11 Mechanically Fastened Composite Joints

The purpose of this section is to provide guidance on the structural design and analysis of mechanically fastened joints where one or more joint members are fiber-reinforced composite materials. The guidance herein is specific to composite materials and should be followed in conjunction with PM-4057 (Section 5.0 Joints, Reference 11-1) and any program specific guidance. This section is organized as shown in the following Table of Contents.

Section 11 Table of Contents

11 Mechanically Fastened Composite Joints 11-1
11.1 References and Nomenclature 11-3
11.2 Introduction 11-8
11.2.1 Bolted Joints in Composites versus Metallics 11-8
11.2.2 Joint Geometry 11-9
11.2.3 Joint Configurations 11-10
11.2.3.1 Single Lap Shear Joints 11-12
11.2.3.2 Double Lap Shear Joints 11-12
11.2.3.3 Multilayer Joints 11-13
11.2.3.4 Composite Fittings 11-13
11.2.3.5 Fastener Rows 11-13
11.2.3.6 Out-of-Plane Loading of Composite Laminates 11-14
11.3 Guidelines for Mechanically Fastened Composite Joints 11-14
11.3.1 Composite Bearing Strength: Guidelines 1-6 11-16
11.3.2 Composite Bolted Joint Geometry: Guidelines 7-11 11-18
11.3.3 Composite Joint Fastener Selection: Guidelines 12-17 11-20
11.3.4 Corrosion Prevention: Guidelines 18-22 11-22
11.4 Basic Theory 11-23
11.4.1 Laminate Strength Failure Modes 11-24
11.4.2 Stresses in Anisotropic Plates with Circular Holes 11-26
11.4.3 Failure Criteria 11-30
11.4.3.1 Fracture Mechanics Based Approach 11-32
11.4.3.2 Point Stress (or Strain) Failure Criterion 11-36
11.4.4 IBOLT Strength Analysis Methodology Overview 11-38
11.4.4.1 Generalization of LEFM Solution for Combined Loads 11-38
11.4.4.2 Finite Geometry Effects 11-42
11.4.4.3 Bearing-Bypass Margin of Safety 11-43
11.4.4.4 Bending Analysis 11-46
11.4.4.5 Bearing Cutoff 11-49
11.4.4.6 Bearing-Bypass Interaction Diagrams 11-54
11.4.4.7 Joint Testing for IBOLT Analysis Calibration 11-56
11.5 Methods of Analysis 11-57
11.5.1 Joint Analysis Overview 11-57
11.5.2 IDAT/IBOLT Strength Analysis 11-58
11.5.2.1 IBOLT Composite Bolted Joint Analysis Overview 11-59
11.5.2.2 IBOLT Analysis Procedure Summary 11-61
11.5.2.3 IBOLT Problem Definition 11-62
11.5.2.4 Element Orientation 11-62
11.5.2.5 Element Dimensions 11-63
11.5.2.6 Element Loads 11-66
11.5.2.7 IBOLT Limitations 11-67
11.5.3 Fastener Pull-Through Analysis 11-68
11.5.4 Other Laminate Strength Checks 11-70

Copyright 2015 Lockheed Martin Corporation.
Note: The current version is always the version on the Lockheed Martin network.

11.5.4.1 Interlaminar Shear Analysis ... 11-71
11.5.4.2 Shear Tear-Out ... 11-73
11.5.4.3 Net Section Tension ... 11-73
11.5.5 Fastener Analysis ... 11-73
11.5.5.1 Fastener Static Strength Installed in Composite Laminates ... 11-74
11.5.5.2 Fatigue ... 11-75
11.6 Determination of Joint Loads ... 11-77
11.6.1 Basic Concepts ... 11-78
11.6.2 Finite Element Analysis Loads ... 11-84
11.6.2.1 Substructure Loads ... 11-88
11.6.2.2 Skin Panel Loads ... 11-89
11.6.2.3 Example Problems – Skin and Substructure Load Transfer ... 11-93
11.6.3 Defining IBOLT Element Free-Body Loads ... 11-96
11.6.3.1 Derived Bearing Load (DBL) Method ... 11-98
11.6.3.2 Fixed Bearing Load (FBL) Method ... 11-100
11.6.3.3 Interior Skin Panel Fasteners: No Edges Free ... 11-103
11.6.3.4 Fasteners along Skin Panel Edges: One Edge Free ... 11-110
11.6.3.5 Fasteners at Skin Panel Corners: Two Edges Free ... 11-117
11.6.4 Multiple Fastener Rows ... 11-123
11.6.5 Coordinate Transformations ... 11-128
11.6.6 Fastener Load Distributions ... 11-130
11.6.6.1 Rigid-Body Fastener Pattern Analysis ... 11-130
11.6.6.2 Elastic Fastener Load Distributions Based on Joint Stiffness ... 11-130
11.6.7 Panel Pressure Induced Membrane and Bending Loads ... 11-131
11.6.8 Pull Off Loads from Panel Pressure ... 11-132
11.6.8.1 Pull-Off Loads from Classical Analysis ... 11-133
11.6.8.2 Pull-Off Loads from Finite Element Analysis ... 11-139
11.7 Special Design Considerations ... 11-141
11.7.1 Multi-Layer Joints ... 11-141
11.7.2 Hybrid Laminates ... 11-142
11.7.3 Countersinks ... 11-143
11.7.4 Hole Reinforcements ... 11-147
11.7.5 Shims and Gaps ... 11-150
11.7.6 Fuel Seals and Seal Grooves ... 11-154
11.7.7 Counterbores ... 11-156
11.7.8 Tapered Joints ... 11-158
11.8 Unix / PC Calculations ... 11-161
11.9 FEA Modeling Conventions and Considerations ... 11-162
11.9.1 Joint Loads from a Coarse Grid Finite Element Model ... 11-162
11.9.1.1 Isolating the Analysis Regions ... 11-163
11.9.1.2 Mapping an IBOLT Element onto a Finite Element Mesh ... 11-164
11.9.1.3 Assigning Free-Body Type ... 11-164
11.9.1.4 Calculating Free-Body Loads ... 11-164
11.9.1.5 Fastener Bearing Load Calculation ... 11-165
11.9.2 Joint Loads from a Fine Grid Finite Element Model ... 11-170
11.9.3 Automated Loads Extraction for Coarse Grid Models ... 11-172
11.9.4 Transforming Nastran Results to IBOLT Coordinates ... 11-173
11.9.5 FEA Modeling of Discrete Fasteners ... 11-175
11.9.6 FEA Modeling for Flange Pull-Off Analysis ... 11-179

Copyright 2015 Lockheed Martin Corporation.
Note: The current version is always the version on the Lockheed Martin network.

11.1 References and Nomenclature

11-1 Flansburg, L.K., *Lockheed Martin Aeronautics Procedures Manual 4057 Metallic Structural Analysis Manual*, Lockheed Martin Aeronautics, Fort Worth, TX, 2008.

11-2 Anon., *Structures Analysis Manual, Volume 1 and Volume 2*, General Dynamics Convair and Space Structures Divisions, 1988.

11-3 Peterson, R. E., *Stress Concentration Design Factors*, John Wiley & Sons, New York, NY, 1953.

11-4 Anon., *Lockheed Composite Stress Memo Manual*, Lockheed Martin Aeronautical Systems, Marietta, GA, Draft Copy 2006.

11-5 Staff, *LTV Composite Structures Analysis Manual*, LTV Aircraft Products Group, Grand Prairie, TX, August, 1984.

11-6 Anon., *DOD/NASA Advanced Composites Design Guide*, Air Force Wright Aeronautical Laboratories, Dayton, OH, prepared by Rockwell International Corporation, 1983.

11-7 Anon., *Composite Materials Handbook CMH-17*, Revision G, Materials Sciences Corporation, Secretariat, Philadelphia, PA, 2012.[1]

11-8 Jones, R. M., *Mechanics of Composite Materials*, Hemisphere Publishing Corp., New York, NY, 1975.

11-9 Hart-Smith, L. J., "Bolted Joint Analyses for Composite Structures—Current Empirical Methods and Future Scientific Prospects," in *Joining and Repair of Composite Structures*, K.T. Kedward and H. Kim, editors, American Society for Testing and Materials, Dec. 2004.

11-10 Vogt, F., "The Load Distribution in Bolted or Riveted Joints in Light Alloy Structures," *NACA TM 1135*, April, 1947.

11-11 Eisenmann, J. R., Taylor, R. M. and Rousseau, C. Q., FZM 9065, *IBOLT Theory Manual*, Lockheed Martin Aeronautics, Fort Worth, TX, 2010.

11-12 Anon., *SS_JOINT Version 4.0 User's Guide*, Lockheed Martin Aeronautics, Fort Worth, TX, 2012.

11-13 Niu, M. C., *Composite Airframe Structures Practical Design Information and Data*, Conmilit Press Ltd., Hong Kong, 1992.

11-14 Lekhnitskii, S. G., *Anisotropic Plates*, Gordon and Breach Science Publishers, 1968.

11-15 Lekhnitskii, S. G., *Theory of Elasticity of an Anisotropic Body*, Mir Publishers 1981.

11-16 Savin, G. N., *Stress Concentrations Around Holes*, Pergamon Press, 1961.

11-17 Garbo, S. P., and Ogonowski, J. M., "Effects of Variances and Manufacturing Tolerances on the Design Strength and Life of Mechanically Fastened Composite Joints," Vol 1, 2 and 3, *AFWAL-TR-81-3041*, April 1981.

11-18 Waddoups, M., Eisenmann, J. and Kaminski, B., "Macroscopic Fracture Mechanics of Advanced Composite Materials," *Journal of Composite Materials*, Vol. 5, October, 1971, pp. 446-454.

11-19 Bowie, O. L., "Analysis of an Infinite Plate Containing Radial Cracks Originating from the Boundary of an Internal Circular Hole," *Journal of Mathematics and Physics*, Vol. 35, 1956.

11-20 Whitney, J. and Nuismer, R., "Stress Fracture Criteria for Laminated Composites Containing Stress Concentrations," *Journal of Composite Materials*, Vol. 8, July, 1974, pp. 253-265.

11-21 Grant, P. and Sawicki, A., "Development of Design and Analysis Methodology for Composite Bolted Joints," Proceedings, *AHS National Technical Specialists Meeting on Rotorcraft Structures*, Williamsburg, VA, October, 1991.

11-22 Eisenmann, J. R. "Bolted Joint Static Strength Model for Composite Materials," *NASA TM X-3377*, Third Conference on Fibrous Composite Materials in Flight Vehicle Design, Part II, April 1976.

11-23 Eisenmann, J. R., *IBOLT Theory Manual for Analysis of Composite Bolted Joints*, FF-93-92, Lockheed Martin Tactical Aircraft Systems, 1994.

11-24 Anon., *IBOLT Version 4.5i User's Guide*, Lockheed Martin Aeronautics, Fort Worth, TX, 2012.

11-25 Eisenmann, J. R. and Rousseau, C. Q., "IBOLT: A Composite Bolted Joint Static Strength Prediction Tool," *Joining and Repair of Composite Structures*, ASTM STP 1455, 2004.

[1] In 2002, administration of MIL-HDBK-17 was transferred to Materials Sciences Corporation. Future releases will be released as Composite Materials Handbook CMH-17, Materials Sciences Corporation, Secretariat.

Copyright 2015 Lockheed Martin Corporation.
Note: The current version is always the version on the Lockheed Martin network.

11-26 Cruse, T., *Boundary Element Analysis in Computational Fracture Mechanics*, Kluwer Academic Publishers, Boston, 1988.

11-27 Waszczak, J. P. and Cruse, T. A., "A Synthesis Procedure for Mechanically Fastened Joints in Advanced Composite Materials", *AFML-TR-73-145*, Volume 2, 1973.

11-28 Paris, P. and Sih, G., "Stress Analysis of Cracks," *Fracture Toughness Testing*, ASTM STP 381, 1970.

11-29 Barrois, W. "Stresses and Displacements Due to Load Transfer by Fasteners in Structural Assemblies", *Engineering Fracture Mechanics*, Vol. 10, 1978, pp. 115-176.

11-30 Ramkumar, R. L., and Tossavainen, E. W., "Bolted Joints in Composite Structures: Design, Analysis and Verification, Task I, Test Results – Single Fastener Joints," *AFWAL-TR-84-3047*, August 1984.

11-31 Nelson, W. D., Bunin, B. L. and Hart-Smith, L. J., "Critical Joints in Composite Aircraft Structure," National Aeronautics and Space Administration Contractor Report *NASA-CR-3710*, 1983.

11-32 Jeans, L. L., Grimes, G. C., and Kan, H. P., "Fatigue Spectrum Sensitivity Study for Advanced Composite Materials, Volume I - Technical Summary," *AFWAL-TR-80-3130*, Vol I, December 1980.

11-33 Walter, R. W., and Tuttle, M. M., "Investigation of Static and Cyclic Failure Mechanisms for GR/EP Laminates," *Proceedings of the Ninth DoD/NASA/FAA Conference on Fibrous Composites in Structural Design*, DOT/FAA/CT-92-25, September 1992, p. I-167.

11-34 Walter, R. W., and Porter, T. R., "Impact of Design Parameters on Static, Fatigue and Residual Strength of GR/EP Bolted Joints," *Proceedings of the Tenth DoD/NASA/FAA Conference on Fibrous Composites in Structural Design*, NAWCADWAR-94096-60, p. III-75, April 1994.

11-35 Anon., "Structural Development Tests, Coupon Tests Results and Evaluation, Volume 05, Graphite Epoxy," *5PPYA081-05*, Lockheed Corporation and The Boeing Company, December 1994.

11-36 Anon., "Structural Development Tests, Coupon Tests Results and Evaluation, Volume 06, Graphite Bismaleimide" *5PPYA081-06*, Lockheed Corporation and The Boeing Company, December 1994.

11-37 Konish, Jr., H. and Cruse, T., "Determination of Fracture Strength in Orthotropic Graphite/Epoxy Laminates," *Composite Reliability*, ASTM STP 580, American Society for Testing Materials, 1975, pp. 490-503.

11-38 Mar, J. and Lin, K., "Fracture Mechanics Correlation for Tensile Failure of Filamentary Composites with Holes," *Journal of Aircraft*, V14, N7, 1977, pp. 703-704.

11-39 Anon., *PULLTHRU Version 3.1 User's Guide*, Lockheed Martin Aeronautics, Fort Worth, TX, 2012.

11-40 Flansburg, L. K., "Derivation of Parameters for Fastener Analysis," *FZM 9379*, Lockheed Martin Aeronautics, 2007.

11-41 Anon., "Structural Development Test Report – Composite Bolted Joint Allowable Tests," *5PC00837-0*, Boeing Military Airplanes, February 1997.

11-42 Fiorenzi, C. J., "Standard Test Procedures for Advanced Fiber Reinforced Composite Materials, Appendix D: Test Methods – Mechanical Properties," *LMA-PT001B*, Lockheed Martin Aeronautics Company, April, 2004.

11-43 Anon., *SPRING Version 2.0 User's Guide*, Lockheed Martin Aeronautics, Fort Worth, TX, 2010.

11-44 Anon., *SPLICE Version 1.2 User's Guide*, Lockheed Martin Aeronautics, Fort Worth, TX, 2006.

11-45 Anon., *PRESS Version 4.13 User's Guide*, Lockheed Martin Aeronautics, Fort Worth, TX, 2008.

11-46 Anon., *FLANGE Version 1.7 User's Guide*, Lockheed Martin Aeronautics, Fort Worth, TX, 2010.

11-47 Anon., "Department of Defense Joint Services Specification Guide, Aircraft Structures, *JSSG-2006*," Department of Defense, ASC/ENSI, Wright Patterson Air Force Base, Ohio, 1998.

11-48 Anon., *Lockheed Martin Aeronautics Procedures Manual 4007 Lockheed Martin Design Manual*, Lockheed Martin Aeronautics, Fort Worth, TX, 2008.

Copyright 2015 Lockheed Martin Corporation.
Note: The current version is always the version on the Lockheed Martin network.

11-49 Hull, M. W., *F-35 Shimming Design Standard*, 2GSA00001 Rev E, Lockheed Martin Aeronautics, Northrop Grumman, BAE Systems, Fort Worth TX, 2007.

11-50 Jackson, T. L., *XG-ST-EL-65 Wing Composite Strap Seal Groove Strength Validation* , Engineering Test Report 2WSA00482-0002, Lockheed Martin Aeronautics, Northrop Grumman, BAE Systems, Fort Worth TX, 2007.

11-51 Hull, M. W. and Dickey, A., *JSF Fuel Sealing Design Standard*, 2ZFA00001 Rev B, Lockheed Martin Aeronautics, Northrop Grumman, BAE Systems, Fort Worth TX, 2007.

11-52 Sewell, J. P., "CV Wing-To-Body Fairing Tapered Edge Analysis Correlation Tests," Engineering Test Report 2WSA00499, Lockheed Martin Corporation, 2008.

11-53 Anon., *BDAT Version 1.6 User's Guide*, Lockheed Martin Aeronautics, Fort Worth, TX, 2011.

Table 11.1-1 Nomenclature

Symbol	Definition	Units
a, b	Panel dimensions; a = hole radius, distance, crack length, or flaw size	in
A, B	IBOLT element edge lengths; A = area (in^2)	in
BCT, BCTX, BCTY	Bearing cutoff with tension reaction (Total, X, Y)	psi
BCC, BCCX, BCCY	Bearing cutoff with compression reaction (Total, X, Y)	psi
BCS, BCSX, BCSY	Bearing cutoff with shear reaction (Total, X, Y)	psi
BRGX, BRGY	Bearing stress components with normal reactions	psi
BRGSX, BRGSY	Bearing stress components with shear reactions	psi
c	Laminate compliance parameter	psi-1
D	Fastener or hole diameter	in
D_{head}	Diameter of the fastener head (flush) or washer (protruding head)	in
d_{sf}	Distance from skin outer surface (OML) to sub-flush fastener	in
e, e_{side} , e_{end}	Edge distance from hole center to panel edge (side or end for clarity)	in
E_X, E_Y, E_θ	Laminate Young's elastic modulus in the X-, Y-, and θ-directions	psi
E_{11}	Lamina Young's modulus 1-direction	psi
edgvec	Unit vector in-plane and parallel to the current element edge	-
f(a/r)	Bowie's LEFM solution function	-
F	Applied stress	psi
F_{all}, F_{allow}	Stress allowable	psi
$f_{applied}$	Maximum fastener bending stress (SFBOLT analysis)	psi
F_{bru}	Ultimate bearing strength	psi
F_{BX}, F_{BY}	β function, bearing stress with tension reaction	-
F_{BXX}, F_{BYY}	β function, bearing stress with shear reaction	-
F_{clr}	Fastener clearance factor (SFBOLT analysis)	-
F_{com}	Joint material combination factor (SFBOLT analysis)	-
F_{fas}	Fastener type factor (SFBOLT analysis)	-
f_{ils}	Interlaminar shear stress	psi
f_{pt}	Fastener pull-through interlaminar shear stress	psi
F_{tu}, F_{cu}	Unnotched tensile and compression strength	psi
F_{TX}, F_{TY}, F_{XY}	β function, bypass stress	-
F_{TXX}, F_{TYY}	β function, membrane stress with shear reaction	-
Fx, Fy, Fz	Fastener load component in the X, Y, Z directions	lbs
F_1	Transverse shear load in panel prior to fastener line	lbs
f_{13}, f_{23}, f_{33}	Interlaminar stress components	psi
F_{13}^{su}, F_{23}^{su}, F_{33}^{tu}	Interlaminar stress allowables	psi
FBF	Cumulative effect of bearing loading factors	-
FBRUBCT	Ratio of F_{bru} to bearing cutoff with tension reaction (BCT)	-
FBTORK	Bearing load fastener off-nominal torque correction factor	-

Copyright 2015 Lockheed Martin Corporation.
Note: The current version is always the version on the Lockheed Martin network.

Symbol	Definition	Units
FCLEAR	Hole-clearance factor	-
FCNTT	Bypass countersink correction factor	-
FCSKBC	Bearing countersink correction factor	-
FDIABC	Fastener diameter factor	-
FDPLY	Effect of adjacent same-oriented tape plies factor	-
FFCBND	Filled countersunk hole factor	-
FFHBND	Filled hole factor	-
FFILL	Filled-hole bypass correction factor	-
FFILLT	Filled-hole tension bypass correction factor	-
FFILLC	Filled-hole compression bypass correction factor	-
FGEOBC	Finite geometry effect factor	-
FGEOBCT	e/d and W/D factor, bearing with tension reaction	-
FGEOBCC	e/d and W/D factor, bearing with compression reaction	-
FGEOBCS	e/d and W/D factor, bearing with shear reaction	-
FOHBND	Open hole factor	-
FPCTBC	Laminate ply percent (0° and 90° plies) factor	-
FPCTBCT	Ply percentage factor, bearing with tension reaction	-
FPCTBCC	Ply percentage factor, bearing with compression reaction	-
FPCTBCS	Ply percentage factor, bearing with shear reaction	-
FPKBC	Peak bearing stress ratio factor	-
FSHIM	Shim factor for bearing strength	-
FSSDS	Single-shear bearing factor	-
FTF	Cumulative effect of bypass loading factors	-
FTFCS	Tangential fibers on compression	-
FTHBC	Bolt load angle, theta	-
FTTORK	Bypass load fastener off-nominal torque correction factor	-
G_{XY}	Laminate X-Y plane shear stiffness	psi
G_0, G_{45},G_{90}	Strain energy release rates of 0º, ±45º, 90º plies	in-lbs/in2
$\Sigma GPF_{i,e}$	Portion of the grid point force resultant at node i	lbs
H	Countersink fastener head height	in
k	Factor locating the centroid of a bearing distribution	-
$K_{FE,shear}$	Finite element joint shear stiffness	lbs/in
K_I	Stress intensity factor	psi-in½
K_{IC}	Critical stress intensity factor	psi-in½
Ksec,i	Secant joint shear stiffness	lbs/in
K_{SS_JOINT}	Single fastener stiffness value determined from SS_JOINT	lbs/in
K_{t_DLS}	4.0 lifetime design limit stress	psi
K_T, K_{TX}, K_{TY}, K_{TXY}	Stress concentration factors, in-plane bypass load	-
KBB	Test-derived bending factor	-
L	Panel length	in
L_{arm}	Moment arm	in
len_e	Length of current element edge	in
L_S	Sleeve length	in
L_{TX}, L_{TY}, L_{XY}	Finite geometry correction, bypass loads	-
L_{TXX}, L_{TYY}	Finite geometry correction, membrane with shear reaction	-
L_{BX}, L_{BY}	Finite geometry correction, bearing with tension reaction	-
L_{BXX}, L_{BYY}	Finite geometry correction, bearing with shear reaction	-
M	Fastener head moment	in-lb
M_h	Moment at the leading edge of the fastener	in-lb
m_B	Flange bending running moment at point B	in-lbs/in

Copyright 2015 Lockheed Martin Corporation.
Note: The current version is always the version on the Lockheed Martin network.

Symbol	Definition	Units
MX, MY, MXY	Moment resultants (running load)	in-lbs/in
M_1	Moment in panel prior to fastener line	in-lb
n	Number of rows of bolts; Laminate elastic stiffness parameter	-
NX, NY, NXY	In-plane force resultants (running load); Also IBOLT bypass loads	lbs/in
NX_{avg}, NY_{avg}, NXY_{avg}	Average in-plane load calculated at the fastener location	lbs/in
NX_{trans}, NY_{trans}, NXY_{trans}	In-plane loads relating average loads to bearing loads	lbs/in
NX1, NY1, NXY1	In-plane force resultants for skin panel Bay 1 (running load)	lbs/in
NX2, NY2, NXY2	In-plane force resultants for skin panel Bay 2 (running load)	lbs/in
NXX, NYY	IBOLT bypass reacted with membrane shear load cases	in-lbs/in
N1, N2, N3, N4	IBOLT element normal force load resultants (running load)	lbs/in
ΔNX1, ΔNX2	Panel load gradient in NX in a given direction	lbs/in
ΔNY1, ΔNY2	Panel load gradient in NY in a given direction	lbs/in
P	Fastener bearing load; Also generic applied joint load	lbs
$P_{bolt\text{-}i}$	Bolt bearing load at the ith fastener	lbs
$P_{byp\text{-}i}$	Bypass load at the ith fastener	lbs
P_{edge}	Fastener load in the edgewise direction	lbs
$P_{node,i}$	Nodal force value determined from the ith finite element solution	lbs
PNX, PNY	IBOLT normal bearing load cases	lbs
P_{shear}	Fastener shear load	lbs
P_{skin}	Axial load in skin	lbs
PSX, PSY	IBOLT shear bearing load cases	lbs
P_{tran}	Fastener load in the edgewise direction	lbs
P_{tu}	Fastener pull through load	lbs
P_{web}	Web load resultant	lbs
PX, PY	IBOLT fastener bearing load components	lbs
PX_{DBL}, PY_{DBL}	Total bearing load calculated using the DBL method	lbs
PX1, PX2, PX3, PTX	PX bearing load components	lbs
PY1, PY2, PY3, PTY	PY bearing load components	lbs
$[\overline{Q}]$	Reduced transformed ply stiffness matrix	psi
q_{edge}	Element edge shear flow	lbs/in
q_{tran}	Element edge transverse running load	lbs/in
q_{web}	Substructure beam web shear flow	lbs/in
q_1, q_2	Panel bay 1 and 2 shear flow	lbs/in
r	Radial coordinate, fastener radius; radius of curvature	in
RNX, RSX, RTX	PX bearing load ratios (normal, shear, balancing NXY shear)	-
RNY, RSY, RTY	PY bearing load ratios (normal, shear, balancing NXY shear)	-
s	Fastener pitch or spacing	in
S_{actual}	Actual fastener spacing as designed	in
S_{FE}	Nodal spacing along component interface in finite element model	in
S_{ij}	Lamina(ply) reduced compliance terms	psi^{-1}
t	Laminate thickness	in
t_{eff}	Laminate effective thickness	in
$t_{eff,skin}$	Skin effective thickness	in
$t_{eff,sub}$	Substructure effective thickness	in
t_{lam}	Total laminate nominal thickness	in
t_{nom}	Skin nominal thickness	in
t_{ns}	Thickness of all of the non-structural material	in
t_{shim}	Shim or gap thickness	in
t_{total}	Total joint thickness (structural members, including shim)	in
tranvec	Unit vector in-plane and normal to the current element edge	-

Copyright 2015 Lockheed Martin Corporation.
Note: The current version is always the version on the Lockheed Martin network.

Symbol	Definition	Units
T1, T2, T3, T4	IBOLT element shear force load resultants (running load)	lbs/in
usec,i	secant displacement at the ith iteration	in
V	Transverse shear heel-toe load	lbs
w	Width of fastener element	in
w_{eff}	effective width	in
W1, W2	Panel bay width	in
X, Y, Z	Reference coordinate system	in
XNSF, YNSF	X- and Y- direction net section factors	-
y	Distance from fastener centerline to stress calculation point	in
α	Countersink angle	deg
$\beta = F_{TX}(a / r)$	Function that accounts for the effects of crack and coupon geometry	-
ν_{XY}	Laminate Poisson's ratio in the X-Y plane	-
σ	Applied stress	psi
σ_b	Bending stress	psi
σ_c	Critical applied stress at failure	psi
σ_θ, σ_{Local}	Local tangential or circumferential stress	psi
σ_{TX}, $\sigma_{Far\text{-}field}$	Applied far-field stress in the X-direction	psi
σ_{TX}, σ_{TY}, σ_{TXY}	Bypass stresses (SIGTX, SIGTY, SIGTXY)	psi
σ_{TXX}, σ_{TYY}	Membrane stress in the x- and y-directions, shear reaction	psi
σ_{BX}, σ_{BY}	Bearing load in the x- and y-directions, tension reaction	psi
σ_{BXX}, σ_{BYY}	Bearing load in the x- and y-directions, shear reaction	psi
$\sigma_{11t,ult}$, $\sigma_{11c,ult}$	Fiber direction ultimate tensile or compression strength	psi
θ	Bearing load orientation angle w.r.t. X-axis	degrees

11.2 Introduction

Structural Joints are an essential feature of all aerospace structural assemblies. At Lockheed Martin, the vast majority of these joints are bolted rather than bonded. This section presents the following introductory level topics related to the design and analysis of mechanically fastened joints for composite structure.

- Bolted Joints in Composites versus Metallics
- Joint Geometry
- Joint Configurations
- Joint Loads

Refer to References 11-1, 11-2 and 11-3 for general guidance on the design and analysis of mechanically fastened joints. Refer to References 11-4, 11-5, 11-6, 11-7, and 11-8 for general guidance on the design and analysis of mechanically fastened joints in composite structures.

11.2.1 Bolted Joints in Composites versus Metallics

Mechanically fastened joints are a primary method of joining aircraft structure and they are also a primary source of failure. They create load path eccentricities, stress concentrations, and analysis complexities. The behavior of composites in bolted joints differs considerably from what occurs with metals. Some of the factors that differentiate the strength and performance of composite bolted joints as compared to metallic joints are discussed below.

- **Anisotropy** – Composites consist of oriented layers of orthotropic laminae with directionally dependent stiffness and strength properties. This increases the analytical complexity of predicting the bearing-bypass stresses and deformation in composite joints as compared to metallic joints.

Copyright 2015 Lockheed Martin Corporation.
Note: The current version is always the version on the Lockheed Martin network.

- **Brittle versus Ductile Material Behavior** – Metallics exhibit ductile material behavior with significant yielding and plastic deformation before final failure. In contrast, fiber-dominated net-section failures in composites exhibit brittle failure behavior with little or no yielding and near linear load-displacement behavior to failure. The brittle material behavior requires that stress peaks be well characterized, such as the stress concentration at the hole edge as well as bearing and bending stress distributions through the laminate thickness. On the other hand, pure bearing failures in composite laminates are complex with nonlinear load-displacement behavior and progressive damage growth with multiple possible local failure modes. The ductile behavior of metallic joint elements helps to smooth out joint loads at higher load levels through the action of yielding, whereas composites are more sensitive to stress concentration and the effects of joint geometry such as edge distance and fastener spacing.
- **Notch Sensitivity** – Composites exhibit a notch sensitivity for both net section and bearing failure modes where, for a given joint width-to-diameter ratio, the joint strength is observed to decrease with increasing hole diameter. Notch sensitivity must be accounted for in any composite joint predictive failure theory or criterion.
- **Through-the-Thickness Strength** – Fiber reinforced composites are known to have relatively low interlaminar tension and shear strength as compared to metallic materials. Composite joint failure modes caused by low interlaminar strength include fastener pull-through and bearing or bending induced damage, progressing into matrix shear cracks and delamination. The susceptibility of composite laminates to fastener pull-through failure has resulted in a need for fasteners with an increased head/tail bearing area to resist these loads.
- **Environmental Effects** – The strength properties of composites are more sensitive to temperature as compared to metallics, and are also sensitive to moisture content. Joint strength properties must be well-characterized over the range of the intended design environment, extending from cold-temperature-dry up through hot-temperature-wet environmental conditions.
- **Fatigue Performance** – Fatigue performance of bolted composite joints is generally very good as compared to metallic joints. Provided that sound joint design practices are implemented, the metallic joint members will typically be the limiting elements for joint fatigue.
- **Galvanic Potential between Joint Materials** – Galvanic corrosion susceptibility between carbon fibers and aluminum have eliminated the use of aluminum fasteners and have required implementation of corrosion barriers in composite joint design.
- **Fastener Selection** – Fasteners for composite joints require high head/tail fixity to reduce joint rotation and peak bearing stresses. Vibration drive fasteners, solid rivets or expanding fasteners should not be used in composites due to risk of laminate damage during installation.

In summary, the local yielding due to ductility in bearing critical metallic joints allows load redistribution among fasteners at higher load levels, relative to linear elastic predictions. Due to the relative brittleness of most composite materials, a similar effect does not occur as readily in composite joints. In addition, bearing stresses or strains generally interact with bypass stresses or strains resulting in a more complex failure mechanism and analysis. Although metal joints also have bypass load, from a static strength standpoint, the anisotropy and ply-by-ply lamination of composites introduce more complexities in dealing with the competing failure modes. Therefore it is important in composite joints to analyze load distributions more accurately and evaluate the structural integrity in bearing and bypass load fields in greater detail.

11.2.2 Joint Geometry

Reference 11-1, PM4057, Section 5.2.3 has a discussion of terminology and joint design considerations for joints in general and metal joints in particular. This section will discuss some of the difference between metal and composite joints. Figure 11.2-1 shows some typical joint geometric features which are important to the strength of a joint. In joint analysis, depending on the context of the discussion, *D* may be the hole diameter or the fastener diameter. For strength calculations and determination of side and end distances and fastener spacing, *D* is the diameter of the hole. For discussions of ratios of thickness-to-diameter, as discussed in Section 11.3, D is the diameter of the fastener. The analyst should be aware of which applies where.

Copyright 2015 Lockheed Martin Corporation.
Note: The current version is always the version on the Lockheed Martin network.

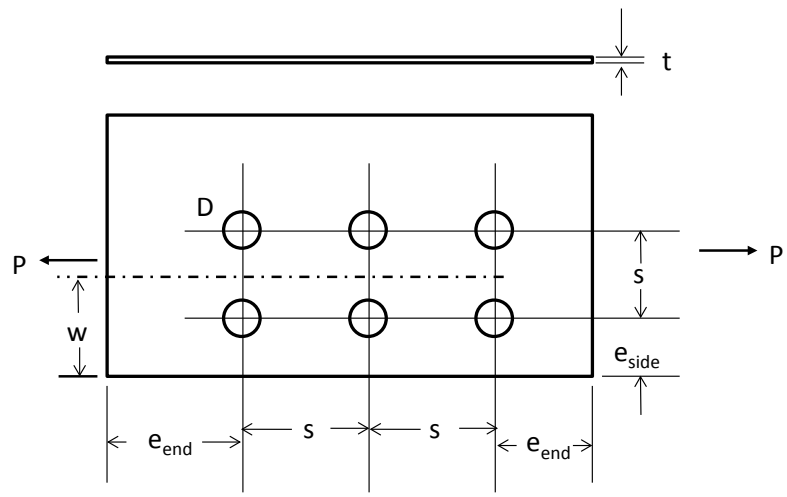

Figure 11.2-1 Definitions of Typical Joint Geometric Features

The fastener pitch or spacing is generically given the dimension *s* and can apply both parallel and perpendicular to the load. The edge and end distances, e_{side} and e_{end}, are often generically given the dimension *e*. The width of a particular joint analysis element is *w* and it can be calculated as 4D, or as half the distance to the adjacent rows or columns, or as the distance to the edge (or end) plus half the distance to the adjacent row on the opposite side, depending on the circumstance. All of these dimensions, *e*, *w* and *s*, have minimum recommended values, generally in terms of a multiple of the hole diameter. In analysis, the laminate nominal thickness dimension is used. This is determined as the nominal per ply thickness times the number of plies.

The minimum recommended edge and end distances for composite materials is 2.5 times the hole diameter while the fastener spacing is recommended to be a minimum of 4 times the hole diameter. This will be discussed in further detail in Sections 11.3 and 11.5.2.5.

11.2.3 Joint Configurations

Mechanically fastened joints vary widely in configuration but can be generally categorized in terms of loading direction, overlap configuration, fastener pattern, and number of layers. This section discusses these joint configuration characteristics, outlining their effect on joint fixity and laminate and bolt loading. The discussion is organized at a top level by joint load direction, focusing on in-plane loading, which is the primary loading direction for composite laminates due to relatively poor out-of-plane properties.

For most composite mechanically fastened joints, the load transfer is primarily in-plane with bolts loaded in shear and holes drilled to close tolerances. The joint is typically formed with an overlap between two or more members being joined and a hole is created at the overlap where fasteners can be inserted.

This section discusses the general configuration of in-plane loaded composite bolted joints in terms of the number shear planes reacting load within the fastener. Single lap shear, double lap shear, and multi-layer joints are defined and discussed. Additional discussion is provided for composite in-plane load fittings and using multiple rows of fasteners for in-plane loaded joints.

Figure 11.2-2 illustrates several different types of joints, generally described in terms of the number of interfaces which create shear planes in the fastener. These will be discussed more in Sections 11.2.3.1 through 11.2.3.3.

Copyright 2015 Lockheed Martin Corporation.
Note: The current version is always the version on the Lockheed Martin network.

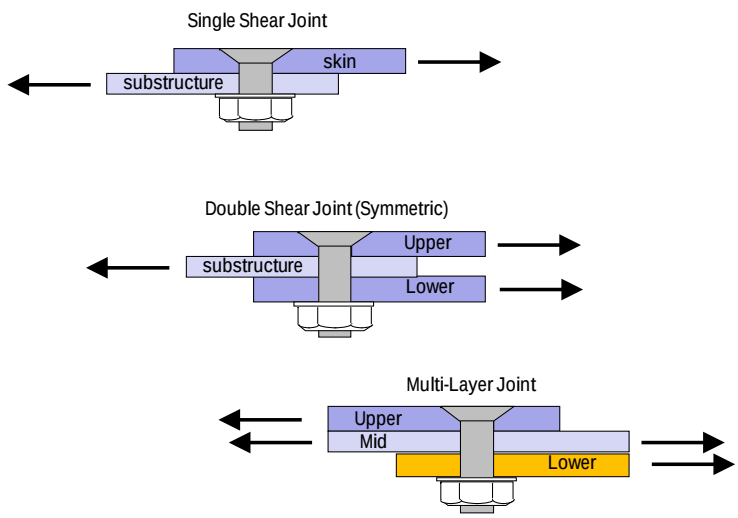

Figure 11.2-2 Joint Configuration Examples

Note that as joints deform and rotate, bending loads can develop in the fasteners. This is primarily the case in unbalanced stack-up joints or single row single lap shear joints. The addition of non-structural shims can also cause bolt bending to occur. Bolt bending analysis is likely required for these joint configurations. Bolt bending analysis is not generally required for double shear joints without gaps between joint layers. Specific guidelines for when bolt bending analysis is required and how to execute the analysis are given in Reference 11-1, Section 5.2.3.4.

Another important concept in joint analysis is the load transferred from one layer to another within the joint. This affects the bearing and bypass loads. The bearing load is the load being transferred from one layer to another at a given fastener through the fastener bearing against the hole surface. The bypass is the load which remains in the layer which continues past the hole to fasteners further along in the joint. This is illustrated in Figure 11.2-3 where a three fastener joint is depicted. Examining the joint from left to right as the load, P, encounters the first fastener in the upper splice member, a portion of load, P_{bolt-1}, is transferred to the lower splice member through the first bolt. The remainder of the load, P-P_{bolt-1}, bypasses hole 1. This bypass load, P_{byp-1}, represents the amount of load in the upper splice member available for transfer at bolts 2 and 3. Similarly at hole 2, P_{bolt-2} represents the load transferred from the upper splice member to the lower splice member through bolt 2. The bypass load, P_{byp-2}, passes around the hole 2 and is available for transfer at hole 3. Because hole 3 is the last hole in the upper splice plate, the remaining load is transferred by bolt 3, and P_{bolt-3}, is equal to P_{byp-2}. There is no load passing around hole 3, so the $P_{byp-3}=0$.

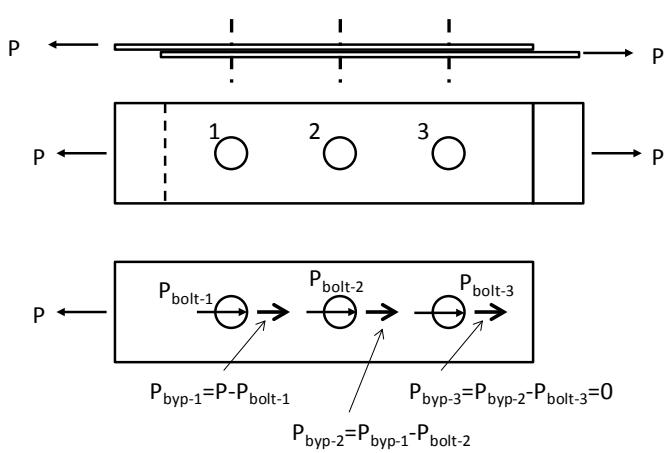

Figure 11.2-3 Bearing-Bypass Loading in a Simple Splice

Copyright 2015 Lockheed Martin Corporation.
Note: The current version is always the version on the Lockheed Martin network.

11.2.3.1 Single Lap Shear Joints

Single lap shear joints consist of two overlapping joint members that have a single shear plane across the body of the fastener at the interface between the layers. This arrangement forms a naturally eccentric joint and rotation occurs as the joint load line tries to straighten out. This can result in bending moments in the fasteners and prying on the head and tail as shown in Figure 11.2-4.

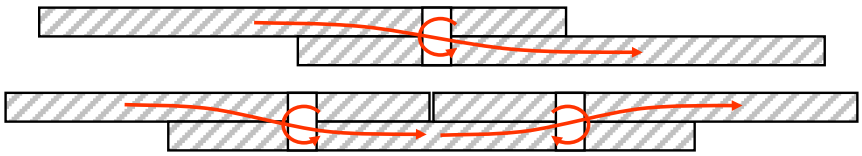

Figure 11.2-4 Single Lap Shear Joints Induce Moment and Rotation Due to Eccentric Load Path

If single lap shear joints are required, they should be stabilized laterally (moments resisted) by supporting structure to reduce bending as shown in Figure 11.2-5.

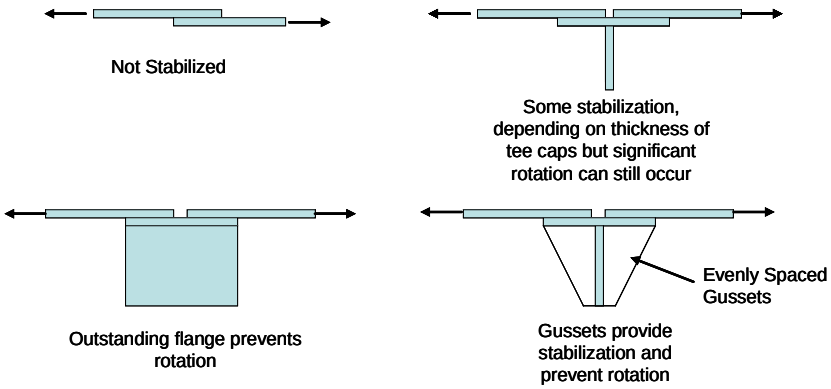

Figure 11.2-5 Single Lap Shear Joint Stabilization

Eccentricity in the load path in a single lap shear joint leads to non-uniform bearing stress through laminate thickness. Because of the brittle nature of composites, there is no local plasticity to redistribute load to alleviate the peak so critical bearing and bypass stresses develop around the hole at the laminate interface at even lower than average bearing stress. Additionally, avoid local reinforcement of unsymmetrical joints by arbitrary laminate thickness pad up because this also increases load eccentricity and bending stress, which counteracts the increase in bearing area. Moment should be reacted in adjacent structures, rather than by bolt bending or in the laminate, to the greatest extent possible.

11.2.3.2 Double Lap Shear Joints

Double lap shear joints have a single load member sandwiched between two load reaction members as shown in the middle illustration of Figure 11.2-2. Double lap shear joints have two shear planes across the body of the fastener at the interface between the layers. As shown in Figure 11.2-6, bending is virtually eliminated in symmetrical double lap shear joints and thus bearing stresses and laminate strains are relatively uniform through the thickness. Symmetry is obtained by having outside members of identical stiffness and thickness.

Copyright 2015 Lockheed Martin Corporation.
Note: The current version is always the version on the Lockheed Martin network.

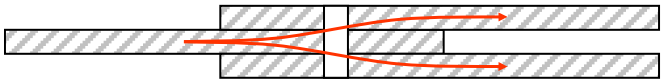

Figure 11.2-6 Symmetrical Double Lap Shear Joint Minimizes Bending

Double lap shear joints are structurally more efficient than single lap shear joints and should be used unless design requirements or space constraints dictate otherwise.

11.2.3.3 Multilayer Joints

Some structural configurations necessitate joining multiple layers of structural materials using mechanical fasteners as shown in Figure 11.2-7 or the bottom figure of Figure 11.2-2. Multilayer joints may have two or more shear planes across the body of the fastener at the interface between the layers. Multilayer joints can take on a number of geometries and the degree of eccentricity and magnitude of the bending moment is dependent on the number, stiffness, thickness and arrangement of the various layers.

For example, chevron panels sometimes use composite straps over bulkhead flanges to avoid excessively wide metallic flanges where panels are attached. Each of the layers in such joints is structural. Additionally, non-structural shims may be included in the layers being joined. These joints may have a complex load distribution due to the mixed stiffness profile of the constituent components. Consequently, fastener load distribution through the layers should be determined using the tools described in Section 11.6.5 or 11.8. A free-body diagram should be constructed to understand the complexities of the load distribution in such a joint.

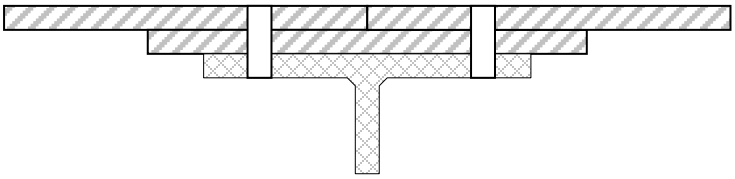

Figure 11.2-7 Multilayer Joint Example

11.2.3.4 Composite Fittings

Discrete composite in-plane load fittings have been used in limited aerospace applications such as rotorcraft blades. Fittings often require multi-axial load transfer, so the inherent strong in-plane and weak out-of-plane properties of composites can result in unique design challenges. The current development of multi-dimensional woven composites may lead to new design alternatives, but development test cost should be taken into consideration.

Most of the current LM Aeronautics analysis methods, tools, material allowables, and experience are all based on thin composite plate structures, thus making analysis of thick composite fittings higher risk. In general, discrete load fittings are better designed using metals and composite materials should not be used. If thick composite fittings are to be considered for structural design, a robust component-level test program must be executed to substantiate analysis predictions.

11.2.3.5 Fastener Rows

Mechanically-fastened joints can use a single row of fasteners or may incorporate multiple rows in order to increase the joint strength and distribute load transfer across a larger number of fasteners. Multiple rows can also be used to minimize induced bending from eccentric loading in unsymmetric joints, such as single lap shear joints. Single fastener row joints may be sufficient up to a certain load magnitude. However, a highly loaded joint, such as a wing root joint, will likely require multiple rows. In determining the number of fastener rows, consideration should be given to failure mode and load distribution.

Copyright 2015 Lockheed Martin Corporation.
Note: The current version is always the version on the Lockheed Martin network.

The benefit of multiple fastener rows depends on the failure mode of the particular joint. Testing and analytical models discussed in Reference 11-9 demonstrated for joint geometries that produce tension failures for a single fastener row, little benefit is gained by the addition of additional fastener rows. When bearing failures occur, however, multi-row fastener patterns can significantly increase the joint strength above that of a single fastener row joint.

In an elastic bolt load distribution, load distributes according to the relative stiffnesses of the bolts and materials being joined. There are two limits on a distribution.

- If the bolts are very flexible the load on the bolts approaches uniformity.
- If the bolts are relatively stiff the distribution depends only on the stiffnesses of the parts being joined.

Further, if the joint members are uniformly stiff across the joint, the bolt distributions shown in Table 11.2-1 are obtained (Reference 11-10). Note the peaking on the first and last bolt for three bolt patterns and above. When relatively stiff bolts are used, an increase in the number of bolts does not significantly reduce the load on the highest loaded first and last bolts, provided no yielding has occurred.

Table 11.2-1 Load Distribution in Bolted Joint of Uniformly Stiff Parts

Number of Bolts	Distribution (Percent)
2	50, 50
3	37.5, 25, 37.5
4	33.3, 16.7, 16.7, 33.3
5	31.9, 13.6, 9.1, 13.6, 31.9
6	31.2, 12.5, 6.3, 6.3, 12.5, 31.2

It is clear from this table that use of more than three rows of bolts in a joint is not efficient since the fasteners in the center of the pattern carry only a small portion of the total load and the fasteners at either end continue to carry approximately ⅓ of the load each. If a tapered or stepped joint is used or fastener diameters are varied then the joint stiffness can be tailored to result in a more uniform distribution.

Section 11.6.6 provides additional discussion on the determination of fastener load distributions.

11.2.3.6 Out-of-Plane Loading of Composite Laminates

Most mechanically fastened composite joints transfer primarily in-plane loads with bolts loaded in shear. Due to relatively weak interlaminar shear and tensile strengths, composite materials should not generally be used in conventional joints and fittings with large **concentrated** out-of-plane load components. An exception is a well-configured bonded joint utilizing a 3-D woven preform.

Many composite panels, however, are required to resist an out-of-plane component of load due to aerodynamic or fuel pressure or other distributed low magnitude source. Such loading induces distributed out-of-plane shear and moments at panel boundaries and attachments to substructure. Laminates must be checked for capability to carry these loads using the analysis methodology defined in Section 11.5.4.

11.3 Guidelines for Mechanically Fastened Composite Joints

Due to the prevalence of bolted joints in aircraft structure, general guidelines to ensure the structural integrity of mechanically fastened joints in composite structures have been developed based on a significant body of structural testing and in-house program successes. These are presented in Table 11.3-1. These guidelines were also presented in Section 2.3.4 and are repeated here for convenience. Each of the guidelines is discussed further in Sections 11.3.1 through 11.3.4.

Copyright 2015 Lockheed Martin Corporation.
Note: The current version is always the version on the Lockheed Martin network.

Table 11.3-1 Guidelines for Mechanically Fastened Joints in Composite Materials

No.	Guideline	Section Remarks
1	Wherever it is practical for the given set of joint design loads, mechanically fastened composite joints should be designed for bearing failure rather than for notched strength, shear out or fastener strength in order to prevent catastrophic failure.	11.3.1 Composite Bearing Strength
2	Laminates subject to bearing loads should be at least 40 percent ±45° plies; at least 8 percent 0° plies; and at least 8 percent 90° plies. Ply dispersion should be maximized.	
3	Fastener diameter to laminate structural thickness ratio for any given composite joint member should be: Single Shear Joints, $t/D \leq 1.0$; Double Shear Joints, $t/D \leq 2.0$.	
4	Total joint thickness including all joint members, shim and gaps shall not exceed 3D, where D is the fastener diameter: $t_{total}/D \leq 3.0$. Note: IBOLT[1] is limited by calibration data to $t_{total}/D \leq 2.0$ and will issue a user warning when this limit is exceeded.	
5	Design countersink depth should not exceed 80% of the nominal structural thickness of a composite joint member.	
6	Use caution increasing the laminate thickness for bearing strength of unsymmetrical single lap shear joints since it is also increasing the load eccentricity.	
7	Fastener edge distance shall be 2.5D minimum, where D is the hole diameter and edge distance is from the hole center to the effective edge of the part. Use 3D minimum edge distance for major-mate joints.	11.3.2 Composite Bolted Joint Geometry
8	Fastener pitch or spacing should be no less than 4D and no greater than 8D, where D is the hole diameter.	
9	Use no less than 4D and no greater than 5D spacing in critical primary load path joints with multiple fasteners.	
10	Multiple fastener rows are recommended along panel edges to react bending loads due to panel pressure and/or eccentric loading induced by single lap shear joints.	
11	Remain cognizant that all joint designs fall within the range of materials, stacking sequences, laminate thicknesses and fastener diameters of existing strength test data.	
12	Fastener hardware should be selected for mechanically fastened composite joints for high head/tail fixity to reduce joint rotation and peak bearing stresses.	11.3.3 Composite Bolted Joint Fastener Selection
13	Appropriate fastener torque should be specified to develop full potential joint fixity.	
14	Only tension head countersunk fasteners should be used in composite joints; shear head countersunk fasteners should not due to their lack of fixity.	
15	Do not use vibration drive fasteners, solid rivets, or expanding fasteners in mechanically fastened composite joints due to risk of damage during installation.	
16	Use close tolerance fit holes for structural composite joints (Diametric bolt-to-hole clearance of 0.000 to +0.004 inches).	

[1] Reference 11-11.

Copyright 2015 Lockheed Martin Corporation.
Note: The current version is always the version on the Lockheed Martin network.

No.	Guideline	Section Remarks
17	Use fasteners designed for composite installation for blind attachments to composite sub-structure or wherever the collar bears against a composite laminate.	
18	Use only titanium, Monel, Inconel, A286, PH13-8MO, PH17-4, MP159, or MP35N fasteners with carbon fiber composite laminates.	11.3.4 Corrosion Prevention
19	Aluminum, cadmium plated steel, or aluminum coated fasteners shall not be used with carbon fiber composites.	
20	Steel fasteners in contact with carbon fiber composites should be permanent and installed wet with sealant.	
21	Use a layer of fiberglass fabric as a galvanic corrosion barrier ply on faying surfaces of carbon fiber composite panels that are joined to aluminum.	
22	Paint or protective coating should be applied to both faying surfaces of mechanically attached carbon fiber composite panels to aluminum substructure.	

These composite joint guidelines are intended to supplement the metallic joint guidelines provided in Section 5.2.3.1 of PM4057 (Reference 11-1). Much of the discussion of metallic bolted joints is also applicable to composite bolted joints but specific items discussed within this section take precedence for composite bolted joints. Analysts should be familiar with the bolted joint concepts in both manuals.

11.3.1 Composite Bearing Strength: Guidelines 1-6

Guidelines 1 through 6 are related to the bearing strength capability of composite joint members. A discussion of the typical failure modes observed in composite bolted joints is provided in Section 11.4.1.

Guideline 1: Mechanically Fastened Composite Joints should be Bearing Critical

Wherever it is practical for a given set of joint design loads, mechanically fastened composite joints should be designed for bearing failure rather than for notched strength, shear tear-out or fastener strength in order to prevent catastrophic failure. The initiation of bearing failure tends to be localized with retention of residual load carrying capability up to a fastener pull through failure. Bearing margins are computed using the IDAT/IBOLT tool. Notched strength failures in particular can result in the release of a large amount of elastic energy which can propagate across a composite panel and trigger the catastrophic failure of major structural components.

Guideline 2: Laminates subject to bearing loads should be at least 40% ±45º plies, at least 8% 0º plies and at least 8% 90º plies. Ply dispersion should be maximized.

Laminates subject to bearing loads should have at least 40 percent ±45° plies; at least 8 percent 0° plies; and at least 8 percent 90° plies with maximized ply dispersion. These stacking sequence percentage guidelines will ensure adequate laminate bearing strength and will mitigate the risk of a laminate shear tear out or cleavage failure. A quasi-isotropic laminate is recommended for laminates that have significant biaxial loading. Additionally the IDAT/IBOLT composite joint analysis tool is limited to [0/±45/90] laminates based on the design of the failure algorithm.[1]

Bearing strength with tension reaction carpet plots for IM7/977-3 carbon/epoxy (RTA typical properties) are shown for tape and fabric in Figure 11.3-1 and 11.3-2, respectively. Note that the bearing strength reaches a maximum

[1] The development and correlation of the IDAT/IBOLT analysis tool has been based on test data for [0/±45/90] laminates. The expansion of the strength analysis tool to other laminate families would require modifications to the analysis tool and the generation of the joint related composite laminate test data for analysis correlation.

Copyright 2015 Lockheed Martin Corporation.
Note: The current version is always the version on the Lockheed Martin network.

above 50 percent ±45° plies; and begins to decrease rapidly below 40 percent ±45° plies. These same trends are also apparent for bearing with compression and shear reactions.

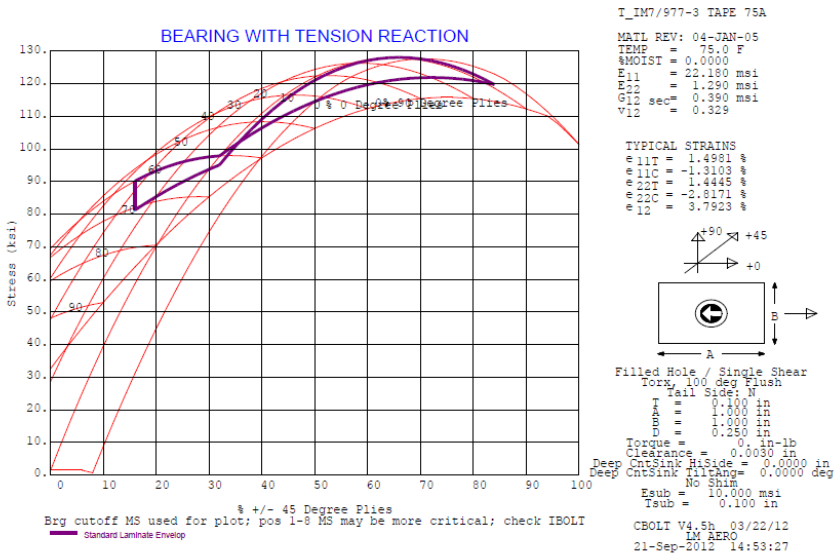

Figure 11.3-1 Sample Bearing with Tension Reaction Carpet Plot: IM7/977-3 Tape, RTA typical

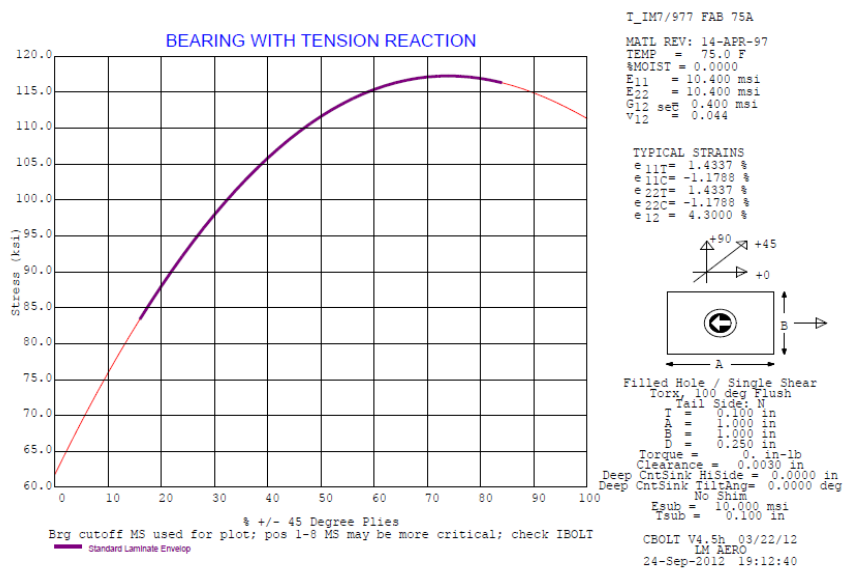

Figure 11.3-2 Sample Bearing with Tension Reaction Carpet Plot : IM7/977-3 Fabric, RTA Typical

<u>Guideline 3: Fastener Diameter to Laminate Thickness Ratio should be greater than 1: (D/t > 1)</u>

Fastener diameter to laminate structural thickness ratio for any given composite joint member should be greater than one ($D/t > 1$) or, alternately the laminate thickness to fastener diameter ratio should be less than 1 ($1 > t/D$). For single lap shear joints, as the laminate thickness increases the load transfer becomes more eccentric which results in increased peak bearing stress and fastener bending. Fastener bending also increases the peak bearing stress. Thus a larger fastener diameter is advisable.

Copyright 2015 Lockheed Martin Corporation.
Note: The current version is always the version on the Lockheed Martin network.

In single lap shear joints, D/t > 1.2 (or inversely, 0.83 > t/D) is preferred wherever possible because as the diameter-to-thickness (D/t) ratio decreases below 1.2, the peak bearing stress increases at a faster rate and the probability of a fastener failure increases. At D/t = 1, a fastener critical failure is almost a certainty. Exceptions can be made for low load transfer, multiple fastener joints where joint configuration is dictated by other considerations such as fuel sealing rather than by load transfer. In that event, the minimum D/t recommended is 0.67 or, alternately the maximum t/D is 1.5.

Guideline 4: Fastener Diameter to Total Joint Thickness Ratio Shall Not Exceed 3: $D/t_{total} \leq 3.0$
Total joint thickness, including all joint members and shim, shall not exceed 3D, where D is the fastener diameter. As discussed above, as the joint thickness is increased, the more that fastener bending can result in increased peaks in bearing stresses.

Guideline 5: Countersink Depth Should Not Exceed 80% of a Given Composite Joint Member
Design countersink depth should not exceed 80% of the nominal structural thickness of a composite joint member. The countersink depth, h, is shown in Figure 11.3-3. Fastener holes that are countersunk too deep can cause a knife edge condition which degrades bearing strength, reduces fastener pull-through strength, increases fastener-hole wear, and could possibly prevent the use of oversize fasteners for discrepant part disposition as it worsens the knife edge condition. A knife edge condition also creates a stress concentration in the laminate that can cause premature failure. IDAT/IBOLT issues a user warning when the countersink depth exceeds 80% of the laminate thickness.

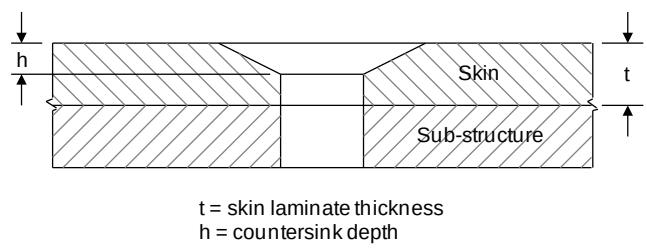

Figure 11.3-3 Countersink Geometry

Specific programs may implement additional countersink depth guidelines. Additionally, deviations from these guidelines may occur during discrepant part disposition. The IDAT/IBOLT tool can be used to assess the strength impact of specific dimensional or manufacturing imperfections.

Guideline 6: Use Caution when Increasing Laminate Thickness for Single Lap Shear Joints
As discussed in conjunction with Guidelines 3 and 4, the greater the laminate thickness in a single lap shear joint, the greater the load path eccentricity, bolt bending and bearing stress peaking. Thus caution is recommended in increasing laminate thickness for bearing strength of unsymmetrical single lap shear joints.

11.3.2 Composite Bolted Joint Geometry: Guidelines 7-11

Guidelines 7 through 11 define limits and guidance for joint design geometry. A discussion of joint geometric definitions and configurations is provided in Section 11.2.

Guideline 7: Fastener Edge (Side or End) Distance is no less than 2.5D: $e/D \geq 2.5$
The nominal fastener hole center-to-edge distance is a minimum of 2.5D, where D is the hole diameter. This guideline applies to either end- or side-edge distance as shown in Figure 11.2-1. Note that edge distance is based on the fastener hole diameter which can be significantly larger than the nominal bolt diameter particularly in interchangeable or replaceable doors or panels. Manufacturing tolerance and repairability must also be considered prior to specifying reduced edge distance in any design applications. See Section 2.4.3 for tolerance considerations.

Copyright 2015 Lockheed Martin Corporation.
Note: The current version is always the version on the Lockheed Martin network.

This requirement exists because notched strength of composite laminates is reduced as side-edge distance is reduced below 2.5D. In addition, composites lose bearing strength and shear tear-out strength with end-edge distance less than 2.5D.

Reduced edge distance may be acceptable for mitigating discrepant part dispositions. IDAT/IBOLT strength analysis should be used to substantiate deviations from the minimum or maximum edge distance guidelines.

Figure 11.2-1 shows a multiple fastener row joint. Note that the minimum spacing and end- and side-edge distances are the same as for single fastener rows.

Guideline 8: Fastener Spacing Distance is between 4D and 8D: $4 \leq s/D \leq 8D$

Fastener pitch should be no less than 4D and no greater than 8D in any direction. Note that bolt spacing is based on the fastener hole diameter which can be larger than the nominal bolt diameter. Fastener hole spacing requirements are defined for joint efficiency and can also be driven by fuel sealing, local buckling, and strength requirements.

As fastener spacing is reduced below 4D, stress concentrations due to the holes begin to interact, in-plane load carrying area is reduced, and the net tension failure can become the primary failure mode. In contrast, larger spacing decreases bearing strength due to a smaller total bearing area. Maximum fastener spacing in both directions should be less than 8D.

Guideline 9: Use 4D Fastener Spacing in Major Joints with Multiple Fasteners

Using analytical predictions, Hart-Smith (Reference 11-9) concluded that overall joint strength is maximized when fastener spacing is approximately 4D (D/w = 0.25) as shown in Figure 11.3-4. It is recommended that the minimum fastener spacing of 4D be used in highly loaded major joints for greatest efficiency.

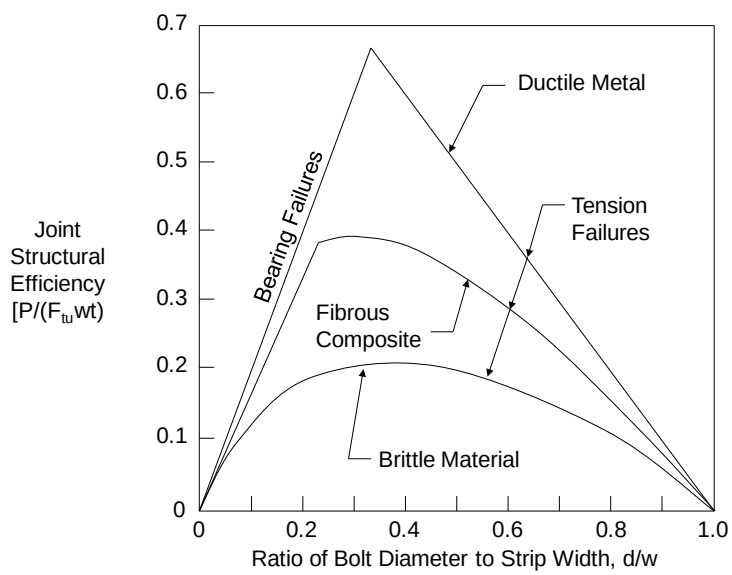

Reference 11-9

Figure 11.3-4 Relative Efficiencies of Bolted Joints in Ductile, Fibrous Composite, and Brittle Materials

Guideline 10: Multiple Fastener Rows should be used to React Significant Panel Moments

Multiple fastener rows are recommended along panel edges to react bending loads due to panel pressure and/or eccentric loading induced by single shear joints. This approach allows for membrane loads to develop in thin skins and allows for redundancy in reaction of the moments where flat plate bending is applicable.

Copyright 2015 Lockheed Martin Corporation.
Note: The current version is always the version on the Lockheed Martin network.

Guideline 11: Joint Designs Should Fall within the Limits of Existing Test Data
Remain cognizant that all joint designs fall within the range of materials, stacking sequences, laminate thicknesses and fastener diameters of existing strength test data. Since the bolt bending and notched composite strength analyses are empirically based this is imperative.

11.3.3 Composite Joint Fastener Selection: Guidelines 12-17

Guidelines 12 through 17 are related to the proper selection of fasteners for use in composite bolted joints.

Guideline 12: Fasteners should be Selected to provide Adequate Joint Fixity
Fastener hardware selection is particularly important for composite bolted joints. Hardware should be selected based on high head/tail fixity to reduce joint rotation and peak bearing stresses.

Fastener fixity refers to the degree of rotational restraint (or stiffness) that the fastener head and nut provides at each end of the fastener shank. The higher the rotational stiffness of the configuration, the more it will contribute to overall joint fixity. Fixity is a function of fastener stiffness, fastener fit, installation forces, installation torque and rotational resistance of the fastener head and the collar or formed backside. Fastener material and geometric stiffness relative to the stiffness of the members being joined influences how load is transferred through the joint. Low fastener stiffness can produce fastener bending and lower bearing strength in the joint and early failures of the fastener. Joint stiffness and bearing load distributions can be calculated using the IDAT/SS_JOINT tool (Reference 11-12) discussed in Section 11.4.4.5.

Fastener fit influences joint stiffness and, further, also affects joint rotation, load peaking, and bearing strength. As bolt-to-hole clearance increases, the reduction in bearing contact area resulting from increased clearance and fastener rotation leads to load peaking at the edge of the hole, thus generating a stress peak that causes bearing failure at a lower load level.

Fasteners designed for use in composite materials, having a larger contact area on the head and the collar or backside, are recommended to ensure the required rotational resistance is achieved while minimizing the damage potential to the laminate. Bearing loads on the fastener result in a net moment on the fastener that must be reacted by opposing moments at the head and tail. Each of these opposing moments are generated by a force couple composed of the shear and bending in the fastener and a prying load on the head or nut. Program allowable development programs should include joint testing with composite material fasteners installed per specification installation force, torque, and clearance.

Guideline 13: Specify Appropriate Fastener Torque
Reference 1, PM4057, Section 5.2.3.1.3 discusses the beneficial effect of preload which is achieved through proper bolt torque. PM4057 Section 5.5 provides a detailed discussion of bolt torque calculations and consideration. As with metallic joints, bolt torque is important to the structural integrity of composite joints. Appropriate fastener torque should be specified to develop full potential joint fixity. Care should be taken to use proper Lockheed Martin Aeronautics process specifications, which define installation forces and torque values specific to composite materials to ensure an installed fastener does not crush or deform the matrix material that binds fibers, thus reducing laminate integrity and pull-through resistance.

Guideline 14: Only Tension Head Countersunk Fasteners should be used in Composite Bolted Joints
Shear head countersunk fasteners do not provide appropriate fixity for laminated composite joints, thus, only tension head countersunk fasteners should be used in composite joints. Fastener head type also influences countersunk hole geometry and thus pull-through and interlaminar shear strength. Tension head 100°countersunk fasteners should be used because the projected area of the tension head fastener is larger than that of a shear head countersunk fastener. The larger area improves pull-through and delamination resistance in composites, while reducing overturning forces from bolt bending. These fasteners are also recommended for double lap shear joints.

Copyright 2015 Lockheed Martin Corporation.
Note: The current version is always the version on the Lockheed Martin network.

Caution should be observed in the use of 130° countersunk head fasteners. Although this fastener increases the pull through load bearing area and permits it to be used in thin laminates, the resistance to prying moments can be adversely affected resulting in early failures of the fastener head.

Guideline 15: Do Not Use Driven or Bucked Fasteners in Composite Bolted Joints

Do not specify vibration drive fasteners, solid rivets, or expanding fasteners in mechanically fastened composite joints due to risk of damage during installation. Composite material properties are sensitive to impact damage, a source of which is manufacturing processes such as bucking or driving fasteners. Additionally, expansion of the diameter of a rivet as it is driven damages fibers at the hole. In order to prevent potential damage to composite laminates, fastener types, including rivets and conventional enlarged end blind fasteners, that must be bucked or driven for proper installation should not be used with composite structures. Fasteners designed for use in composite materials should always be used.

Additionally, exercise caution when using Lockbolts or other pull-type fasteners that can generate appreciable dynamic loads in certain composite applications. Without proper process control, delaminations can occur during such fastener installations.

Guideline 16: Close Fit Fastener Hole Tolerance is Recommended for Composite Bolted Joints

Classes of fastener fit are discussed in Section 5.2.3.1.2 of Reference 11-1. Close fit holes in composites are required to achieve the highest possible static load and joint fatigue life. Although close tolerance fit fasteners are desirable for use with composites, interference fit fasteners cannot, in general, be used due to potential delamination or crushing of fibers at the fastener hole, as shown in Figure 11.3-5.

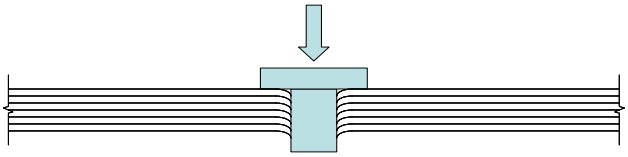

Reference 11-13

Figure 11.3-5 Hole Damage Caused by Interference Fit Fastener in Laminated Composite Part

In general, use close tolerance fit holes for structural composite joints. This is defined as a diametric bolt-to-hole clearance of -0.000 to +0.004 inches. Looser fits may be suitable in non-structural removable panels and non-structural joints as described in Section 5.2.3.1.2 of Reference 11-1.

Guideline 17: Use Fasteners Designed for Use with Composites

Use fasteners designed for composite installation for blind attachments to composite substructure or wherever the collar bears against a composite laminate. Do not install blind fasteners in oversize holes since the formation of the tail can malfunction if the hole is oversize and cause delamination or crushing of the laminate. This is shown in Figure 11.3-6.

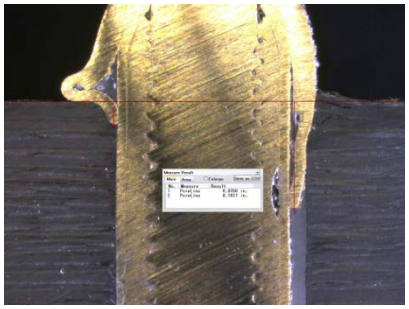

Figure 11.3-6 Cross Section (20X magnification) of Blind Fastener Installed in Second Oversized Hole

Copyright 2015 Lockheed Martin Corporation.
Note: The current version is always the version on the Lockheed Martin network.

Fasteners designed for use in composite materials, having a larger contact area on the head and the collar or backside, should be used in composite joints. These fasteners should prevent damage to the composite laminate from locking collars and will improve clamp-up, bearing, and pull-through strengths over smaller contact fasteners. Use a washer under a collar or a wide bearing head or tension protruding head fastener to ensure adequate pull-through strength.

11.3.4 Corrosion Prevention: Guidelines 18-22

Galvanic corrosion occurs when two metals or alloys having different compositions are electrically coupled while exposed to an electrolyte such as humid, salty air. A galvanic couple exists when two metals are connected electrically in an electrolyte fluid wherein one metal becomes an anode and corrodes, while the other metal acts as a cathode. Large differences in electric potential between joint materials in the presence of an electrolyte can therefore result in galvanic corrosion.

A ranking of the relative reactivity of common engineering materials in sea water is provided in Table 11.3-2. Corrosion potential is minimal for material within the same electromotive group. Pairing materials from widely separated electromotive groups without significant protection can be catastrophic. Reference 11-1, PM4057 Section 3.4 has an extensive discussion of all types of corrosion and a more comprehensive table. PM4057 Section 3.4.8 discusses galvanic corrosion.

Table 11.3-2 Galvanic Resistance of Common Materials in Order of Electric Potential

Active (Anodic or Least Noble)		
Material or Alloy	**Electromotive Group**	**Specific Alloy, if applicable**
Magnesium and Magnesium Alloys	I	AZ-31B; HK-31A
Aluminum Alloy	II	Al 7072 clad on 7075; Al 2014-T3; Al 1160-H14; Al 7079-T6
Cadmium	II	
Mild Steel	II	
Aluminum Alloy	II	Al 218 (die cast); Al 5052-0; Al 5052-H12; Al 5456-0, H353; Al 5052-H32; Al 6061-T6; Al 7075-T6; Al 6061-0
Aluminum Alloy[1]	III	Al 2014-0; Al 2024-T4; Al 5052-H16
Nickel	III	plated
Chromium	III	plated
Stainless Steel	IV	310 (active), 301 (active), 304 (active), 430 (passive), 410 (passive), PH15-5Mo (Active), 17-7PH (active), A-286
Stainless Steel	IV	321 (active), 316 (active), 17-7PH (passive), PH15-5Mo (passive) 304 (passive), 301 (passive), 321 (passive), 201 (passive), 286 (passive), 316L (passive), AM355 (active), 202 (active), Carpenter 20 (passive), AM350 (passive), A286 (passive), Monel, MP35, MP159
Titanium Alloy[1]	IV	5A1-2.5 Sn; 6AL-4V (STA); 6AL-4V (annealed)
Silver	V	
Gold	V	
Graphite	V	
Least Active (Cathode or Noble)		

Table 11.3-2 shows that the three materials commonly used in aircraft construction: carbon, steel and aluminum, have large differences in electric potential. This can result in galvanic corrosion between conductive carbon fiber

[1] In actual practice, test, and aircraft structure aluminum and titanium are much more compatible than this table would imply due to active titanium being reported. However, since titanium rapidly oxidizes, passive titanium has an EMF that puts it in close proximity with aluminum. Appropriate protective coatings should be used.

Copyright 2015 Lockheed Martin Corporation.
Note: The current version is always the version on the Lockheed Martin network.

composite laminates and fasteners and/or substructure made from certain metals, including aluminum, aluminum alloys, low alloy steels, martensitic stainless steels, and magnesium alloys. Conventional plating materials on these materials are insufficient to prevent galvanic corrosion due to rapid deterioration of the plating. Fasteners made of these materials should be avoided or wet installed with reliable corrosion inhibiting-coatings in accordance with applicable Lockheed Martin Aeronautics material and process specifications. Such corrosion-inhibiting coatings may be used with recommended fastener materials as well. Also note that cadmium plated steel fasteners shall not be used in carbon fiber laminates.

Guideline 18: Use only titanium, Monel, Inconel, A286, PH13-8MO, PH17-4, MP159, or MP35N fasteners with carbon fiber composite laminates.
This guideline specifies the fastener materials that are acceptable for use based on their galvanic resistance in mechanically fastened joints with carbon fiber composite members. Titanium fasteners are preferred. Stainless steel fasteners are acceptable in a low corrosion environment only.

Guideline 19: Aluminum, cadmium plated steel, or aluminum coated fasteners shall not be used with carbon fiber composites.
Based on their galvanic potential relative to carbon fiber composites, the fastener materials and coatings specified above should not be used in mechanically fastened joints with carbon fiber composite members.

Guideline 20: Steel fasteners in contact with carbon fiber composites should be permanent and installed wet with sealant.
The permanent wet installation of steel fasteners with sealant is intended to provide a galvanic barrier between the steel fastener and carbon fiber composite.

A286 and PH13-8MO CRES alloys and some other austenitic and semi-austenitic alloys are acceptable in many environments. However, in a severe marine or industrial corrosion environment, such as might be found in aircraft fuel tanks, sump areas, gear bays, or other bays exposed to the environment, superficial rusting and staining develops on the fastener that, while usually objectionable, has not been connected to loss of fastener integrity.

In all cases, Lockheed Martin Aeronautics Materials and Processes personnel should be consulted when composite structural designs using fasteners of non-recommended materials are being considered.

Guidelines 21 and 22 describe recommended guidelines for the use of protective fabric barrier plies and coatings at fay surfaces to prevent direct contact between carbon fiber composites and aluminum substructure.

Guideline 21: Use a layer of fiberglass (0.005 inch minimum) on faying surfaces of carbon fiber composite composite panels that are joined to aluminum.
A fiberglass fabric ply or group of plies is recommended as a corrosion barrier to separate the carbon fiber composite layers from direct (fay surface) contact with the aluminum substructure.

Guideline 22: Paint or protective coating should be applied to both faying surfaces of mechanically attached carbon fiber composite panels to aluminum substructure.
A fiberglass ply or group of plies is recommended as a corrosion barrier but adhesive, liquid shim, sealant or paint can also be used in certain situations. Lockheed Martin Aeronautics Materials and Processes personnel should be consulted when alternative corrosion barrier materials are being considered.

11.4 Basic Theory

This section provides an overview of the basic theory that is used for strength analysis of mechanically fastened composite joints. Section 11.4.1 begins with a discussion of the failure modes that are typically observed in composite bolted joints. The section describes the importance of predicting laminate net-section and bearing strength as these are the primary failure modes for composite bolted joints.

Copyright 2015 Lockheed Martin Corporation.
Note: The current version is always the version on the Lockheed Martin network.

Section 11.4.2 describes the prediction of stresses in laminated composite joints. Closed-form two-dimensional elasticity solutions have been developed for infinite homogenous, anisotropic plates with elliptic or circular holes subjected to in-plane membrane loads and a bearing load distribution at the hole boundary. The influence of finite plate geometry can be accounted for using boundary integral solutions. Other effects such as bending, filled holes, environment, countersink, hole clearance and fastener torque can be accounted for analytically and through empirically based correction factors.

Section 11.4.3 describes the failure criteria used for the prediction of laminate net-section failure. Two effective laminate failure criteria are presented that have been successfully used for composite bolted joint strength analysis. These include a fracture mechanics based approach that is the basis for the Lockheed Martin IBOLT (Interactive BOLTed Joint) strength analysis, and a point stress (or strain) fracture criteria that has been used by the BJSFM (Bolted Joint Stress Field Model) strength analysis as well as an effective criterion for composite cutouts in general. Section 11.4.4 concludes with a theoretical overview of the Lockheed Martin IBOLT strength analysis methodology.

11.4.1 Laminate Strength Failure Modes

Laminate strength failure modes that are observed experimentally in composite bolted joints are dependent upon many factors. These factors include joint configuration (single lap shear, double lap shear, multilayer), fastener type (protruding head, flush head), joint geometry, loading, laminate ply percentage and stacking sequence. The potential failure modes observed in composite bolted joints are described below and shown in Figure 11.4-1.

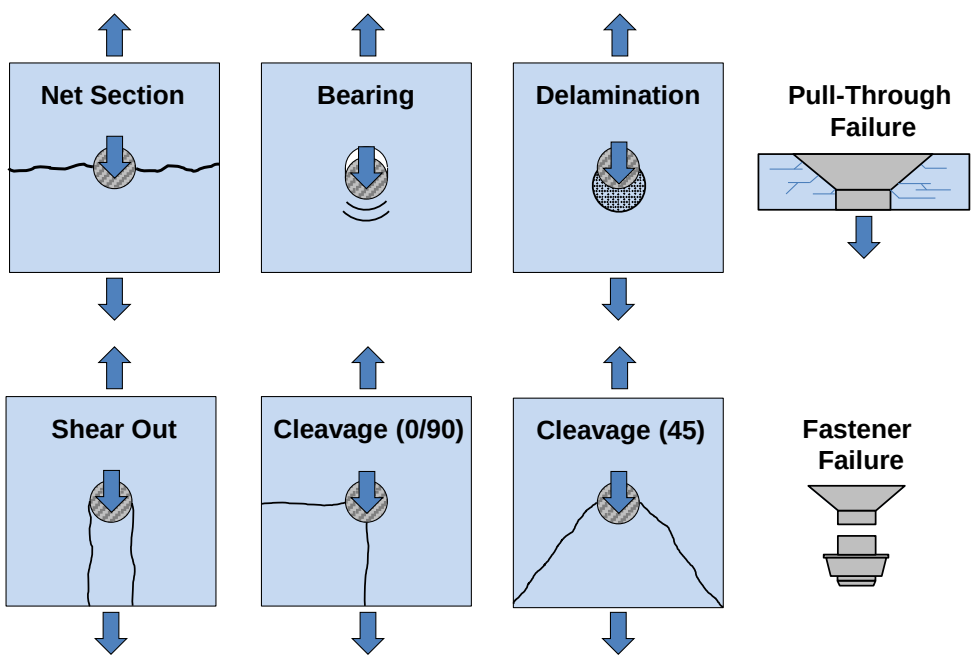

Figure 11.4-1 Potential Failure Modes in Mechanically Fastened Composite Joints

Net section failure – Net section failures are fiber dominated failures that occur at a peak circumferential stress location along the hole edge. These failures typically occur in locations where the loaded fiber is tangential to the hole edge. The peak stress causing fiber failure may be in tension or compression and its location is depending upon the stacking sequence and loading conditions. Net section failures occur under high bypass loading conditions or when the bolt diameter is large compared to the laminate width.

Copyright 2015 Lockheed Martin Corporation.
Note: The current version is always the version on the Lockheed Martin network.

Bearing failure – Bearing stresses are caused by fastener bearing loads transferred to the laminate along the hole boundary. Bearing failure initiates when these stresses exceed the laminate strength. The initiation of bearing failure is complex and can be a combination of local fiber failures, matrix cracking and delamination between layers. The failure location is usually centered on the peak of the bearing load distribution along the hole perimeter. However, the distribution of bearing stresses can vary significantly through the depth of the laminate thickness. This topic will be treated in greater detail later within this section.

Delamination failure – Delaminations that initiate at or near hole edges can be caused by bearing stresses, laminate bending or pull through loads. The initiation of a delamination is caused by high localized interlaminar stresses. High interlaminar stresses can arise directly from out-of-plane loads (tension or shear) or indirectly from a mismatch in material properties between adjacent layers reacting to in-plane loads and bending. Peak in-plane stresses that are the result of bearing or bending loads can result in the initiation of delaminations as adjacent layers separate under the action of high local interlaminar stresses. Since three-dimensional (3-D) interlaminar stress fields are complex and difficult to predict with accuracy, and the delaminations are considered secondary to the primary failure modes of bearing, bending or pull-through, failure prediction models focus on the primary failure modes.

Pull through failure – A fastener pull through failure occurs when the fastener tension load causes the fastener to be partially or completely pulled through the composite laminate. This failure mode is usually the result of a high fastener "pull off" or "pull through" load such as that caused by normal panel pressure reacted at a substructure spar or rib attachment. The strength analysis for a fastener pull through failure mode is discussed in Section 11.5.3. A pull-through failure mode may also occur as a secondary failure mode after severe bearing damage has occurred and the fastener begins to rotate under loading, particularly for single lap shear joints where a high degree of joint rotation can occur.

Shear out failure – Shear out failures can be considered as a special case of bearing failure and usually occur in joints with short edge distance and/or within highly orthotropic laminates. Shear out failures can be mitigated by following Guidelines 2 and 7 in Table 11.3-1.

Cleavage failure – Cleavage-tension failures are similar to the shear out failures in that they are usually the result of short edge distance and/or highly orthotropic laminates. These failures initiate at the hole and then propagate catastrophically to the nearest edges. The failures propagate along the weak directions of the laminate such as along the 0/90 or +45/-45 directions shown. As with shear out failures, cleavage failures can be mitigated by following Guidelines 2 and 7 in Table 11.3-1.

Bolt failure – Fastener failure modes can vary greatly and may be the result of insufficient fastener static strength or fatigue loading. The static strength and fatigue analysis for fasteners are discussed in Section 11.5.5.

Summarizing the above discussion, the primary failure modes for laminate strength in bolted composite joints are net section and bearing failures. Shear out and cleavage-tension failure modes can be eliminated through good laminate design practice. In the absence of fastener tension loads that can be analyzed using the method of Section 11.5.3, fastener pull through can be considered a secondary failure mode that follows bearing failure. Similarly, fastener failure can be analyzed using the methods of Section 11.5.5.

Composite bolted joints exhibit two distinct types of load versus deflection behavior when loaded to static failure under either combined bearing-bypass loading or pure bearing loading. The load versus deflection response for net section failure under combined bearing-bypass loading is nearly linear to failure exhibiting brittle fracture behavior with little to no yielding or plastic deformation. The load versus deflection behavior for bearing failure, however, displays significant non-linearity very similar to that of a metal-to-metal joint. A typical load-deflection curve for bearing failure in a composite laminate is shown in Figure 11.4-2.

Copyright 2015 Lockheed Martin Corporation.
Note: The current version is always the version on the Lockheed Martin network.

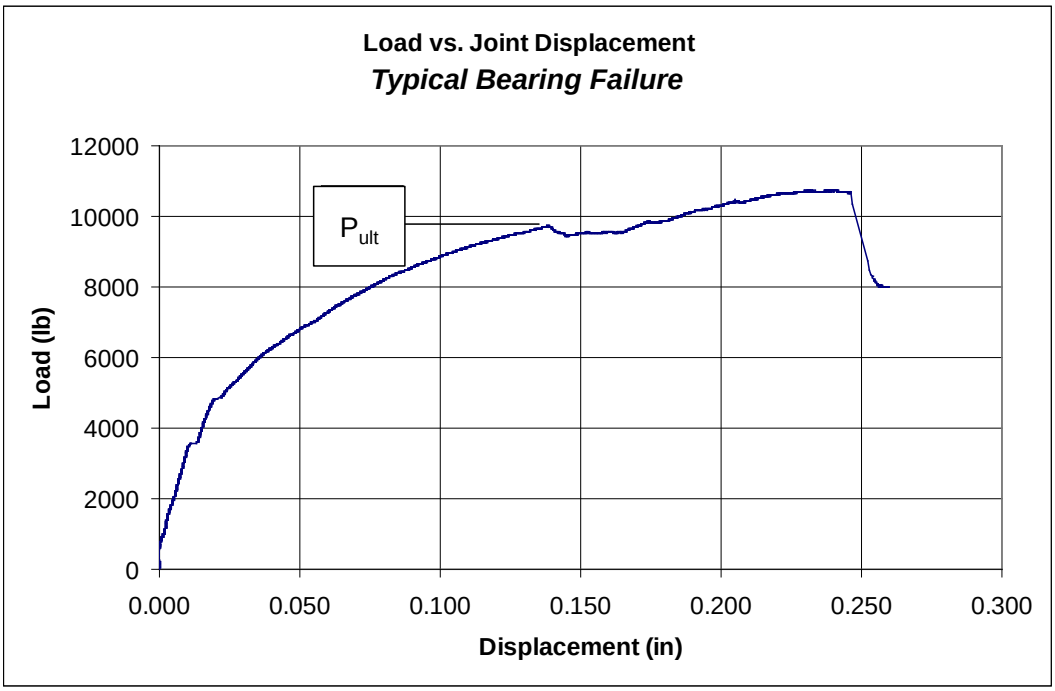

Figure 11.4-2 Typical load-deflection curve for bearing failure

The objective of developing an analytical approach for predicting laminate bolted joint strength may be summarized as follows:

- Determine the laminate stress state when subjected to fastener bearing loads and far-field stresses
- Develop an empirically based failure criteria that characterizes both net-section and bearing failure

The next two sections will focus on the prediction of stresses in composite bolted joints and the failure criteria for laminate net-section and bearing failure modes.

11.4.2 Stresses in Anisotropic Plates with Circular Holes

Closed form analytical solutions for stresses in homogenous, anisotropic infinite plates with elliptical holes have been developed from anisotropic elasticity (References 11-14, 11-15, 11-16). The solutions are based on the assumption of generalized plane deformation which reduces to a two-dimensional problem that is solved using complex stress functions.

Key features of the solution are summarized:

- Homogenous, anisotropic infinite plate with an elliptical hole
- Assumed generalized plane deformation reduces to a two-dimensional boundary value problem
- Lekhnitskii complex stress function approach is used to obtain a series solution
- 4th order characteristic equation is obtained with complex roots

Copyright 2015 Lockheed Martin Corporation.
Note: The current version is always the version on the Lockheed Martin network.

Closed form elasticity solutions have been determined for a number of loading conditions including the following conditions applicable to strength analysis of composite bolted joints:

- Uniaxial tension loading at an angle to the principal direction of the plate (Figure 11.4-3)
- Bearing load distribution which is assumed to be a radial cosine load distribution, $P_r = P\cos\theta$

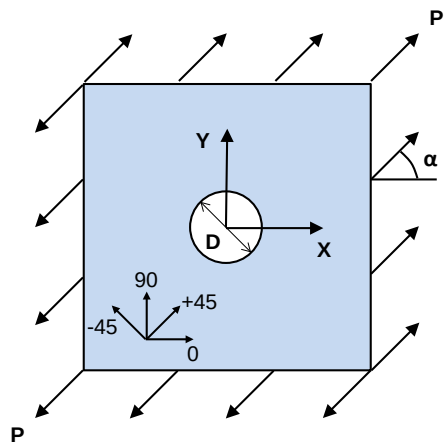

Figure 11.4-3 Uniaxially Loaded Anisotropic Infinite Plate with a Circular Hole (Reference 11-17)

Solutions for uniaxial loading at various orientations can be superimposed to obtain a general solution for combined in-plane far-field loading: NX, NY, and NXY. The closed form solution for an anisotropic infinite plate with an elliptical or circular hole subjected to combined loads is available in the IDAT/CUTOUT computer program. The program also supports the strength analysis of metallic or composite doubler reinforcement of the holes.

As shown in Figure 11.4-4, the combined in-plane loading solution can be superimposed with the bearing load solution along the hole boundary to obtain the full two-dimensional stress state for a composite bolted joint.

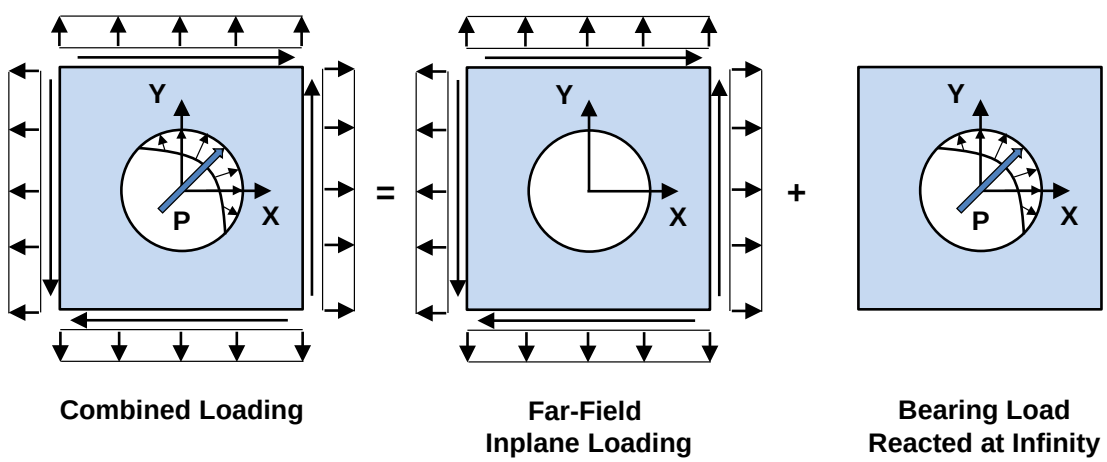

Figure 11.4-4 Superposition of Anisotropic Elasticity Solutions for Bolted Joint Analysis (Reference 11-17)

Copyright 2015 Lockheed Martin Corporation.
Note: The current version is always the version on the Lockheed Martin network.

Although the stress solutions are relatively complex, useful expressions can be obtained at the hole boundary. The stress concentration factor at the hole boundary is defined in Equation 11.4-1 and is illustrated in Figure 11.4-5. The stress concentration factor, K_{TX}, at a given position θ on the hole boundary is defined as the ratio of the local tangential (or circumferential) stress σ_θ to the far-field applied stress σ_{TX}.

$$K_{TX} = \frac{\sigma_\theta}{\sigma_{TX}} = \frac{\sigma_{Local}}{\sigma_{Far-field}}$$ **Equation 11.4-1**

Where
σ_θ, σ_{Local} = local tangential or circumferential stress (psi)
σ_{TX}, $\sigma_{Far-field}$ = Far-field applied stress (psi)

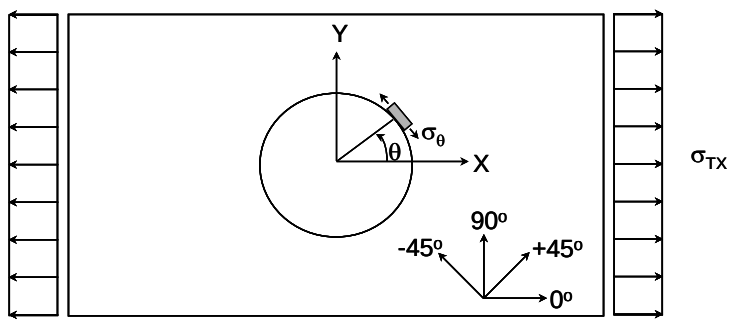

Figure 11.4-5 Circumferential stress along a hole edge in an anisotropic plate subjected to uniaxial loading

Equation 11.4-2, Equation 11.4-3, and Equation 11.4-4 provide simple formulas for the stress concentration factor K_{TX} for an orthotropic, infinite plate loaded in the X-direction as shown in Figure 11.4-5.

$$K_{TX} = \frac{E_\theta}{E_X}\left[-\sqrt{\frac{E_X}{E_Y}}\cos^2\theta + (1+n)\sin^2\theta\right]$$ **Equation 11.4-2**

Where
θ = angular position on hole boundary (deg)
E_X, E_Y = laminate x-and y-direction stiffnesses (psi)
E_θ is given in Equation 11.4-3 (psi)
n is given in Equation 11.4-4

$$E_\theta = \left[\frac{\sin^4\theta}{E_X} + \left(\frac{1}{G_{XY}} - \frac{2\cdot\nu_{xy}}{E_X}\right)\sin^2\theta\cos^2\theta + \frac{\cos^4\theta}{E_Y}\right]^{-1}$$ **Equation 11.4-3**

Where
G_{XY} = laminate in-plane shear stiffness (psi)
ν_{XY} = laminate in-plane Poisson's ratio

$$n = \sqrt{2\cdot\left(\sqrt{\frac{E_X}{E_Y}} - \nu_{xy}\right) + \frac{E_X}{G_{XY}}}$$ **Equation 11.4-4**

Copyright 2015 Lockheed Martin Corporation.
Note: The current version is always the version on the Lockheed Martin network.

Note that for θ = 90°, the equation for K_{TX} simplifies to:

$$K_{TX} = n + 1$$ **Equation 11.4-5**

As a comparison, the circumferential stress for a uniaxially loaded infinite isotropic plate with a circular hole (hole radius = *a*) is given by:

$$\sigma_{\theta(Isotropic)} = \frac{\sigma_{TX}}{2}\left(1+\frac{a^2}{r^2}\right) - \frac{\sigma_{TX}}{2}\left(1+\frac{3a^4}{r^4}\right)\cos 2\theta$$ **Equation 11.4-6**

As seen in the equations above, the stress concentration factor is a strong function of position on the hole boundary denoted by θ. The stress concentration factor at a given value of θ is also highly dependent on the percentage of 0, ±45, and 90-degree plies as shown in Figure 11.4-6 for three different laminates. The angle θ is measured positive counterclockwise from the x-axis where the x-axis is parallel to the 0-degree ply direction. Laminate ply percentages are defined by (XX/YY/ZZ) where XX is the percent of 0-degree plies, YY is the percent of ±45-degree plies, and ZZ is the percentage of 90-degree plies.

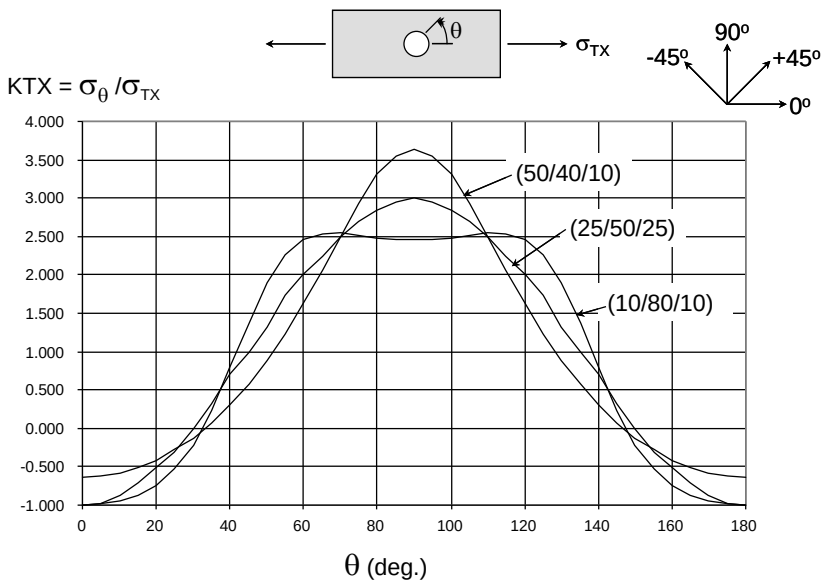

Figure 11.4-6 Stress Concentration Factor (K_{TX}) Variation Due to Percentage of Plies

The stress concentration factor is also a strong function of the type of applied loading. Figure 11.4-7 shows the variation of stress concentration factor with position θ for three different types of applied loading. σ_{TX} is a constant membrane stress applied in the x-direction, σ_{TY} is a constant membrane stress applied in the y-direction, and τ_{XY} is a constant shear stress. In IBOLT terminology, these are SIGTX, SIGTY, and SIGTXY and are applied as shown.

Copyright 2015 Lockheed Martin Corporation.
Note: The current version is always the version on the Lockheed Martin network.

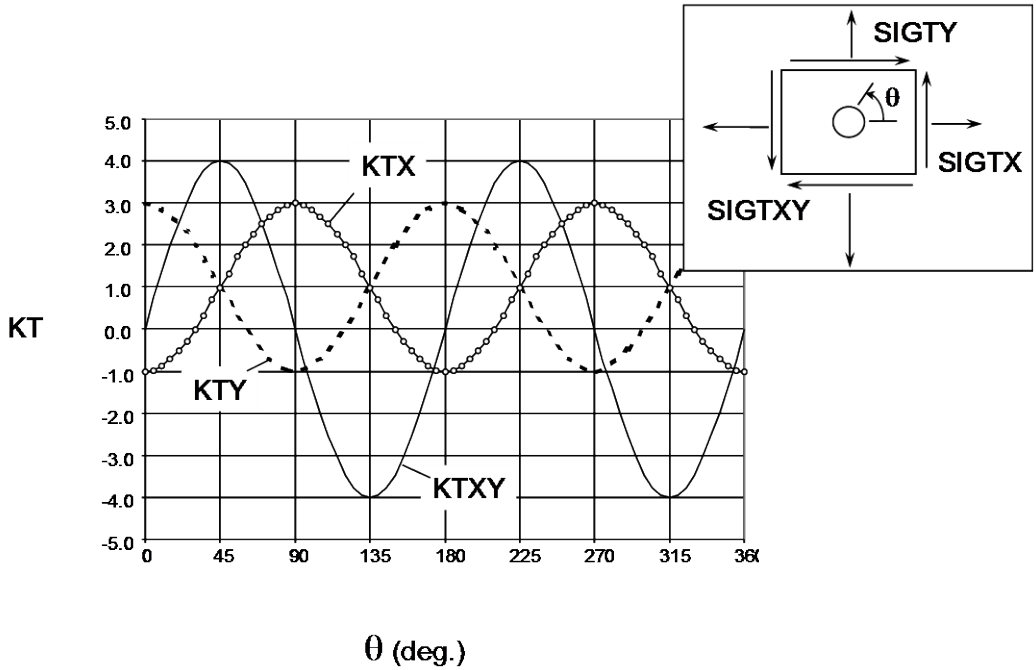

Figure 11.4-7 Stress Concentration Factor Variation Due to Type of Loading

Closed form equations from Reference 11-14 are available for calculating the values of KTX, KTY, and KTXY for orthotropic laminates. These equations can be derived through load case superposition using the equations above. These solutions, however, are valid only for infinite plates with an elliptic or circular hole, plates which have length and width dimensions very much larger than the diameter of the hole. The analysis of composite bolted joints must account for additional effects of the following:

- Environmental effects of temperature and moisture on material properties (stiffness, strength)
- Corrections for finite plate geometry
- Single and double lap shear joint configurations
- Countersink
- Filled holes
- Bending
- Fastener Installation Torque (clamp up)
- Fastener-to-Hole Diameter Clearance

The discussion of these factors will be deferred to Section 11.4.4 as part of the IBOLT Methodology Overview.

11.4.3 Failure Criteria

One failure characteristic of composite laminates containing holes is a sensitivity to the hole diameter. For a constant width-to-hole diameter ratio, the net-section tension strength of notched laminates varies with hole size as shown by the example in Figure 11.4-8. As the hole becomes very small, the strength approaches the unnotched laminate tension strength. This variation of notched strength with hole size is also observed for compression loading. This variation with hole size is also observed for bearing strength as shown in Figure 11.4-9.

Copyright 2015 Lockheed Martin Corporation.
Note: The current version is always the version on the Lockheed Martin network.

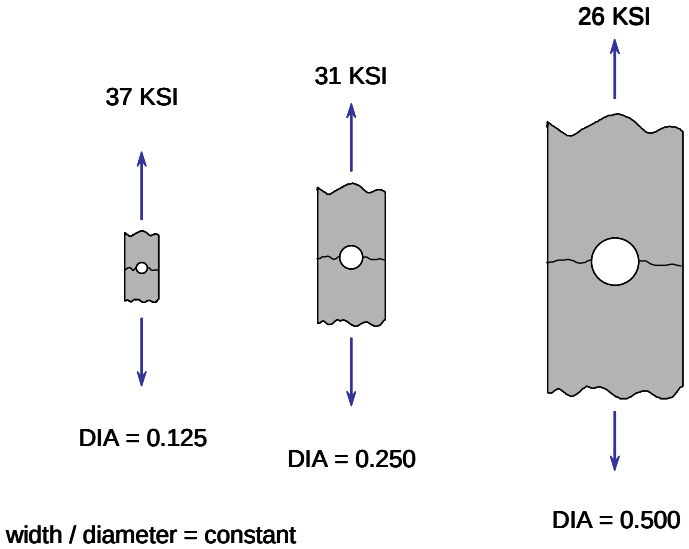

Figure 11.4-8 Laminate Net Section Tension Strength Variation with Hole Diameter

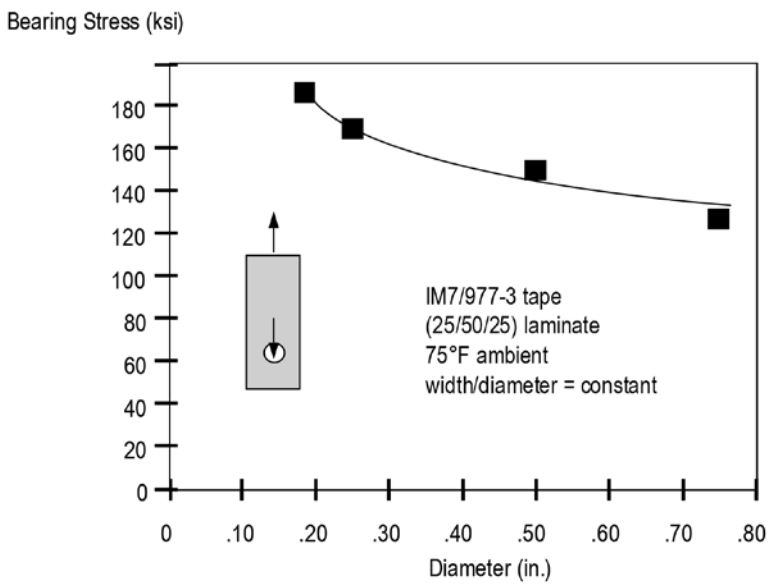

Figure 11.4-9 Laminate Bearing Strength Variation with Hole Diameter

Conventional strength-based failure theories are not applicable for this type of behavior. Two common strength-based failure models are shown in Figure 11.4-10. For ductile materials, the net section stress at failure is equal to the unnotched strength. For a constant width-to-hole diameter ratio, the value of remote stress at failure is then a constant value. For brittle materials, the far-field stress at failure would be equal to the unnotched strength divided by the elastic stress concentration factor at the critical location – on the hole boundary at the narrowest section. This also provides a constant value of remote stress at failure as indicated by the lower horizontal line in Figure 11.4-10. Neither of these criteria show a variation in strength with hole diameter as observed in the test data.

Copyright 2015 Lockheed Martin Corporation.
Note: The current version is always the version on the Lockheed Martin network.

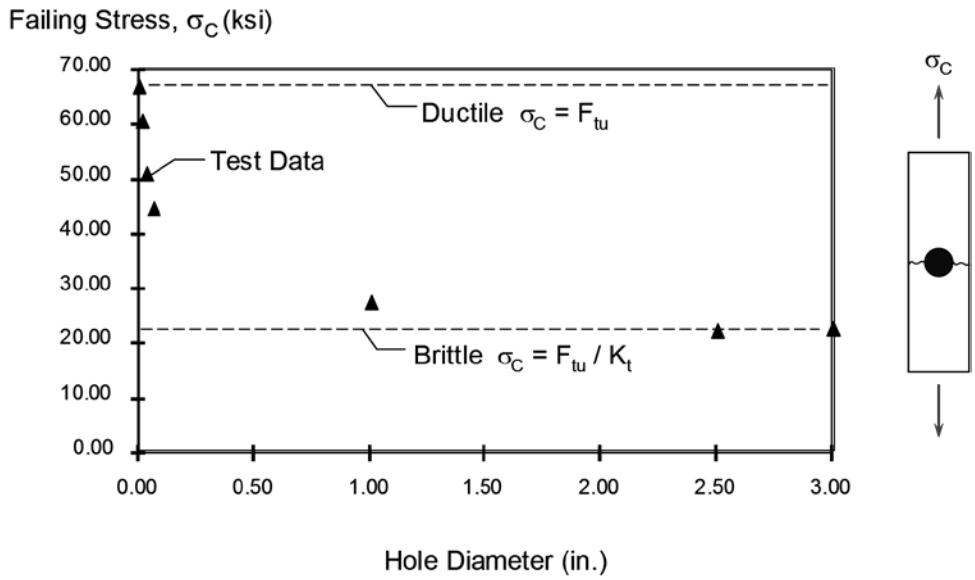

Figure 11.4-10 Strength-Based Failure Models

The next section presents two approaches to accounting for notch sensitivity in predicting the net section strength of composite laminates. The two approaches are:

- A Fracture Mechanics Based Approach (used for the IBOLT analysis methodology)
- Point Stress (or Strain) Fracture Criteria

The discussion of bearing failure and bearing-bypass interaction is deferred until the IBOLT methodology discussion in Section 11.4.4

11.4.3.1 Fracture Mechanics Based Approach

Waddoups, Eisenmann and Kaminski (Reference 11-18) proposed a linear elastic fracture mechanics (LEFM) based approach for defining a failure criterion. Bowie (Reference 11-19) developed a solution for the stress intensity factor, K_I, for the problem of symmetric edge cracks originating from a circular hole in a homogenous, isotropic plate subjected to uniaxial tension loading (Figure 11.4-11).

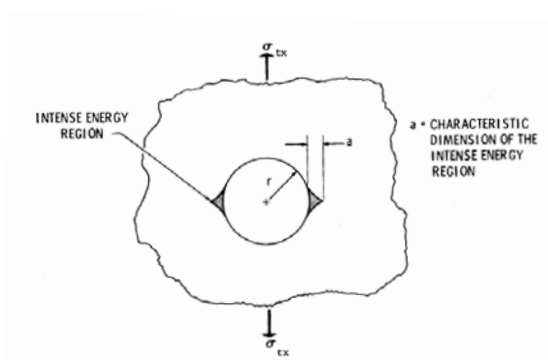

Figure 11.4-11 Fracture Problem of Edge Cracks Originating from a Circular Hole in an Isotropic Plate

Copyright 2015 Lockheed Martin Corporation.
Note: The current version is always the version on the Lockheed Martin network.

As shown in Figure **11.4-12**, it was observed that the Bowie solution utilized a curve that had a shape similar to the notch sensitivity exhibited by composite laminates.

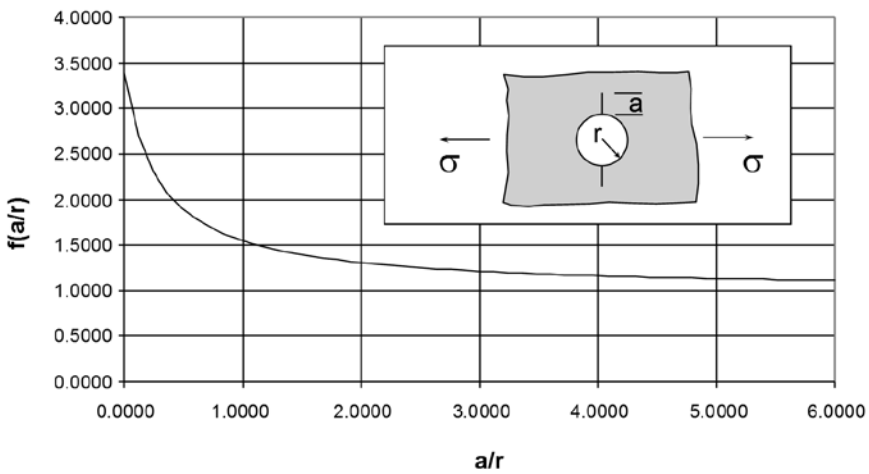

Figure 11.4-12 **Bowie Solution Has Same Shape as Bearing Strength Variation**

This solution provides values of the function *f(a/r)*, which is dependent on *a/r*, where *a* is the length of each edge crack, *r* is the radius of the hole, and K_I is the stress intensity factor as given in Equation 11.4-7.

$$K_I = \sigma\sqrt{\pi a}\, f\left(\frac{a}{r}\right) \qquad \text{Equation 11.4-7}$$

Where
K_I = stress intensity factor (psi-in$^{1/2}$)
σ = applied far-field stress (psi)
a = length of each edge crack (in)
f(a/r) = Bowie's function; serves as an effective stress concentration factor that incorporates the effects of both hole size (*r*) and a fixed effective flaw size (*a*)

In order to apply a fracture mechanics based failure theory to composite laminates, it must be understood how fracture mechanics can be used to predict static strength. An overview of basic fracture mechanics is shown in Figure 11.4-13. The stress intensity factor is given in Equation 11.4-8.

$$K_I = \sigma\sqrt{\pi a}\,\beta \qquad \text{Equation 11.4-8}$$

Where
β = a function that accounts for the effects of crack and coupon geometry

As the applied stress is increased, the stress intensity factor K_I increases proportionally. As the value of K_I reaches its critical value K_{IC}, failure occurs. The value of applied stress at failure is denoted by σ_C, the critical stress. Each of the coupon geometries shown has a corresponding geometry function, β.

Copyright 2015 Lockheed Martin Corporation.
Note: The current version is always the version on the Lockheed Martin network.

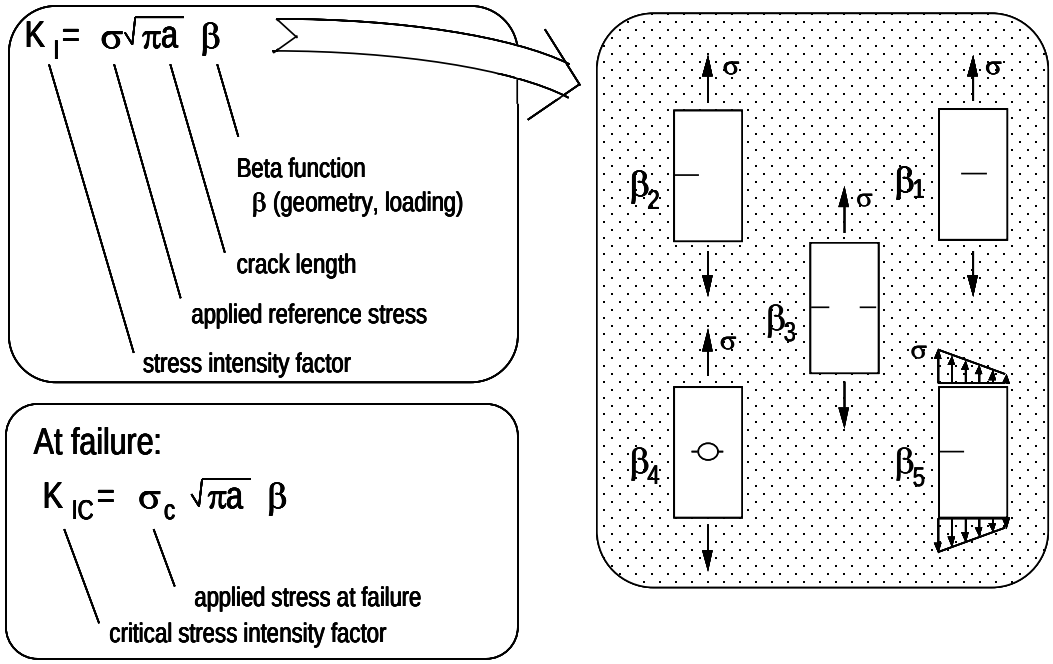

Figure 11.4-13 Basics of Fracture Mechanics

The application of the Bowie solution to a composite coupon is described as follows. Two composite laminate uniaxial tension coupons are shown in Figure 11.4-14, one without a notch (a) and one with a notch (b) or circular hole. Failure occurs in the unnotched coupon when the applied far-field stress σ meets the critical applied stress, F_{tu}. Similarly, the notched coupon fails when the applied far-field stress σ meets the critical applied stress, σ_C. For the notched coupon with a circular hole as shown in Figure 11.4-14 (b), *f(a/r)* is substituted for β in Equation 11.4-8 giving the stress intensity factor previously shown in Equation 11.4-7.

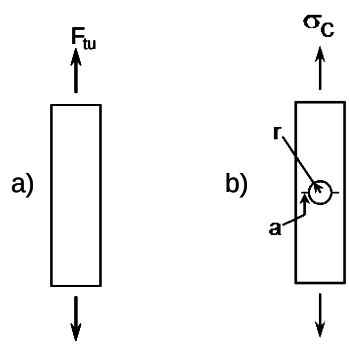

Figure 11.4-14 Failure Condition for Composite Tensile Coupon: Unnotched (a) and Notched (b)

In applying the Bowie solution to a composite coupon with a hole without edge cracks, it is assumed that the crack length is an inherent material property at that point and has a constant value. A solution is sought that is capable of predicting failure for all hole diameters and which converges to the unnotched tension strength as the hole diameter approaches zero. For this condition, the geometry function *f(a/r)* approaches 1.00 as *r* approaches 0.0 as shown previously in Figure **11.4-12**. Therefore, for an unnotched tensile coupon at failure, the Bowie solution for stress intensity given in Equation 11.4-7 becomes Equation 11.4-9.

Copyright 2015 Lockheed Martin Corporation.
Note: The current version is always the version on the Lockheed Martin network.

$$K_{IC} = F_{tu}\sqrt{\pi a}$$ Equation 11.4-9

Where
F_{tu} = laminate unnotched tension strength (psi)

For the case of a tensile coupon with a hole at failure, the Bowie solution for stress intensity is:

$$K_{IC} = \sigma_c \sqrt{\pi a}\, f(a/r)$$ Equation 11.4-10

Where
σ_c = critical applied stress at failure (psi)

Setting these two expressions equal to each other gives:

$$\sigma_c = \frac{F_{tu}}{f(a/r)}$$ Equation 11.4-11

Equation 11.4-11 implies that the notched strength of the laminate is equal to the unnotched strength of the laminate divided by Bowie's function *f(a/r)*. Taken in this form, the Bowie *f(a/r)* function acts like an effective stress concentration factor that is dependent on both the laminate (the value of crack length, *a*) and on the hole diameter (the hole radius, *r*).

A comparison of net-section strength predicted by Equation 11.4-11 with test results is provided in Figure 11.4-15. As shown in the figure, the Bowie solution provides a suitable model for predicting the static strength behavior of open hole tensile coupons. Since all tests were conducted on the same laminate, a single value of "a" was chosen to provide the curve shown in Figure 11.4-15. As shown, the equation matches the experimental behavior very well. A detailed discussion of this formulation is given in Reference 11-18.

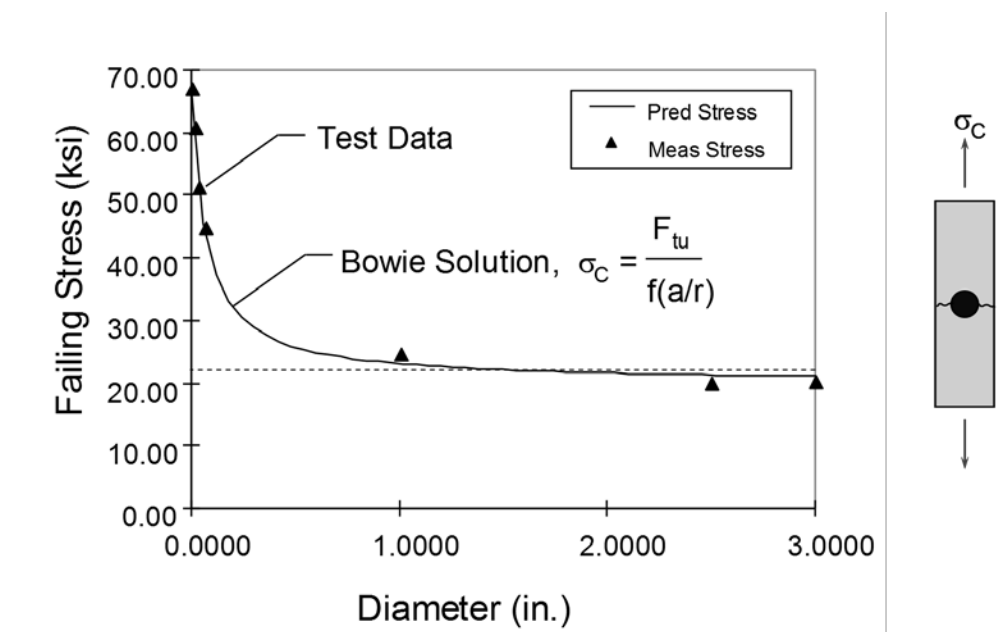

Figure 11.4-15 Fracture Mechanics Models the Strength Behavior for Circular Holes (Reference 11-18)

Copyright 2015 Lockheed Martin Corporation.
Note: The current version is always the version on the Lockheed Martin network.

11.4.3.2 Point Stress (or Strain) Failure Criterion

Whitney and Nuismer (Reference 11-20) proposed a failure criterion for in-plane failure modes such as net-section laminate failures. The basis of the approach is to evaluate a ply level circumferential stress (or strain) level at a characteristic distance, d_0, away from the hole edge. The characteristic distance accounts for two experimentally observed effects. First, the laminate strength is greater than that described for a brittle material in Figure 11.4-10 where the far-field stress at failure would be equal to the unnotched strength divided by the stress concentration factor at the critical location. Second, the laminate strength exhibits the notch sensitivity described in Figure 11.4-8 where the strength decreases with increasing hole diameter. The application of a characteristic distance simulates these observed experimental effects as shown in Figure 11.4-16.

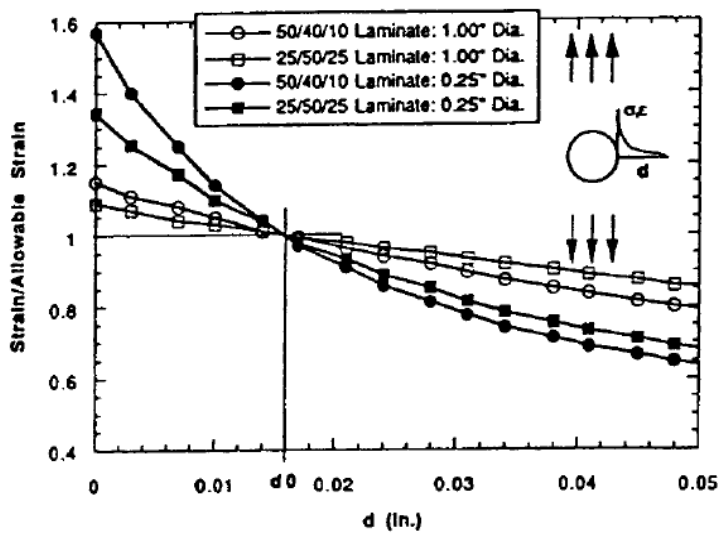

Figure 11.4-16 Strain distributions near an open hole for different hole diameters and tape laminates with characteristic distance, d_0 (Reference 11-7)

The criterion assumes that failure occurs when the stress (or strain) some characteristic distance from the hole edge meets the unnotched strength. The characteristic distance is obtained by correlating the analysis to the ratio between test derived unnotched and notched strengths. This characteristic distance is assumed to be a material property that is independent of the laminate geometry and stress distribution, although more extensive correlation may indicate a dependence on ply percentages. The characteristic distance will also depend upon the ply level failure criterion used.

Typical unnotched and notched test data may be used for correlation purposes in establishing the characteristic distances to be used for strength analysis. However, B-Basis unnotched allowables must be used for application of the method for sizing and drawing release strength analysis. Using B-basis unnotched allowables, the characteristic distance may also be correlated to predict B-basis open hole strength.

Different characteristic distances are to be determined for tension and compression loading using the corresponding unnotched allowables. Different characteristic distances may be needed for analysis correlation to allowables at different environmental conditions. For combined loads, a search must be performed to determine the most critical location around the hole edge. It is important that the hole diameters of the test data cover the entire range of design hole diameters. This method can also be applied to composite cutouts provided that the test data covers the range of design cutout diameters.

Copyright 2015 Lockheed Martin Corporation.
Note: The current version is always the version on the Lockheed Martin network.

As described above, the correlation with test data may indicate a dependence on ply percentages. Grant and Sawicki have described an Angle Minus Longitudinal (AML) Plies method to account for this ply percentage dependence (Reference 11-21). Using the stress concentration factor as defined in Equation 11.4-2, typical filled-hole tension data is used to determine unique characteristic distances for laminate ply percentages with corresponding stress concentration factors, K_t. This data is plotted in Figure 11.4-17 which implies a relationship between characteristic distance, d_0, and the inverse of the stress concentration factor, $1/K_t$. To facilitate the use of this relationship for design, the inverse stress concentration factor, $1/K_t$, has been plotted in Figure 11.4-18 against a laminate configuration parameter, defined as Angle Minus Longitudinal Plies (AML). The AML plies parameter is defined as percent ±45° plies − percent 0° plies. As shown in the figure, the relationship is almost linear between the inverse stress concentration factor, $1/K_t$, and the laminate configuration parameter AML. This approach allows for the development and use of relationships between the characteristic distance d_0 versus $1/K_t$ or AML for evaluating tension or compression net-section failures.

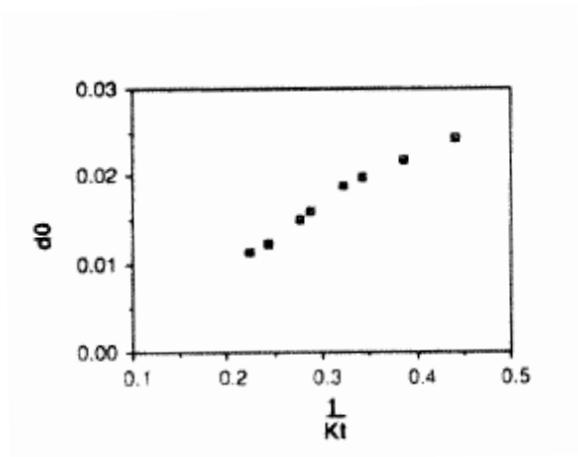

Figure 11.4-17 Characteristic Distance d_0 versus $1/K_t$ (Reference 11-21)

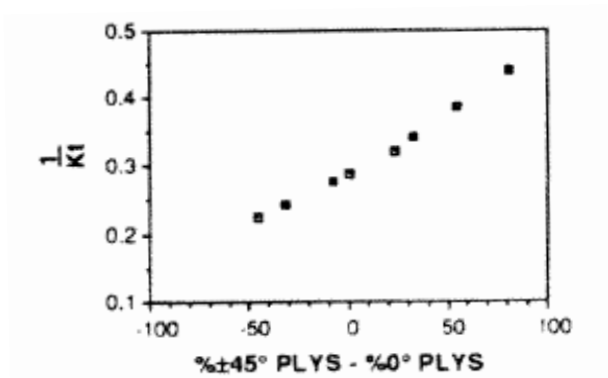

Figure 11.4-18 1 / Kt versus % ±45° Plies Minus % 0° Plies (Reference 11-21)

Copyright 2015 Lockheed Martin Corporation.
Note: The current version is always the version on the Lockheed Martin network.

11.4.4 IBOLT Strength Analysis Methodology Overview

This section provides a theoretical overview of the Lockheed Martin IDAT/IBOLT strength analysis methodology. For more detailed information, refer to the IBOLT Theory Manual (Reference 11-11) and References 11-22, 11-23, 11-24). The following discussion has been adapted from Reference 11-25.

The Bowie solution described in Section 11.4.3.1 was generated for application to metals and strictly applies to isotropic materials only. However, corresponding solutions for orthotropic materials can be obtained from the isotropic curve by scaling the solution with the ratio of the orthotropic-to-isotropic K_T at the hole boundary as shown in Figure 11.4-19.

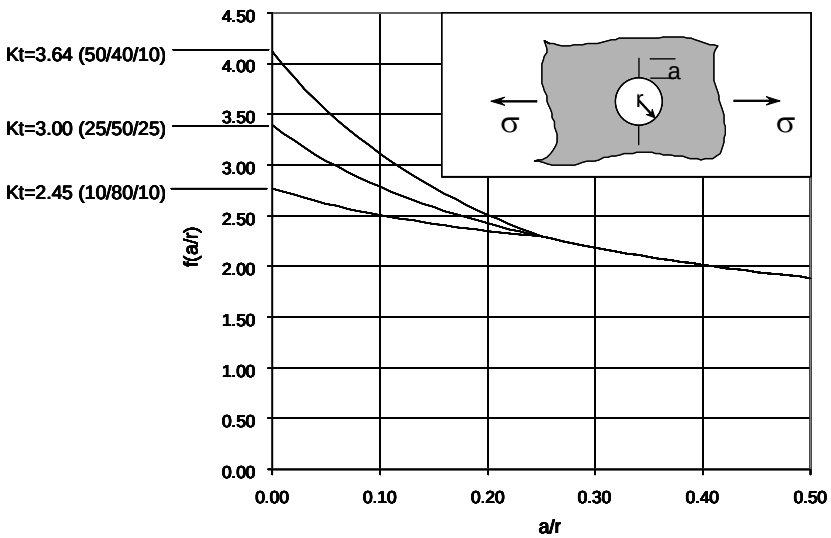

Figure 11.4-19 Orthotropic Kt is used to scale the Isotropic f(a/r) Curve

It was noted that the Bowie function *f(a/r)* at a/r = 0.0 is equal to a 1.13 factor times the isotropic $K_T = 3.00$ at the hole boundary: $f(0.0) = 1.13 \cdot K_{T(Isotropic)} = 1.13 \cdot 3.00 = 3.39$. Note also that the quasi-isotropic (25/50/25) laminate also has a value of $f(0.0) = 3.39$ since it also has a $K_T = 3.00$. As *a/r* becomes large, the function *f(a/r)* approaches 1.00 for all materials, isotropic or orthotropic. Given these two boundary conditions, an algorithm was developed to scale the Bowie solution up and down as required to match the orthotropic K_T value$\cdot 1.13$ at $a/r = 0.0$ and to converge to 1.00 for large values of *a/r*.

11.4.4.1 Generalization of LEFM Solution for Combined Loads

Up to this point, the LEFM solution has been applied only for bypass tensile loading of an unloaded hole. To analyze joint elements taken from complex joints containing multiple fasteners, the type of general loading shown in Figure 11.4-20 must be addressed.

Copyright 2015 Lockheed Martin Corporation.
Note: The current version is always the version on the Lockheed Martin network.

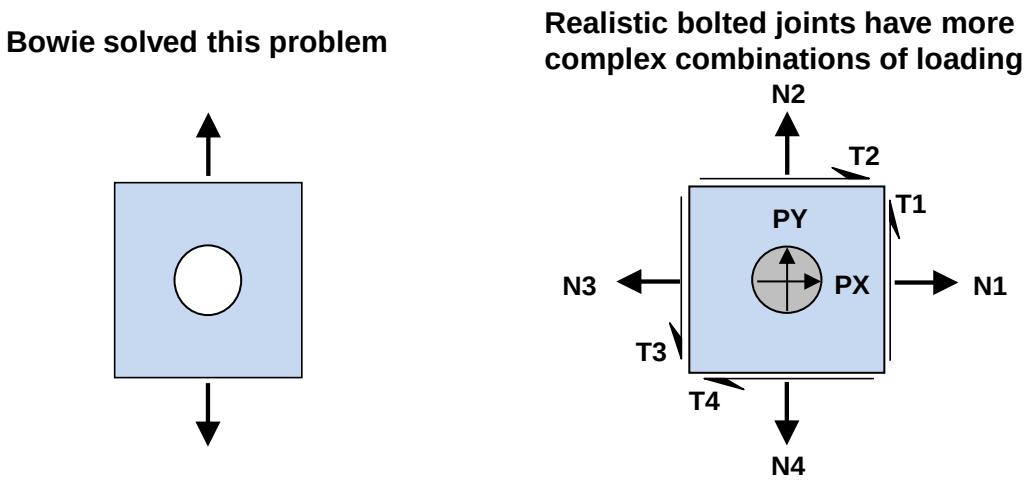

Figure 11.4-20 Complex Bolted Joint Loading

Figure 11.4-21 shows a set of nine basic load cases that can be combined to treat a realistic joint element loading condition. These include five types of bypass loading: X-direction tensile (NX), Y-direction tensile (NY), shear (NXY), and membrane loads reacted in shear in the X-direction (NXX) and Y-direction (NYY). Bearing loads reacted in tension in the X-direction (PNX) and Y-direction (PNY) are included as well as bearing loads reacted in shear in both the X-direction (PSX) and Y-direction (PSY). The sign of the loading may be reversed for any of the nine basic load cases. Bowie-type LEFM solutions were generated numerically using the boundary element method (Reference 11-26, Reference 11-27) to treat each of these nine basic load cases so that superposition could be used to analyze complex loading situations formed by combinations of the basic load cases.

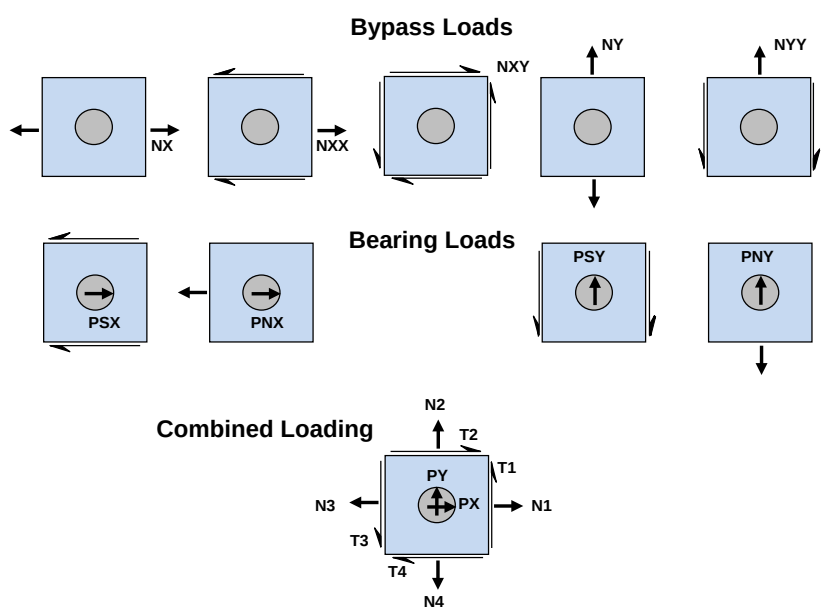

Figure 11.4-21 Nine Basic Load Cases Can Be Combined for General Loading

This set of basic load cases can be combined to treat a typical joint element subjected to a complex loading condition. In the example of Figure 11.4-22, three of the nine basic load cases are combined to form the complex

Copyright 2015 Lockheed Martin Corporation.
Note: The current version is always the version on the Lockheed Martin network.

load state representing a joint element at the edge of a structural panel having a single free edge. Loads acting on the element boundaries are given as constant tractions with units of lbs/in. Fastener loads acting on the hole-boundary are expressed in pounds. For simplicity, the example shown assumes the element dimensions are 1.0 inch by 1.0 inch to allow the edge tractions (lbs/in) and bolt load (lbs) to be summed directly. Since each basic load case is in equilibrium, any combination of basic load cases will result in a balanced element freebody diagram. IBOLT Subroutine RLDCONV decomposes the user-input element loads into the equivalent set of 9 basic load cases of Figure 11.4-21.

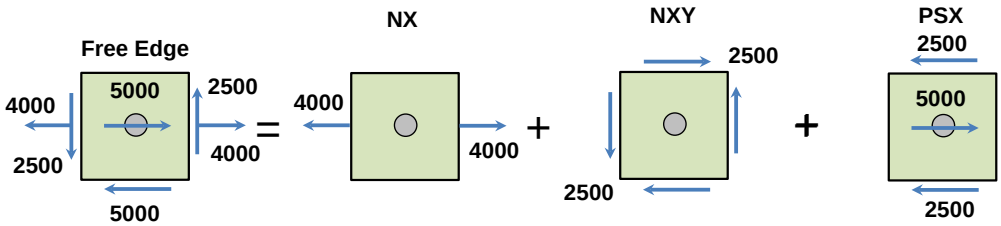

Figure 11.4-22 Example of Superimposed Basic Load Cases

For an open hole tensile coupon, the failure location is expected to be on the hole boundary at the net section of the coupon. For more complicated loading conditions, the failure location is not as easy to determine. Ideally all locations on the hole boundary would be evaluated for possible failure, and the most critical location would be selected. Based on the observations of many failed composite coupons, a simplifying assumption was made to reduce the scope of the required analysis. It was observed that for the [0/±45/90] family of laminates, failure occurred at or near one of the eight locations shown in the Figure 11.4-23. These are the eight locations where fibers are tangent to the hole boundary. Each failure appears to initiate as a through-the-thickness radial crack. The coupons evaluated had been loaded to failure with bypass loading, bearing loading, and combined bearing-bypass loading. These eight failure positions are numbered sequentially counterclockwise at 45-degree intervals. Position 1 is located at the intersection of the hole boundary with the X-axis. The local element X-Y coordinate system has its origin at the center of the fastener hole. The X-axis is defined to be parallel to the 0-degree ply direction.

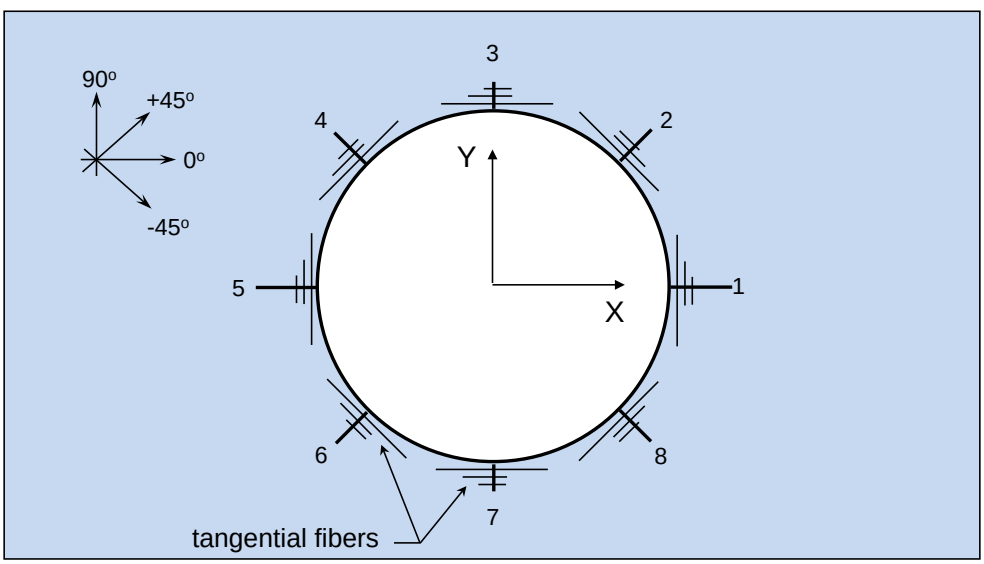

Figure 11.4-23 Observed Failure Locations

Copyright 2015 Lockheed Martin Corporation.
Note: The current version is always the version on the Lockheed Martin network.

The unnotched laminate strength in the tangential direction is not constant at the eight failure positions around the hole. Table 11.4-1 and Figure 11.4-24 show how the percentages of tangential, off-axis, and radial plies vary with position for a (50/40/10) laminate. Tangential plies are those plies oriented tangent to the hole boundary at a given position. Radial plies are those oriented in a direction normal to the tangential plies (radial with respect to the center of the hole). Off-axis plies are those plies oriented at ±45 degrees to the tangential direction.

Table 11.4-1 Percentage Plies Vary With Position—50/40/10 Laminate Example

Position	Percent Tangential Plies	Percent Off-axis Plies	Percent Radial Plies
1	10	40	50
2	20	60	20
3	50	40	10
4	20	60	20
5	10	40	50
6	20	60	20
7	50	40	10
8	20	60	20

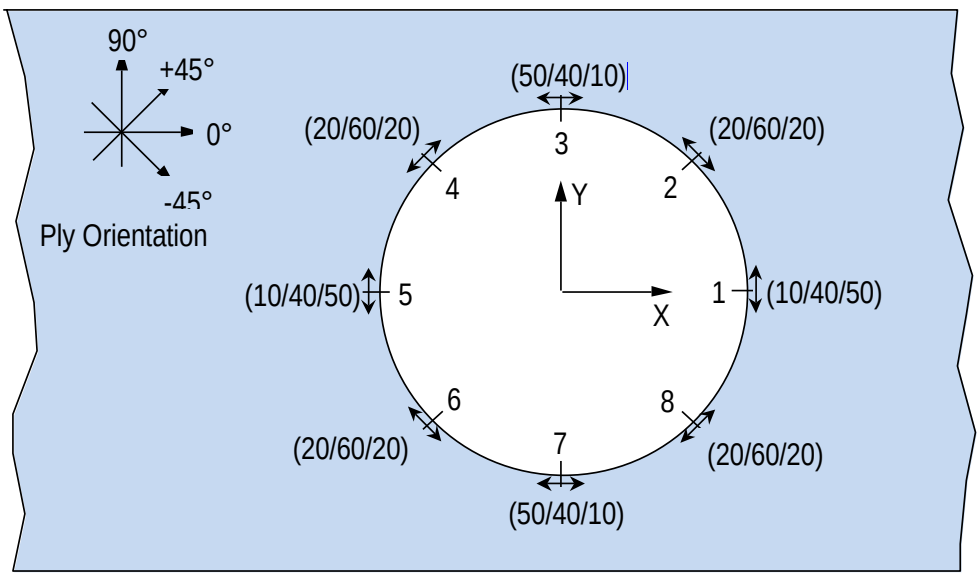

Figure 11.4-24 Circumferential Variation of Laminate Ply Percentages—50/40/10 Laminate Example

Since the ply content of the laminate in the tangential direction varies from one failure position to another, the value of the effective flaw size "a" also changes with position. Given the thickness fractions of the tangential, off-axis, and radial plies at the eight failure positions, the value of “a” can be calculated as:

$$a = \left(G_0 \left[\frac{t_{\tan}}{t_{total}} \right] + G_{45} \left[\frac{t_{oa}}{t_{total}} \right] + G_{90} \left[\frac{t_r}{t_{total}} \right] \right) \bullet \left(\frac{1}{cF_{tu}^2 \pi} \right)$$ Equation 11.4-12

Where

G_0 = strain energy release rate of the 0º plies (in-lbs/in^2)

Copyright 2015 Lockheed Martin Corporation.
Note: The current version is always the version on the Lockheed Martin network.

G_{45} = strain energy release rate of the ±45º plies (in-lbs/in^2)
G_{90} = strain energy release rate of the 90º plies (in-lbs/in^2)
t = thickness (in)
F_{tu} = unnotched tension strength (psi)

The constant "c" is defined in Paris and Sih (Reference 11-28) relating critical strain energy release rate to fracture toughness.

$$c = \sqrt{\frac{S_{11}S_{22}}{2}\left[\sqrt{\frac{S_{11}}{S_{22}}} + \frac{2S_{12} + S_{66}}{2S_{22}}\right]} \qquad \text{Equation 11.4-13}$$

Where
S_{ij} = lamina compliance matrix terms (psi^{-1}).

G_0, G_{45}, and G_{90} are defined early in the model calibration process using open hole tension (OHT) data from three or more laminates.

Figure 11.4-25 shows typical values of "a" calculated from the equation above for a (50/40/10) laminate. In addition to position on the hole, “a” is also a function of material properties and ply percentages. The Bowie-type LEFM solutions that were developed for the nine basic load cases included treatment of through-the-thickness radial cracks at each of the eight failure positions. The ability for the effective flaw size “a” to be a function of laminate ply percentages rather than a fixed value provides the strength model with the ability to better reflect the physics of damage development over a wide range of laminate configurations. This flexibility thus provides a better prediction of joint strength over the full extent of the design space.

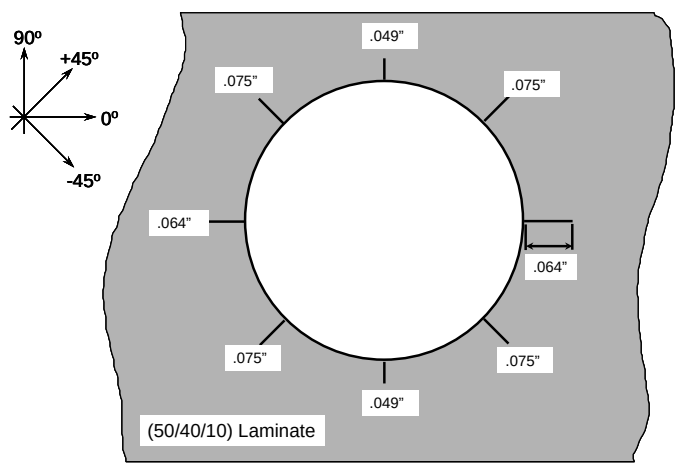

Figure 11.4-25 Typical values of "a" as a function of position for a (50/40/10) laminate

11.4.4.2 Finite Geometry Effects

Each IBOLT solution is based on infinite plate equations which are then corrected for the finite dimensions of the joint element. These finite geometry correction factors were generated numerically using boundary element method (Reference 11-26) for all nine basic load cases and eight failure positions for the usable range of laminate ply

Copyright 2015 Lockheed Martin Corporation.
Note: The current version is always the version on the Lockheed Martin network.

percentages and element geometries as summarized in Figure 11.4-26. These finite geometry factors are stored within IBOLT in a large lookup table that allows rapid retrieval of the values appropriate for each analysis.

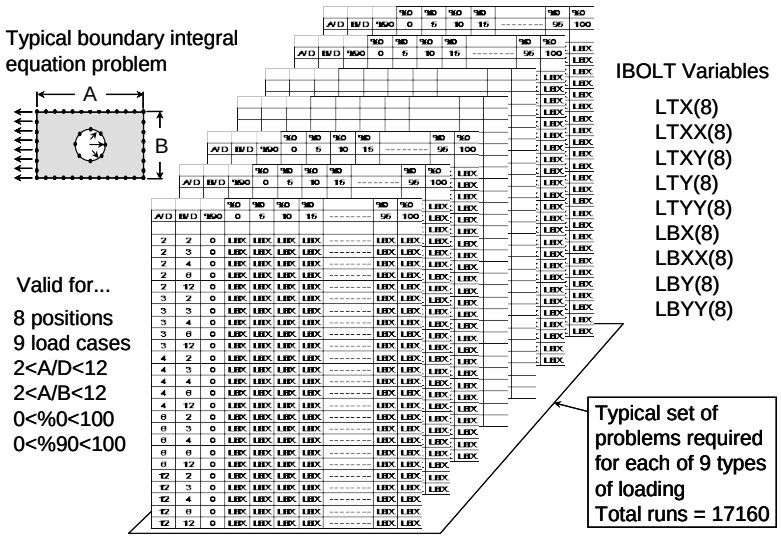

Figure 11.4-26 Finite Geometry Correction Factors

11.4.4.3 Bearing-Bypass Margin of Safety

The failure strength for an infinite plate with an open hole, loaded in uniaxial tension can be predicted by dividing the unnotched laminate strength F_{tu} by the Bowie function $f(a/r)$:

$$\sigma_c = \frac{F_{tu}}{f\left(\frac{a}{r}\right)} \qquad \text{Equation 11.4-14}$$

Where
σ_c = open hole tension strength (psi)
F_{tu} = unnotched laminate strength (psi)
$f(a/r)$ = Bowie function

The Bowie function $f(a/r)$ serves as an effective stress concentration factor that includes the effect of the hole diameter (hole radius "r") and an effective flaw size (crack length "a"). The open hole coupon fails at locations 3 and 7 at the net section. F_{tu} is the unnotched strength of the laminate in the tangential direction at locations 3 and 7 shown in Figure 11.4-23. Each of the eight locations on the hole boundary has a value of unnotched strength $F_{tu,i}$ and effective flaw size a_i. Equation 11.4-14 can be rewritten to apply to each of the eight locations on the hole boundary (denoted by index "i") and corrected for finite geometry effects using the correction factor $L_{TX,I}$. The resulting equation shows the far-field applied axial X-direction tensile stress required to initiate failure at location i:

$$\sigma_{TX} = \frac{F_{tu,i}}{F_{TX,i}\left(\frac{a_i}{r}\right) \bullet L_{TX,i}} \qquad \text{Equation 11.4-15}$$

Where

Copyright 2015 Lockheed Martin Corporation.
Note: The current version is always the version on the Lockheed Martin network.

σ_{TX} = applied far-field X-direction tension stress load (psi)
$F_{tu,i}$ = unnotched laminate strength at hole position i (psi)
$F_{TX,i}(a_i / r)$ = beta function at hole position i
$L_{TX,i}$ = finite geometry correction factor at hole position i

Rearranging Equation 11.4-15 gives:

$$F_{tu,i} = \sigma_{TX} \bullet L_{TX,i} \bullet F_{TX,i}\left(\frac{a_i}{r}\right) \qquad \text{Equation 11.4-16}$$

For the purpose of combining stresses contributed by each of the nine load cases, Equation 11.4-16 can be expanded as shown:

$$\begin{aligned}
F_i &= \sigma_{TX} \bullet L_{TX,i} \bullet F_{TX,i}\left(\frac{a_i}{r}\right) \bullet FTF && \text{Bypass Load, X-direction} \\
&+ \sigma_{TXX} \bullet L_{TXX,i} \bullet F_{TXX,i}\left(\frac{a_i}{r}\right) \bullet FTF && \text{Membrane Reacted in Shear, X-direction} \\
&+ \sigma_{TY} \bullet L_{TY,i} \bullet F_{TY,i}\left(\frac{a_i}{r}\right) \bullet FTF && \text{Bypass Load, Y-direction} \\
&+ \sigma_{TYY} \bullet L_{TYY,i} \bullet F_{TYY,i}\left(\frac{a_i}{r}\right) \bullet FTF && \text{Membrane Reacted in Shear, Y-direction} \\
&+ \sigma_{TXY} \bullet L_{TXY,i} \bullet F_{TXY,i}\left(\frac{a_i}{r}\right) \bullet FTF && \text{Bypass Shear Load, X-Y plane} \qquad \text{Equation 11.4-17} \\
&+ \sigma_{BX} \bullet L_{BX,i} \bullet F_{BX,i}\left(\frac{a_i}{r}\right) \bullet FBF && \text{Bearing Reacted in Tension, X-direction} \\
&+ \sigma_{BXX} \bullet L_{BXX,i} \bullet F_{BXX,i}\left(\frac{a_i}{r}\right) \bullet FBF && \text{Bearing Reacted in Shear, X-direction} \\
&+ \sigma_{BY} \bullet L_{BY,i} \bullet F_{BY,i}\left(\frac{a_i}{r}\right) \bullet FBF && \text{Bearing Reacted in Tension, Y-direction} \\
&+ \sigma_{BYY} \bullet L_{BYY,i} \bullet F_{BYY,i}\left(\frac{a_i}{r}\right) \bullet FBF && \text{Bearing Reacted in Shear, X-direction}
\end{aligned}$$

Where
$\sigma_{TX}, \sigma_{TY}, \sigma_{TXY}$ = contribution from applied far-field bypass loads (psi)
$\sigma_{TXX}, \sigma_{TYY}$ = contribution from membrane load reacted by shear (psi)
σ_{BX}, σ_{BY} = contribution from bearing load reacted by normal load (psi)
$\sigma_{BXX}, \sigma_{BYY}$ = contribution from bearing load reacted by shear load (psi)
$F_{TX,i}(a_i / r)$ = beta function at hole position i
$L_{TX,i}$ = finite geometry correction factor at hole position i
FTF = cumulative effect of additional factors that affect bypass loading as given in Equation 11.4-18
FBF = cumulative effect of additional factors that affect bearing loading as given in Equation 11.4-19

Equation 11.4-17 shows the total effective tangential stress at location "i" resulting from the contributions of all nine load cases. The first line in the equation is the contribution resulting from an applied tensile stress in the x-direction ($\sigma_{TX,i}$) and is equal to Equation 11.4-16 multiplied by a joint configuration factor. Each successive line represents the contribution to the effective tangential stress at location "i" resulting from a different load case for a total of nine load cases. Each line in the equation is the product of the applied load, the finite geometry correction factor, the effective stress concentration factor (the appropriate Bowie function for load type and location on hole boundary), and the empirical factor FTF or FBF. The FTF term represents the cumulative effect of additional factors that affect bypass loading. These include filled hole effects, countersink effects, torque, and clearance effects. The FBF term represents the cumulative effect of additional factors that affect bearing loading such as single/double shear effects,

Copyright 2015 Lockheed Martin Corporation.
Note: The current version is always the version on the Lockheed Martin network.

countersink effects, and torque effects. The functional form of these terms is given for FTF in Equation 11.4-18 and FBF in Equation 11.4-19.

$$FTF = FCNTT \cdot FFILL \cdot FTTORK \cdot FCLEAR \qquad \text{Equation 11.4-18}$$

Where
FCNTT = bypass countersink correction factor
FFILL = filled-hole bypass correction factor
FTTORK = bypass load fastener off-nominal torque correction factor
FCLEAR = hole-clearance factor

$$FBF = FSSDS \cdot FCSKBC \cdot FBTORK \qquad \text{Equation 11.4-19}$$

Where
FSSDS = single-shear bearing factor
FCSKBC = bearing countersink correction factor
FBTORK = bearing load fastener off-nominal torque correction factor

All such empirical correction factors, as well as the bearing cut-off factors discussed in Section 11.4.4.5 are derived from multivariate regression analysis of open- and filled-hole tension and compression test data; and tension-, compression-, and shear-loaded bearing test data.

Finally, the bearing-bypass margin of safety is calculated. While tensile loads and stresses have been used to develop the bearing-bypass analysis methodology given in the preceding sections, F_i, given in Equation 11.4-17 can also be compressive. The developed methodology is also valid for compressive loads and stresses. In this case, all factors are calculated the same as for the tensile case but the margin of safety calculation uses unnotched compressive strength, F_{cu}. The bypass margin of safety at location "i" is given by:

$$M.S. = \frac{F_{all,i}}{F_i} - 1.0 \qquad \text{Equation 11.4-20}$$

Where
$F_{all,i} = F_{tu,i}$ if F_i is greater than 0, indicating tensile stress, $F_{cu,i}$ if F_i is less than 0, indicating compressive stress
$F_{tu,i}$ = the unnotched tangential tensile stress allowable in the tangential direction at location i (psi)
$F_{cu,i}$ = the unnotched tangential compressive stress allowable in the tangential direction at location i (psi)

A margin of safety is calculated at each of the eight locations on the hole boundary. The lowest of these eight values is the critical margin of safety for bearing-bypass loading. This margin is compared with the bearing cutoff margin of safety to determine the critical margin of safety for the joint element.

At this point, the basic bolted joint static strength model (summarized in Figure 11.4-27) has the following features:

- Applies to orthotropic laminates, [0/±45/90] laminate family
- Treats rectangular, finite-geometry joint element
- Predicts strength as a function of hole diameter
- Employs fracture-mechanics-based failure theory
- Allows combinations of 9 basic types of loading
- Analyzes for possible failure at 8 positions on hole boundary
- Defines flaw size as a function of ply percentage

Copyright 2015 Lockheed Martin Corporation.
Note: The current version is always the version on the Lockheed Martin network.

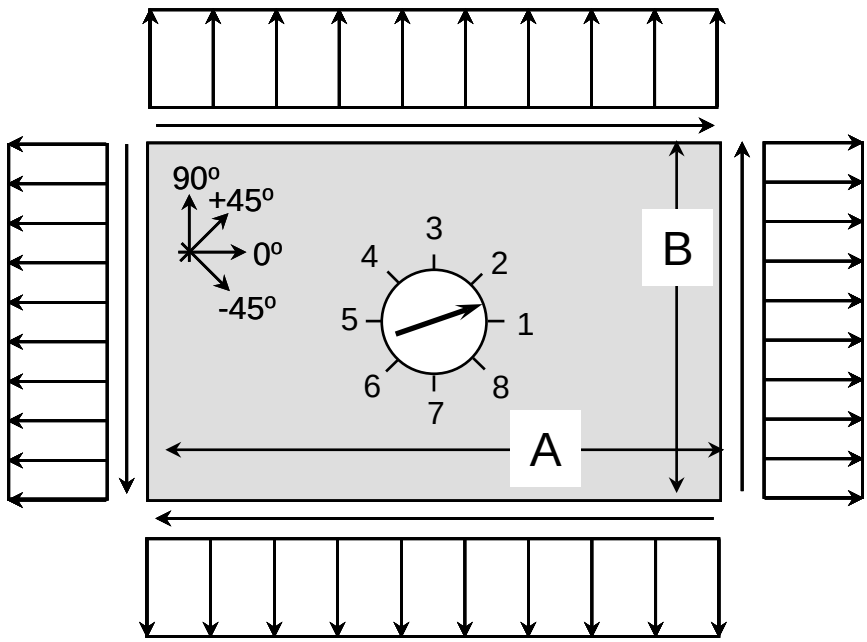

Figure 11.4-27 Features of Basic Strength Model

11.4.4.4 Bending Analysis

Up to this point, all applied loads have been in the plane of the composite joint element. IBOLT also accounts for the effect of out-of-plane moment resultants, MX, MY, and MXY. These applied moments per unit length (units: in.-lb/in.) are positive when applied in the directions shown in Figure 11.4-28.

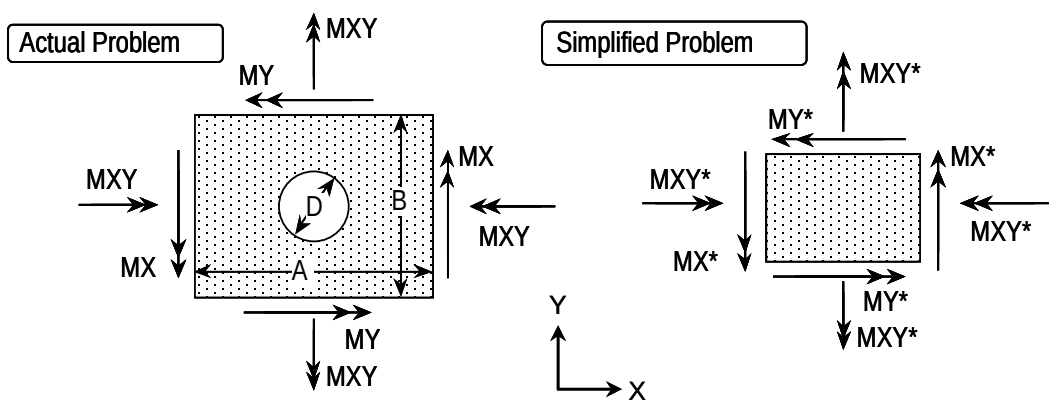

Figure 11.4-28 Bending Problem Simplification

The sign convention shown assumes the IBOLT element is viewed looking down on the fastener head where the highest numbered ply is in view, and ply number 1 is on the back side at the interface with the substructure member.

Copyright 2015 Lockheed Martin Corporation.
Note: The current version is always the version on the Lockheed Martin network.

The actual problem of moment resultants MX, MY, and MXY applied to a rectangular element with a central hole has been simplified by omitting the central hole and performing a ply-by-ply point moment analysis on the remaining unnotched laminate using lamination theory. The simplified analysis assumes that moments MX*, MY*, and MXY* are applied as given in the following equations.

$$MX^* = \frac{MX}{XNSF \cdot KBB}$$ Equation 11.4-21

$$MY^* = \frac{MY}{YNSF \cdot KBB}$$ Equation 11.4-22

$$MXY^* = \frac{MXY}{0.5 \cdot (XNSF + YNSF) \cdot KBB}$$ Equation 11.4-23

Where
MX, MY, MXY = applied out-of-plane moments (in-lbs/in)
XNSF, YNSF = x- and y- direction net section factors
KBB = test-derived bending factor

The original moments are increased to account for the net section of the joint element using the bending factor and the section factors. The bending factor, KBB, is a bending factor that is a function of fastener head type and whether or not the hole is filled by a fastener. The KBB factor is derived from notched flexure. The net section factors, XNSF and YNSF, are calculated as given in the equations below. For countersunk holes, the second term in the equations removes the area of the countersunk head in the values of XNSF and YNSF. Head height and countersink angle for specific fasteners are stored in the IDAT fastener database. The second term in these equations reduces to zero for holes with no countersink.

$$XNSF = \frac{B-D}{B} - \frac{H^2 \cdot \tan\frac{\alpha}{2}}{B \cdot t}$$ Equation 11.4-24

$$YNSF = \frac{A-D}{A} - \frac{H^2 \cdot \tan\frac{\alpha}{2}}{A \cdot t}$$ Equation 11.4-25

Where
A, B = gross section widths in the x- and y- directions, respectively (in)
D = hole diameter (in)
H = countersink head height (in)
α = countersink angle (deg)
t = laminate thickness (in)

The bending margin of safety is calculated ply-by-ply. Ply stresses are transformed into the local ply coordinate system and a strength-based margin of safety is calculated. The tensile and compression margins of safety for the set of all plies j with ply orientation angle θ are given by:

$$M.S._{ten}(\theta) = MIN_{all,j}\left(\frac{\sigma_{11t,ult}}{\sigma_{j,\theta}} - 1.0\right) \text{ for j=1,n plies}$$ Equation 11.4-26

Copyright 2015 Lockheed Martin Corporation.
Note: The current version is always the version on the Lockheed Martin network.

$$M.S._{comp}(\theta) = MIN_{all,j}\left(\frac{\sigma_{11c,ult}}{\sigma_{j,\theta}} - 1.0\right) \text{ for j=1,n plies} \qquad \text{Equation 11.4-27}$$

Where

$\sigma_{j,\theta}$ = stress for ply j at angle θ in global coordinate system (psi)

$\sigma_{11t,ult}$ = fiber direction ultimate tensile strength (psi)

$\sigma_{11c,ult}$ = fiber direction ultimate compression strength (psi)

The margins of safety are calculated for each of the four ply angles 0, +45, -45, and 90 degrees. These eight values of strength-based margins (one tension and one compression value for each of four ply angles) are used to calculate the tension and compression stress contributions due to bending for each ply angle (8 values of stress, 4 positive and 4 negative values). The tension and compression stress contributions are given by

$$+\sigma_b(\theta) = \frac{F_{tu}(\theta)}{M.S._{ten}(\theta)+1} \qquad \text{Equation 11.4-28}$$

$$-\sigma_b(\theta) = \frac{F_{cu}(\theta)}{M.S._{com}(\theta)+1} \qquad \text{Equation 11.4-29}$$

Where

$F_{tu}(\theta)$ =unnotched tensile strength for ply angle θ in the global coordinate system (psi)

$F_{cu}(\theta)$ =unnotched compression strength for ply angle θ in the global coordinate system (psi)

These eight values of bending stress contributions are assigned to their proper positions on the hole boundary according to ply angle in subroutine BEND as shown in Table 11.4-2 and illustrated in Figure 11.4-29.

Table 11.4-2 Bending Stress Contributions

Position	Tension	Compression
1	$+\sigma_B(90)$	$-\sigma_B(90)$
2	$+\sigma_B(-45)$	$-\sigma_B(-45)$
3	$+\sigma_B(0)$	$-\sigma_B(0)$
4	$+\sigma_B(+45)$	$-\sigma_B(+45)$
5	$+\sigma_B(90)$	$-\sigma_B(90)$
6	$+\sigma_B(-45)$	$-\sigma_B(-45)$
7	$+\sigma_B(0)$	$-\sigma_B(0)$
8	$+\sigma_B(+45)$	$-\sigma_B(+45)$

At each of the 8 positions, the stresses due to membrane and bending loading are combined where the most critical bending stress (either $+\sigma_B$ or $-\sigma_B$) is used that results in the lowest margin of safety for the combined stress state.

Copyright 2015 Lockheed Martin Corporation.
Note: The current version is always the version on the Lockheed Martin network.

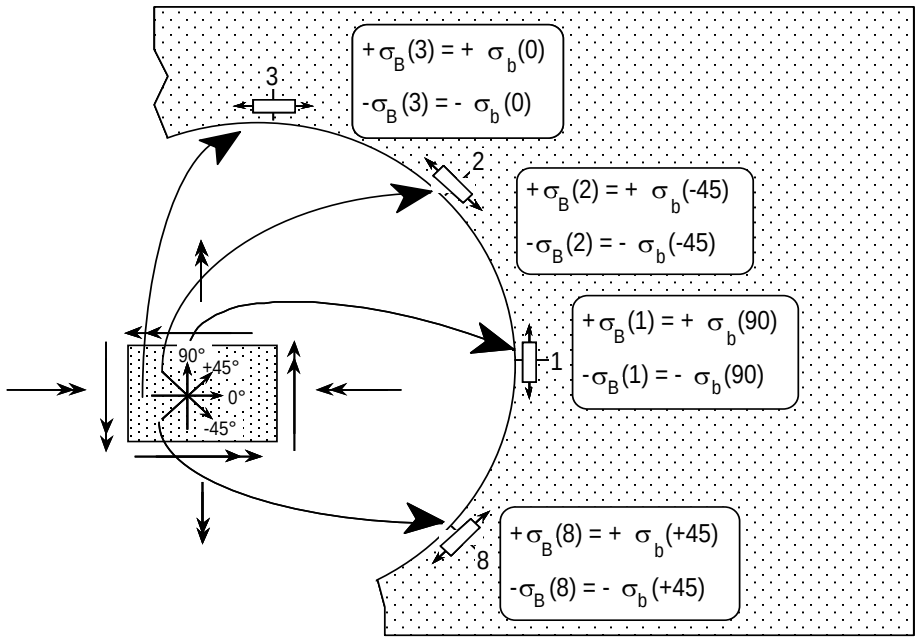

Figure 11.4-29 Combination of Bending Stress Components with Membrane Stress Components

11.4.4.5 Bearing Cutoff

The basic strength model used in IBOLT only deals with the net section failure mode with the progression of a radial, through-the-thickness crack from the edge of the hole. For the pure bearing case (no bypass loading), additional failure modes may be involved. A separate check on bearing strength for the no bypass condition called the "bearing cutoff" calculation has been included in IBOLT.

The starting point for the bearing cutoff check is the measured bearing strengths from the three test methods illustrated in Figure 11.4-30. The test methods determine bearing strengths for tension (BCT), compression (BCC), and shear reactions (BCS).

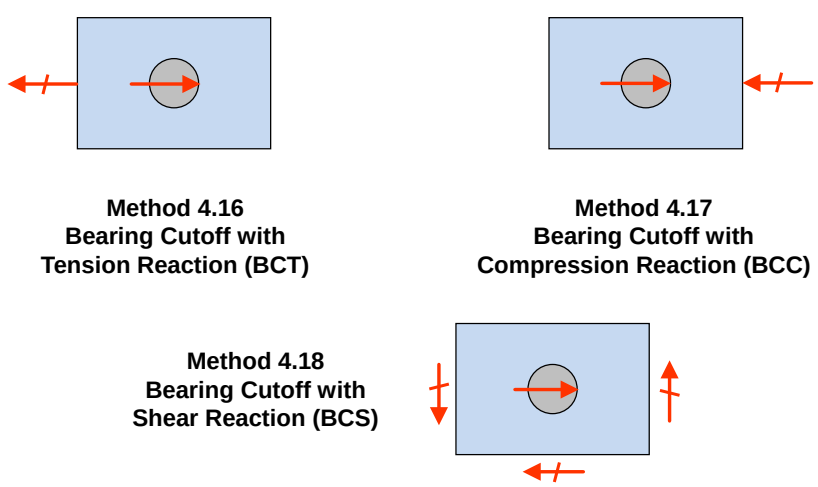

Figure 11.4-30 Three Types of Bearing Strength Test Reaction Methods

Copyright 2015 Lockheed Martin Corporation.
Note: The current version is always the version on the Lockheed Martin network.

As described in Figure 11.4-31, these are single lap shear bearing strength values obtained for a (25/50/25) quasi-isotropic laminate with a protruding head fastener attached to a rigid steel fixture approximately 0.80 inch thick. The value of thickness-to-hole diameter for these tests is approximately 0.50. Values of e/D and W/D are approximately 2.5 and 5.0, respectively. Loading for the test is in the 0º ply direction. The goal of the bearing cutoff check is to provide a bearing value appropriate for the actual structural joint being analyzed. To provide this, it is necessary to correct the data file value for fastener head type, e/D, W/D, laminate ply percentages, bolt load direction, t/D ratio, hole diameter, and substructure modulus and thickness.

A SEPARATE CHECK ON BEARING STRENGTH FOR THE NO-BYPASS CONDITION

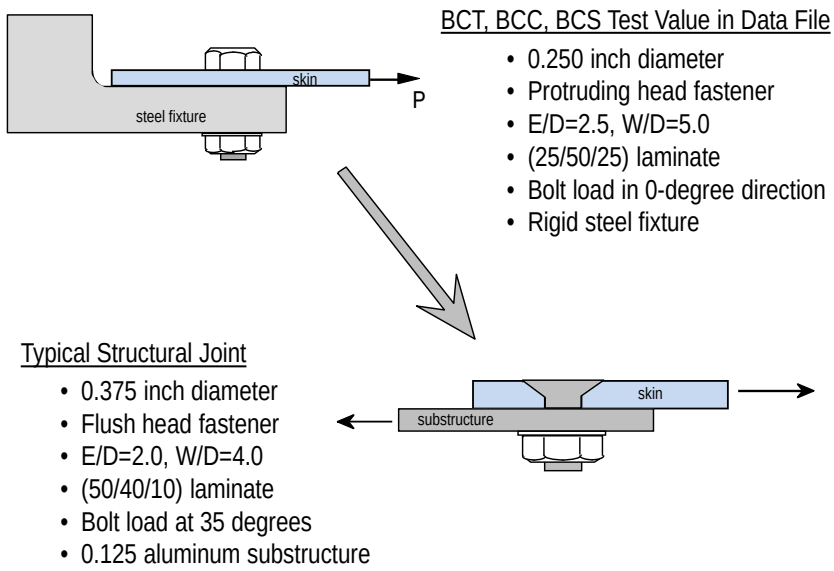

Figure 11.4-31 Bearing Cutoff Value Description

A primary and a secondary method are used to provide the bearing cutoff value as outlined in Figure 11.4-32. The lower value obtained from these two methods are used to calculate the bearing cutoff margin of safety.

Copyright 2015 Lockheed Martin Corporation.
Note: The current version is always the version on the Lockheed Martin network.

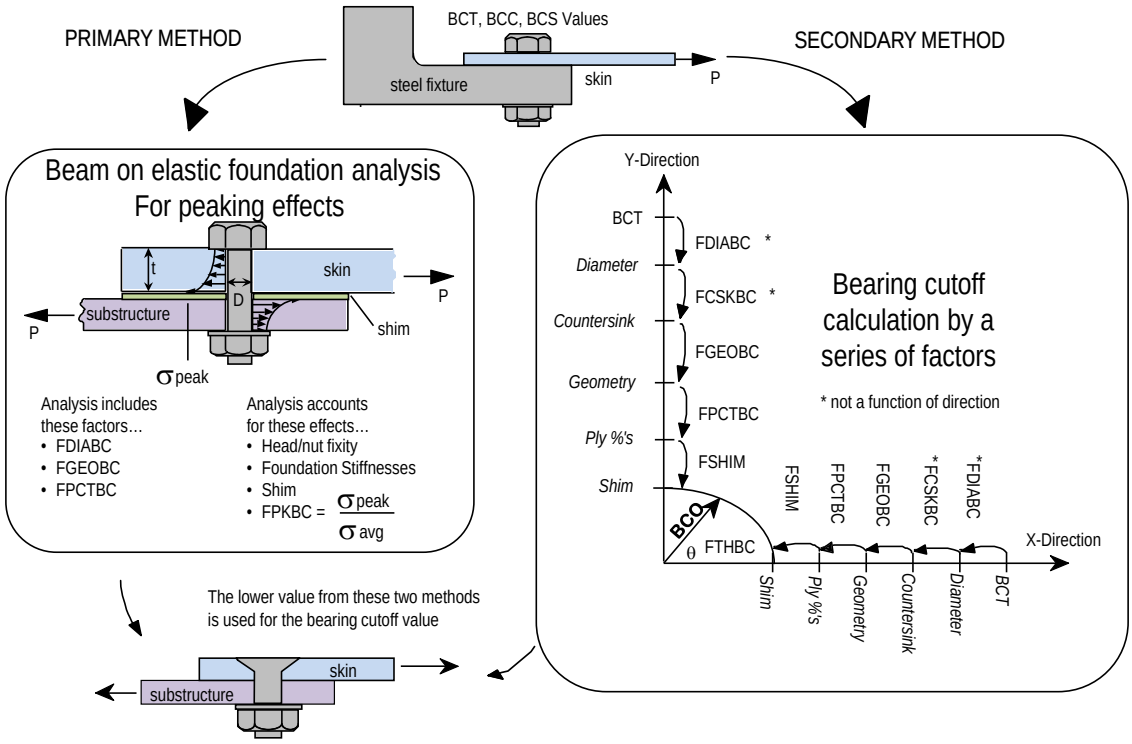

Figure 11.4-32 Two Bearing Cutoff Methods

The primary method of calculation uses a beam-on-elastic-foundation analysis to provide a bearing stress profile through the thickness of the laminate. The beam-on-elastic-foundation analysis included in IBOLT also exists as a stand-alone program SS_JOINT, which is included in the IDAT toolset. As shown in Figure 11.4-33, this analysis models the fastener, the skin, the substructure, and a shim (if present). The skin and substructure serve as elastic foundations with appropriate elastic moduli and thicknesses. The shim is modeled as an unsupported length of fastener between the two foundations. Fixity provided at the ends of the beam (fastener) by the fastener head and nut are modeled as springs that resist rotation at these two points. Values for the spring constants are correlated with test results for a given fastener system. SS_JOINT program output includes the bearing stress profile through the thickness, joint stiffness, and shear and bending moment values along the length of the fastener.

The SS_JOINT analysis is based on a method proposed by Barrois (Reference 11-29) and modified to add an unsupported beam length representing a shimmed gap (See Section 11.7.5 for more discussion on shimmed gaps). This method accounts for laminate and substructure modulus and thickness, fixity provided by the head and nut, and provides a factor FPKBC that is the ratio of peak bearing stress to average bearing stress. Other factors, as shown in Figure 11.4-32, are used to account for fastener diameter (FDIABC), countersink (FCSKBC), e/D and W/D (FGEOBC), ply percentages (FPCTBC), shim (FSHM), and bolt load direction (FTHBC). Two factors, SSDS and FBRUBCT, provide empirical calibration to account for bearing strength differences between single- and double-lap shear configurations. Because the bearing with tension reaction (BCT) test is the only configuration that is able to be done in both single- and double-shear modes, these two factors are used to account for strength differences between single- and double-shear configurations in all three bearing cutoff calculations in the primary method. The peak bearing stress provided by this analysis is compared to the ultimate bearing stress measured in a double-shear test (minimal peaking in bearing stress) to determine the margin of safety.

Copyright 2015 Lockheed Martin Corporation.
Note: The current version is always the version on the Lockheed Martin network.

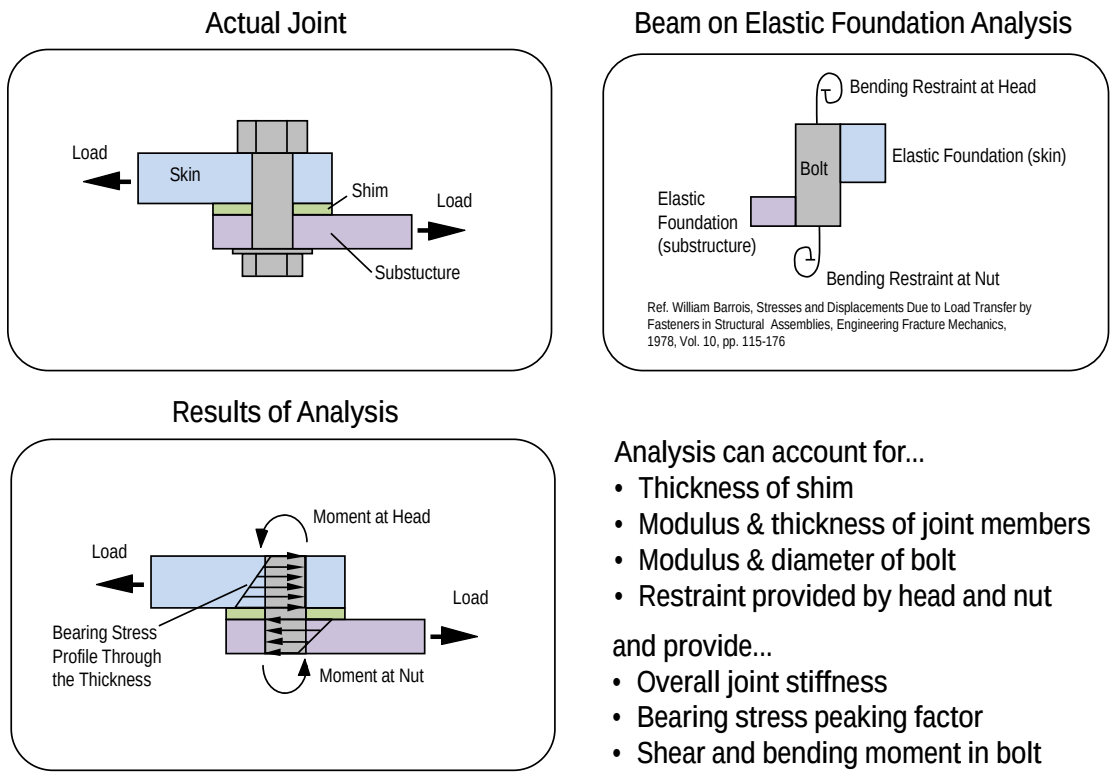

Figure 11.4-33 Beam-On-Elastic-Foundation Fastener Model (IDAT/SS_JOINT)

The equations used by IBOLT for the primary bearing cutoff calculation are shown below. Bearing cutoff values are calculated in both the X- and Y-directions. The FGEOBCT, FGEOBCC, and FGEOBCS factors will have different values in the X- and Y-directions if the A and B dimensions are not the same. The FPCTBCT, FPCTBCC, and FPCTBCS factors will have different values in the X- and Y-directions if the percent 0º plies and percent 90º plies are not the same.

The primary calculation for bearing cutoff with tension reaction in the X- and Y-directions is given below.

$$BCTX,BCTY = BCT \cdot \frac{FDIABC \cdot FGEOBCT \cdot FPCTBCT \cdot FBRUBCT}{FPKBC \cdot SSDS}$$ **Equation 11.4-30**

Where
BCT = material allowable for bearing with tension reaction (psi)
FDIABC = hole diameter factor
FGEOBCT = e/d and W/D factor (where e is edge distance, W is IBOLT element width, and D is hole diameter)
FPCTBCT = %0º and %90º plies factor
FBRUBCT = ratio of F_{bru} to bearing cutoff with tension reaction (BCT) material allowable
FPKBC = ratio of peak bearing stress to average bearing stress calculated by beam-on-elastic-foundation analysis
SSDS = single to double shear ratio factor

The primary calculation for bearing cutoff with compression reaction in the X- and Y-directions is given below.

$$BCCX, BCCY = BCC \cdot \frac{FDIABC \cdot FGEOBCC \cdot FPCTBCC \cdot FBRUBCT}{FPKBC \cdot SSDS}$$ **Equation 11.4-31**

Where
BCC = material allowable for bearing with compression reaction (psi)

Copyright 2015 Lockheed Martin Corporation.
Note: The current version is always the version on the Lockheed Martin network.

The primary calculation for bearing cutoff with shear reaction in the X- and Y-directions is given below.

$$BCSX,BCSY = BCS \cdot \frac{FDIABC \cdot FGEOBCS \cdot FPCTBCS \cdot FBRUBCT}{FPKBC \cdot SSDS}$$ **Equation 11.4-32**

Where
BCS = material allowable for bearing with shear reaction (psi)

The secondary method of bearing cutoff calculation applies a series of factors to the reference bearing cutoff value in the data file (BCT, BCC, BCS) to account for hole diameter (FDIABC), countersink (FCSKBC), e/D and W/D (FGEOBC), ply percentages (FPCTBC), and bolt load direction (FTHBC). These reductions are applied in both the X- and Y-directions since FGEOBC and FPCTBC are functions of ply percentages, edge distance, and width and have different values in these two directions. A final correction is applied for bolt load angle.

The secondary bearing cutoff analysis method applies to the rigid substructure case, and no correction is made for substructure thickness and modulus. For rigid substructure, the primary method can over-predict the bearing strength. Use of the secondary analysis (when it predicts a lower bearing cutoff value) insures that bearing strength predictions will not be unconservative.

The equations used by IBOLT for the secondary bearing cutoff calculations are shown below. As with the Primary method, bearing cutoff values are calculated in both the X- and Y-directions. The FGEOBCT, FGEOBCC, and FGEOBCS factors will have different values in the X- and Y-directions if the A and B dimensions are not the same. The FPCTBCT, FPCTBCC, and FPCTBCS factors will have different values in the X- and Y-directions if the percent 0º plies and percent 90º plies are not the same.

The secondary calculation for bearing cutoff with tension reaction in the X- and Y-directions is given below.

$$BCTX\,,BCTY = BCT \cdot \frac{FDIABC \cdot FGEOBCT \cdot FPCTBCT}{FCSKBC \cdot FSHIM}$$ **Equation 11.4-33**

Where
BCT = material allowable for bearing with tension reaction (psi)
FDIABC = hole diameter factor
FGEOBCT = e/d and W/D factor (where e is edge distance, W is IBOLT element width, and D is hole diameter)
FPCTBCT = %0º and %90º plies factor
FCSKBC = countersunk fastener head factor
FSHIM = shim factor

The secondary calculation for bearing cutoff with compression reaction in the X- and Y-directions is given below.

$$BCCX\,,BCCY = BCC \cdot \frac{FDIABC \cdot FGEOBCC \cdot FPCTBCC}{FCSKBC \cdot FSHIM}$$ **Equation 11.4-34**

Where
BCC = material allowable for bearing with compression reaction (psi)

The secondary calculation for bearing cutoff with shear reaction in the X- and Y-directions is given below.

$$BCSX\,,BCSY = BCS \cdot \frac{FDIABC \cdot FGEOBCS \cdot FPCTBCS}{FCSKBC \cdot FSHIM}$$ **Equation 11.4-35**

Where
BCS = material allowable for bearing with shear reaction (psi)

Once the various bearing cutoff allowable values have been defined for the three types of bearing in both the X- and Y-directions, a final bearing cutoff margin of safety can be calculated. The peak bearing stress provided by this analysis is compared to the ultimate bearing stress measured in a double-shear test (minimal peaking in bearing stress) to determine the margin of safety as shown in Equation 11.4-36 below. This calculation is performed for

Copyright 2015 Lockheed Martin Corporation.
Note: The current version is always the version on the Lockheed Martin network.

both the primary and the secondary methods in subroutine SBEARMS. The method providing the lower margin of safety value will be reported in the final margin of safety summary. Note that all bearing stress values are taken as positive numbers; however, the choice of tension or compression cutoff is based on the sign of the applied stress.

Equation 11.4-36

$$M.S. = \frac{1.0}{\sqrt{\left[\frac{BRGX}{BCX} + \frac{BRGSX}{BCSX}\right]^2 + \left[\frac{BRGY}{BCY} + \frac{BRGSY}{BCSY}\right]^2}} - 1.0$$

Where
BRGX, BRGY = bearing stress components with normal reactions in X- and Y-directions, respectively (psi)
BRGSX, BRGSY = bearing stress components with shear reactions in X- and Y-directions, respectively (psi)
BCX = bearing cutoff allowable (either BCTX or BCCX as appropriate) in X-direction (psi)
BCY = bearing cutoff allowable (either BCTY or BCCY as appropriate) in Y-direction (psi)
BCSX, BCSY = bearing cutoff allowable in X- and Y-directions, respectively (psi)

11.4.4.6 Bearing-Bypass Interaction Diagrams

Bearing-bypass interaction diagrams are a very useful means to visualize the failure modes predicted by IBOLT bearing-bypass analysis. Bearing-bypass interaction plots can be generated for a given laminate using either the LAMINATE or LAM_PERCT IDAT tool.

A bearing-bypass interaction diagram for a 32-ply (25/50/25)% IM7/5250-4 Bismaleiminide (BMI) tape laminate (RTA Typical) is presented in Figure 11.4-34. The average joint strength is plotted as *Total stress (N3/t)* versus *bearing stress PX/(Dt)* for the IBOLT element shown.

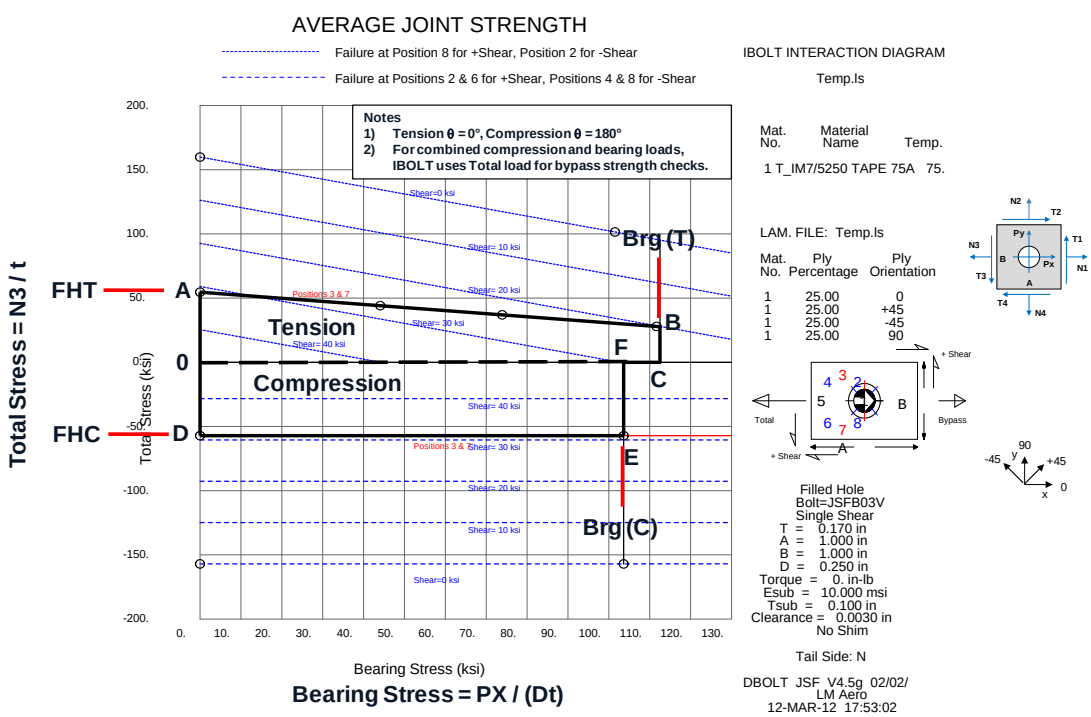

Figure 11.4-34 Bearing-Bypass Interaction Plot, Total Stress versus Bearing Stress

Copyright 2015 Lockheed Martin Corporation.
Note: The current version is always the version on the Lockheed Martin network.

For pure bypass loading with no bearing stress, the intersections with the Total stress axis correspond to the filled hole tension (FHT, point A) and filled hole compression (FHC, point D) strength of the laminate. For pure bearing loading with no bypass stress, the intersections correspond to the bearing cutoffs with a tension reaction (point C) or a compression reaction (point F).

For combined bearing-tension bypass loading (segment AB) there is in an interaction in stresses at the hole edge. The laminate strength is observed to decrease with increasing bearing stress up to point B, above which the laminate becomes purely bearing critical (segment BC).

For combined bearing-compression loading, the load orientations on the IBOLT element diagram are reversed. The total and bypass stress are reversed in direction and act in compression. Similarly, the bolt bearing load PX is also reversed and acts 180 degrees from the X-direction.

For combined bearing-compression bypass (segment DE), the experimental data generated for IM7/977-3 epoxy and IM7/5250-4 bismaelimide (tape and fabric) for IBOLT correlation indicated that failure occurs at the same total load level for a given laminate. Since the combined stress state predicted by IBOLT theory does not capture this behavior, IBOLT uses the total load level for a bypass stress state check to generate a margin of safety. IBOLT makes this adjustment automatically based on the loads input, so there is no action required by the user. Thus, segment DE is a flat line equivalent to filled hole compression.strength. For bearing stress beyond point E, the laminate becomes purely bearing critical (segment EF). It should be noted that this observed behavior for combined bearing-compression bypass may not be the case for other composite material systems. Therefore, new materials should be carefully correlated to determine if analysis adjustments are required.

Figure 11.4-35 shows a bearing-bypass interaction plot for the same laminate, but with *Bypass stress (N1/t)* versus *bearing stress* instead of *Total stress (N3/t)*. Once again, for zero bearing stress, points A and D are the filled hole tension and filled hole compression strengths, respectively. For zero bypass stress, points C and F are the bearing cutoff for tension and compression loading, respectively. For combined bearing-tension bypass, the predicted interaction results in the segment AB, beyond which the failure becomes purely bearing critical (segment BC).

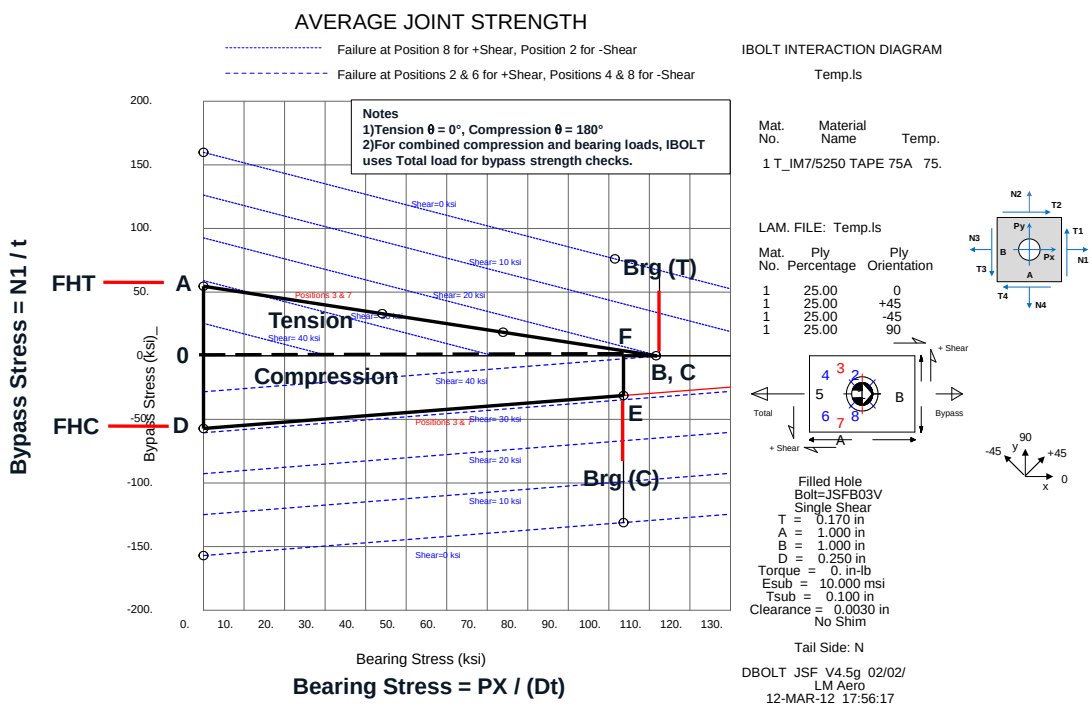

Figure 11.4-35 Bearing-Bypass Interaction Plot, Bypass Stress versus Bearing Stress

Copyright 2015 Lockheed Martin Corporation.
Note: The current version is always the version on the Lockheed Martin network.

For combined bearing-tension bypass interaction, point B *approximately* coincides with point C; that is, the bearing-bypass interaction failure mode is predominant up to a pure bearing failure (point C) with tension.

Again, for combined bearing-compression loading, the load orientations on the IBOLT element diagram are reversed. The total and bypass stress are reversed in direction and act in compression. Similarly, the bolt bearing load PX is also reversed and acts 180 degrees from the x-direction.

For combined bearing-compression bypass, the line segment D-E has a slope that results from the observation that failure occurs at the same total load level for a given laminate discussed above. That is, the laminate strength decreases as the bearing stress is increased. For bearing stress beyond point E, the laminate becomes purely bearing critical (segment EF).

11.4.4.7 Joint Testing for IBOLT Analysis Calibration

For a given material system and environment, the IBOLT program must be calibrated with a series of lamina and laminate coupon tests as outlined in Figure 11.4-36. The calibration process is sequential in nature and begins by comparing lamination theory predictions of laminate modulus (average of tension and compression) with experimental values provided by strain-gaged unnotched tension (UNT) and unnotched compression coupons (UNC). The lamina modulus value of E11 in the material data file is adjusted to provide the best correlation between measured and predicted laminate moduli.

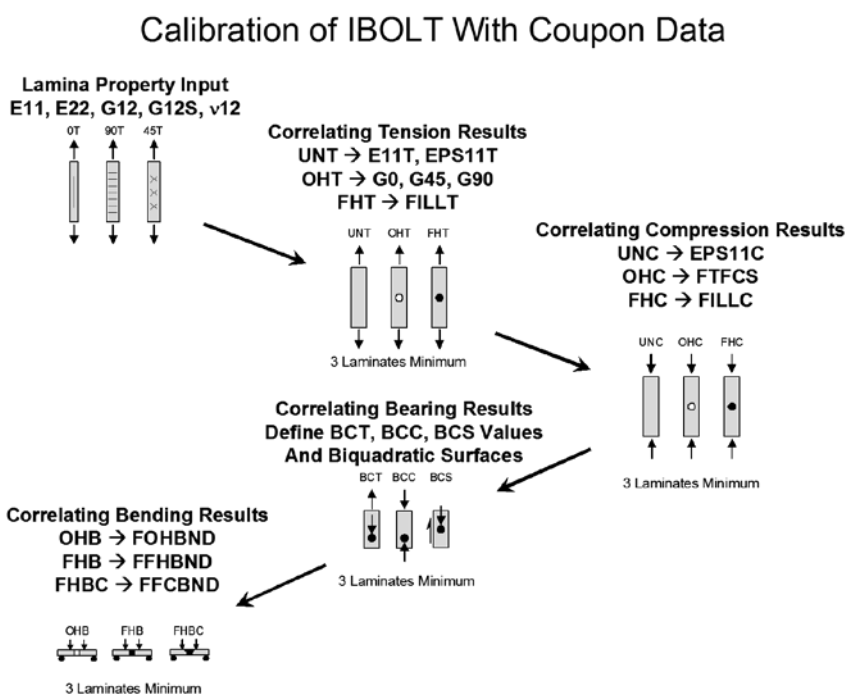

Figure 11.4-36 Empirical Calibration of IBOLT

Predicted unnotched laminate tension strength values for three or more laminates are then compared with test results to define an appropriate single value of laminate failing tensile strain EPS11T. The tested laminates exhibit fiber-dominated behavior having 0º ply percentages typically ranging from 15 to 60 percent. Since the 0º plies are the major load carrying component of the laminate, the theoretical laminate failing strain should equal the failure strain of the 0º plies – a constant value. This approach differs from the common industry practice of assigning higher failing strains to soft laminates and lower failing strains to hard laminates, but provides a sufficiently accurate estimate of the unnotched strength for use in predicting bolted joint strength. Following this, IBOLT-predicted open

Copyright 2015 Lockheed Martin Corporation.
Note: The current version is always the version on the Lockheed Martin network.

hole tension (OHT) strengths for three or more laminates are compared with test results, and values of critical ply strain energy release rate G0, G45, and G90 are adjusted to match predictions with experimental values. Next, IBOLT-predicted values of filled hole tension strength for the same set of laminates are compared with test results. Parameters defining the fill factor for tension (FFILLT) are adjusted to provide the best correlation.

A similar path is followed for correlation of compression test results with IBOLT predictions using UNC coupon data to define the best single value of laminate failing compression strain EPS11C, open hole compression (OHC) data to define compression correlation parameters (FTFCS), and filled hole compression data to specify parameters for the compression fill factor FFILLC.

The effect of ply percentage on bearing strengths involves creating biquadratic surface fits to the available test results for BCT, BCC, and BCS. The effects of fastener torque, countersink fastener head geometry and countersink depth, width, and edge distance are typically not sensitive to material type and thus can often be determined from legacy test results from previous material systems.

In the final step, notched flexure coupons containing open, filled, and filled countersunk holes are used to set parameters controlling prediction of out-of-plane moment effects (FOHBND, FFHBND, FFCBND). This process is repeated for each material system and environment of interest to define the required set of material property values. For design purposes, linear interpolation of property values for intermediate temperatures is permitted.

11.5 Methods of Analysis

Bolted joints are the most common form of joint in composite aircraft structure and are also often the limiting factor for structural efficiency and load-carrying capability. As discussed in Section 11.4.1, the behavior of composite joints leading up to failure differs significantly from metallic joints due to the relatively inhomogeneous nature of composites and their relative brittleness that leads to high stress concentrations. The specific failure mode is a function of the laminate configuration, including ply percentages, stacking sequence, thickness, and fiber/matrix material system properties. Consequently, sound fundamental theory must underlie robust analysis methodologies for mechanically fastened composite joints to maintain structural integrity, ensure efficient structural performance and to avoid unnecessary conservatism.

The composite bolted joint analysis methods discussed in this section rely on empirically calibrated analysis that is coded into the Lockheed Martin Aeronautics IDAT software tools that access a database of composite material system properties and allowables specifically prepared to support these methods. The scope of configurations and materials supported by these analysis methods is bounded by good design practices and guidelines as discussed in Section 11.3. Joint and laminate configurations that extend outside this scope cannot reliably be analyzed and IDAT Software tools will give warnings in such cases. Specific limitations for IBOLT are discussed in Section 11.5.2.7

11.5.1 Joint Analysis Overview

As discussed in Section 11.3, wherever it is practical for the given set of joint design loads, composite bolted joints should be designed to fail first in laminate bearing in order to prevent sudden, catastrophic failure, which can occur with other failure modes as described in Section 11.4. The aerospace industry has devoted considerable effort to the development of methods and tools to accurately predict bearing-bypass failure in composite bolted joints. Composite bolted joint static stress analysis methods were the subject of much early analytical development in the field of advanced composite mechanics[1]. While Garbo and Ogonowski's [2] Bolted Joint Stress Field Model (BJSFM), and purely empirical bearing/bypass interaction curve fits[3] are widely used throughout the aerospace industry, a

[1] See References 11-17, 11-18, 11-20, 11-26, 11-2811-37,11-29, 11-37, and 11-38
[2] Reference 11-17
[3] Reference 11-21

Copyright 2015 Lockheed Martin Corporation.
Note: The current version is always the version on the Lockheed Martin network.

proprietary method generally referred to by one of its FORTRAN program names, IBOLT[1] was developed by Lockheed Martin Ft Worth and is the standard across Lockheed Martin Aeronautics. IBOLT is a part of the IDAT tool Suite.

This section provides a brief overview of the IBOLT bearing and bypass analysis methodology as follows:

- IBOLT Analysis Overview
- IBOLT Analysis Procedure Summary
- IBOLT Usage

Testing reported in the literature and also conducted by Lockheed Martin Aeronautics has shown fatigue performance of properly designed and installed bolted composite joints to be generally very good as compared to metal joints. The composite portion of such joints has been shown to be fairly insensitive to fatigue in tension loading at normal operating loads. Composite bolted joints can endure long fatigue life with minimal reduction in residual strength under maximum cyclic load levels as high as 70% of the static strength. Test results have also shown that composite bolted joints are insensitive to fatigue even in severe environments. The predominant damage mechanism under cyclic loads is usually bearing failure in the form of hole elongation with net section failure for static residual test.

Section 6.3.4 of Reference 11-7 provides an overview of fatigue behavior of composite bolted joints, including sensitivity to parameters such as fastener fit, fastener torque, countersink, laminate lay-up, and environment. References 11-30, 11-32, 11-33 and 11-34 investigate the effects of variable amplitude cyclic loading on the fatigue performance of composite bolted joints. Reference 11-30 reports two lifetimes of variable amplitude cyclic loading on composite bolted joints without fatigue failure. Reference 11-33 investigates the influence of spectrum profile and load truncation levels and reports no distinguishable difference in the fatigue life for the spectrum loading investigated. Reference 11-32 generated a spectrum sensitivity database for bolted composite joints load and studied sensitivity to parameters that included frequency, spectrum truncation, stress level, extended life, temperature and moisture, and specimen size. The study reported no fatigue failures within the composite portion of bolted joint specimens.

Reference 11-32 generated extensive residual strength data that showed excellent static strength retention in composite bolted joints with the largest percentage of fatigue strength reduction observed, when compared with static strength, was 8 percent. LM Aero legacy program testing, discussed in Section 4.2.2.6 of References 11-35 and 11-36, further demonstrated composite bolted joint residual strength capability. The results of constant amplitude fatigue tests showed capability to endure the cyclic bearing loadings encountered in service. In the testing, fastener failure occurred prior to reaching any composite laminate failure criteria. Residual strength tests showed 89 percent retention of static ultimate bearing strength relative to control specimens used to set fatigue load levels and 96 percent retention of corresponding static yield strengths. This indicates that no significant degradation of the material's properties occurred during testing and that no knockdown factors are necessary to compensate for the durability of composite material experiencing cyclic bearing loading.

While the composite laminate portion of a bolted joint has been shown to be resistant to fatigue, fastener failures under fatigue loading have occurred, sometimes precipitated by composite stiffness or hole fit. The IDAT/SFBOLT program is used to analyze fastener fatigue capability in a composite bolted joint.

11.5.2 IDAT/IBOLT Strength Analysis

This section provides an overview of IDAT/IBOLT analysis and analysis procedure, along with guidelines on problem definition, analysis element orientation and dimensions and loading. This section also discusses IBOLT limitations. Refer to Section 11.4.4 and Reference 11-11 for more detailed information on the background theory.

[1] Interactive BOLTed joint analysis, Reference 11-11

Copyright 2015 Lockheed Martin Corporation.
Note: The current version is always the version on the Lockheed Martin network.

11.5.2.1 IBOLT Composite Bolted Joint Analysis Overview

For a constant width-to-diameter ratio, the bearing strength in a composite laminate depends on hole size. A fracture mechanics approach to analysis, discussed in detail in Section 11.4.4 and in the IBOLT Theory Manual[1], has shown good correlation to bearing test results and forms the basis for the IDAT/IBOLT analysis methodology. This section is extracted from Section 2.0 of Reference 11-11.

As shown in Figure 11.5-1, IBOLT performs a fracture-mechanics-based static strength prediction for a rectangular [0/±45/90] laminate family composite element with a single open or filled circular hole. The element may be subjected to a combination of biaxial membrane loads, shear loads, and an off-axis bolt bearing load. Out-of-plane bending moments are also treated. The membrane loads and shear loads are assumed to be constant along a given edge and are defined as running loads (lb/in). The bending moments are also assumed to be constant along a given edge (in-lb/in). The bolt bearing load is defined by a magnitude (lb) and an angle (deg) measured counterclockwise from the x-axis.

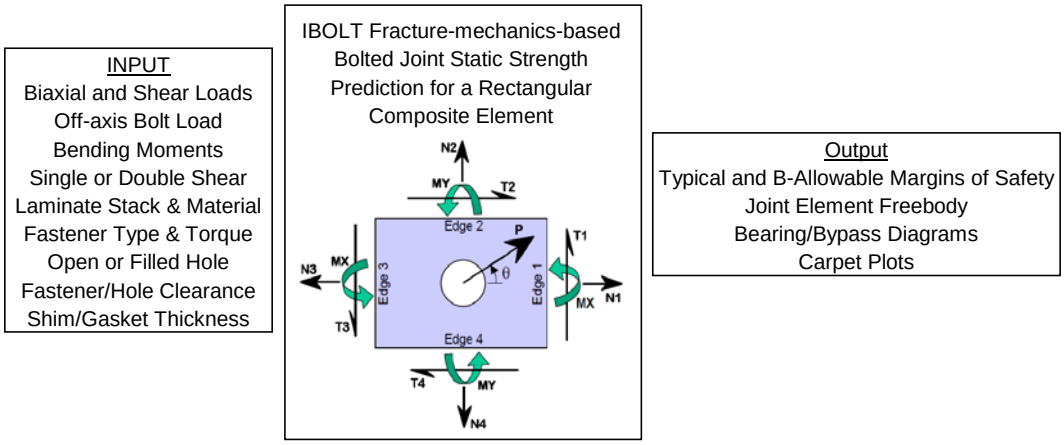

Figure 11.5-1 IBOLT Input, Joint Element, and Output

It has been observed in test results that for the [0/±45/90] family of laminates, failure occurs at or near one of the eight locations shown in Figure 11.5-2. These are the eight locations where fibers are tangent to the hole boundary. These eight failure positions are numbered sequentially counterclockwise at 45º intervals. Position 1 is located at the intersection of the hole boundary with the x-axis. The local element x-y coordinate system has its origin at the center of the fastener hole. The x-axis is defined to be parallel to the 0º ply direction. IBOLT calculates a static margin of safety at each of these eight failure locations.

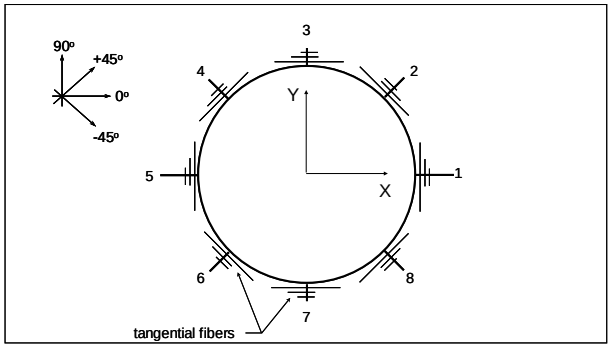

Figure 11.5-2 Observed Failure Locations for 0/45/90 Laminate Family

[1] Reference 11-11

Copyright 2015 Lockheed Martin Corporation.
Note: The current version is always the version on the Lockheed Martin network.

Composite bolted joints exhibit two distinct types of load versus deflection behavior when loaded to static failure under either combined bearing-bypass loading or pure bearing loading. The load versus deflection response for combined bearing-bypass loading is nearly linear to failure. The load versus deflection behavior for bearing load only, however, displays significant non-linearity very similar to that of a metal-to-metal joint. IDAT/IBOLT performs separate static failure analyses for these two types of loading. The basic strength model used in IDAT/IBOLT only deals with a single failure mode that addresses combined bearing-bypass failure: failure of tangential fibers near the fastener hole. For the pure bearing case with no bypass loading shown in Figure 11.5-3, other failure modes may be involved as well. IDAT/IBOLT satisfies this with a separate check on bearing strength for the no-bypass condition. This is called the bearing cutoff calculation.

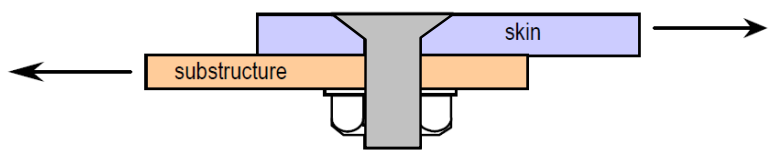

Figure 11.5-3 Pure Bearing Loading

The primary method of bearing cutoff calculation uses a beam-on-elastic-foundation analysis to provide a bearing stress profile through the thickness of the laminate. The fastener is treated as a beam resting on elastic foundations provided by the laminate and the substructure. This method accounts for laminate and substructure modulus and thickness, fixity provided by the head and nut, and provides a factor, F_{PKBC}, that is the ratio of peak bearing stress to average bearing stress. Additional factors are used to account for

- Fastener diameter, F_{DIABC}
- Edge distance- and element width-to-diameter ratio, F_{GEOBC}
- Percent 0° and 90° plies, F_{PCTBC}

To determine the margin of safety, the peak bearing stress provided by this analysis is compared to the ultimate bearing stress allowable as measured in a double-shear test which results in minimal peaking in bearing stress.

The secondary method of bearing cutoff calculation applies a series of reduction factors to the base allowable bearing cutoff values in the data file. The base allowable cutoffs represent three possible reaction states within the analysis element: bearing cutoff with tension reaction, bearing cutoff with compression reaction, or bearing cutoff with shear reaction. The applied reduction factors account for

- Diameter, F_{DIABC}
- Countersunk fastener head, F_{CSKBC}
- Edge distance-to-diameter and element width-to-diameter ratios, F_{GEOBC}
- Percent 0° and 90° plies, F_{PCTBC}

These reductions are applied in both the X- and Y-directions since F_{GEOBC} and F_{PCTBC} are functions of ply percentages, edge distance, and width and thus have different values in these two directions.

The secondary bearing cutoff analysis method applies to the rigid substructure case and no correction is made for substructure thickness and modulus. For rigid substructure, the primary method can over-predict the bearing strength. Use of the secondary analysis, if it predicts a lower bearing cutoff value, ensures that bearing strength will not be over-predicted.

In addition to the loading, other effects are treated in the IBOLT analysis. Joint configuration effects (single- or double-shear) are included in the beam-on-elastic-foundation analysis to account for the thickness and stiffness of the joint members as well as the bolt bending and shear stiffness. Empirical equations are included to account for fastener head geometry, effects of filled versus open holes, fastener-to-hole clearance, and fastener torque.

Required input, in addition to the usual geometry, loads, fastener, and substrate elastic properties, includes a variety of special laminate-level joint properties, which are included in the IDAT material files and not provided by the stress analyst. The laminate level joint properties are empirically based and must be generated for each material.

Copyright 2015 Lockheed Martin Corporation.
Note: The current version is always the version on the Lockheed Martin network.

Uniaxial notched, unnotched, and bolted-joint coupon tests are conducted to develop these properties. In addition to these uniaxial coupon tests, bearing-bypass tension and bearing-bypass compression tests have been performed to validate the accuracy of IBOLT strength predictions.

Several forms of output are provided for the analyst's convenience. Hardcopy output is available in a short one-page summary or a detailed four-page summary, depending on the level of information and insight desired. Both include an echo of input data and B-allowable and/or typical margins of safety depending on the type of material file used. Graphical output includes a free-body diagram of the joint element with an abbreviated input echo and all margins of safety. A companion program, DBOLT, creates bearing/bypass interaction diagrams for a given combination of laminate, geometry, and environment. DBOLT is accessed via IDAT from the *Reports* menu option in the LAMINATE program. A second companion program creates carpet plots of 15 different notched and unnotched properties for the [0/±45/90] laminate family. This feature is also available in IDAT using the *Carpet Plots* menu item in the MATUTL program.

11.5.2.2 IBOLT Analysis Procedure Summary

IDAT/BOLT predicts the static strength of the composite laminate in the immediate vicinity of an individual fastener hole. An individual fastener within a typical multiple fastener pattern is idealized using an IBOLT fastener element as shown in Figure 11.5-4. To apply the analysis to a typical multiple fastener pattern, the analysis is performed for each fastener of interest in the pattern using the following sequence of steps:

1. Determine the load transferred by each fastener (magnitude and direction). This task is usually done with the aid of a finite element model (FEM), but can be accomplished by spring models or by hand calculation for simple joints.
2. Define the membrane loads and bending moments present in the composite laminate in the vicinity of the fastener.
3. Select a rectangular element of composite laminate of appropriate size and draw a balanced free-body diagram of this "joint element".
4. Run the IBOLT program to obtain the margin of safety for static strength for this joint element.
5. Repeat steps 1 through 4 for each joint element of interest. The margin of safety for the joint is the minimum margin of safety obtained from any of the joint elements that were analyzed.

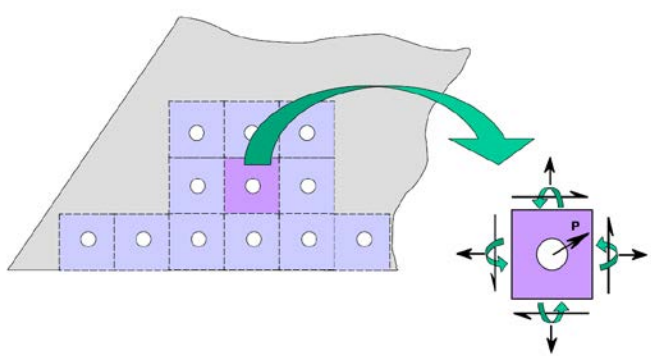

Figure 11.5-4 Composite Bolted Joint Analysis Element Definition

Section 11.6 describes in detail the process for the determination of appropriate element and fastener loads for a range of loading scenarios and joint types. The IBOLT Users Guide, Reference 11-18, provides comprehensive details for execution of IBOLT, formats for input and output, and instructions for selection of parameters and options discussed in this manual.

Copyright 2015 Lockheed Martin Corporation.
Note: The current version is always the version on the Lockheed Martin network.

11.5.2.3 IBOLT Problem Definition

Proper definition of the IBOLT joint input parameters is a key step in the analysis process and crucial to obtaining valid margins of safety. These parameters include definition of the operating environment, selection of the statistical basis for the material properties, definition of the ply stacking sequence, joint element and hole geometries, all load components, and various joint parameters. The joint parameters include information which has a direct effect on the strength of the joint such as whether it is an open or filled hole, and if filled, what type of fastener, hole clearance, the applied fastener torque and whether the head or tail is against the composite material. Other inputs include whether the joint is single or double shear, the stiffness of the substructure in the form of substructure modulus and thickness, if there is a shim or gap and how thick it is. The input parameters required for IDAT/IBOLT input are summarized in Table 11.5-1.

Table 11.5-1 IBOLT Input Parameter Summary

Category	Units	Description	Category	Units	Description
Laminate		Material	Joint		Hole Type (Filled, Open)
		Environment (Temperature, Moisture)			Bolt Part Number
		Statistical Bases for Properties (Design/Typical)			Bolt Orientation (Head, Tail)
		Stacking Sequence (Layup)			Interface Type (Frictionless, Other)
Geometry	in	Hole Diameter		in	Hole Clearance
	in	Element Length (A) and Width (B)		in-lb	Torque
Loads	lb/in	Normal: N1, N2, N3, N4		in	Deep Countersink High Side
	lb/in	Shear: T1, T2, T3, T4		deg	Deep Countersink Angle
	lb	Bolt Load			Joint Type (Single Shear, Double Shear)
	deg	Bolt Load Orientation Angle		psi	Substructure Modulus
	in-lb/in	Mx, My, Mxy		in	Substructure Thickness
		Moment Type: Unconstrained or No Curvature along x or y axis			Shim Type (None, Gap, Hard Shim)
				in	Shim Thickness

Accurate composite bolted joint analysis with IBOLT requires the analyst to ensure that IBOLT problem formulation aligns with theoretical assumptions coded in IBOLT. Modeling practices must ensure appropriate IBOLT problem formulation to address assumptions such as

- Definition of the IBOLT joint element discussed in Section 11.5.2.4
- Development of IBOLT Free-Body loads (discussed in Sections 11.5.2.6 and Section 11.6)
- Limitations in the IBOLT formulation discussed in Section 11.5.2.7

In the selection of statistical basis for the material properties, the analyst should always choose “design” unless predicting failures for test articles.

11.5.2.4 Element Orientation

Correct orientation of the IBOLT element is achieved by aligning the element x-axis with one of the four fiber directions for the [0/±45/90] laminate family. Figure 11.5-5 shows four elements, A-D, that are correctly aligned and one element, E, that is incorrectly aligned. As discussed previously, the 8 failure locations evaluated by IBOLT

Copyright 2015 Lockheed Martin Corporation.
Note: The current version is always the version on the Lockheed Martin network.

are located at the 8 points where the plies are tangent to the boundary of the fastener hole as shown in Figure 11.5-2. Unless the element is aligned with one of the four laminate ply directions, these failure locations will not correspond with the tangency points, and the analysis will be invalid. Along structural boundaries that are not parallel to one of the four ply directions, one corner of the IBOLT element boundary may be allowed to extend beyond the physical edge of the structure as shown in Element D, Figure 11.5-5. Note that Element E orientation could be brought into proper alignment by rotating in -15º so that it matches the alignment of Element D.

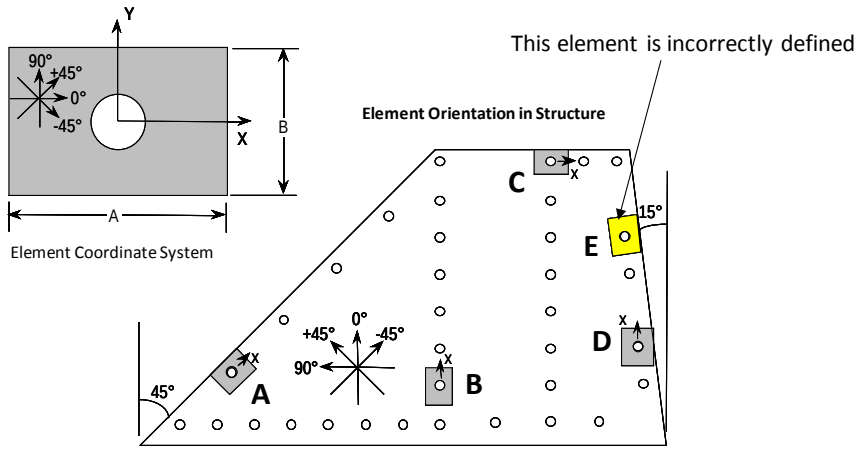

Figure 11.5-5 Example IBOLT Element Orientations

The element may be aligned with any one of the four fiber directions as convenient and loads must be oriented to correspond to the element. If the element x-axis is aligned with a fiber direction other than the 0º direction, the laminate ply percentages will have to be redefined. For example, Element A, shown in the lower left of Figure 11.5-5**,** is aligned with the -45º fiber direction. If the laminate in the structure orientation is a (50/20/20/10) laminate, the IBOLT ply percentages must be redefined as in Table 11.5-2.

Table 11.5-2 Laminate Redefinition for IBOLT Element A of Figure 11.5-5 Reoriented to Align with -45º Fiber Direction

Ply Angle (degrees)	Laminate (percent)	IBOLT Analysis (percent)
0	50	20
+45	20	50
-45	20	10
90	10	20

11.5.2.5 Element Dimensions

The IBOLT analysis routine treats each joint element as an isolated entity with uniform loads applied along the element edges as shown Figure 11.5-6. Since fasteners are typically embedded in a fastener row or pattern, the fastener pitch or spacing, *s*, is used to establish the IBOLT element dimensions A and B.

Copyright 2015 Lockheed Martin Corporation.
Note: The current version is always the version on the Lockheed Martin network.

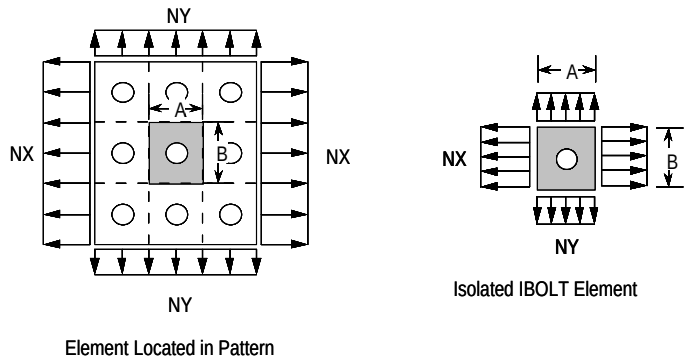

Figure 11.5-6 Standard Joint Element Boundary Midway between Fastener Locations

Per the fastener design guidelines discussed in Section 11.3, fastener spacing should be between 4D and 8D and the hole center to edge distance should be 2.5D or greater where D is the fastener hole dimension. For fastener spacing within the fastener spacing guidelines, the usual assumption is to define element boundaries midway between the adjacent fastener locations as shown in the left hand side of Figure 11.5-6. This is a conservative assumption since the proximity of the other fastener holes tends to lessen the stress concentration effects when compared to those of the isolated element. This is due to the "shadowing" relief effect that is provided by the adjacent fasteners.[1]

The A and B element dimensions do not necessarily have to be equal, but the fastener hole should always be centered within the IBOLT element. The dimension in a given direction can be extended if there are no neighboring fasteners or structural boundaries in that direction. However, the strength reduction effect of a neighboring hole or structural boundary tends to dampen out at a distance of approximately 2.5D from the fastener hole center.

For fastener spacing between 4D and 5D, the IBOLT analysis element fastener hole center-to-edge-distance is below the minimum of 2.5D and the resulting reduction in strength is conservative since there is really not an edge effect in a continuous panel. For this spacing, the IBOLT element dimensions can be extended to 5D to mitigate this knockdown provided that the same running loads (load per unit length) for the multi-fastener region are applied to the isolated IBOLT element.

For non-routine situations, such as the material review of discrepant parts, in which the fastener spacing is below the recommended minimum of 4D but greater than or equal to 3D, the short edge distance of the analysis element will result in a conservative strength knockdown. In order to mitigate margins in such situations, an exception can be made whereby the IBOLT element dimension can be extended to 5D or to the center of the adjacent hole, whichever is less, provided that the same running loads for the multi-fastener region are applied to the isolated IBOLT element. **This approach should never be used for design.**

For non-routine situations in which the fastener spacing is above the recommended guideline of $s \geq 8D$, such as for mitigation of a material review issue, the actual fastener spacing may be used for up to 10D which is the IBOLT maximum allowable dimension for analysis. **This approach should never be used for design.**

The recommended guidelines for setting IBOLT element dimensions are summarized in Table 11.5-3.

[1] Parametric studies of open hole stress concentration factors (SCF) in isotropic plates have been conducted to compare models of multi-fastener patterns versus an idealized isolated finite plate with a single hole. The results for fastener spacing from 4D to 8D indicate that the peak SCF is approximately 6 to 25% greater for the isolated finite plate with boundaries midway between adjacent fasteners.

Copyright 2015 Lockheed Martin Corporation.
Note: The current version is always the version on the Lockheed Martin network.

Table 11.5-3 IBOLT Element Dimension Guidelines

Fastener Pitch or Spacing, *s*	IBOLT Element Dimensions	Comment
3D ≤ s < 4D Discrepant Material Review only	A=B=5D	Below Recommended fastener spacing guidelines of 4D ≤ s ≤ 8D
4D ≤ s < 5D		Within recommended fastener spacing guideline. IBOLT dimension can be extended to 5D
5D ≤ s < 8D	A=B=S	Within recommended fastener spacing guideline
8D ≤ s < 10D Discrepant Material Review only		Exceeds recommended fastener spacing guidelines of 4D ≤ s ≤ 8D
s ≥ 10D Discrepant Material Review only	A=B=10D	Exceeds recommended fastener spacing guidelines of 4D ≤ s ≤ 8D

For IBOLT elements located on structural boundaries, the loading determines the appropriate element A and B dimensions. As stated in Section 11.3, the recommended guideline is that the fastener hole center-to-edge-distance should be 2.5D minimum. As an example, four cases are shown in Figure 11.5-7 and the predominant loading is as shown.

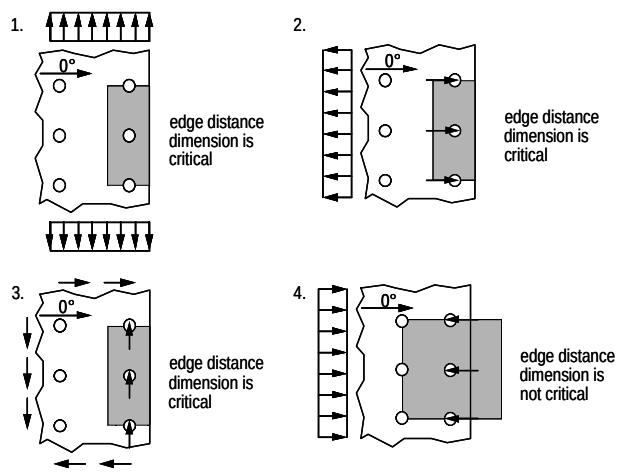

Figure 11.5-7 Example of IBOLT Element Defined as a Function of Predominant Load

For Cases 1 through 3, the location of the structural boundary, *i.e.*, edge distance is critical to the strength of the joint element because of the loading direction. In these cases, the joint element boundary must coincide with the actual structural boundary. In the direction parallel to the boundary, the element can extend to the center of the next fastener hole. For case 4, the bearing load is acting away from the edge of the part, and the element boundary can be extended as shown to reduce the short edge distance effect within the IBOLT element. If loading is a combination of load Cases 1 and 4, the element size shown in Case 1 would be appropriate to avoid unconservative results.

In actual practice, panel loads are not always as predominately unidirectional as shown in Figure 11.5-7 and engineering judgment must be used to determine if the transverse load is sufficiently small enough to allow the element dimension to be extended as shown in Case 4. Two guidelines should be considered in this case:

- The critical bearing-bypass strength margin should be located on the compression side of the hole.
- For the bearing cutoff strength margin, the fastener load angle should be normal to the edge within 30º, which equates to a ratio of load components, *PX/PY*, less than 0.58.

Four additional cases are shown in Figure 11.5-8. In each of the four cases in this figure, the element boundaries are not aligned with the structural boundaries. The same guidelines discussed above for Figure 11.5-7 apply to these

Copyright 2015 Lockheed Martin Corporation.
Note: The current version is always the version on the Lockheed Martin network.

four cases. In all cases, the IBOLT elements should be oriented as discussed in Section 11.5.2.4, the hole must be located in the center of the IBOLT element and the element must be aligned with one of the four fiber directions.

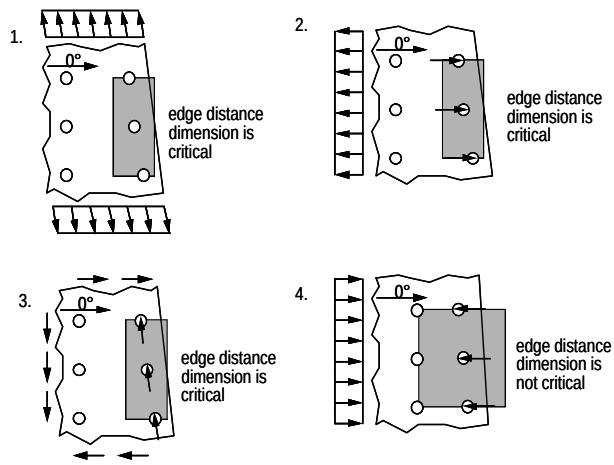

Figure 11.5-8 Example of IBOLT Element Defined as a Function of Predominant Load: Angled Boundary

11.5.2.6 Element Loads

This section provides insight to what is expected for each of the load inputs to IDAT/IBOLT. Section 11.6 provides a discussion of how the loads may be determined for a given set of load components and element scenarios. Figure 11.5-9 depicts the IBOLT free-body loads.

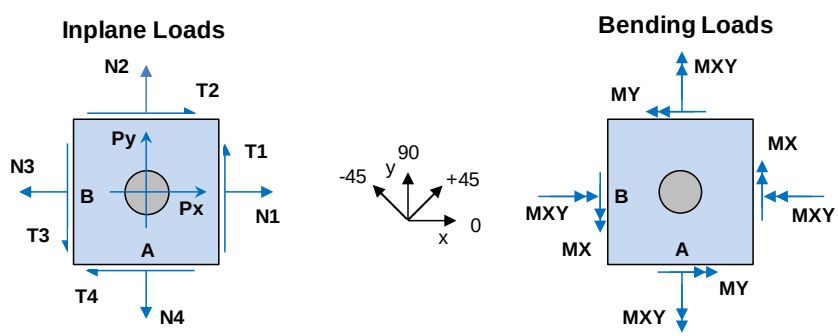

Figure 11.5-9 IBOLT Fastener Element and Free-Body Loads

The bolt load, P (lbs), is the magnitude of the resultant fastener load applied on the element hole boundary. The individual component bolt loads, P_x and P_y are depicted in Figure 11.5-9. The resultant fastener load is the bearing load transfer between the composite skin panel and substructure member. IBOLT assumes the fastener hole is centered within the IBOLT element. The bolt load is input as a positive number.

The resultant fastener load may be oriented in any direction within the IBOLT element. The orientation is input by specifying the angle between the resultant bolt load and the x-axis. This angle, θ, is measured in degrees and is counterclockwise positive with respect to the x-axis. The angle θ must be between ±360 degrees. IBOLT uses the angle and the resultant bolt load to calculate the x and y components of the bolt load, P_x and P_y, as

$$P_x = P\cos\theta$$
$$P_y = P\sin\theta$$

Copyright 2015 Lockheed Martin Corporation.
Note: The current version is always the version on the Lockheed Martin network.

The normal and shear in-plane force resultants acting along the four element boundaries are given as N_1 through N_4 and T_1 through T_4. These are running loads with units of lbs/in. These loads are a combination of fastener bearing load reaction and skin bypass loads transferred across the joint. The positive orientation of each force resultant is shown in Figure 11.5-9. A different constant value may be input for each of the force resultants provided that the element is in static equilibrium. This is described in more detail in Section 11.6.

The flexural bending moment resultants that act along the element boundaries are given by M_x, M_y, M_{xy}. These are given per unit length so the units are in-lbs/in. The moment resultants are bypass type loads meaning that they are assumed to be applied along the edges of the IBOLT element as opposed to reacted at the fastener. All three moment resultants can be specified by the user.

The user may also specify curvature constraints on the element in conjunction with or in lieu of specifying moments in each of the directions. There are various options:

- Unconstrained – User inputs all three out-of-plane moment values.
- M_x specified plus no curvature along the y-axis – Analyst specifies M_x, IBOLT calculates the values of M_y and M_{xy} required to maintain cylindrical curvature
- M_x specified but unconstrained along the y-axis – M_x is specified but IBOLT allows the laminate to deform freely without constraint
- M_y specified plus no curvature along the x-axis – Analyst specifies M_y, IBOLT calculates the values of M_x and M_{xy} required to maintain cylindrical curvature
- M_y specified but unconstrained along the x-axis - M_y is specified but IBOLT allows the laminate to deform freely without constraint

More information can be found in The IBOLT User's Guide, Reference 11-24.

Moment resultants are usually neglected for preliminary sizing. Moment resultants predicted by geometrically linear finite element analysis may not be accurate and should be used with caution. In-plane (N_x, N_y, N_{xy}) and bending (M_x, M_y, M_{xy}) loads induced by panel curvature and/or normal panel pressure usually require geometrically nonlinear analysis for accurate load prediction to account for membrane-flexural coupling.

11.5.2.7 IBOLT Limitations

It is important that the analyst is knowledgeable about and understands the limitations of the IBOLT program in order to ensure that the analysis is valid and correct. Table 11.5-4 summarizes the program limitations and provides design guidance.

Copyright 2015 Lockheed Martin Corporation.
Note: The current version is always the version on the Lockheed Martin network.

Table 11.5-4 Summary of IBOLT Program Limitations and Design Guidance

Description	IBOLT Program Limitations	Recommended Design Limitations
[0/45/90] Laminate Family	Only valid for this family of laminate orientations; **no other ply angle permitted**	Use [0/45/90] Laminate Family
Minimum and maximum percent of plies, each orientation[1]	7% < 0 < 60% 7% < -45 < 60% 7% < +45 < 60% 7% < 90 < 60%	8% ≤ 0 ≤ 60% 8% ≤ -45 ≤ 60% 8% ≤ +45 ≤ 60% 8% ≤ 90 ≤ 60%
Orientation of IBOLT element	The IBOLT element edges must be aligned with one of the four ply directions	Align element edges with one of four ply directions and and not necessarily with the edges of the structural boundary.
Element loading	The boundary loads are assumed to have a constant magnitude along any given element boundary.	Define element loads appropriately using combinations of load components to achieve appropriate variations in loads. See Section 11.6 for assistance.
Bearing strength calculation	Empirically based. The smaller of 2 failure calculations as described in Section 11.5.2.1	Automatically done in IBOLT – no further action required
Element Geometry	The IBOLT element must be rectangular with length and width values between 2 fastener diameters and 10 fastener diameters. Hole is in the center of the IBOLT element.	**Design:** Fastener spacing must comply with 4D minimum and 8D maximum for design. Table 11.5-3 and associated discussion describes definition of IBOLT element within these parameters. **Discrepant material disposition only:** Fastener spacing may deviate to as low as a minimum of 3D and above 10D; see Table 11.5-3 and associated discussion for definition of IBOLT element.
Number of different materials	3	Use no more than 3 materials in definition of hybrid laminates
Maximum allowable hole size	1.0 in based on testing up to 0.75 in.	For holes above 1.0 in diameter use alternative methods of analysis.
Materials available for analysis	For an IBOLT analysis to be performed on a particular material, IBOLT empirical constants must be developed.	Select available materials for design or plan to perform coupon level testing to develop empirical constants.

11.5.3 Fastener Pull-Through Analysis

Composite laminates are weak in the out-of-plane direction, and interlaminar, matrix failure modes. Any design features that induce loads in this direction must be checked. All composite skin and cover structure subjected to fastener tension induced loads from panel pressure and curvature effects must be analyzed at the substructure

[1] The IDAT/IBOLT analysis tool is capable of analyzing laminates with a minimum of 7% 0, +45, -45 or 90 degree plies. The recommended design minimum of 8% is intended to mitigate the risk of a shear out or cleavage tension failure.

Copyright 2015 Lockheed Martin Corporation.
Note: The current version is always the version on the Lockheed Martin network.

attachment for fastener pull-through and interlaminar shear (ILS) failure modes. Fastener pull-through is a failure mode where the fastener head or tail pulls partially or completely through the laminate due to a tension load parallel to the axis of the fastener trying to separate one layer from another. This section provides guidance for performing these analyses.

Fastener pull-through should be analyzed at the fastener location using loads derived per the method defined in Section 11.6. The interlaminar shear analysis should consider the worst case out-of-plane shear load due to the applied load and substructure attachment heel-toe reaction.

Figure 11.5-10 defines the pull-through analysis geometry. The analysis methodology described below makes the following assumptions:

1. The bolt pull-through load, *P*, is the only load acting and does not account for any other sources of interlaminar shear that may be present. Note that the methodology for analysis of interlaminar shear in bolted joints is discussed in Section 11.5.4.
2. Moments applied to the bolt are not considered. The bolt should be analyzed separately for combined bending, tension, and shear.
3. For hybrid laminates consisting of two or more composite material systems, the interlaminar shear allowable for the material with the lowest value of F_{13}^{su} should be used to calculate the margin of safety. The exception to this is an all tape laminate with fabric surface plies where the interlaminar shear allowable for the tape plies is the appropriate value.
4. For flush head fasteners, the fastener head diameter is used as shown in Figure 11.5-10. If the fastener head is recessed, the laminate thickness is not accounted for.

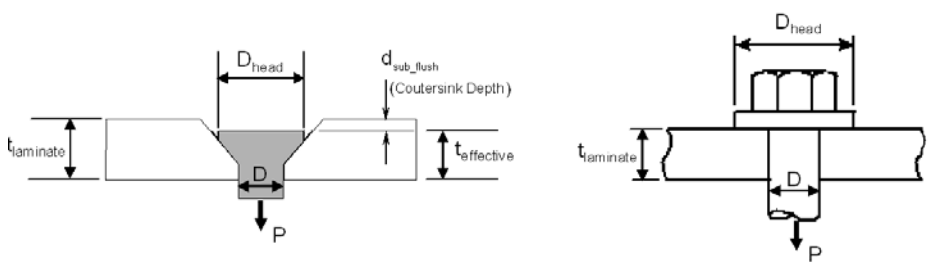

Figure 11.5-10 Fastener Pull-Through Analysis Geometry

The total pull-through load for analysis is the sum of the pull-through loads due to panel pressure loading and due to curvature effects. Panel pressure loading is discussed in Section 11.6.6.

$$P = (p_{tu})_{pressure} + (p_{tu})_{curvature} \qquad \textbf{Equation 11.5-1}$$

Where
p_{tu} is the fastener pull-off load (lbs)

Flush head fasteners located on external skins and panels may have program requirements to be countersunk below the skin surface some prescribed distance, d_{sf}. This sub-flush distance must be accounted for in the analysis since it reduces the ability of the laminate to resist pull-through. As a reference, recent LM programs have used a sub-flush depth value of 0.011 inch for fixed skins and 0.002 inch for removable panels. This is generally documented in fastener installation specifications.

Additionally, external skins may have non-structural plies such as random fiber mat and expanding copper mesh or other lightning strike protection. The thickness of these plies must also be discounted in the calculation of the pull-through allowable since they are considered ineffective in resisting pull-though.

Copyright 2015 Lockheed Martin Corporation.
Note: The current version is always the version on the Lockheed Martin network.

The pull-through effective thickness can be calculated as

$$t_{eff} = t_{lam} - (d_{sf} + t_{ns}) \qquad \textbf{Equation 11.5-2}$$

where
t_{lam} is the total laminate nominal thickness (in)
d_{sf} is the distance below the surface that the countersink head is located (in)
t_{ns} is the thickness of all of the non-structural material (in)

The fastener pull-through shear stress, f_{PT}, is calculated using the following equation:

$$f_{PT} = \frac{P}{\pi D_{head} t_{eff}} \qquad \textbf{Equation 11.5-3}$$

where
t_{eff} is the effective laminate thickness, defined by Equation 11.5-2 (in)
D_{head} is the diameter of the fastener head, if countersink fastener is used, as shown in Figure 11.5-11(in)
D_{head} is the diameter of the washer, if protruding head fastener is used, as shown in Figure 11.5-11 (in)

The fastener pull-through margin of safety is calculated using the following equation:

$$M.S. = \frac{F_{13}^{su}}{f_{PT}} - 1 \qquad \textbf{Equation 11.5-4}$$

where
F_{13}^{su} = B-basis interlaminar shear stress allowable (TAU13) in the IDAT MATUTL database (psi)

This analysis approach has been codified into the IDAT program PULLTHRU, with a few exceptions. Rather than using the fastener head diameter from the fastener specification, as would be done by hand, the fastener head diameter is calculated based on the fastener shank diameter input by the user along with coefficients for a linear fit contained in the IDAT fastener database. Therefore, the fastener head diameter used in the pull-through analysis and reported in the PULLTHRU output will not exactly match the fastener head diameter reported in the fastener specification and the resulting allowable will be slightly different. IDAT/PULLTHRU is fully documented in Reference 11-39. Table 11.5-5 provides a list of pertinent parameters for PULLTHRU and recommended inputs. Note that the laminate thickness input to the program should be that calculated from Equation 11.5-2.

Table 11.5-5 Input Guidance for IDAT/PULLTHRU

IDAT/PULLTHRU Input	Units	Discussion
Laminate thickness	in	Enter t_{eff} from Equation 11.5-2
Bolt Diameter	in	Nominal Bolt Diameter
Bolt Load	lbs	P = total bolt pull-through load from Equation 11.5-1
Material Definition		Select material from a pull down menu. If a hybrid material, select material with lowest τ_{13}, unless second material is only outer ply protection.
Bolt Part		Select appropriate bolt from pull down menu. If bolt is not available, select bolt with same head geometry.

11.5.4 Other Laminate Strength Checks

There are some additional laminate analyses required at joints. All of these are not applicable in all situations but only when the loading or geometry dictates. The sections below describe both the applicable situations and the analysis.

Copyright 2015 Lockheed Martin Corporation.
Note: The current version is always the version on the Lockheed Martin network.

11.5.4.1 Interlaminar Shear Analysis

Interlaminar shear strength analysis is sometimes required at panel edges where large panel shear and moments are reacted. In the case of skin joint shown in Figure 11.5-11, the skin moment is effectively reacted by the double fastener row. The panel moment is reacted by pull-off load on the inner fastener and heel-toe reaction at the edge. In this configuration, the combination of IDAT/IBOLT and IDAT/PULLTHRU analyses is sufficient to cover all expected failure modes in the composite laminate. A balanced free-body diagram, including all relevant shears, moments, and heel-toe reactions must be developed in order to determine the proper value of the induced fastener tensile load, p_{tu}. IBOLT analyses in these instances should use the moment at the fastener line, and (usually) the "No Curvature along y(x)-axis" option.

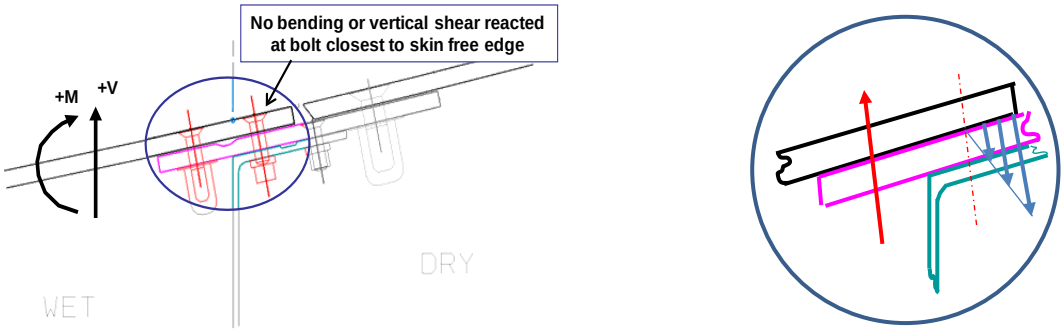

Figure 11.5-11 Typical Edge-of-Part Fastener Configuration

In the case of the skin joint, shown in Figure 11.5-12, the panel moment is reacted by a single fastener row. The moment can become sufficiently large such that IBOLT and PULLTHRU analyses do not cover a potential free-edge delamination failure mode due to the heel-toe reaction force between the fastener row and the edge of the part.

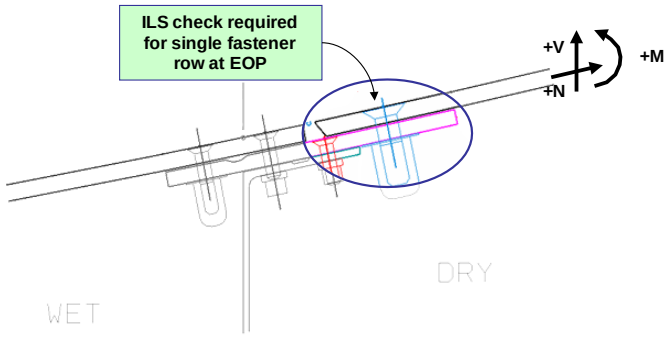

Figure 11.5-12 Single Row Edge-of-Part Fastener Configuration

Thus, if a heel-toe reaction is occurring at the edge of part of a single-row bolted joint such as is shown in Figure 11.5-12, an additional strength check must be made. The applied loads and free-body diagram for this configuration are shown in Figure 11.5-13.

Copyright 2015 Lockheed Martin Corporation.
Note: The current version is always the version on the Lockheed Martin network.

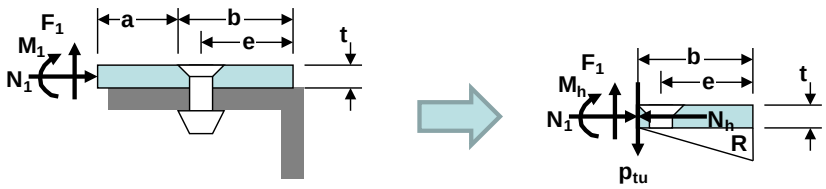

Figure 11.5-13 Applied Loads and Free-Body Diagram of Single Row Edge-of-Part Fastener Joint (Positive Sign Convention)

Note that the heel-toe reaction force is a contact force that changes location if the moment, M_h, at the fastener is reversed. For the positive sign convention, shown in Figure 11.5-13, M_h, given by Equation 11.5-5, is greater than zero and produces the heel-toe reaction on the outside of the single fastener row toward the free edge of the part. The moments reacted by the fastener and from in-plane load path eccentricity in the bolted joint are assumed to be small relative to the other moments and are therefore neglected. In this positive loading case, the interlaminar shear margin must be calculated. If M_h is reversed, resulting from one or both of M_1 and F_1 being of opposite sign from that depicted in Figure 11.5-13, it produces the heel-toe reaction on the inside of the single fastener row, *i.e.*, away from the free edge of the panel. In this case, the interlaminar shear stress outside the fastener row is benign and does not need to be checked and the pull-through check discussed in Section 11.5.3 is sufficient to show interlaminar shear strength at the fastener.

The moment at the fastener head, M_h, must be determined from a suitable loads model. Typically, in-plane axial load, out-of-plane shear and bending moment values are extracted from a finite element model some distance away from the fastener and an equivalent moment is calculated as follows

$$M_h = M_1 + F_1 \cdot a \qquad \textbf{Equation 11.5-5}$$

Where
M_h is the moment at the leading edge of the fastener, *i.e.*, toward panel (in-lb)
M_1 is the moment in panel prior to fastener line(in-lb)
$F_1$is the transverse shear load in panel prior to fastener line (lb)
a is distance from the load to the leading edge of the fastener (in)

Alternatively, a detailed finite element model that matches fastener location to node location and adequately captures the heel-toe behavior may provide a suitable moment value at the fastener node which can be used directly as M_h.

The interlaminar shear stress, f_{ILS}, is computed at design ultimate load (DUL) using the formulation for maximum shear stress in a rectangular section and assuming the resultant heel-toe shear, V, is acting 2/3 of the distance from the fastener leading edge to the edge of part as shown in Figure 11.5-13. The interlaminar shear stress may be determined as follows:

$$A = w_{eff} t$$

$$V = \frac{M_h}{\frac{2}{3} b} = \frac{3M_h}{2b}$$

$$f_{ils} = 1.5 \frac{V}{A} = 1.5 \left(\frac{3M_h}{2b}\right)\left(\frac{1}{w_{eff} t}\right) = 2.25 \frac{M_h}{w_{eff}} tb \qquad \textbf{Equation 11.5-6}$$

where
V is the transverse shear heel-toe load (lbs)
A is the cross-sectional area (in^2)
M_h = moment at the leading edge of the fastener (in-lb)
w_{eff} = lower of fastener spacing or 4D (where D = fastener hole diameter) (in)
t = laminate structural thickness (in), t_{eff} of Equation 11.5-2
b = e + D_h/2 (where D_h is fastener head diameter) (in)

Copyright 2015 Lockheed Martin Corporation.
Note: The current version is always the version on the Lockheed Martin network.

The dimension *b*, the distance from the leading edge of the hole to the edge of part, rather than *e*, should be used for the heel-toe reaction force distribution based on coupon test correlation results. Note also that no net section reduction factor is needed beyond the proper use of w_{eff}.

The margin of safety is calculated as follows:

$$MS = \frac{F_{13}^{su}}{f_{ils}} - 1 \qquad \textbf{Equation 11.5-7}$$

Where
F_{13}^{su}= B-basis interlaminar shear stress allowable (TAU13) in the IDAT/MATUTL database. (psi)

The interlaminar shear stress allowable, F_{13}^{su}, should correspond to the appropriate critical environmental condition. Also for hybrid laminates with more than two plies of fabric, the lowest F_{13}^{su} allowable should be selected.

11.5.4.2 Shear Tear-Out

If a fastener is located less than the recommended 2.5D from the edge of the part, in a metallic material a calculation would be made for shear tear-out. Shear tear-out is a mode of failure when the material between the fastener and the edge of the part fails in shear as is shown in Figure 11.5-14.

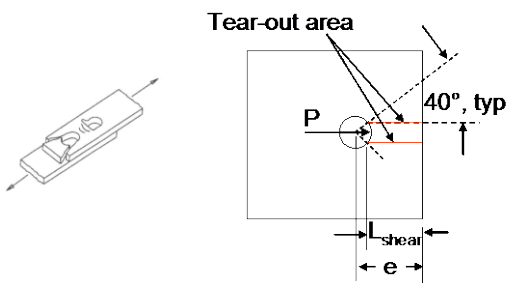

Figure 11.5-14 Illustration of Shear Tear-Out Failure

This mode of failure does not require a separate hand check in composite materials analyzed using IDAT/IBOLT. Shear tear-out is covered in the IDAT/IBOLT analysis through reductions in bearing allowables due to reduced edge distance.

11.5.4.3 Net Section Tension

Net section tension and compression are some of the failure modes checked by IDAT/IBOLT which factors in ply orientations, ply percentages, bolt-to-hole clearances, countersink or no countersink, notch sensitivity and so forth. No additional check for net section is required.

11.5.5 Fastener Analysis

Joint stiffness and development of individual fastener loads within a fastener pattern is discussed in 11.6.5. In that section, theory and margin calculations focus on characterizing the capability of the composite laminate at the bolted joint near the fastener. The high stiffness and brittle nature of the composite material also create special considerations for the analysis of the fastener in a composite material.

Copyright 2015 Lockheed Martin Corporation.
Note: The current version is always the version on the Lockheed Martin network.

This section discusses the preferred methodology for fastener static and fatigue analysis in a composite laminate. This methodology is encapsulated in the IDAT/SFBOLT tool. The purpose of SFBOLT is to provide static and fatigue margins of safety for the fastener in a single-shear bolted joint.

11.5.5.1 Fastener Static Strength Installed in Composite Laminates

The fastener static strength analysis methodology in PM4057, Section 5.2.3.3, Reference 11-1 with minor adjustment, is valid for a fastener in a joint with a composite member. This section identifies the differences in the analysis that are specific to a fastener in a composite bolted joint and should be used in the method of Reference 11-1. These differences involve assumptions related to load distribution, effective thickness, and moment arm calculation. These differences are implemented in the IDAT/SFBOLT tool.

In the analysis of bolted joints, whether all metal, hybrid metal-composite or all composite, the following assumptions are made:

- Friction loads between joint members are neglected
- Bolt bending moment caused by load eccentricity is reacted within the bolt and at bolt head and nut
- Moment reactions at bolt head and nut induce tensile stresses in the fastener shank

The first difference from the method of Reference 11-1 is the assumed load distribution in the composite material. An assumed distribution of bearing stress is utilized to calculate bolt bending moment and bending-induced tensile load in the bolt. The bolt free-body diagram shown in Figure 11.5-15 is used for the static analysis. The assumed through-the-thickness distribution of bearing stress in each of the joint members is dependent on the type of material present. For metallic joint members a uniform distribution of bearing stress is assumed, while for composite joint a triangular bearing stress distribution is assumed up to the thickness of the composite layer, transitioning to a trapezoidal and finally a uniform distribution at increasingly higher bolt loads.

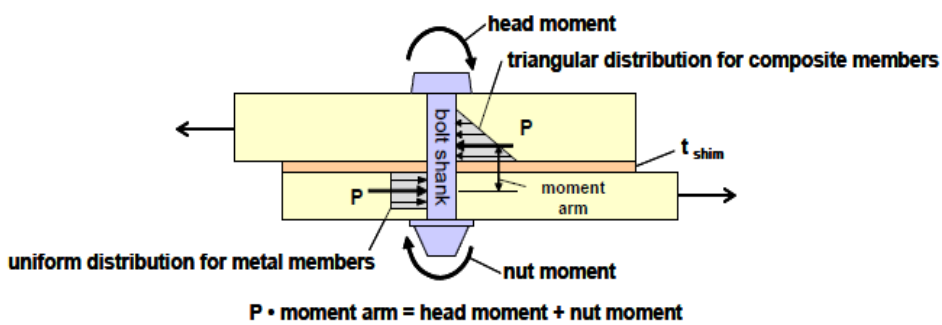

Figure 11.5-15 Bolt Free-Body for Static Analysis

The effective thickness required to support the bearing load is dependent on the ultimate bearing stress value for the joint member. The effective thickness is the minimum value required to support the applied load and is given by the following equations for composites, based on a triangular stress distribution.

$$P = \frac{1}{2} F_{bru} D t_{eff}$$

$$t_{eff} = \frac{P}{\frac{1}{2} F_{bru} D}$$ **Equation 11.5-8**

where
t_{nom} = Nominal laminate thickness (in)
t_{eff} = Calculated effective thickness (in), not to exceed t_{nom}
P = Applied load (lbs)
F_{bru} = Ultimate bearing strength (psi)
D = Fastener diameter (in)

Copyright 2015 Lockheed Martin Corporation.
Note: The current version is always the version on the Lockheed Martin network.

If the applied load requires more bearing area than provided by the triangular distribution across the full laminate thickness, t_{nom}, then the triangular distribution transitions to a trapezoidal distribution and eventually to a uniform distribution until the full applied load can be supported. For the purpose of calculating t_{eff}, the peak bearing stress is held at F_{bru} as long as the full applied load can be supported. The resultant bearing load, irrespective of distribution shape, is assumed to act at the centroid of the distribution. The generalized equation for calculating the moment arm, L_{arm}

$$L_{arm} = kt_{eff,skin} + t_{shim} + kt_{eff,sub}$$ **Equation 11.5-9**

where
$t_{eff,skin}$ is the skin effective thickness (in)
$t_{eff,sub}$ is the substructure effective thickness (in)
t_{shim} is the shim (or gap) thickness (in)
k is the factor locating the centroid of the bearing distribution and is 0.333 for triangular bearing distribution in composites, 0.5 for trapezoidal and rectangular bearing distribution in composites and 0.5 for the rectangular bearing distribution in metals

The effective thickness for skin and substructure should be calculated as appropriate for the material from which they are made. Similarly k should be chosen to be consistent with the material and stress level for the individual layer. Note that as the effective skin calculation for composite transitions from triangular, to trapezoidal, and then rectangular the value for k transitions from 0.333 for triangular to 0.5 for trapezoidal and rectangular bearing distributions.

The bolt moment is then given by

$$M = 0.65 \cdot P \cdot L_{arm}$$ **Equation 11.5-10**

Where
0.65 is the empirical correlation factor, which is discussed in Reference 11-40, PM4057, Section 5.2.3.3

Refer to Reference 11-1, PM4057 Section 5.2.3.3 for guidance on fastener allowables, fitting and other factors, margin calculation, and interaction equations.

11.5.5.2 Fatigue

The preferred methodology for fatigue analysis of a fastener in a composite laminate is implemented in the IDAT/SFBOLT tool and outlined in this section. For fatigue analysis, SFBOLT calculates a margin of safety for the fastener in a single-shear bolted joint using an analytical method that is calibrated with empirically derived modification factors.

The SFBOLT-based fatigue analysis is applicable only to shear-loaded joints and any tensile component of loading in the fastener is not accounted for in the fatigue life prediction. SFBOLT bolt tension load input is used for the static analysis only to account for secondary induced tension loads. That is, SFBOLT is not intended for static or fatigue analysis of tension joints.

For cases in which there are significant fastener tension loads, where fatigue analysis using the SFBOLT tool is not applicable, an appropriate hand analysis of the fastener should be performed using an appropriate IMAT based durability allowable stress.

Bolt fatigue analysis is not required for double lap shear joints or for metal-to-metal, single lap shear joints that meet the following conditions.

- $t/D < 1.0$ for skin and $t/D < 1.0$ for substructure
- $t/D < 2.0$ for skin, substructure, and shim combined
- $t_{shim}/D < 0.15$
- Fastener shank is solid

Copyright 2015 Lockheed Martin Corporation.
Note: The current version is always the version on the Lockheed Martin network.

- Fastener/hole clearance is 0.000 to 0.004 inch in both skin and substructure
- Joint is stabilized to prevent out-of-plane motion

All joints are assumed to be single lap shear configuration assembled with low-density sealant per AMS 3281 in the joint interface and around the fasteners. Variables accounted for in the fastener fatigue analysis include the following:

- Skin and substructure material (and ply layup, if composite)
- Fastener type, diameter, and material
- Fastener/hole clearance
- Presence of shims
- Load spectrum effects

The bolt free-body shown in Figure 11.5-16 is used for SFBOLT fatigue analysis of a fastener. A beam-on-elastic foundation analysis is executed by IDAT/SS_JOINT and is used to predict the value of bending moment at the fastener head. This analysis accounts for bolt bending and shear deflections, modulus and thickness of the skin and substructure, and the presence of a shim (treated as a gap) at the interface between the two joint members. The fatigue response of the fastener is assumed to be driven by bending stress at the fastener head.

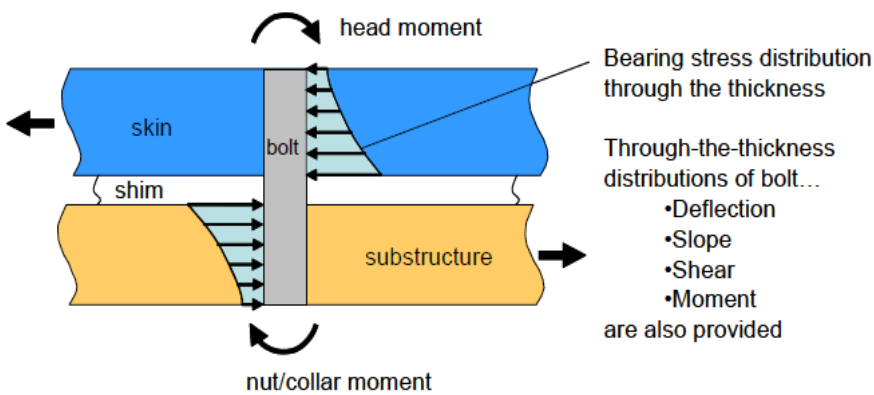

Figure 11.5-16 Beam-on-Elastic-Foundation Analysis Free-Body of Fastener/Joint Element

The maximum stress occurring in the fastener is based on the fastener head moment, M, and is given by

$$f_{applied} = \frac{My}{I} = \frac{4Mr}{\pi r^4} = \frac{32M}{\pi D^3} \qquad \textbf{Equation 11.5-11}$$

where
M = Fastener head moment (in-lbs)
y = Distance from fastener centerline to stress calculation point. The maximum stress value is at the fastener surface, *i.e.*, y = r (in)
r = Fastener radius, D/2 (in)
D = Fastener diameter (in)

The calculated bending stress is multiplied by three empirical factors to account for fastener type (F_{fas}), material combination in the joint (F_{com}), and for fastener/hole clearance (F_{clr}) to best correlate with the available joint fatigue test data. These factors are bolt dependent and stored in the IDAT/Fastener Database. The resulting equation for fatigue margin of safety is given by

$$M.S. = \frac{F_{allow}}{F_{fas}F_{com}F_{clr}f_{applied}} - 1 \qquad \textbf{Equation 11.5-12}$$

where
F_{fas} = Fastener type factor

Copyright 2015 Lockheed Martin Corporation.
Note: The current version is always the version on the Lockheed Martin network.

F_{com} = Joint material combination factor
F_{clr} = Fastener clearance factor
F_{allow} = Stress allowable (psi) that is a function of fastener material and is related to the IMAT-generated $K_{t\text{-}DLS}$ value for Titanium as follows:

- $F_{allow} = K_{t\text{-}DLS}$ for titanium fasteners (psi)
- $F_{allow} \cong 0.4652 \cdot K_{t\text{-}DLS} + 104{,}410$ for corrosion resistant steel fasteners (psi)
- $F_{allow} \cong 1.1360 \cdot K_{t\text{-}DLS} + 39{,}348$ for Inconel fasteners (psi)

$K_{t\text{-}DLS}$ = The 4.0 lifetime design limit stress for Ti-6Al-4V titanium (mill-annealed plate, 0% load transfer, $K_t = 1.0$) for the load spectrum applicable to this joint.

The user should always input the $K_{t\text{-}DLS}$ value for titanium, and SFBOLT will generate the value of F_{allow} appropriate for the fastener material selected. Similarly, once a fastener is selected from the IDAT fastener database, the appropriate values of F_{fas}, F_{com}, and F_{clr} will be provided. These three factors were empirically derived during correlation of the analysis procedure with the results of over 400 multi-fastener fatigue tests as discussed in Reference 11-41. The ranges of variable values included in the test database and, hence the limits of validity for the applicability of SFBOLT are listed in Table 11.5-6. Use of this analysis beyond these parameters will require further testing to verify applicability.

Table 11.5-6 Limits of Validity for SFBOLT Analysis

Variable	Minimum	Maximum
Bolt diameter (in.)	0.188	0.375
Head Thickness (in.)	0.075	0.356
Tail Thickness (in.)	0.075	0.560
Shim Thickness (in.)	0.000	0.090
Head Clearance (in.)	0.000	0.008
Tail Clearance (in.)	0.000	0.052
Total Joint Thickness/Fastener Diameter Ratio	0.791	3.210
Shim Thickness/Fastener Diameter Ratio	0.000	0.360

While margins of safety are not generally developed for fatigue analysis, in this case an exception is made. A fatigue margin of safety equal to 0.0 indicates that the fastener is predicted to survive for 4.0 lifetimes. It should be noted that the margin of safety is not a linear function of load. For example, a 10% increase in load could result in a much larger decrease in life. The analysis must be repeated with the increased load to determine the new life prediction.

11.6 Determination of Joint Loads

This section provides suggested guidelines for determining joint loads input for IBOLT strength analysis from finite element results. The section begins with a discussion of basic joint loads concepts that include: IBOLT element free-body loads required for problem definition, free-body equations of equilibrium, an overview of IBOLT basic load cases, and a discussion of useful load case combinations.

The section then provides an overview of finite element analysis loads results that includes: typical finite element representations used for aircraft structure; substructure loads; skin panel loads; and examples of load transfer between substructure members and composite skin panels.

A methodology is then presented for defining IBOLT free-body loads that includes: an introduction to two methods for defining loads (one treats the bearing load as known; the other treats it as an unknown); followed by load equation tables and application examples for fastener elements with no free edges (interior skin panel fasteners), one edge free (fasteners along skin panel edges), and two edges free (for fasteners at the corner of a skin panel).

Copyright 2015 Lockheed Martin Corporation.
Note: The current version is always the version on the Lockheed Martin network.

The section concludes with a series of joint loads related topics that include: treatment of multi-fastener rows; determination of fastener load distributions; coordinate transformations between finite element model results, fastener geometry, and laminate coordinate systems; and determination of pull-off loads from panel pressure.

11.6.1 Basic Concepts

A typical IBOLT element for an interior skin panel fastener is shown in Figure 11.6-1. The element in-plane free-body loads required for IBOLT strength analysis are shown. Refer back to Section 11.5.2.6 for a more detailed description of these load components.

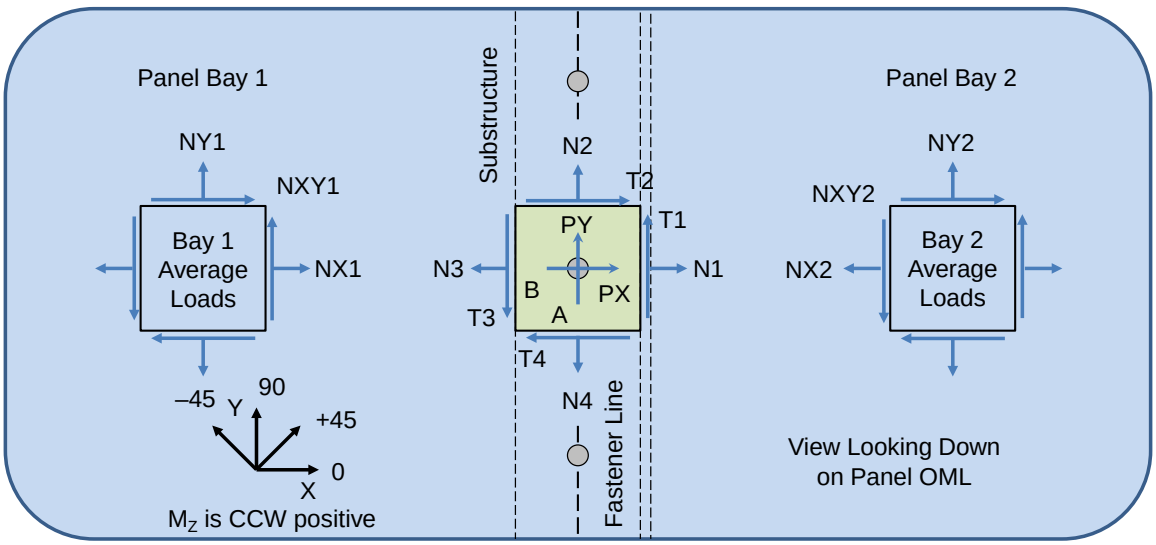

Figure 11.6-1 Typical Fastener Element and Free-Body Loads Required for IBOLT Strength Analysis

This is a view looking down on a composite skin panel outer surface. The fastener line is aligned with the Y-coordinate axis and attaches the composite skin to the substructure hidden below. The fastener line divides the composite skin into two bays: Bay 1 on the left and Bay 2 on the right. The positive conventions for the in-plane loads in adjacent bays are shown.

Any state of combined in-plane loading for an IBOLT element must satisfy the conditions of static equilibrium as expressed in Equation 11.6-1. The equations are based on the assumption that the hole is centered within the IBOLT element. IBOLT performs an equilibrium check during input and alerts the user to an imbalanced load set.

$$\sum F_X = B\cdot(N1-N3)+A\cdot(T2-T4)+PX=0$$

$$\sum F_Y = A\cdot(N2-N4)+B\cdot(T1-T3)+PY=0 \qquad \textbf{Equation 11.6-1}$$

$$\sum M_Z = 0.5\cdot A\cdot B\cdot(T1+T3-T2-T4)=0$$

where
N1-N4 = IBOLT element boundary normal running loads (lb/in)
T1-T4 = IBOLT element boundary shear running loads (lb/in)
A, B = IBOLT element dimensions (in)
PX, PY = IBOLT fastener bearing loads in the x and y directions, respectively (lbs)

Copyright 2015 Lockheed Martin Corporation.
Note: The current version is always the version on the Lockheed Martin network.

These equations can be rearranged into more useful forms:

$$PX = B \cdot (N3 - N1) + A \cdot (T4 - T2)$$

$$PY = A \cdot (N4 - N2) + B \cdot (T3 - T1) \qquad \textbf{Equation 11.6-2}$$

$$T1 + T3 = T2 + T4$$

IBOLT strength analysis uses the superposition of stress field solutions from the nine basic load cases shown in Figure 11.6-2 to obtain the predicted stresses for any combined load state. Bowie-type linear elastic fracture mechanics (LEFM) solutions for each load case were generated numerically using the boundary element method.

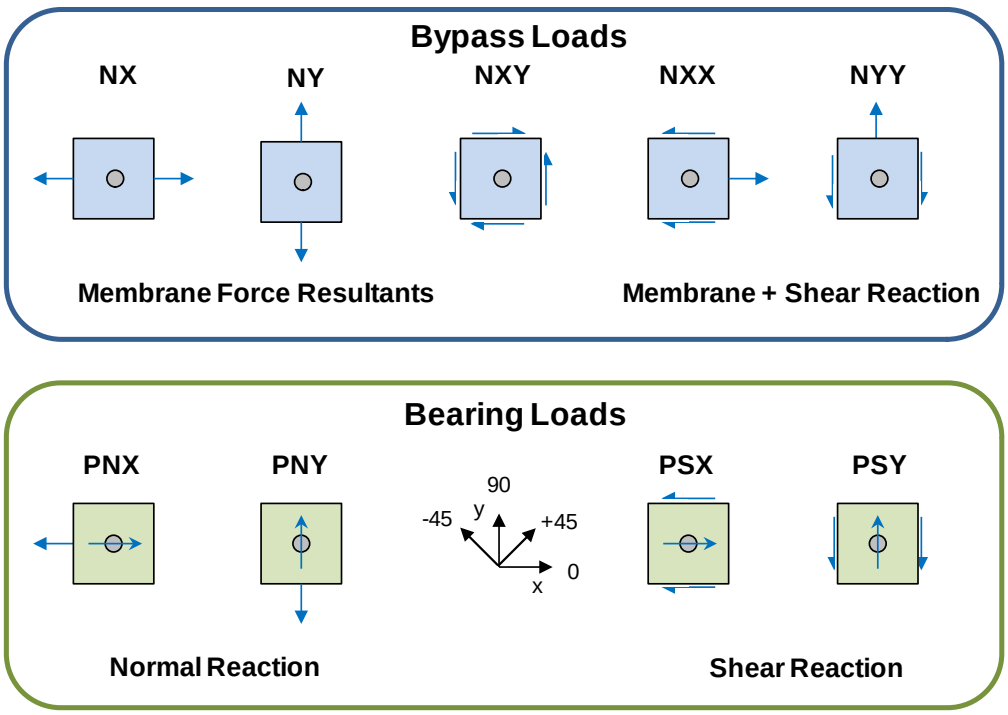

Figure 11.6-2 Nine Basic Load Cases for Combined In-Plane Loading

These load cases include five types of in-plane bypass loading and four types of fastener bearing and reaction loads. Bypass loads are the portion of the total loads that are not reacted by the fastener as discussed in Section 11.2.3. In contrast, the bearing loads are the loads acting upon the fastener that represents the load transfer between the joint elements (skin and substructure) and the corresponding bearing reaction or balancing load acting on the IBOLT element boundary. The sign of the loading may be reversed for any of the nine basic load cases.

Loads acting on the element boundaries are given as constant running loads with units of lbs/in. Fastener loads acting on the hole-boundary are given in lbs. For simplicity, the example shown assumes the element dimensions are 1.0 inch by 1.0 inch to allow the edge tractions (lbs/in) and bolt load (lbs) to be summed directly. Since each basic load case is in equilibrium, any combination of basic load cases will result in a balanced element free-body diagram.

The bypass load cases NX (x-direction tensile), NY (y-direction tensile), NXY (x-y plane shear) are identical to the in-plane membrane force resultants from classical laminated plate theory. The NXX, NYY bypass load cases are

Copyright 2015 Lockheed Martin Corporation.
Note: The current version is always the version on the Lockheed Martin network.

membrane bypass loads (x- and y-directions, respectively) reacted by two equal shear load resultants acting on opposite edges.

Bearing load cases PNX, PNY are bearing loads reacted by a normal load resultant. The reaction may be tension or compression acting on the corresponding edge as shown in Figure 11.6-3. The load cases shown are analogous to tests for bearing strength reacted by tension or compression[1] used for IBOLT bearing strength correlation. The figure illustrates how Bearing with a Compression Reaction is decomposed by IBOLT analysis into a superposition of NX and PNX load cases. The same can be shown for the Y-direction using PNY and NY load cases.

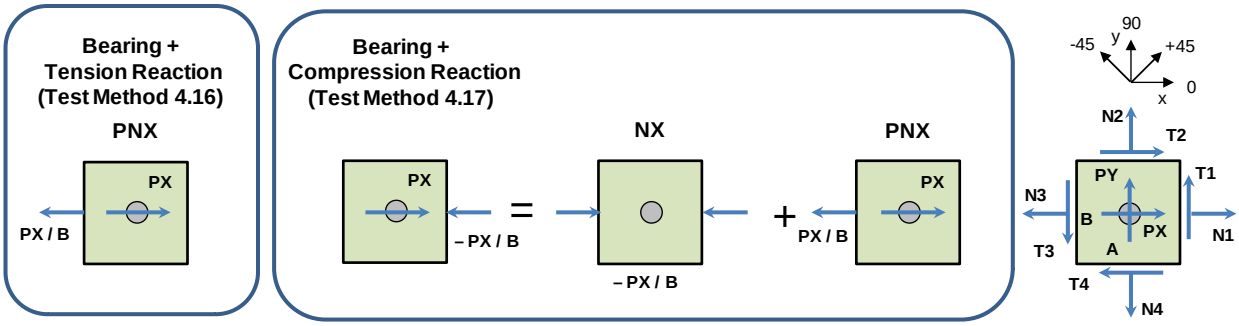

Figure 11.6-3 Fastener Bearing Load Cases with a Normal Reaction (X-direction shown)

Bearing load cases PSX and PSY are bearing loads reacted by two equal shear load resultants acting on opposing edges as shown as the load case PSX at the right of Figure 11.6-4. This load case can be combined with in-plane shear bypass load (NXY = 0.5 • PX / A) to create a useful condition in which the bearing load is reacted in shear along one edge and is rotationally balanced by a shear couple on the other edges. This combined load case is analogous to testing of bearing strength reacted in shear used for IBOLT bearing correlation[2].

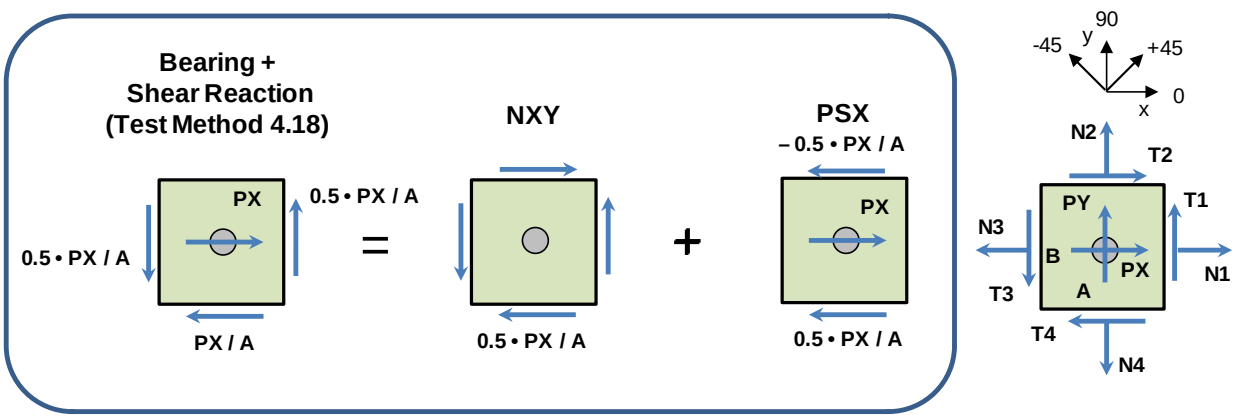

Figure 11.6-4 Fastener Bearing Load Case with a Shear Reaction (X-direction shown)

[1] Reference 11-42, Test Methods 4.16 (Bearing with Tension) and 4.17 (Bearing with Compression)
[2] Reference 11-42, Test Methods 4.18 (Bearing with Shear)

Copyright 2015 Lockheed Martin Corporation.
Note: The current version is always the version on the Lockheed Martin network.

Bearing load cases PNX and PNY can be combined with NX and NY bypass load cases to create a uniaxial bearing-bypass load condition as shown in Figure 11.6-5. These combined load cases correspond to bearing-bypass testing[1] with a tension or compression reaction, not shown.

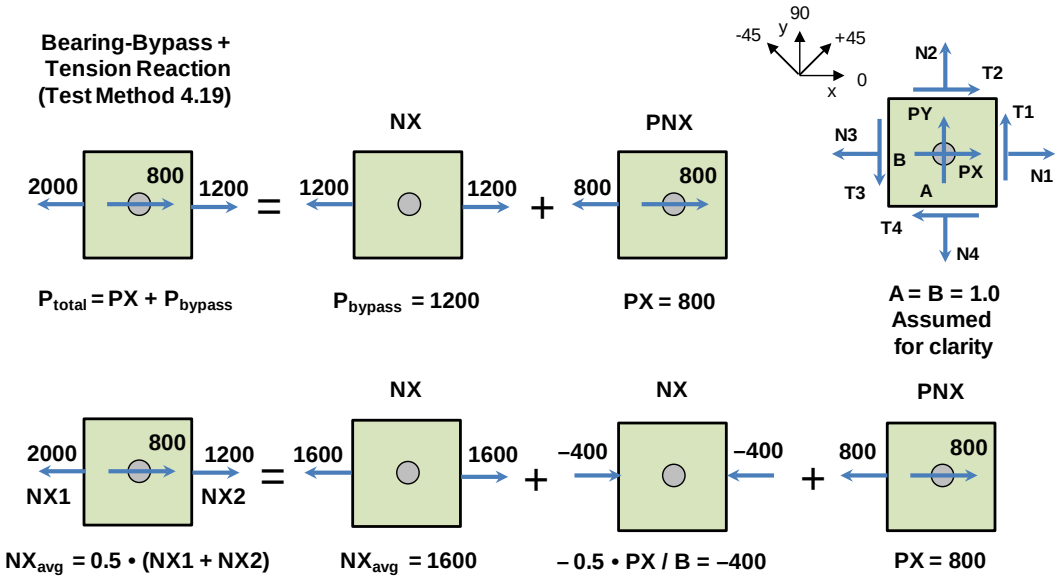

Figure 11.6-5 Bearing-Bypass Load Case with a Normal Reaction (X-direction shown)

The upper example of the uniaxial bearing-bypass is a simple combination of NX and PNX load cases. The lower example shows a decomposition in which the NX load case is subdivided into the average NX load level at the fastener and a NX transformation load case that is equal to NX = – 0.5 • PX / B. This is a useful form when the bearing load is known. The bearing-bypass load state can then be calculated using the average NX load at the fastener location. This form will be used in the methods for defining IBOLT element loads in Section 11.6.3.

Some useful numerical examples for combined NXY and PSX load cases are provided in Figure 11.6-6.

- The upper combined load example is the combination: NXY = + 0.5 • PX / A; and PSX = PX. This creates a free edge condition on the upper edge of the fastener element and the bearing load is reacted on the lower edge.
- The middle combined load example shows the effect of reversing the in-plane bypass shear, NXY = – 0.5 • PX / A. This creates a free edge condition on the lower edge of the fastener element and the bearing load is reacted on the upper edge.
- The lower combined load example has an in-plane bypass shear, NXY = + PX / A. This creates a combined load condition where the bearing load (1200 lbs) is reacted on the lower edge, but there is an additional load increment (600 lbs) required to react the opposite side shear.

In all cases, there is a balancing couple on the other edges to preserve Mz equilibrium (T1 + T3 = T2 + T4).

[1] Reference 11-42, Test Method 4.19 (Bearing-Bypass Tension) and 4.20 (Bearing-Bypass Compression)

Copyright 2015 Lockheed Martin Corporation.
Note: The current version is always the version on the Lockheed Martin network.

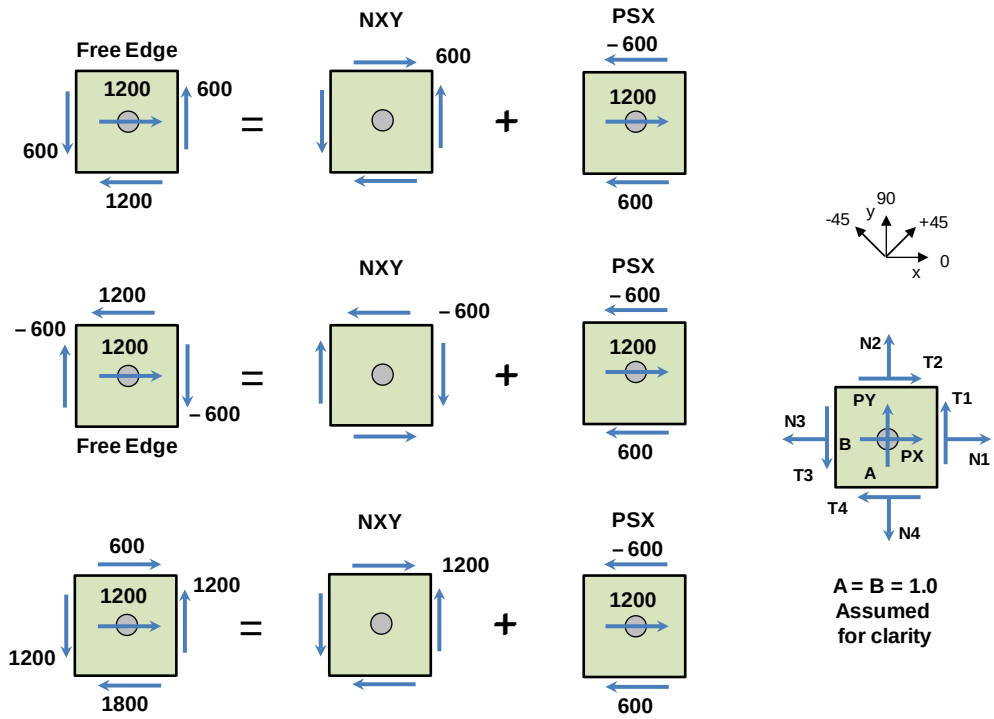

Figure 11.6-6 Bearing-Bypass Load Cases with a Shear Reaction (X-direction shown)

An example that demonstrates the combination of three load cases to represent a fastener with a combined load state along a skin panel free edge is shown in Figure 11.6-7. The decomposition of a general load case into an equivalent set of the 9 basic load cases shown Figure 11.6-2 is processed internally with IBOLT by the subroutine RLDCONV.

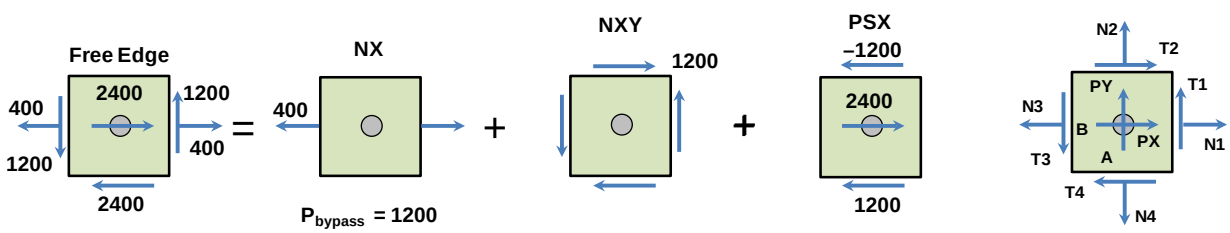

Figure 11.6-7 Example of a Combined Load Case with a Single Free Edge

Another example that demonstrates a combination of five load cases to represent a fastener with a combined load state at a panel corner with two free edges is shown in **Figure 11.6-8**. The fastener element has free edge conditions that require: N1 = T1 = N2 = T2 = 0. The requirement of element rotational equilibrium ($M_Z = 0$) requires that T3 = T4. The combined load cases NXY, PSX and PSY are used to produce the shear boundary force resultants, where: NXY = 0.5 • PSX / A = 0.5 • PSY / B.

Copyright 2015 Lockheed Martin Corporation.
Note: The current version is always the version on the Lockheed Martin network.

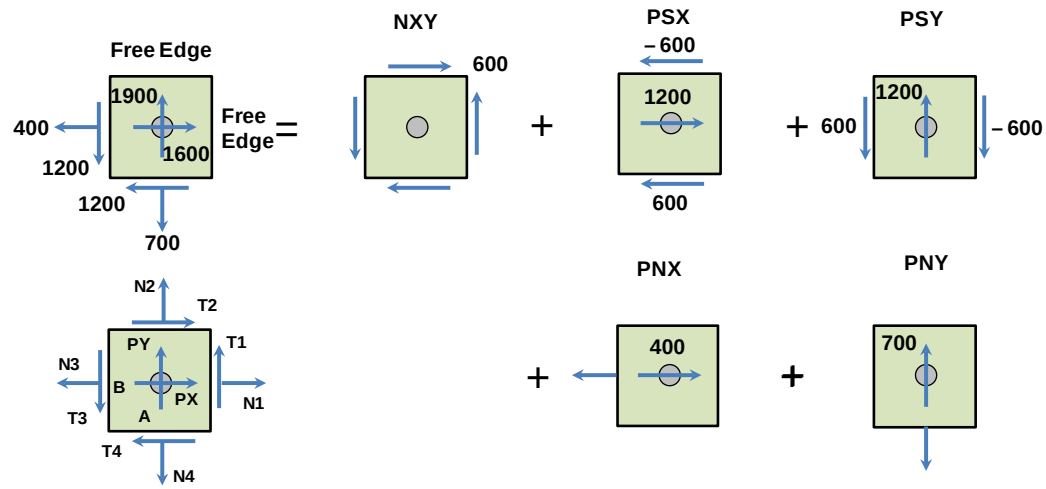

Figure 11.6-8 Example of a Combined Load Case with Two Free Edges at a Panel Corner

Returning to the basic bypass load cases, the membrane with shear reaction load cases (NXX, NYY) were added to the IBOLT analysis routine to address special combined load cases that can occur along panel edges and corners. Two IBOLT element load decomposition examples are provided in Figure 11.6-9 and Figure 11.6-10 to illustrate special cases in which the NXX load case is used to generate combined load states.

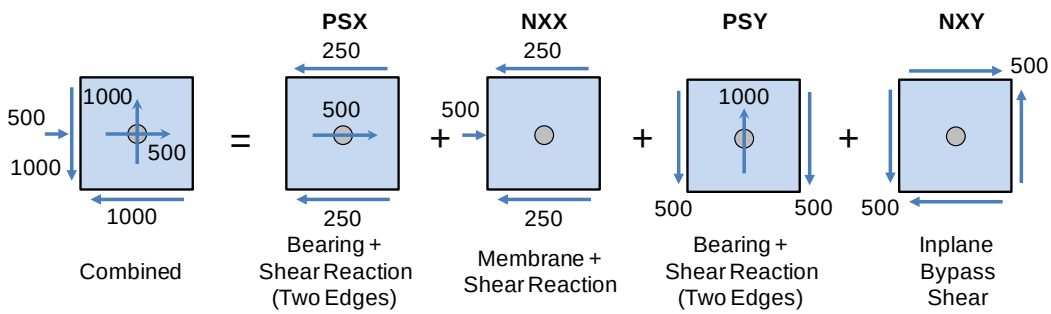

Figure 11.6-9 NXX Bypass Loading Example for Combined Loads at a Corner Fastener

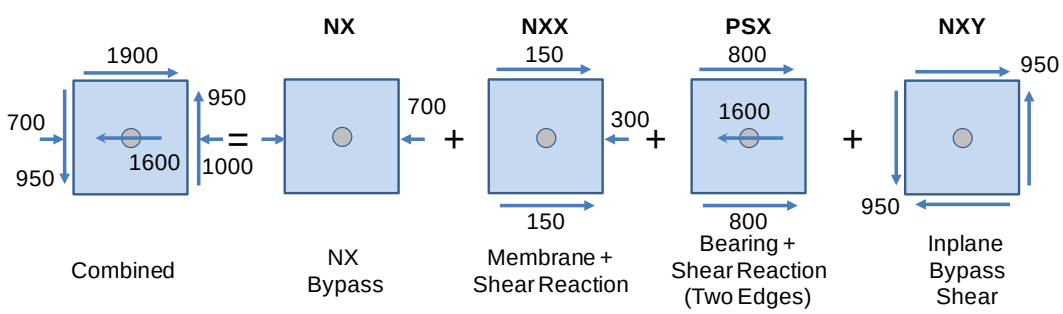

Figure 11.6-10 NXX Bypass Loading Example for Combined Loads at a Rib Cap Fastener

A summary of the possible options for IBOLT bearing-bypass combined load cases is illustrated in Figure 11.6-11. The figure shows the IBOLT element loads on the left with the possible constituent load cases on the right. As shown, the IBOLT element combined load state can be decomposed into bypass loads and bearing loads. Bypass

Copyright 2015 Lockheed Martin Corporation.
Note: The current version is always the version on the Lockheed Martin network.

loads can be composed of any of the five basic bypass load cases (NX, NY, NXY, NXX, and NYY). Bearing loads can be grouped according to their reaction loads. The fastener bearing load may be reacted by:

- Normal load cases: PNX, PNY
- Shear load cases along two edges: PSX, PSY

And, as demonstrated above, the PSX and PSY load cases can be combined with NXY bypass to create any necessary free edge conditions along with a couple to preserve M_Z static equilibrium.

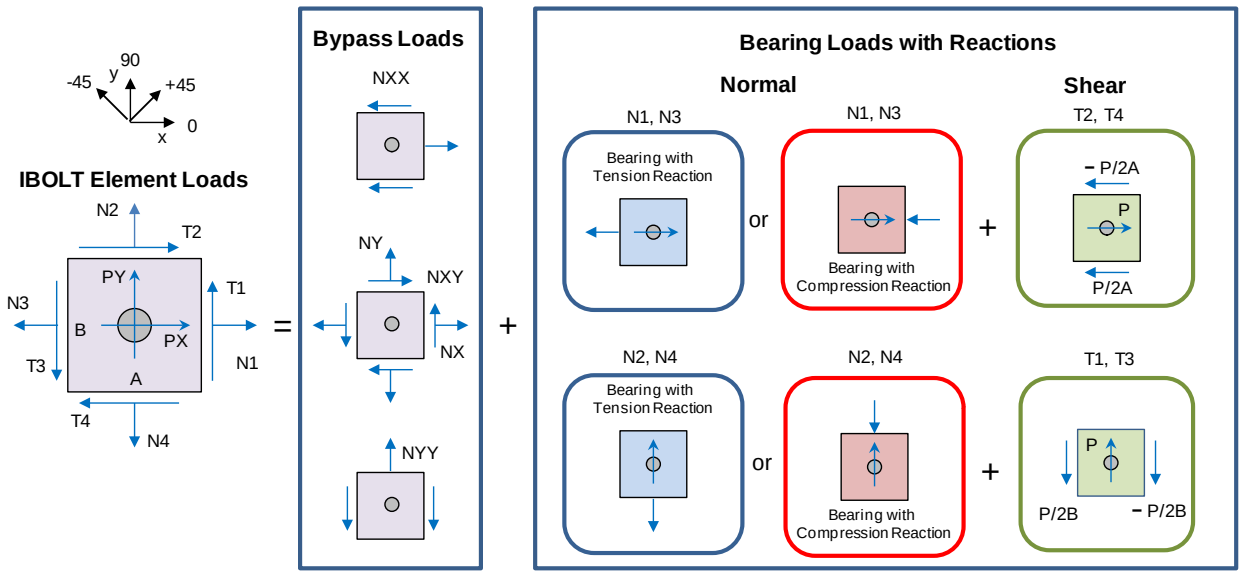

Figure 11.6-11 A Summary of Possible Options for IBOLT Bearing-Bypass Load Case Combinations

A discussion of joint loads that can be obtained using finite element analysis is presented in the next section. This is followed by a discussion of methods used to define IBOLT element input loads from finite element analysis results with examples.

11.6.2 Finite Element Analysis Loads

This section provides suggested guidelines for determining IBOLT joint element loads from finite element results. Also, refer to Section 11.9 for more discussion on Finite Element Modeling (FEM) conventions and considerations. For purposes of illustration, the discussion of joint loads is oriented toward a common example of aircraft structure such as the wing structure shown in **Figure 11.6-12**.

Copyright 2015 Lockheed Martin Corporation.
Note: The current version is always the version on the Lockheed Martin network.

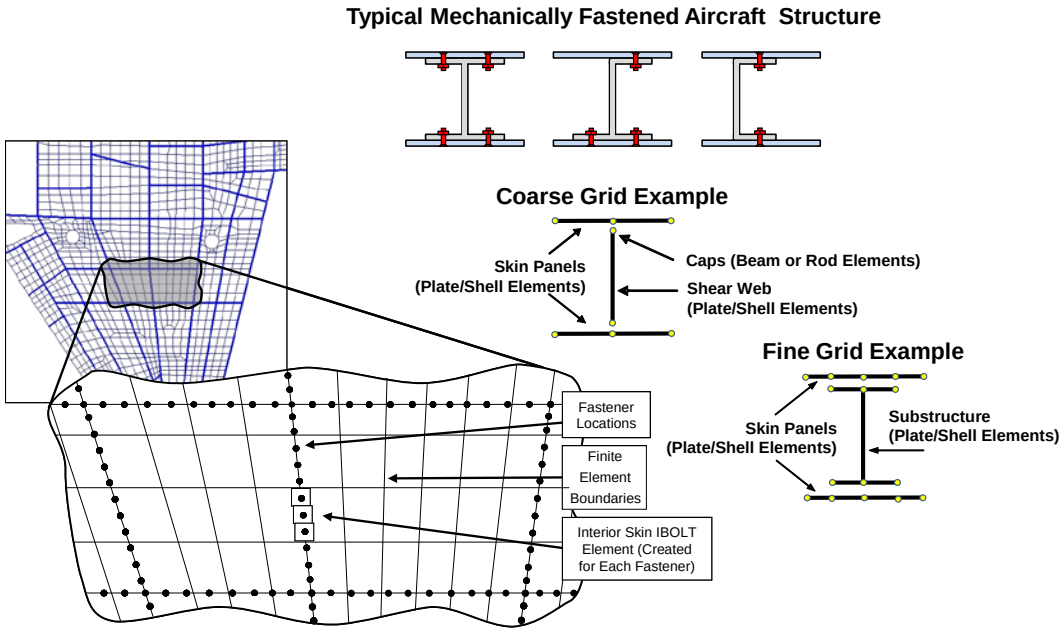

Figure 11.6-12 A Finite Element Model of Aircraft Wing Structure

The bolted assembly shown is comprised of upper and lower composite skins attached to an internal framework of substructure members, such as metallic or composite spars and ribs. Single shear joints are predominantly used to fasten the skins to the substructure members. Multi-layer joints may exist at spar-rib intersections where fasteners join the skins to both a spar and rib; or at locations where specialized fittings are installed (for example: doublers, splices, bathtub fittings, fuel/weapon pylons, etc.) Single row fastener lines may be used for C or J section members; double row fastener lines may be used for I, J or extended C section members. At each fastener location, it is important to verify that the fastener diameter-to-thickness ratio, countersink depth, pitch, and edge distances are within recommended guidelines.

Outer skin panels are modeled using quadrilateral (or triangular) plate or shell elements as shown in Figure 11.6-13. Finite element analysis predictions for stresses, strains and displacements can be obtained at the element nodes and centroid. Membrane (NX, NY, NXY) and flexural (MX, MY, MXY) load resultants can also be obtained which is a convenient form of results for determining joint loads.

Substructure members such as spars, ribs, bulkheads and frames are usually modeled as beams using a combination of plate or shell elements for the webs and beam or rod elements for the beam caps. C, J and I section beams can be modeled through assignment of the appropriate cap properties. For more refined models, the caps or flanges of the beam may be explicitly modeled using plate or shell elements.

Copyright 2015 Lockheed Martin Corporation.
Note: The current version is always the version on the Lockheed Martin network.

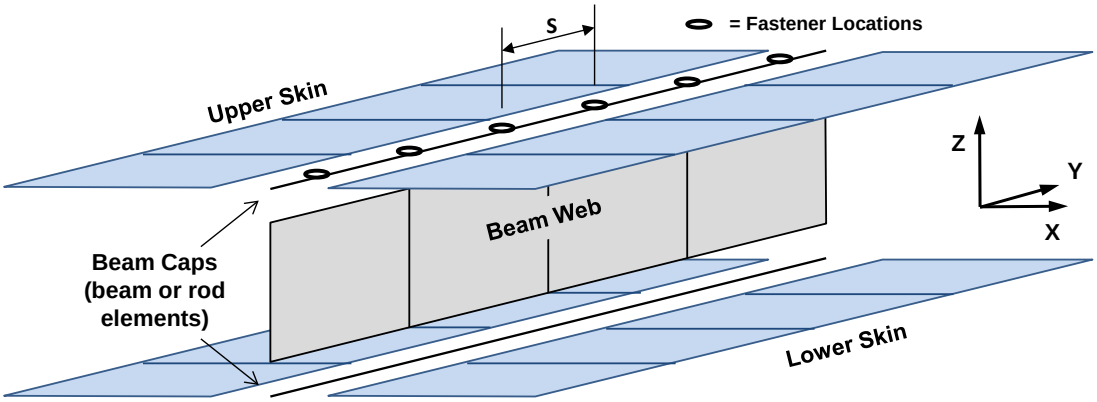

Plate or Shell elements are used for Skin Panels and Beam Webs.

Figure 11.6-13 Skin Panel and Substructure Elements

Models of substructure members can range from coarse grid models used for airframe loads development to complex fine grid models with detailed structural features. Coarse grid models may have a single plate or shell element spanning the web depth and multiple fasteners present along the element length. Fine grid models may have multiple plate or shell elements spanning the web depth with nodes and even spring elements corresponding to each fastener location. Fine grid models may explicitly model structural details such as web cutouts, system penetrations, fuel flow and vent holes. Taller, thin beams will tend to act as shear beams where the webs primarily carry shear and bending loads are reacted in the beam caps. Shorter beams with relatively thick webs will tend to carry bending in the webs as well as the caps. Truss structure is sometimes used for substructure where a framework of beam or rod elements may be necessary to model the truss members.

Web shear is transferred to the beam from the skins along the fastener lines at the beam perimeter as shown in Figure 11.6-14 and Figure 11.6-15. Figure 11.6-14 illustrates in-plane shear NXY1 and NXY2 in skin panel Bays 1 and 2. The NXY shear is shown as shear flow q_1 and q_2, respectively. From equilibrium along the fastener line, the substructure web shear, q_s, is equal to the difference in shear flow between the bays, $q_w = q_2 - q_1$.

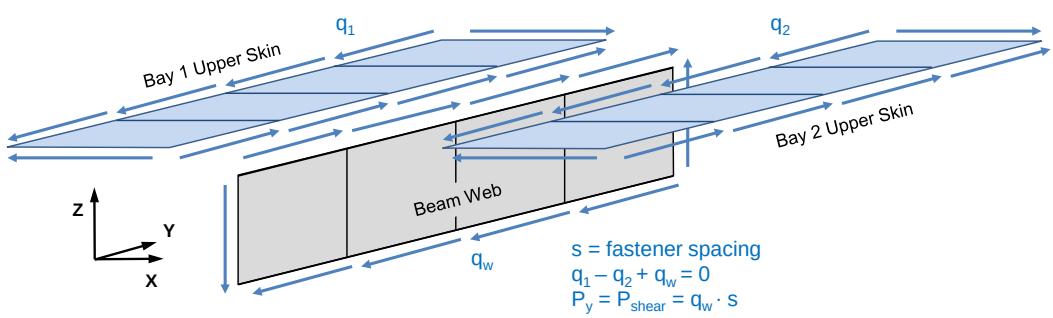

Figure 11.6-14 Example Load Transfer between Skin Panels and Substructure for NXY Skin Loads

Figure 11.6-15 illustrates in-plane normal loads NY1 and NY2 within skin panel Bays 1 and 2. As shown, the NY load is increasing in the Y-direction along the length of the bay. This increase or change in load is designated as load gradient ΔNY1 and ΔNY2. The load gradients ΔNY1 and ΔNY2 are introduced into the skin panels as shear transfer that occurs along the fastener lines. As with the previous example, the beam shear can be calculated through Y-direction force equilibrium along the fastener line.

Copyright 2015 Lockheed Martin Corporation.
Note: The current version is always the version on the Lockheed Martin network.

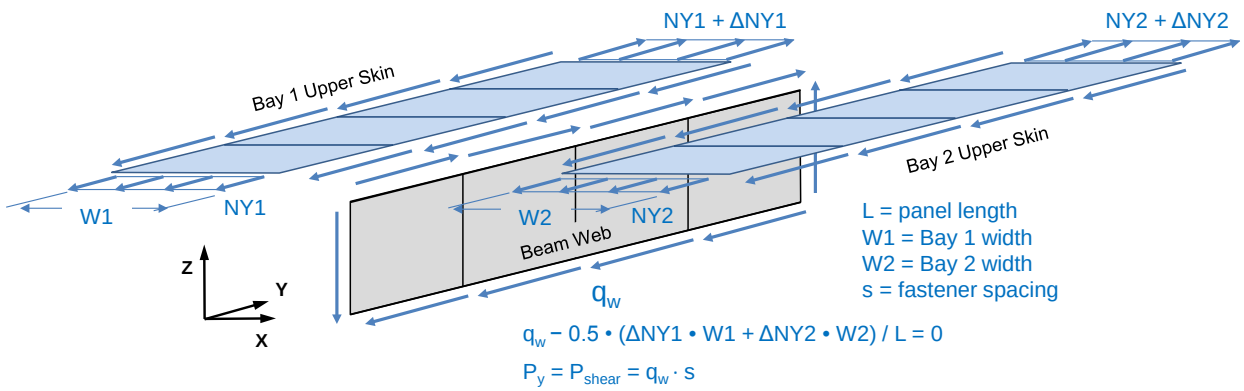

Figure 11.6-15 Example Load Transfer between Skin Panels and Substructure for ΔNY Skin Load Gradient

Skin panel to substructure attachment may be direct through shared nodes or grid points or through the use of spring elements in which the fastener stiffness is explicitly modeled. As shown in Figure 11.6-16, grid points may not necessarily align with fastener locations. Springs elements may represent a single fastener or a small fastener group for which the loads may be distributed by hand calculation.

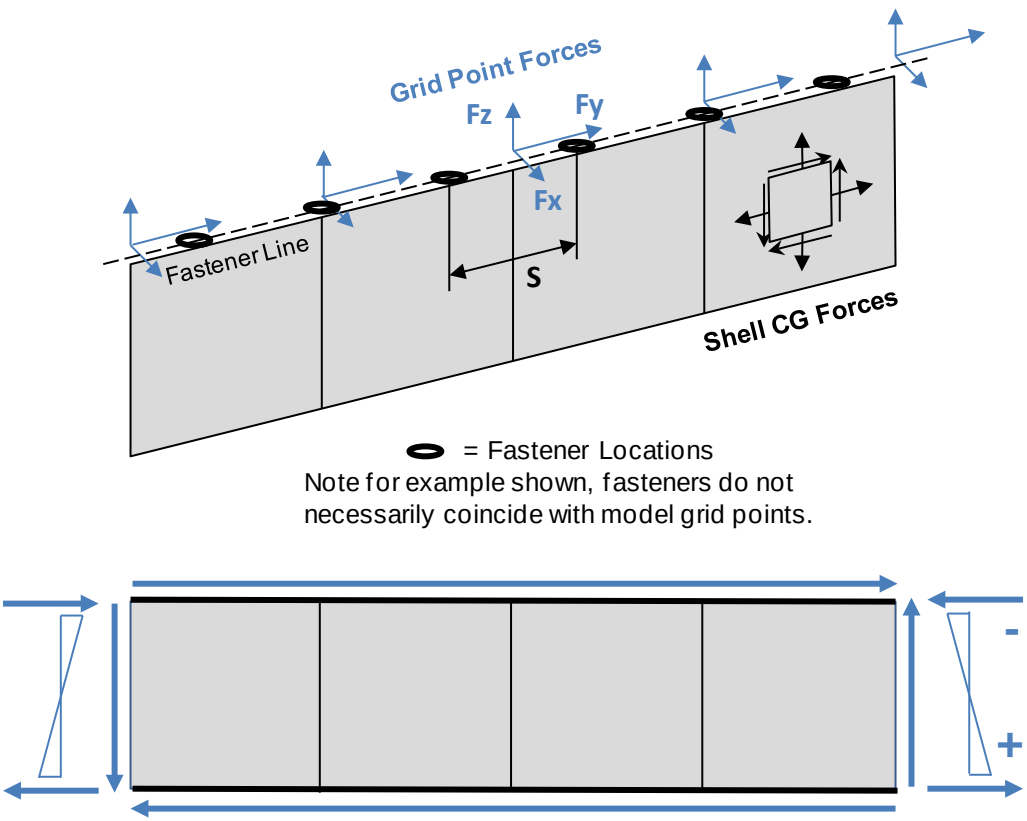

Figure 11.6-16 Substructure Load Transfer through Fasteners

Fastener loads acting transverse to the fastener line occur primarily along panel edges, as shown in Figure 11.6-16 as the F_X component. They can also develop near intersections with other transverse running structural members.

Copyright 2015 Lockheed Martin Corporation.
Note: The current version is always the version on the Lockheed Martin network.

Away from edges and intersections, these transverse loads should be small or even negligible since the skin continuity across the joint provides the stiffer load path. The normal load component F_Z can be used for evaluation of fastener pull-through or flange bending strength.

11.6.2.1 Substructure Loads

There are a number of methods that can be used to determine fastener loads from substructure element results. Three example methods are illustrated in Figure 11.6-17:

1) Web Shear Flow from a coarse grid model;
2) Grid Point Forces from a coarse grid model; and
3) Discrete Spring Elements at Fastener Locations from a fine grid model.

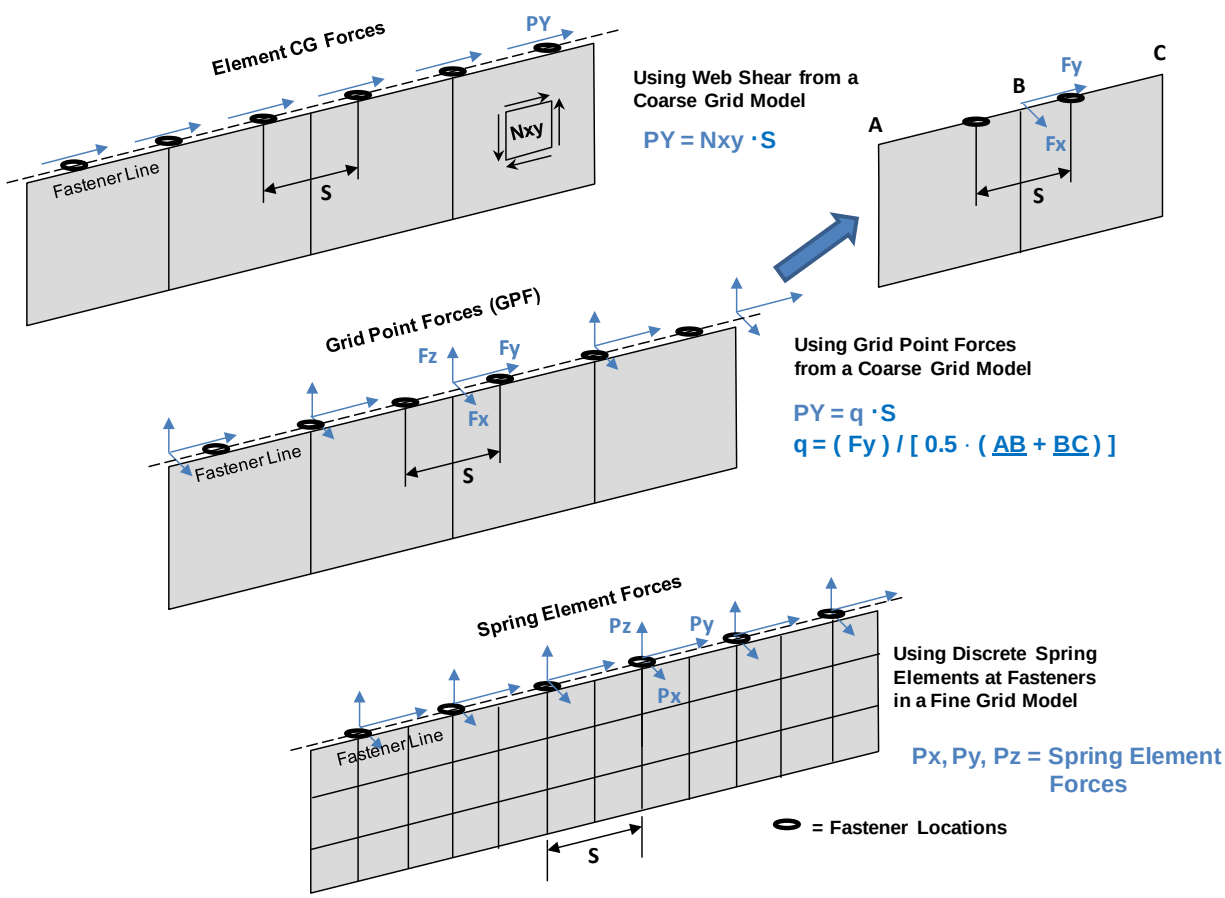

Figure 11.6-17 Load Transfer from Substructure Elements

Web Shear Flow from a Coarse Grid Model – The fastener load PY is based on the web shear from the beam web element that is adjacent to the fastener. The web shear is obtained from the element $\mathbf{N_{XY}}$ shear resultant at the element centroid. The fastener shear load is the product of the $\mathbf{N_{XY}}$ running load and the nominal fastener spacing **s.** If the fastener is located at an element boundary, then an average of the element shears is used.

Copyright 2015 Lockheed Martin Corporation.
Note: The current version is always the version on the Lockheed Martin network.

Grid Point Forces from a Coarse Grid Model – Local nodal or grid point forces are used to calculate a web shear running load **q**. There are a number of ways that a local shear running load can be calculated. One example is shown in the upper right where the shear running load is equal to the local grid point force F_Y divided by one half the sum of the adjacent element lengths AB and BC along the fastener line. The fastener shear load is the product of the shear flow **q** and the nominal fastener spacing **s.** Any method used should account for any observed gradient in the shear running load along the beam length and should be consistent with adjacent panel running loads.

Spring Element Forces from a Fine Grid Model – A spring element is used to model a fastener (or small fastener group) to connect a substructure node to a corresponding skin node. This method provides the fastener load components directly as finite element results. As shown in the figure, this level of modeling is typically reserved for fine grid models used for detailed structural analysis. For implementation, the fastener locations must be known and considerable effort must be expended to model each fastener location.

11.6.2.2 Skin Panel Loads

As shown in the previous section, the fastener bearing loads can be determined from the substructure. The skin panel loads must also be evaluated to determine the complete state of bearing-bypass loads at the IBOLT joint element. Several examples of skin panel load conditions and edge reactions are provided below to illustrate the type of loads that can be introduced at a fastener line. For fastener lines within the interior of a panel, these loads may be transferred from bay-to-bay across the joint, or they may be partially or completely transferred into the substructure through the fastener line. In the case of fasteners along panel edges and at corners, the panel loads must be completely reacted through the fastener line.

A typical composite skin panel is shown in Figure 11.6-18. The rectangular bay has dimensions of lengths **a** and **b** in the X and Y directions, respectively. An origin for a reference x_0-y_0 coordinate system is shown in the lower left corner of the panel. The skin panel is subjected to uniform in-plane loads equal to NX_p, NY_p and NXY_p.

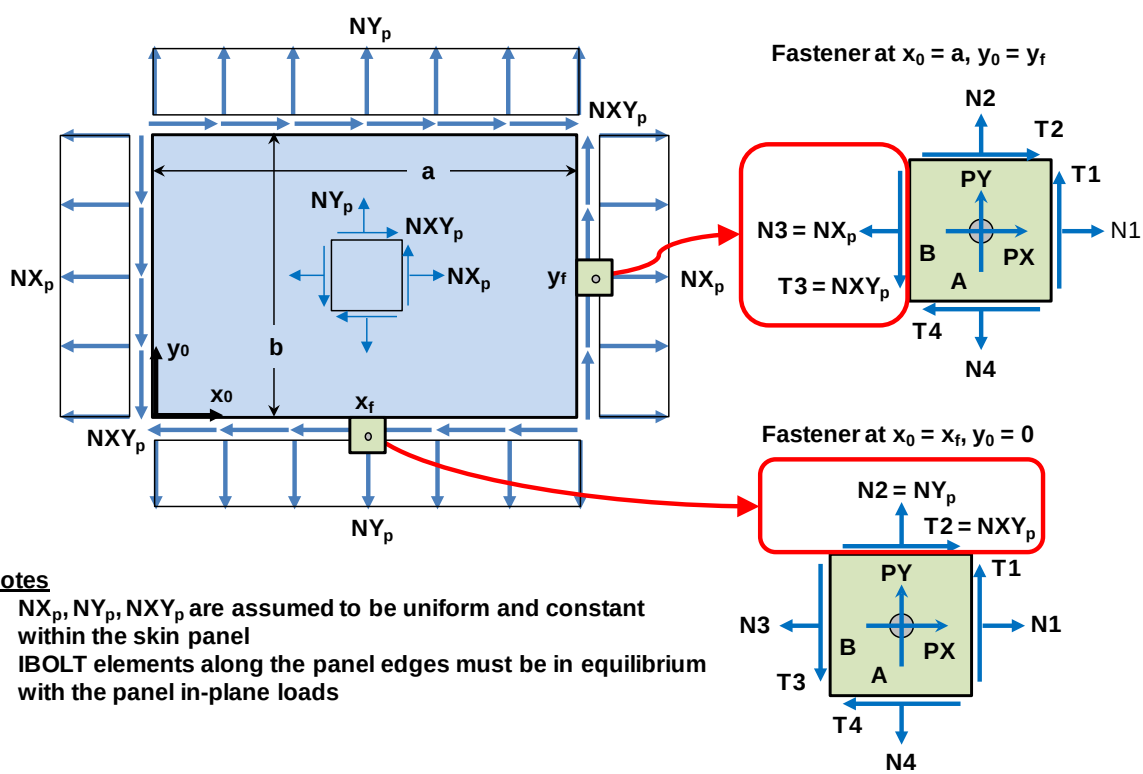

Notes

- **NX_p, NY_p, NXY_p are assumed to be uniform and constant within the skin panel**
- **IBOLT elements along the panel edges must be in equilibrium with the panel in-plane loads**

Figure 11.6-18 Example Skin Panel Loads: Uniform In-Plane Loads

Copyright 2015 Lockheed Martin Corporation.
Note: The current version is always the version on the Lockheed Martin network.

Two fasteners are shown along the edges of the panel at locations: $x_0 = x_f$, $y_0 = 0$ and $x_0 = a$, $y_0 = y_f$. The uniform in-plane loads have constant normal and shear reactions along the edges of the panel. As shown, the normal and shear force resultants on the edges of the IBOLT element must be in equilibrium with the panel edge loads. In turn, these element normal and shear force resultants must also be in equilibrium with the remaining element loads.

A more complex loading example shown in Figure 11.6-19 is a composite skin panel subjected to NX and NY in-plane loads which each have gradients with respect to the X-direction.

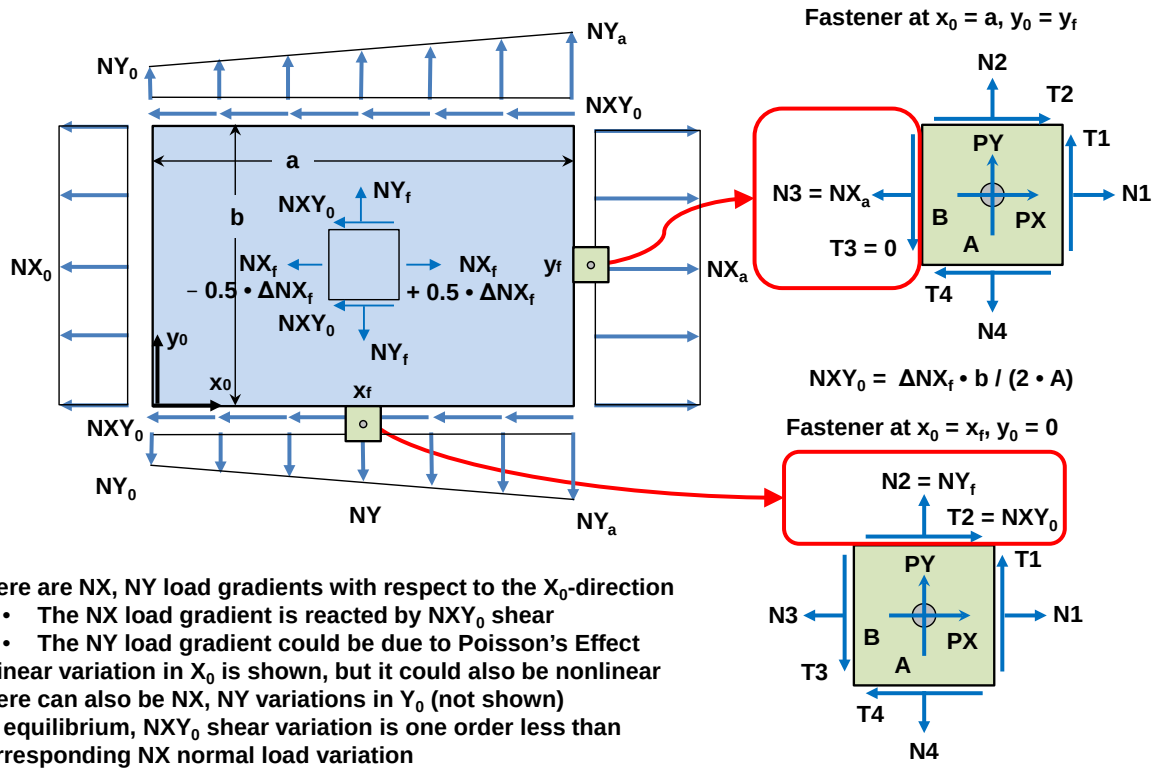

Notes

- **There are NX, NY load gradients with respect to the X_0-direction**
  - **The NX load gradient is reacted by NXY_0 shear**
  - **The NY load gradient could be due to Poisson's Effect**
- **A linear variation in X_0 is shown, but it could also be nonlinear**
- **There can also be NX, NY variations in Y_0 (not shown)**
- **By equilibrium, NXY_0 shear variation is one order less than corresponding NX normal load variation**

Figure 11.6-19 Example Skin Panel Loads: NX and NY load gradients in the X-direction

The NX load gradient varies linearly with the x_0 coordinate from $x_0 = 0$ to $x_0 = a$. The linear increase in NX is reacted or induced by a constant NXY_0 shear load along the panel edges $y_0 = 0$ to $y_0 = b$. The edge shear acts in the same direction on opposite edges. This is in contrast to the equal and opposite shear due to NXY exhibited by the uniform in-plane load conditions. The NX gradient can also be nonlinear and that, by equilibrium, the variation of the NXY boundary shear will be one order lower than the corresponding NX variation. A linear NY variation is also shown which could be due to a Poisson's effect. Note that the anisotropy of the panel could also result in a more complex edge distribution.

Again, two fasteners are shown along the edges of the panel at locations: $x_0 = x_f$, $y_0 = 0$ and $x_0 = a$, $y_0 = y_f$. As shown, the normal and shear force resultants on the edges of the IBOLT element must be in equilibrium with the panel edge loads.

The loading example shown in Figure 11.6-20 is a composite skin panel subjected to normal panel pressure. For thin panels, the normal pressure is typically reacted by combined membrane and bending loads. A geometrically nonlinear plate or shell analysis is required to properly account for the membrane-flexural coupling. The solution will also depend upon the edge fixity and may also need to account for any panel curvature. The resulting panel deflections and edge loads can be determined using the IDAT/Press analysis tool or through a geometrically nonlinear finite element analysis.

Copyright 2015 Lockheed Martin Corporation.
Note: The current version is always the version on the Lockheed Martin network.

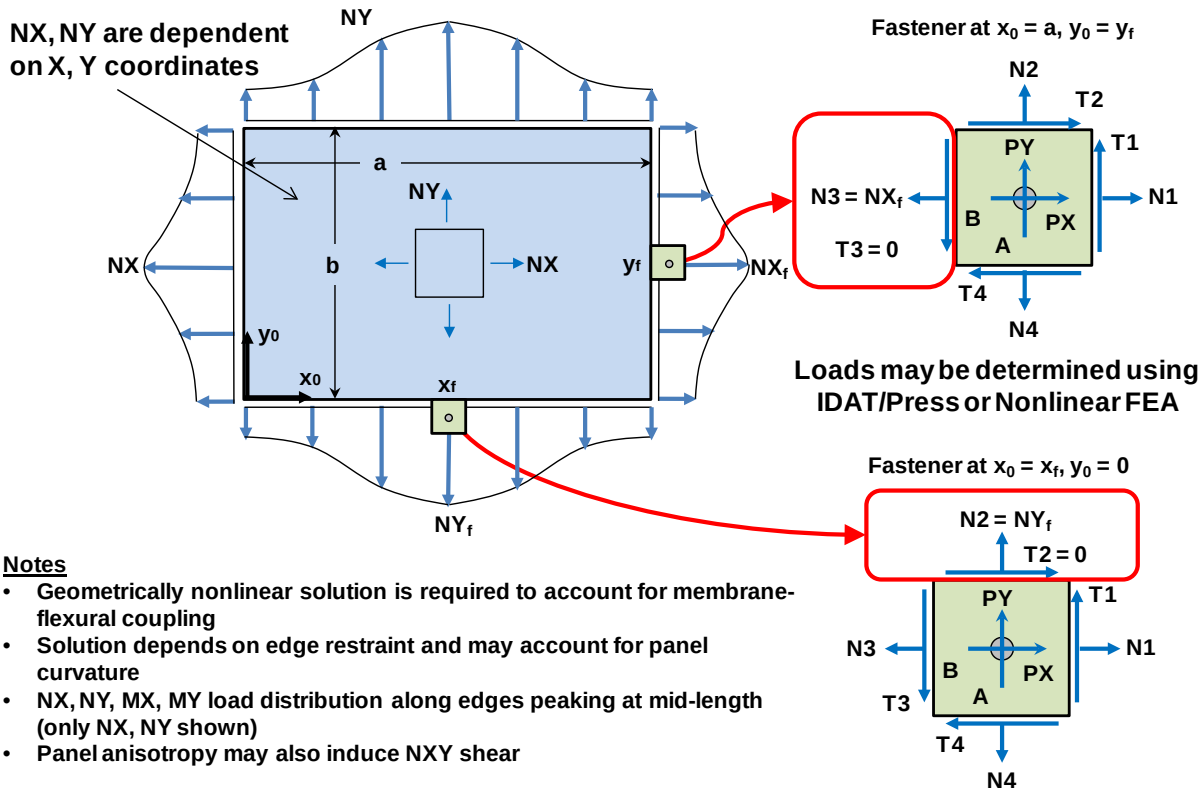

Notes

- **Geometrically nonlinear solution is required to account for membrane-flexural coupling**
- **Solution depends on edge restraint and may account for panel curvature**
- **NX, NY, MX, MY load distribution along edges peaking at mid-length (only NX, NY shown)**
- **Panel anisotropy may also induce NXY shear**

Figure 11.6-20 Example Skin Panel Loads: Normal Panel Pressure

As shown in the figure, nonlinear analysis results will provide NX, NY, MX and MY distributions along the panel edges (only NX and NY are shown). The peak edge reaction loads typically occur at the panel mid-lengths. Be aware that panel anisotropy can also induce panel NXY shear.

The examples shown in Figure 11.6-18, Figure 11.6-19, and Figure 11.6-20 illustrate how the normal and shear force resultants can vary along panel edges and that normal load gradients in a direction parallel with the edge can induce a shear force resultant along the panel edge that is dependent on the panel width.

There are a number of methods that can be used to determine skin panel loads from finite element results. Three examples of methods are illustrated in Figure 11.6-21:

1) Skin Bay Average
2) Skin Adjacent Element
3) Maximum-Minimum (Max-Min) Survey of Skin Elements

Copyright 2015 Lockheed Martin Corporation.
Note: The current version is always the version on the Lockheed Martin network.

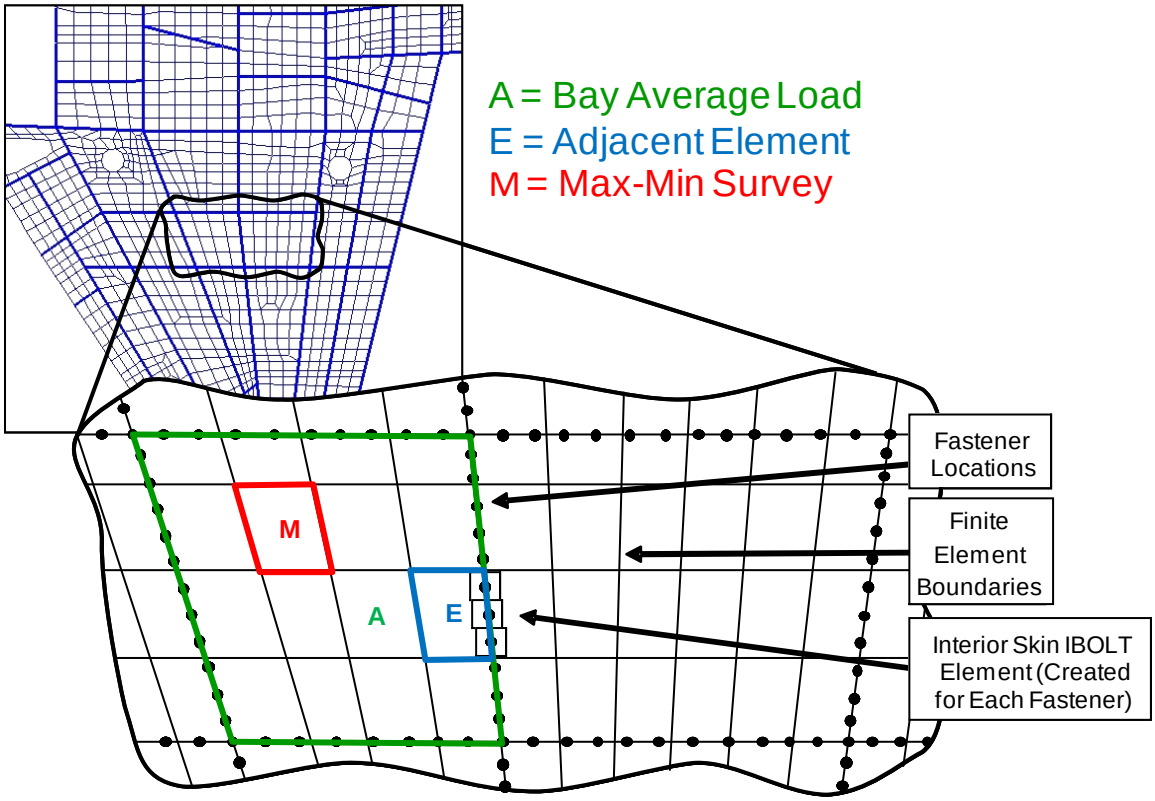

Figure 11.6-21 Methods for Determining Skin Loads from Adjacent Bays

Skin Bay Average – Each of the load components (NX, NY, NXY) are averaged to obtain a bay representative value. The averages can be area weighted to account for variability in element size and is done on a load case by load case basis to obtain consistent load case sets. The bay elements should be surveyed for maximum and minimum values and for any load gradients in the X or Y directions that would not be captured in this averaging method.

Skin Adjacent Element – Adjacent element running loads are used for fastener analysis. Overall, the bay elements should be surveyed for consistency. For fine grid models with multiple elements in the vicinity of the fastener, average loads for a local group of the adjacent elements can be used. The averaging of elements would be done on a load case by load case basis to obtain load case consistent load sets.

Maximum-Minimum Survey – This is a conservative approach for which the bay elements are surveyed for the maximum or minimum values of each load component. Engineering judgment is then used to select bay representative values. The bay elements should also be surveyed for any load gradients in the X or Y directions that would not be captured in this method. This method is typically **only** used in conceptual design or early stages of preliminary design and never for drawing release analysis.

Observed load gradients across the bay should correlate with the fastener loads at the bay boundaries; engineering judgment should be used to verify all load gradients. Another helpful approach is to survey principal loads and directions for the bay elements. This approach may help to evaluate the overall bay load state and can help identify load gradients.

Copyright 2015 Lockheed Martin Corporation.
Note: The current version is always the version on the Lockheed Martin network.

11.6.2.3 Example Problems – Skin and Substructure Load Transfer

This section concludes with two examples of load transfer between composite skin panels and the adjoining substructure before presenting general methods for defining IBOLT element free-body loads in Section 11.6.3. Each example demonstrates how fastener loads can be determined from either skin panel loads or from the substructure loads.

The examples are based on a small section of composite skin panel that is connected to a corresponding section of substructure through a single row of three identical fasteners. Free-bodies of the skin and substructure are shown along with the internal loads acting upon them. An IBOLT element is provided for reference. The examples demonstrate how to determine the load transfer through the fasteners using: a) the skin panel loads; and b) the shear flow in the substructure web.

Example 1 illustrates skin-to-substructure load transfer with the skin panel subjected to NXY in-plane shear only. This is the same as the loading condition described in Figure 11.6-14. The example shows how bay-to-bay NXY load differences are reacted through the fastener line.

Example 2 illustrates skin-to-substructure load transfer with the skin panel subjected to ΔNY load gradient in the Y-direction. This is the same as the loading condition described in Figure 11.6-15. The example shows load gradients running parallel to the fastener line are reacted through the fastener line.

If the ΔNY gradients in the Y-direction were different in each bay, this would be evident in a difference in shear running load introduced along the Bay 1 and 2 edges. This difference would result in an additional component of PY bearing load reacted at the fasteners. These more general load cases will be addressed in the next section.

It should be recognized that these are idealized loads examples. In actual practice, the skin panel loads and substructure shear flow can be extracted from the finite element results using a variety of methods and assumptions, with each possibly yielding a slightly different result. So although the fastener load determined from either the skin or substructure loads should theoretically be the same value, in practice there are likely to be differences observed. Large differences should be investigated to identify possible model anomalies or errors. Engineering judgment will sometimes be required to discern the best method for determining most accurate fastener load.

Copyright 2015 Lockheed Martin Corporation.
Note: The current version is always the version on the Lockheed Martin network.

11.6.2.3.1 Example 1 – Skin and Substructure Load Transfer with NXY Loads

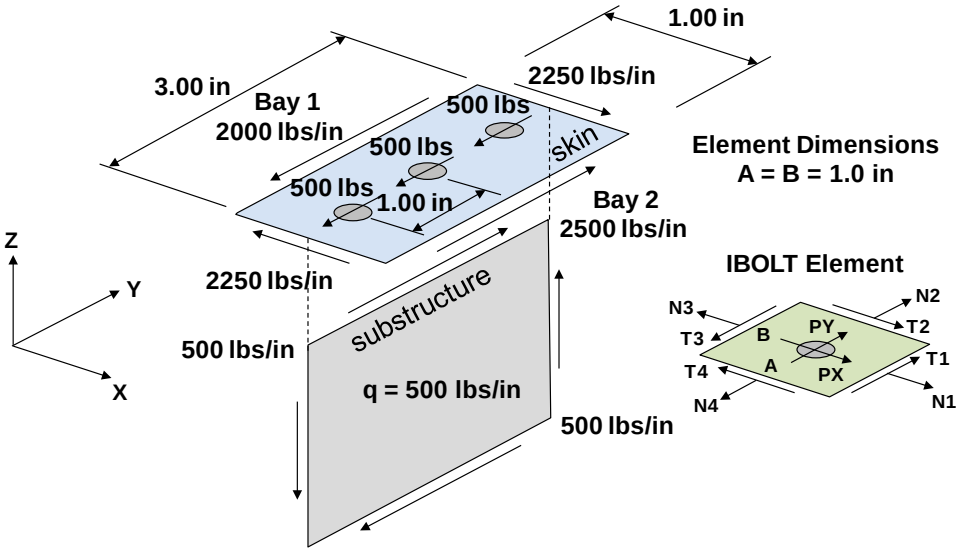

Problem Statement: Determine the IBOLT element fastener bearing loads (PX, PY) for the center fastener based on equilibrium using: a) Skin Panel Loads; and b) Substructure Load.

Known:

q = 500 lbs/in, Beam web shear flow
Bay 1 shear load = 2000 lbs/in
Bay 2 shear load = 2500 lbs/in
$NXY_{nearside}$ = 2250 lbs/in, $NXY_{farside}$ = 2250 lbs/in
s = 1.0 in, Fastener spacing
A = B = 1.0 in, Element dimensions

a) ***Solution using Skin Panel Loads***

N1 = 0 lbs/in
N2 = 0 lbs/in
N3 = 0 lbs/in
N4 = 0 lbs/in

T1 = 2500 lbs/in
T2 = 2250 lbs/in
T3 = 2000 lbs/in
T4 = 2250 lbs/in

Using equilibrium equations 11.6-2:
PX = B • (N3 − N1) + A • (T4 − T2)
PX = 1.0 • (0 − 0) + 1.0 • (2250 − 2250)
PX = 0 lbs

PY = A • (N4 − N2) + B • (T3 − T1)
PY = 1.0 • (0 − 0) + 1.0 • (2000 − 2500)
PY = −500 lbs

Verify M_Z equilibrium:
T1 + T3 = T2 + T4
2500 + 2000 = 2250 + 2250 = 4500 lb/in ✓

b) ***Solution using Substructure Load***

There are no transverse loads acting on the web:
PX = 0 lbs

Web shear flow:
q_{web} = NYZ = 500 lbs/in
PY = q_{web} • s = 500 lbs/in • 1.0 in
PY = 500 lbs per fastener

Note: This is the fastener bearing load acting on the web or beam upper flange (not shown). This load is equal and opposite the bearing load acting on the skin panel.

Copyright 2015 Lockheed Martin Corporation.
Note: The current version is always the version on the Lockheed Martin network.

11.6.2.3.2 Example 2 – Skin and Substructure Load Transfer with a ΔNY Load Gradient

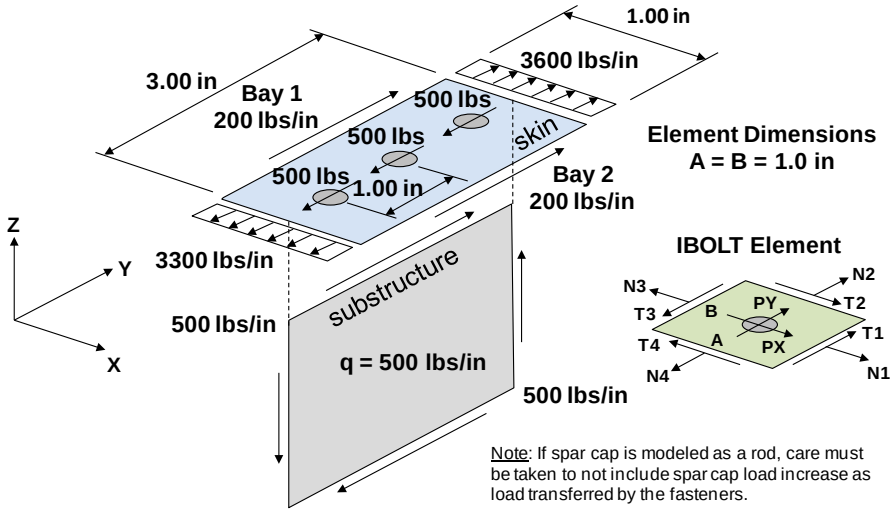

Problem Statement: Determine the IBOLT element fastener bearing loads (PX, PY) for the center fastener based on equilibrium using: a) Skin Panel Loads; and b) Substructure Load.

Known:

q = 500 lbs/in, Beam web shear flow
Bay 1 shear load = −200 lbs/in
Bay 2 shear load = 200 lbs/in
$NY_{nearside}$ = 3300 lbs/in, $NY_{farside}$ = 3600 lbs/in
s = 1.0 in, Fastener spacing
A = B = 1.0 in, Element dimensions

a) ***Solution using Skin Panel Loads***

Assuming a linear gradient in NY along Y:
N1 = 0 lbs/in
N2 = 3500 lbs/in (Center fastener, element far edge)
N3 = 0 lbs/in
N4 = 3400 lbs/in (Center fastener, element near edge)

T1 = 200 lbs/in
T2 = 0 lbs/in
T3 = −200 lbs/in
T4 = 0 lbs/in

Using equilibrium equations 11.6-2:
PX = B • (N3 − N1) + A • (T4 − T2)
PX = 1.0 • (0 − 0) + 1.0 • (0 − 0)
PX = 0 lbs
PY = A • (N4 − N2) + B • (T3 − T1)
PY = 1.0 • (3400 − 3500) + 1.0 • (−200 − 200)
PY = −500 lbs

Verify M_Z equilibrium:
T1 + T3 = T2 + T4
200 − 200 = 0 lbs/in ✓

b) ***Solution using Substructure Load***

There are no transverse loads acting on the web:
PX = 0 lbs

Web shear flow:
q_{web} = NYZ = 500 lbs/in
PY = q_{web} • s = 500 lbs/in • 1.0 in
PY = 500 lbs per fastener

Note: This is the fastener bearing load acting on the web or beam upper flange (not shown). This load is equal and opposite the bearing load acting on the skin panel.

Copyright 2015 Lockheed Martin Corporation.
Note: The current version is always the version on the Lockheed Martin network.

11.6.3 Defining IBOLT Element Free-Body Loads

This section provides suggested methods for defining IBOLT element free-body loads from finite element results. There are two methods presented for deriving IBOLT element loads:

1) Fixed Bearing Load (FBL) Method – for which the fastener bearing loads (PX, PY) are known; and
2) Derived Bearing Load (DBL) Method – for which the fastener bearing loads (PX, PY) are unknown.

The loads methods defined within this section are suggested analytical approaches that are based on a survey of best practices developed from Legacy Programs and may be modified by program guidance.

The two methods are introduced through consideration of a typical fastener line located within an interior skin panel as shown in Figure 11.6-22. These two methods will be applied to the practical problems of fasteners with: no edges free as is found in interior skin panel fasteners; one edge free such as fasteners along skin panel edges; and two edges free for fasteners at skin panel corners.

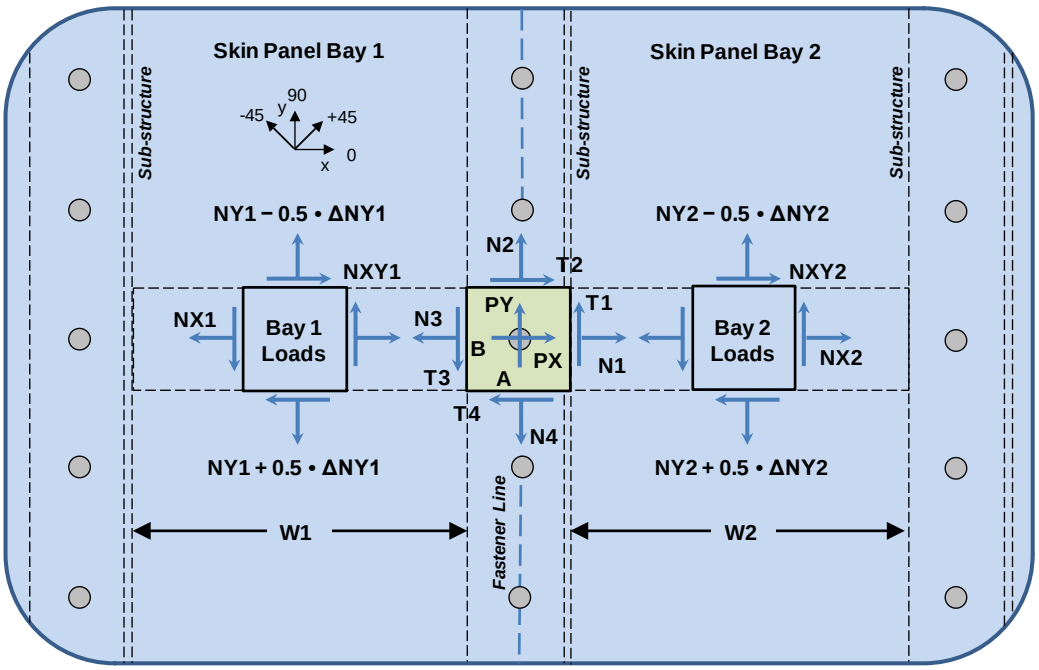

Figure 11.6-22 Interior Skin Panel Fastener within a Fastener Line Aligned with the Y-axis

The IBOLT element is centered on the fastener and is highlighted in green with element lengths of A and B in the X- and Y-directions, respectively. The fastener is an interior skin panel fastener with no free edges. The fastener belongs to a single row of fasteners that are aligned with the Y-axis. The fastener line divides the composite skin panel into two adjacent bays, designated as Bay 1 on the left and Bay 2 on right.

The known problem parameters are defined as:

- IBOLT element dimensions (in): A, B
- Bay widths (in), in a direction normal to the fastener line: W1, W2
- Bay 1 in-plane loads and NY load gradient (lbs/in): NX1, NY1, NXY1, ΔNY1
- Bay 2 in-plane loads and NY load gradient (lbs/in): NX2, NY2, NXY2, ΔNY2

Copyright 2015 Lockheed Martin Corporation.
Note: The current version is always the version on the Lockheed Martin network.

The bay in-plane force resultants, NX, NY and NXY, are finite element running loads that have been determined from the adjacent bays. ΔNY represents any change or gradient in NY load with respect to the Y-direction that is observed to occur over the element length B (Refer to Section 11.6.2 for more information). It is centered on the fastener and is thus expressed in terms of plus/minus one half quantities. ΔNY is assumed to be linear across the element length. The bay width W is required to determine the magnitude of the shear load due to the NY gradient that is reacted at the fastener element.

Note that any ΔNX load gradient in the Y-direction within a skin bay is accounted for through the use of the local NX loads that correspond to the fastener element in each adjacent bay. Similarly, ΔNX and ΔNY load gradients in the X-direction can also be accounted for through the use of the local NX and NY loads that correspond to the fastener element. For these reasons, only the ΔNY load gradient in the Y-direction has been illustrated in the figure since its magnitude will be required to calculate its contribution to the fastener bearing load. Note also that the sign convention of the ΔNY has been selected such that it corresponds to a positive PY bearing load.

The unknowns that must be determined are the IBOLT element loads:

- Fastener Bearing Loads (lbs): PX, PY
- Element Boundary Normal Force Resultants (lbs/in): N1, N2, N3, N4
- Element Boundary Shear Force Resultants (lbs/in): T1, T2, T3, T4

As stated in the Joint Design Guidelines of Section 11.3, it is desirable that joint design should be bearing critical. Therefore, it is important to obtain an accurate bearing load. Typically, the bearing load should be predetermined through an analysis of substructure to skin load transfer as this is usually more accurate than a bearing load derived from skin loads only. As discussed in Section 11.6.2, bearing load may be determined from a discrete spring element, skin/substructure grid point forces, substructure shear flow, a detailed fastener loads analysis (Refer to Section 11.6.5), or similar joint loads analysis. For these reasons, the Fixed Bearing Load Method, for which the bearing load has been predetermined, should be used.

Although both the FBL and DBL methods are valid approaches that should theoretically produce the same IBOLT element loads, there are likely to be observed differences due to the finite element mesh fidelity (element size, shape, geometry, etc.); and the specific method selected for determining adjacent skin loads and/or substructure to skin load transfer. In practice, the Fixed Bearing Load should be used, while the Derived Bearing Load method can be used as a check. Large differences between the two methods should be scrutinized for possible modeling anomalies or errors. An overview of each method is provided below:

Derived Bearing Load (DBL) Method

- Assumes that the fastener bearing load (PX, PY) is unknown.
- Adjacent skin panel loads are evaluated first to determine IBOLT element boundary running loads (N1–N4, T1–T4) such that:
    - The IBOLT element is in equilibrium with adjacent skin panels.
- Fastener bearing load components (PX, PY) are then calculated from element free-body equilibrium.

The DBL method is relatively straight forward, even for realistically complex combined loading conditions.

Fixed Bearing Load (FBL) Method

- Assumes that the fastener bearing load (PX, PY) has been predetermined from an analysis of substructure to skin load transfer.
- Adjacent skin panel loads are then evaluated to determine IBOLT element boundary running loads (N1–N4, T1–T4) such that:
    - Fastener bearing loads (PX, PY) are reacted exactly; and
    - Bypass loads are based on average skin panel loads at the joint.

The FBL method is relatively more complicated and uses elements of the DBL method for resolving bearing load components.

Copyright 2015 Lockheed Martin Corporation.
Note: The current version is always the version on the Lockheed Martin network.

Both methods are based on the simplifying assumptions:

- Element normal loads acting parallel to the fastener line are assumed equal to the bay-to-bay average.
- Element shear loads acting normal to the fastener line are assumed to be a balancing couple to preserve M_Z equilibrium.

Since the Derived Bearing Load method is relatively straight forward to implement and is used by the Fixed Bearing Load method to determine bearing load components, it will be presented first followed by the FBL method.

11.6.3.1 Derived Bearing Load (DBL) Method

The DBL method is illustrated through consideration of the IBOLT element shown in Figure 11.6-22. The IBOLT fastener element is an interior fastener with no free edges that is part of a fastener row aligned with the Y-axis. The IBOLT element free-body loads acting on the fastener element are shown in Figure 11.6-23.

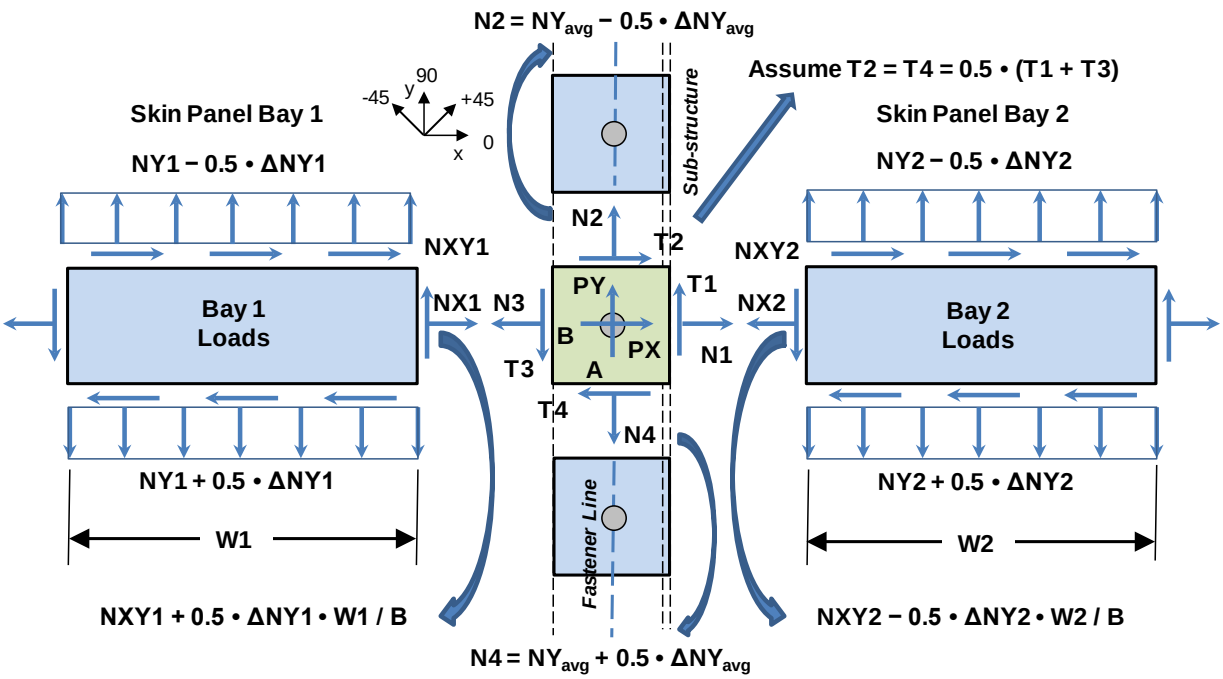

Figure 11.6-23 Free-Body Loads for a Skin Panel Fastener within a Fastener Line Aligned with the Y-axis

As summarized in Table 11.6-1, the normal element running loads N1 and N3 are set equal to the NX component of the adjacent panel loads. As for N2 and N4, the average in-plane load resultants are assumed to occur at the center of the IBOLT element, so the normal loads on the upper and lower edges are the NY_{avg} element average load minus and plus the $0.5 \bullet \Delta NY_{avg}$ increment. The T1 and T3 shear element running loads are equal and opposite to the NXY load components of the adjacent bays plus any shear induced that react the ΔNY load gradients in each bay. The T2 and T4 element running loads are a resultant couple that develops to preserve M_Z element equilibrium. This couple arises from restraint provided by adjacent fasteners in the fastener row. Once the element boundary loads are defined, the bearing load components (PX, PY) are determined using the element equilibrium equations in the X- and Y-directions.

Copyright 2015 Lockheed Martin Corporation.
Note: The current version is always the version on the Lockheed Martin network.

Table 11.6-1 IBOLT Loads using the DBL Method for a Fastener Line Aligned with the Y-axis

Loads	Units	Equations
N1	lbs/in	NX2
N2	lbs/in	$NY_{avg} - 0.5 \cdot \Delta NY_{avg}$
N3	lbs/in	NX1
N4	lbs/in	$NY_{avg} + 0.5 \cdot \Delta NY_{avg}$
T1	lbs/in	NXY2 − 0.5 • ΔNY2 • W2 / B
T2	lbs/in	0.5 • (T1 + T3)
T3	lbs/in	NXY1 + 0.5 • ΔNY1 • W1 / B
T4	lbs/in	0.5 • (T1 + T3)
PX	lbs	B • (N3 − N1) + A • (T4 − T2)
PY	lbs	A • (N4 − N2) + B • (T3 − T1)
Average In-Plane Load Resultants		
NX_{avg}	lbs/in	0.5 • (NX1 + NX2)
NY_{avg}	lbs/in	0.5 • (NY1 + NY2)
NXY_{avg}	lbs/in	0.5 • (NXY1 + NXY2)
ΔNY_{avg}	lbs/in	0.5 • (ΔNY1 + ΔNY2)

The bearing loads can be divided into constituent components that isolate different types of boundary reactions. Bearing load components are illustrated in Figure **11.6-24** with equations provided in Table 11.6-2.

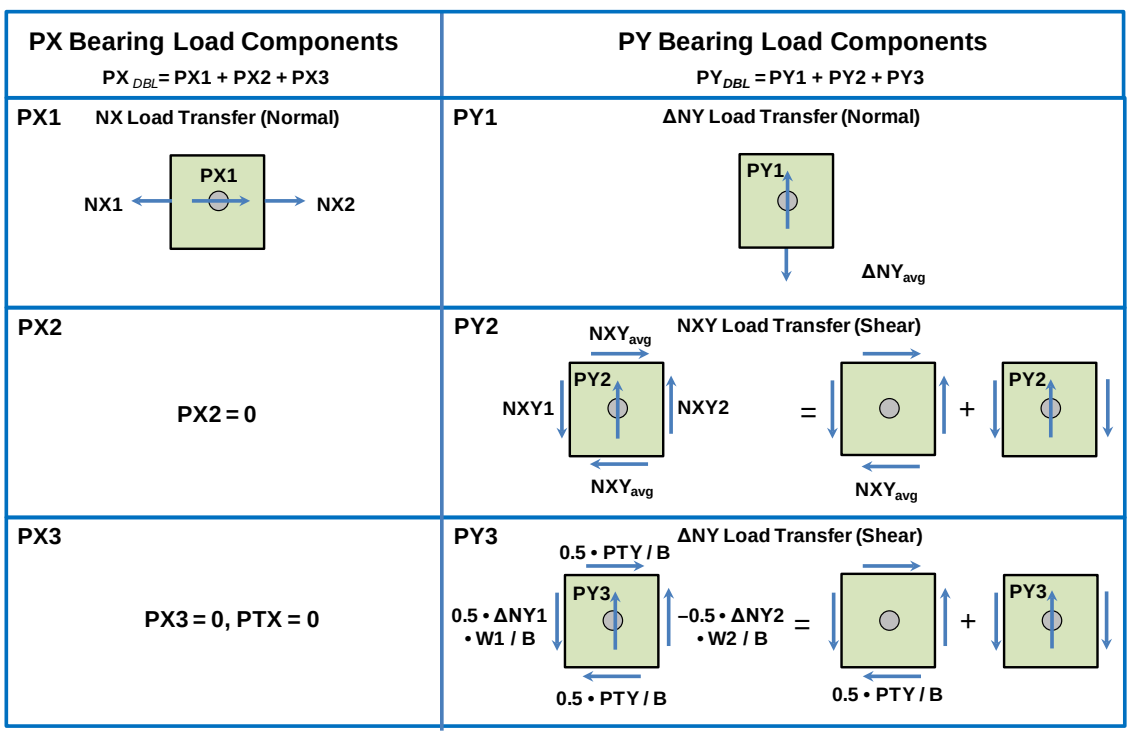

Figure 11.6-24 **Bearing Load Components using the DBL Method for a Fastener Line Aligned with the Y-axis**
Table 11.6-2 DBL Method: Bearing Load Components for a Fastener Line Aligned with the Y-axis

Copyright 2015 Lockheed Martin Corporation.
Note: The current version is always the version on the Lockheed Martin network.

Units	PX_{DBL} = PX1 + PX2 + PX3	PY_{DBL} = PY1 + PY2 + PY3
lbs	PX1 = (NX1 − NX2) • B	PY1 = ΔNY_{avg} • A
lbs	PX2 = 0	PY2 = (NXY1 − NXY2) • B
lbs	PX3 = 0	PY3 = 0.5 • (ΔNY1 • W1 + ΔNY2 • W2)
lbs	PTX = 0	PTY = 0.5 • (ΔNY1 • W1 − ΔNY2 • W2)

Notes:

1) If NX1 = NX2, then PX1 = 0.

2) If NXY1 = NXY2, then PY2 = 0.

3) If ΔNY1 = ΔNY2 = 0, then PY1 = PY3 = PTY = 0.

4) If ΔNY1 • W1 = ΔNY2 • W2 = 0, then PTY = 0.

For fastener lines aligned with the Y-axis, the PX bearing load component has a single component which will be designated as PX1. This is the X-direction lateral load transferred between the skin panel and substructure. It is calculated from the N1 and N3 load change in normal NX load that occurs from bay to bay across the fastener line. This load component directly depends upon the lateral stiffness provided by the substructure. The stiffer and more direct load path is provided by the skin continuity from bay-to-bay, so any large lateral loads should be verified. The lateral loads would be expected to increase as fasteners approach intersections with other transverse running substructure members since this increases the effective substructure stiffness.

In contrast, the PY bearing load has three possible contributing components designated as PY1, PY2, and PY3. The PY1 component is associated with N2 and N4 loads and is due to the normal load gradient in the Y-direction, ΔNY_{avg}. The PY2 and PY3 load components are due to T1 and T3 shear load transfer at edges 1 and 3. The PY2 load component is due to changes in the NXY load components from bay to bay across the fastener line. The PY3 load component is the portion of shear load transfer due to the ΔNY normal load gradient in each adjacent bay. The PTY load is the magnitude of the balancing couple required to keep the element in equilibrium when ΔNY1 • W1 does not equal to ΔNY2 • W2.

For fasteners lines aligned with the X-axis, there will be similar relationships for the bearing load components, PX and PY. In that case, there will be three possible PX bearing load components: PX1, PX2, PX3 along with a possible PTX shear balancing load, and only one PY bearing load component, PY1, where PY2 = PY3 = PTY = 0.

11.6.3.2 Fixed Bearing Load (FBL) Method

The Fixed Bearing Load method is intended to define loads for fasteners for which the bearing load has already been determined. The objective is to determine element boundary loads that reacts exactly the predetermined bearing loads. Fastener bearing loads may be reacted by either normal or shear loads at the element boundaries. The bearing loads and the assumed normal and shear reactions at the element boundaries are illustrated in Figure 11.6-25.

Copyright 2015 Lockheed Martin Corporation.
Note: The current version is always the version on the Lockheed Martin network.

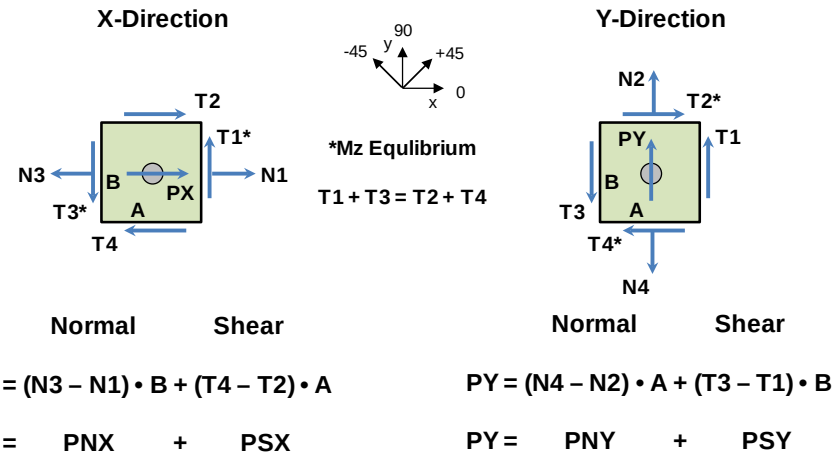

Figure 11.6-25 Fixed Bearing Load Method: Bearing Loads and Reactions

The PX bearing load component is a combination of the PNX and PSX bearing load cases shown in Figure 11.6-2 with normal and shear reactions, respectively. Similarly, the PY load component is a combination of the PNY and PSY bearing load cases with normal and shear reactions.

While PX and PY are already known, the contributing components need to be determined so that the proper element boundary forces can be calculated. As seen in the previous section, the DBL method can be used to determine the bearing load components. These DBL bearing load components will be used to determine load ratios that can be multiplied by the known bearing loads to determine the contributing components. The relevant equations are presented in Table 11.6-3.

Table 11.6-3 Using the DBL Method to Define FBL Bearing Load Factors

Units	PX = (RNX + RSX) • PX	PY = (RNY + RSY) • PY
---	RNX = PX1 / PX_{DBL}	RNY = PY1 / PY_{DBL}
---	RSX = (PX2 + PX3) / PX_{DBL}	RSY = (PY2 + PY3) / PY_{DBL}
---	RTX = PTX / PX_{DBL}	RTY = PTY / PY_{DBL}
---	1.0 = RNX + RSX	1.0 = RNY + RSY
---	RNX = 1.0 − RSX	RNY = 1.0 − RSY

The portions of normal and shear load can be expressed in terms of non-dimensional bearing load ratios or factors, as defined as: RNX, RSX, RNY and RSY. Since the sum of the bearing load factors is one (i.e., 1.0 = RNX + RSX), the normal bearing load factors can be defined in terms of the shear load factors (RNX = 1.0 – RSX). PX_{DBL} and PY_{DBL} are the total bearing loads as determined using the DBL method defined in Table 11.6-2.

Two additional load factors are also defined in Table 11.6-3, RTX and RTY. These load factors are used to represent NXY shear induced within the IBOLT element by a difference in load gradient ΔNY between the adjacent bays. Since the induced NXY shear is proportional to the bearing load component associated with the ΔNY load gradient, it is defined in terms of a bearing load factor.

An important point to note is how these equations simplify for the case when only in-plane loads exist (NX, NY, NXY) and there is no ΔNY load gradient. Under these conditions, PY1 = PY3 = PTY = 0 and the bearing load

Copyright 2015 Lockheed Martin Corporation.
Note: The current version is always the version on the Lockheed Martin network.

factors simplify to: RNX = 1, RSX = 0, RNY = 0, RSY = 1. Similarly, when only in-plane loads exist for the case of a fastener line aligned with the X-axis, the bearing load factors simplify to: RSX = RNY = 1, RNX = RSY = 0.

Using the bearing load factors defined above, the bearing-bypass loads for fastener line aligned with the Y-axis using the Fixed Bearing Load method are summarized in Figure 11.6-26.

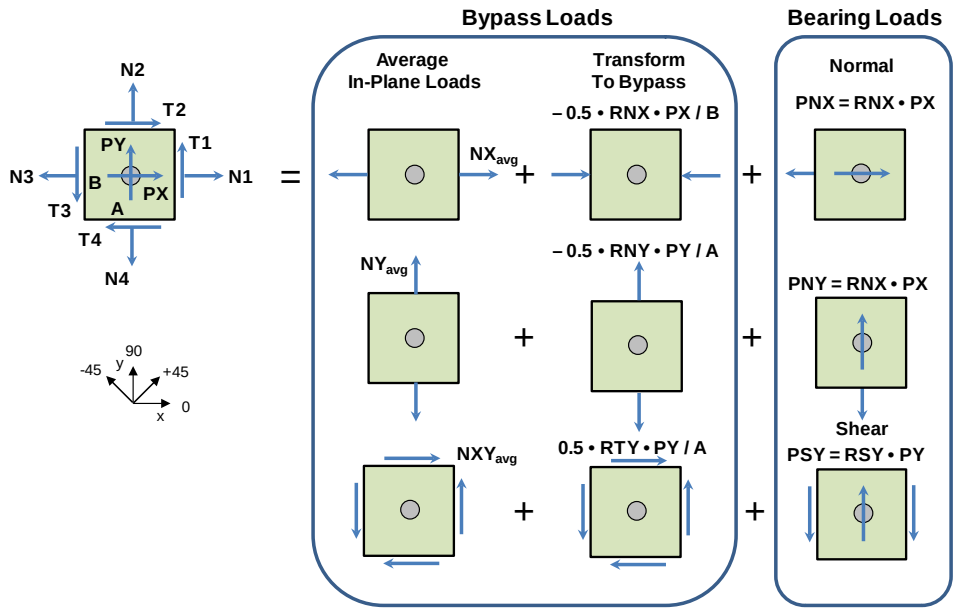

Figure 11.6-26 Bearing-Bypass Loads for a Fastener Line aligned with the Y-Axis using the FBL Method

The bearing loads for a fastener line aligned with the Y-axis are shown with normal (PNX, PNY) and shear (PSY) reactions in the right hand side of the figure. The bypass loads shown in the center are grouped into a convenient form. The bypass loads have been grouped into the average in-plane loads at the joint location and transform terms that are dependent on the bearing load and relate the average loads to the bearing basic load cases. This allows the calculation of average in-plane loads betweens bays and simplifies the overall load equations.

Figure 11.6-27 summarizes all of the Basic Load Cases that are required by the FBL and DBL methods to define IBOLT Element loads. Note that the NXX and NYY bypass cases of membrane load reacted by shear were not required.

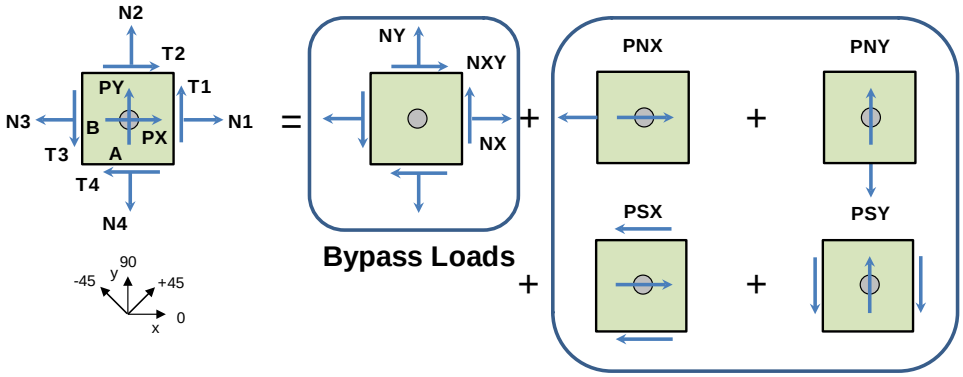

Figure 11.6-27 Basic Load Cases used to Define IBOLT Element Loads

Copyright 2015 Lockheed Martin Corporation.
Note: The current version is always the version on the Lockheed Martin network.

The associated equations for the basic load cases are summarized in Table 11.6-4.

Table 11.6-4 Bearing and Bypass Load Equations for the FBL Method

Bypass Loads	Units	Equations
FBL Method: Bypass Loads		
NX	**lbs/in**	$NX_{avg} + NX_{trans}$
NY	**lbs/in**	$NY_{avg} + NY_{trans}$
NXY	**lbs/in**	$NXY_{avg} + NXY_{trans}$
FBL Method: Transform Terms Relating Average Loads to Bearing Loads		
NX_{trans}	**lbs/in**	**−0.5 • (1 − RSX) • PX** / B
NY_{trans}	**lbs/in**	**−0.5 • (1 − RSY) • PY** / A
NXY_{trans}	**lbs/in**	**0.5 • (RTX • PX / A + RTY • PY / B)**
FBL Method: Bearing Loads and Factors		
PX	**lbs**	**PNX + PSX**
PY	**lbs**	**PNY + PSY**
PNX	**lbs**	**RNX • PX = (1 - RSX) • PX**
PSX	**lbs**	**RSX • PX**
PTX	**lbs**	**RTX • PX**
PNY	**lbs**	**RNY • PY = (1 - RSY) • PY**
PSY	**lbs**	**RSY • PY**
PTY	**lbs**	**RTY • PX**

IBOLT element loads equations for the following classes of fastener problems are presented with examples in the sections shown below:

1) Interior Skin Panel Fasteners: No Edges Free (Section 11.6.3.3);
2) Fasteners along Skin Panel Edges: One Edge Free (Section 11.6.3.4); and
3) Fasteners at Skin Panel Corners: Two Edges Free (Section 11.6.3.5).

11.6.3.3 Interior Skin Panel Fasteners: No Edges Free

This section provides IBOLT element load equations for interior skin panel fasteners with no edges free. The load equations are classified into fastener lines that are aligned with either the X-axis or Y-axis. The reference geometry for each condition is shown in Figure 11.6-28. The reference geometry for skin Bays and 1 and 2 are shown along with the positive components of bay loads. The orientations of the IBOLT element loads are also shown.

Copyright 2015 Lockheed Martin Corporation.
Note: The current version is always the version on the Lockheed Martin network.

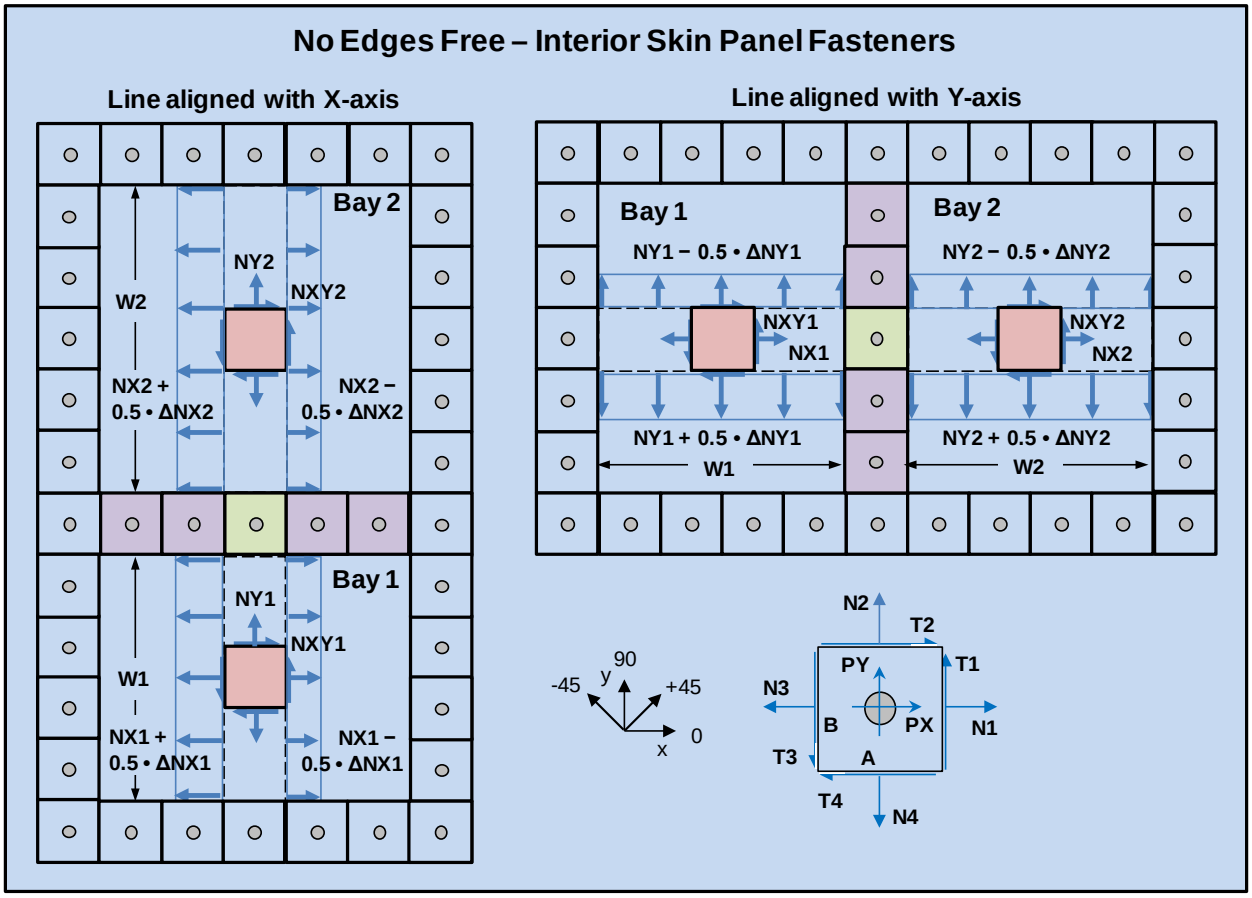

Figure 11.6-28 Reference Geometry for No Edges Free – Interior Skin Panel Fasteners

Figure 11.6-28 is to be used with the load equations provided in **Table 11.6-5** and Table **11.6-6**. The IBOLT element load equations for the Fixed Bearing Load (FBL) method in which PX and PY are known are given in Table 11.6-5. The IBOLT element load equations for the Derived Bearing Load (DBL) method for which PX and PY are unknown are given in Table 11.6-6**.**

For each method, there are two columns of load equations, one column for fastener lines aligned with the X-axis, the other for fastener lines aligned with the Y-axis. The known quantities are presented first, followed by the loads equations. The adjacent panel bay loads are in-plane loads (NX, NY and NXY) and any existing load gradients (ΔNX or ΔNY). The bay widths W1 and W2 are needed for any load gradients to calculate the shear induced on the fastener element.

For the FBL method, average in-plane loads are calculated at the joint location using the equations provided at the bottom of the table. These are a simple average of the Bay 1 and Bay 2 loads. These are the same average loads that were shown in Figure 11.6-26.

The X-direction bearing load ratios for fastener lines aligned with the Y-axis are RNX = 1, RSX = 0, RTX = 0. The Y-direction bearing load ratios are calculated based on the bearing load components: PY1, PY2, PY3 and PTY. PY1 is the normal load contribution due to a ΔNY load gradient acting across the element. PY2 is the shear load contribution due to NXY load in the adjacent panels. The PY3 is the shear load contribution due to ΔNY load gradients acting across the adjacent panels. PTY is the balancing shear due to ΔNY load differences between bays.

Copyright 2015 Lockheed Martin Corporation.
Note: The current version is always the version on the Lockheed Martin network.

If the load gradients ΔNY1 = ΔNY2 = 0, then PY1 = PY3 = 0 and PNY = PTY = 0 and PSY = 1. Another check is to make sure that PY_{DBL} or PY is non-zero. If either value equals zero, then the DBL method should be used to calculate the IBOLT element loads.

As shown in Table 11.6-6, the load equations for the DBL method are relatively straight forward. The normal boundary force resultants are set equal to the adjacent skin panel loads (NX and NY). The shear boundary force resultants are set equal and opposite the adjacent shear skin panel loads (due to NXY and/or ΔNY). PX and PY are then calculated using the equilibrium equations.

Table 11.6-5 IBOLT Element Loads for Interior Fasteners using FBL Method with Bolt Loads Known

Quantity	Units	Fastener Line aligned with X-axis	Fastener Line aligned with Y-axis
Known	**lbs**	**PX, PY**	**PX, PY**
	in	**A, B, W1, W2**	**A, B, W1, W2**
	lbs/in	**NX1, NY1, NXY1, NX2, NY2, NXY2**	**NX1, NY1, NXY1, NX2, NY2, NXY2**
	lbs/in	**ΔNX1, ΔNX2**	**ΔNY1, ΔNY2**
IBOLT Element Loads			
N1	**lbs/in**	$NX_{avg} - (1 - RSX) \cdot 0.5 \cdot PX / B$	$NX_{avg} - 0.5 \cdot PX / B$
N2	**lbs/in**	$NY_{avg} - 0.5 \cdot PY / A$	$NY_{avg} - (1 - RSY) \cdot 0.5 \cdot PY / A$
N3	**lbs/in**	$NX_{avg} + (1 - RSX) \cdot 0.5 \cdot PX / B$	$NX_{avg} + 0.5 \cdot PX / B$
N4	**lbs/in**	$NY_{avg} + 0.5 \cdot PY / A$	$NY_{avg} + (1 - RSY) \cdot 0.5 \cdot PY / A$
T1	**lbs/in**	$0.5 \cdot (T2 + T4)$	$NXY_{avg} + (RTY - RSY) \cdot 0.5 \cdot PY / B$
T2	**lbs/in**	$NXY_{avg} + (RTX - RSX) \cdot 0.5 \cdot PX / A$	$0.5 \cdot (T1 + T3)$
T3	**lbs/in**	$0.5 \cdot (T2 + T4)$	$NXY_{avg} + (RTY + RSY) \cdot 0.5 \cdot PY / B$
T4	**lbs/in**	$NXY_{avg} + (RTX + RSX) \cdot 0.5 \cdot PX / A$	$0.5 \cdot (T1 + T3)$
Bearing Load Components and Factors			
Define	**lbs**	$PX1 = \Delta NX_{avg} \cdot B$	$PY1 = \Delta NY_{avg} \cdot A$
	lbs	$PX2 = (NXY1 - NXY2) \cdot A$	$PY2 = (NXY1 - NXY2) \cdot B$
	lbs	$PX3 = 0.5 \cdot (\Delta NX1 \cdot W1 + \Delta NX2 \cdot W2)$	$PY3 = 0.5 \cdot (\Delta NY1 \cdot W1 + \Delta NY2 \cdot W2)$
	lbs	$PTX = 0.5 \cdot (\Delta NX1 \cdot W1 - \Delta NX2 \cdot W2)$	$PTY = 0.5 \cdot (\Delta NY1 \cdot W1 - \Delta NY2 \cdot W2)$
	lbs	$PX_{DBL} = PX1 + PX2 + PX3$	$PY_{DBL} = PY1 + PY2 + PY3$
	---	**RNY = 1, RSY = 0, RTY = 0**	**RNX = 1, RSX = 0, RTX = 0**
	---	$RNX = PX1 / PX_{DBL}$	$RNY = PY1 / PY_{DBL}$
	---	$RSX = (PX2 + PX3) / PX_{DBL}$	$RSY = (PY2 + PY3) / PY_{DBL}$
	---	$RTX = PTX / PX_{DBL}$	$RTY = PTY / PY_{DBL}$

Copyright 2015 Lockheed Martin Corporation.
Note: The current version is always the version on the Lockheed Martin network.

Checks	---	**1) If ΔNX1 = ΔNX2 = 0, Set RSX = 1, RTX = 0**	**1) If ΔNY1 = ΔNY2 = 0, Set RSY = 1, RTY = 0**
	---	**2) If (PX_{DBL} or PX = 0), Use DBL Method**	**2) If (PY_{DBL} or PY = 0), Use DBL Method**
Average In-Plane Load Resultants			
Define	**lbs/in**	**NX_{avg} = 0.5 • (NX1 + NX2)**	**NX_{avg} = 0.5 • (NX1 + NX2)**
	lbs/in	**NY_{avg} = 0.5 • (NY1 + NY2)**	**NY_{avg} = 0.5 • (NY1 + NY2)**
	lbs/in	**NXY_{avg} = 0.5 • (NXY1 + NXY2)**	**NXY_{avg} = 0.5 • (NXY1 + NXY2)**
	lbs/in	**ΔNX_{avg} = 0.5 • (ΔNX1 + ΔNX2)**	**ΔNY_{avg} = 0.5 • (ΔNY1 + ΔNY2)**

Table 11.6-6 IBOLT Element Loads for Interior Fasteners using DBL Method with Bolt Loads Unknown

Quantity	Units	Fastener Line aligned with X-axis	Fastener Line aligned with Y-axis
Known	**in**	**A, B, W1, W2**	**A, B, W1, W2**
	lbs/in	**NX1, NY1, NXY1, NX2, NY2, NXY2**	**NX1, NY1, NXY1, NX2, NY2, NXY2**
	lbs/in	**ΔNX1, ΔNX2**	**ΔNY1, ΔNY2**
IBOLT Element Loads			
N1	**lbs/in**	**$NX_{avg} - 0.5 \cdot \Delta NX_{avg}$**	**NX2**
N2	**lbs/in**	**NY2**	**$NY_{avg} - 0.5 \cdot \Delta NY_{avg}$**
N3	**lbs/in**	**$NX_{avg} + 0.5 \cdot \Delta NX_{avg}$**	**NX1**
N4	**lbs/in**	**NY1**	**$NY_{avg} + 0.5 \cdot \Delta NY_{avg}$**
T1	**lbs/in**	**0.5 • (T2 + T4)**	**NXY2 − 0.5 • ΔNY2 • W2 / B**
T2	**lbs/in**	**NXY2 − 0.5 • ΔNX2 • W2 / A**	**0.5 • (T1 + T3)**
T3	**lbs/in**	**0.5 • (T2 + T4)**	**NXY1 + 0.5 • ΔNY1 • W1 / B**
T4	**lbs/in**	**NXY1 + 0.5 • ΔNX1 • W1 / A**	**0.5 • (T1 + T3)**
PX	**lbs**	**PX = B • (N3 − N1) + A • (T4 − T2)**	
PY	**lbs**	**PY = A • (N4 − N2) + B • (T3 − T1)**	
Average In-Plane Load Resultants			
Define	**lbs/in**	**NX_{avg} = 0.5 • (NX1 + NX2)**	**NX_{avg} = 0.5 • (NX1 + NX2)**
	lbs/in	**NY_{avg} = 0.5 • (NY1 + NY2)**	**NY_{avg} = 0.5 • (NY1 + NY2)**
	lbs/in	**NXY_{avg} = 0.5 • (NXY1 + NXY2)**	**NXY_{avg} = 0.5 • (NXY1 + NXY2)**
	lbs/in	**ΔNX_{avg} = 0.5 • (ΔNX1 + ΔNX2)**	**ΔNY_{avg} = 0.5 • (ΔNY1 + ΔNY2)**

Example problem 3 provides a numerical example for an interior panel fastener line that is aligned with the Y-axis. The example demonstrates the use of the DBL and FBL methods in determining IBOLT element loads. Bay 1 and

Copyright 2015 Lockheed Martin Corporation.
Note: The current version is always the version on the Lockheed Martin network.

Bay 2 in-plane loads and ΔNY load gradients are given along with the bay widths, W1 and W2. The IBOLT element is assumed to have dimensions A = B = 1.0 in. for clarity.

The PX, PY loads used in the Fixed Bearing Load method example have been idealized for clarity in that it matches the calculated PX, PY loads in the Derived Bearing Load method. In practice, these loads are likely to vary and large differences should be investigated to determine the cause. Engineering judgment may be required to resolve the differences and determine which approach is more accurate.

11.6.3.3.1 Example 3 – Interior Panel Fastener Line Aligned with the Y-Axis

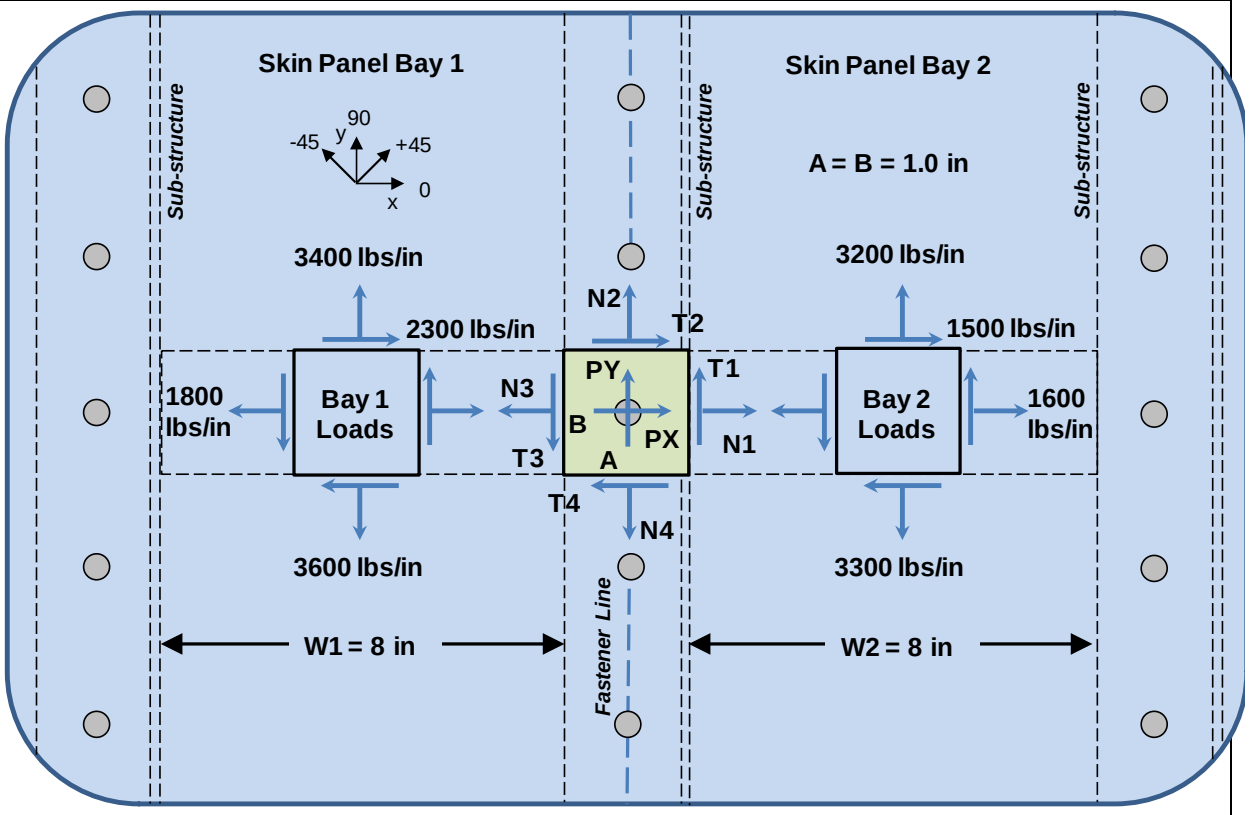

Problem Statement: Determine the IBOLT element loads for the center fastener using: a) the Fixed Bearing Load method; and b) the Derived Bearing Load method.

Known:

PX = 200 lbs, PY = 2150 lbs	A = B = 1.0 in, Element dimensions
Bay 1	Bay 2
NX1 = 1800 lbs/in	NX2 = 1600 lbs/in
NY1 = 0.5 • (3400 + 3600) = 3500 lbs/in	NY2 = 0.5 • (3200 + 3300) = 3250 lbs/in
NXY1 = 2300 lbs/in	NXY2 = 1500 lbs/in
ΔNY1 = 3600 – 3400 = 200 lbs/in	ΔNY2 = 3300 – 3200 = 100 lbs/in
W1 = 8.0 in	W2 = 8.0 in

a) ***Solution using the Fixed Bearing Load method***

Known: PX = 200 lbs, PY = 2150 lbs
Determine: N1, N2, N3, N4, T1, T2, T3, T4 (Refer to Table 11.6-5)

Copyright 2015 Lockheed Martin Corporation.
Note: The current version is always the version on the Lockheed Martin network.

11.6.3.3.1 Example 3 Continued

Preliminary observations:
a. The fastener is part of an interior fastener line that is aligned with Y-axis.
b. Is there a ΔNY load gradient in Y in either Bay? Yes, no load factor simplifications are applicable.
c. Is the bearing load PY = 0? No, then proceed with the FBL method.

1) Begin by calculating the average in-plane loads at the fastener center:
$NX_{avg} = 0.5 \cdot (NX1 + NX2) = 0.5 \cdot (1800 + 1600) = 1700$ lbs/in
$NY_{avg} = 0.5 \cdot (NY1 + NY2) = 0.5 \cdot (3500 + 3250) = 3375$ lbs/in
$NXY_{avg} = 0.5 \cdot (NXY1 + NXY2) = 0.5 \cdot (2300 + 1500) = 1900$ lbs/in
$\Delta NY_{avg} = 0.5 \cdot (\Delta NY1 + \Delta NY2) = 0.5 \cdot (200 + 100) = 150$ lbs/in

2) Calculate the bearing load components. For a fastener line aligned with the Y-axis:
PX1 = PX = 200 lbs
PX2 = PX3 = PTX = 0 lbs/in

$PY1 = \Delta NY_{avg} \cdot A = 150 \cdot 1.0 = 150$ lbs
$PY2 = (NXY1 - NXY2) \cdot B = (2300 - 1500) \cdot 1.0 = 800$ lbs
$PY3 = 0.5 \cdot (\Delta NY1 \cdot W1 + \Delta NY2 \cdot W2) = 0.5 \cdot (200 \cdot 8.0 + 100 \cdot 8.0) = 1200$ lbs
$PY_{DBL} = PY1 + PY2 + PY3 = 150 + 800 + 1200 = 2150$ lbs

Magnitude of shear required to maintain M_Z equilibrium for the case of $\Delta NY1 \cdot W1 \neq \Delta NY2 \cdot W2$:
$PTY = 0.5 \cdot (\Delta NY1 \cdot W1 - \Delta NY2 \cdot W2) = 0.5 \cdot (200 \cdot 8.0 - 100 \cdot 8.0) = 400$ lbs

3) Calculate bearing load factors:
$RSY = (PY2 + PY3) / PY_{DBL} = (800 + 1200) / 2150 = 0.930$
$RNY = 1.0 - RSY = 0.070$
$RTY = PTY / PY_{DBL} = 400 / 2150 = 0.186$

4) Calculate running loads along the IBOLT element boundary:
$N1 = NX_{avg} - 0.5 \cdot PX / B = 1700 - 0.5 \cdot 200 / 1.0 = 1600$ lbs/in
$N2 = NY_{avg} - (1 - RSY) \cdot 0.5 \cdot PY / A = 3375 - 0.070 \cdot 0.5 \cdot 2150 = 3375 - 75 = 3300$ lbs/in
$N3 = NX_{avg} + 0.5 \cdot PX / B = 1700 + 0.5 \cdot 200 / 1.0 = 1800$ lbs/in
$N4 = NY_{avg} + (1 - RSY) \cdot 0.5 \cdot PY / A = 3375 + 0.070 \cdot 0.5 \cdot 2150 = 3375 + 75 = 3450$ lbs/in

$T1 = NXY_{avg} + (RTY - RSY) \cdot 0.5 \cdot PY / B = 1900 + (0.186 - 0.930) \cdot 0.5 \cdot 2150 / 1.0 = 1100$ lbs/in
$T2 = 0.5 \cdot (T1 + T3) = 2100$ lbs/in
$T3 = NXY_{avg} + (RTY + RSY) \cdot 0.5 \cdot PY / B = 1900 + (0.186 + 0.930) \cdot 0.5 \cdot 2150 / 1.0 = 3100$ lbs/in
$T4 = 0.5 \cdot (T1 + T3) = 2100$ lbs/in

5) Verify using equilibrium equations 11.6-2:
$PX = B \cdot (N3 - N1) + A \cdot (T4 - T2)$
$PX = 1.0 \cdot (1800 - 1600) + 1.0 \cdot (2100 - 2100)$
PX = 200 lbs ✓

$PY = A \cdot (N4 - N2) + B \cdot (T3 - T1)$
$PY = 1.0 \cdot (3450 - 3300) + 1.0 \cdot (3100 - 1100)$
PY = 2150 lbs ✓

T1 + T3 = T2 + T4
3100 + 1100 = 2100 + 2100 = 4200 lb/in ✓

Copyright 2015 Lockheed Martin Corporation.
Note: The current version is always the version on the Lockheed Martin network.

11.6.3.3.1 Example 3 Continued

b) ***Solution using the Derived Bearing Load method***

Determine: N1, N2, N3, N4, T1, T2, T3, T4, PX, PY (Refer to Table 11.6-6)

1) Begin by calculating the average in-plane loads at the fastener center:
$NX_{avg} = 0.5 \cdot (NX1 + NX2) = 0.5 \cdot (1800 + 1600) = 1700$ lbs/in
$NY_{avg} = 0.5 \cdot (NY1 + NY2) = 0.5 \cdot (3500 + 3250) = 3375$ lbs/in
$NXY_{avg} = 0.5 \cdot (NXY1 + NXY2) = 0.5 \cdot (2300 + 1500) = 1900$ lbs/in
$\Delta NY_{avg} = 0.5 \cdot (\Delta NY1 + \Delta NY2) = 0.5 \cdot (200 + 100) = 150$ lbs/in

2) Calculate running loads along the IBOLT element boundary:
$N1 = NX2 = 1600$ lbs/in
$N2 = NY_{avg} - 0.5 \cdot \Delta NY_{avg} = 3375 - 0.5 \cdot 150 = 3375 - 75 = 3300$ lbs/in
$N3 = NX1 = 1800$ lbs/in
$N4 = NY_{avg} + 0.5 \cdot \Delta NY_{avg} = 3375 + 0.5 \cdot 150 = 3375 + 75 = 3450$ lbs/in

$T1 = NXY2 - 0.5 \cdot \Delta NY2 \cdot W2 / B = 1500 - 0.5 \cdot 100 \cdot 8.0 / 1.0 = 1100$ lbs/in
$T2 = 0.5 \cdot (T1 + T3) = 2100$ lbs/in
$T3 = NXY1 + 0.5 \cdot \Delta NY1 \cdot W1 / B = 2300 + 0.5 \cdot 200 \cdot 8.0 / 1.0 = 3100$ lbs/in
$T4 = 0.5 \cdot (T1 + T3) = 2100$ lbs/in

3) Calculate PX, PY from equilibrium equations 11.6-2:
$PX = B \cdot (N3 - N1) + A \cdot (T4 - T2)$
$PX = 1.0 \cdot (1800 - 1600) + 1.0 \cdot (2100 - 2100)$
$PX = 200$ lbs

$PY = A \cdot (N4 - N2) + B \cdot (T3 - T1)$
$PY = 1.0 \cdot (3450 - 3300) + 1.0 \cdot (3100 - 1100)$
$PY = 2150$ lbs

Verify M_Z equilibrium:
$T1 + T3 = T2 + T4$
$3100 + 1100 = 2100 + 2100 = 4200$ lb/in ✓

Copyright 2015 Lockheed Martin Corporation.
Note: The current version is always the version on the Lockheed Martin network.

11.6.3.4 Fasteners along Skin Panel Edges: One Edge Free

This section provides IBOLT element load equations for fasteners along panel edges with one edge free. The reference geometry for panel edges and corners are shown in Figure 11.6-29. Table 11.6-7 describes the position and designation for each IBOLT element analysis. The loads equations for the four edge cases will be discussed within this section, while the loads equations for the corner cases are discussed in Section 11.6.3.5.

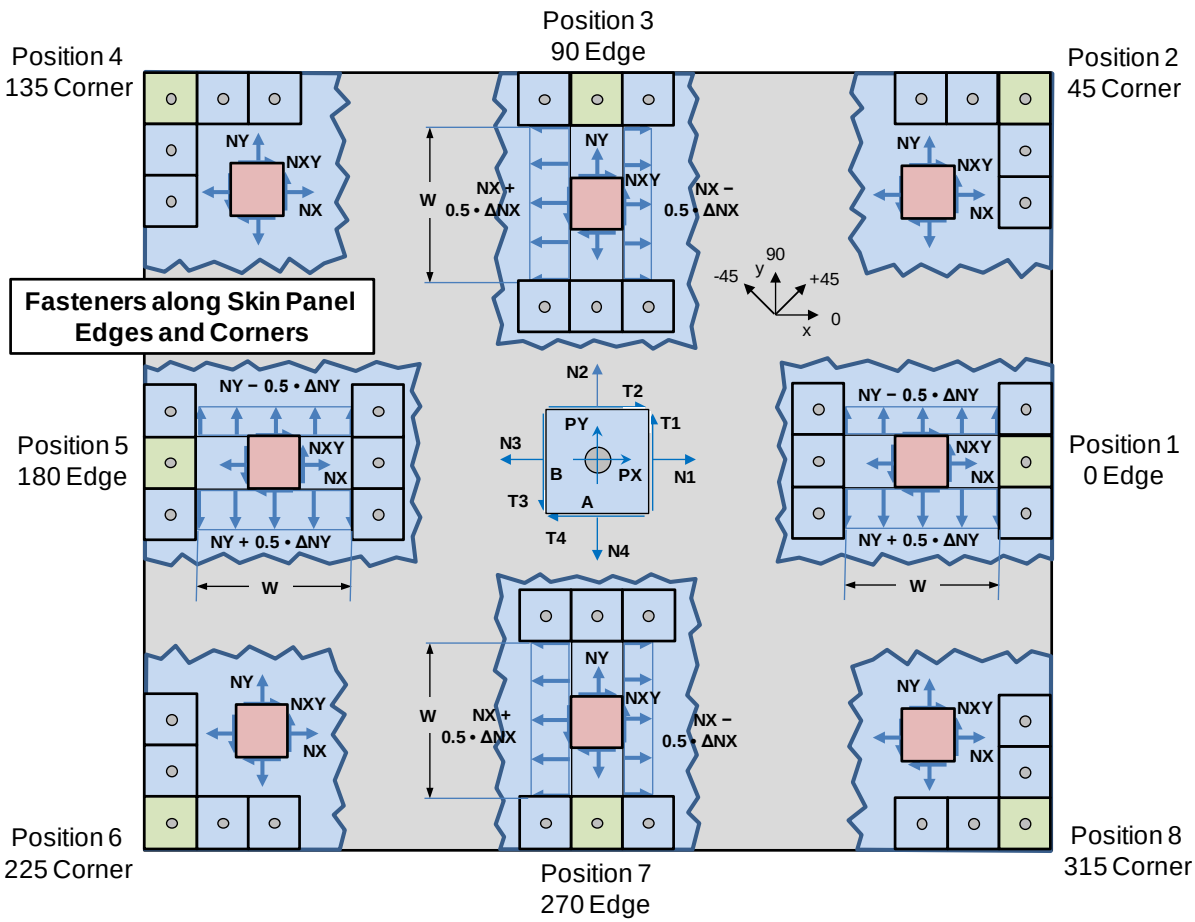

Figure 11.6-29 Reference Geometry for One or Two Edges Free (Panel Edge or Corner)

Copyright 2015 Lockheed Martin Corporation.
Note: The current version is always the version on the Lockheed Martin network.

Table 11.6-7 IBOLT Element Edge and Corner Positions and Designations

Location	Corner or Edge	Angle	Position	Edge Condition
Right Edge	Edge	0	1	One-Edge-Free
Upper Edge	Edge	90	3	One-Edge-Free
Left Edge	Edge	180	5	One-Edge-Free
Lower Edge	Edge	270	7	One-Edge-Free
Upper Right Corner	Corner	45	2	Two-Edges-Free
Upper Left Corner	Corner	135	4	Two-Edges-Free
Lower Left Corner	Corner	225	6	Two-Edges-Free
Lower Right Corner	Corner	315	8	Two-Edges-Free

The orientation of the IBOLT element loads are shown in the center of the panel figure. A typical fastener element for each edge is highlighted in green. Examining the one edge free edge locations, Positions 1, 3, 5 or 7, load components may exist along three of the four element edges. These edges are denoted as 0, 90, 180 and 270, respectively. The adjacent skin panel loads associated with each position is shown within the same breakout area. The positive sign conventions for the local skin panel loads are indicated for each edge. Pertinent dimensions are also shown.

The key assumptions for one edge free are as follows:
1) The normal and shear boundary force resultant on the free edge must be equal to zero.
2) M_Z equilibrium (T1 + T3 = T2 + T4) must be satisfied.
As an example, the assumed boundary shear force resultants for Edge Position 1 are shown in Figure 11.6-30.

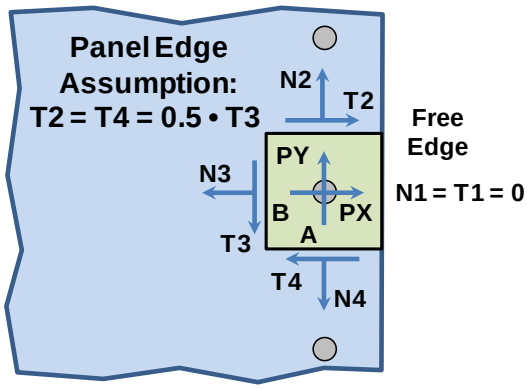

Figure 11.6-30 Assumed Panel Boundary Shear Loads for Edge Position 1

The IBOLT element load equations for the Fixed Bearing Load (FBL) method in which PX and PY are known are given in Table **11.6-8**. The IBOLT element load equations for the Derived Bearing Load (DBL) method for which PX and PY are unknown are given in Table **11.6-9**.

For each method, there are four columns of load equations, one column for each of the Edge Positions 1, 3, 5 and 7. The known quantities are presented first, followed by the loads equations. The adjacent panel loads are in-plane loads (NX, NY and NXY) and any existing load gradients (ΔNX or ΔNY). The bay width W is needed for any load gradients to calculate the shear induced on the fastener element.

Copyright 2015 Lockheed Martin Corporation.
Note: The current version is always the version on the Lockheed Martin network.

Table 11.6-8 **IBOLT Element Loads for Panel Edges using FBL Method with Bolt Loads Known**

Quantity	Units	1 − 0 Edge	3 − 90 Edge	5 − 180 Edge	7 − 270 Edge
Known	lbs	PX, PY	PX, PY	PX, PY	PX, PY
	in	A, B, W	A, B, W	A, B, W	A, B, W
	lbs/in	NX, NY, NXY, ΔNY	NX, NY, NXY, ΔNX	NX, NY, NXY, ΔNY	NX, NY, NXY, ΔNX
IBOLT Element Loads					
N1	lbs/in	0	NX − (1 − RSX) • 0.5 • PX / B	− PX / B	NX − (1 − RSX) • 0.5 • PX / B
N2	lbs/in	NY − (1 − RSY) • 0.5 • PY / A	0	NY − (1 − RSY) • 0.5 • PY / A	− PY / A
N3	lbs/in	PX / B	NX + (1 − RSX) • 0.5 • PX / B	0	NX + (1 − RSX) • 0.5 • PX / B
N4	lbs/in	NY + (1 − RSY) • 0.5 • PY / A	PY / A	NY + (1 − RSY) • 0.5 • PY / A	0
T1	lbs/in	0	0.5 • T4	− RSY • PY / B	0.5 • T2
T2	lbs/in	0.5 • T3	0	0.5 • T1	− RSX • PX / A
T3	lbs/in	RSY • PY / B	0.5 • T4	0	0.5 • T2
T4	lbs/in	0.5 • T3	RSX • PX / A	0.5 • T1	0
Bearing Load Components and Factors (RTX = RTY = 0)					
Define	lbs	PY1 = ΔNY • A	PX1 = ΔNX • B	PY1 = ΔNY • A	PX1 = ΔNX • B
	lbs	PY2 = NXY • B	PY2 = NXY • A	PY2 = − NXY • B	PY2 = − NXY • A
	lbs	PY3 = 0.5 • ΔNY • W	PX3 = 0.5 • ΔNX • W	PY3 = 0.5 • ΔNY • W	PX3 = 0.5 • ΔNX • W
	lbs	PY_{DBL} = PY1 + PY2 + PY3	PX_{DBL} = PX1 + PX2 + PX3	PY_{DBL} = PY1 + PY2 + PY3	PX_{DBL} = PX1 + PX2 + PX3
	---	RNX = 1, RSX = 0	RNY = 1, RSY = 0	RNX = 1, RSX = 0	RNY = 1, RSY = 0
	---	RNY = PY1 / PY_{DBL}	RNX = PX1 / PX_{DBL}	RNY = PY1 / PY_{DBL}	RNX = PX1 / PX_{DBL}
	---	RSY = (PY2 + PY3) / PY_{DBL}	RSX = (PX2 + PX3) / PX_{DBL}	RSY = (PY2 + PY3) / PY_{DBL}	RSX = (PX2 + PX3) / PX_{DBL}
Checks	---	1) If ΔNY = 0, Set RSY = 1	1) If ΔNX = 0, Set RSX = 1	1) If ΔNY = 0, Set RSY = 1	1) If ΔNX = 0, Set RSX = 1
	---	2) If (PY_{DBL} or PY = 0), Use DBL Method	2) If (PX_{DBL} or PX = 0), Use DBL Method	2) If (PY_{DBL} or PY = 0), Use DBL Method	2) If (PX_{DBL} or PX = 0), Use DBL Method

Copyright 2015 Lockheed Martin Corporation.
Note: The current version is always the version on the Lockheed Martin network.

Table 11.6-9 **IBOLT Element Loads for Panel Edges using DBL Method with Bolt Loads Unknown**

Quantity	Units	1 − 0 Edge	3 − 90 Edge	5 − 180 Edge	7 − 270 Edge
Known	in	A, B, W	A, B, W	A, B, W	A, B, W
	lbs/in	NX, NY, NXY	NX, NY, NXY	NX, NY, NXY	NX, NY, NXY
	lbs/in	ΔNY	ΔNX	ΔNY	ΔNX
IBOLT Element Loads					
N1	lbs/in	0	NX − 0.5 • ΔNX	NX	NX − 0.5 • ΔNX
N2	lbs/in	NY − 0.5 • ΔNY	0	NY − 0.5 • ΔNY	NY
N3	lbs/in	NX	NX + 0.5 • ΔNX	0	NX + 0.5 • ΔNX
N4	lbs/in	NY + 0.5 • ΔNY	NY	NY + 0.5 • ΔNY	0
T1	lbs/in	0	0.5 • T4	NXY − 0.5 • ΔNY • W / B	0.5 • T2
T2	lbs/in	0.5 • T3	0	0.5 • T1	NXY − 0.5 • ΔNX • W / A
T3	lbs/in	NXY + 0.5 • ΔNY • W / B	0.5 • T4	0	0.5 • T2
T4	lbs/in	0.5 • T3	NXY + 0.5 • ΔNX • W / A	0.5 • T1	0
PX	lbs	PX = B • (N3 − N1) + A • (T4 − T2)			
PY	lbs	PY = A • (N4 − N2) + B • (T3 − T1)			

Copyright 2015 Lockheed Martin Corporation.
Note: The current version is always the version on the Lockheed Martin network.

Examining Table **11.6-8**, the load equations for the FBL method are relatively straightforward to calculate. For example, referring to the equations for Edge Position 1,

- Element dimensions (A and B) and bearing loads (PX and PY) are known.
- The adjacent panel load NY is adopted as the element average.
- PX bearing load ratios for Edge Position 1 are RNX = 1, RSX = 0.
- PY bearing load ratios are calculated based on the bearing load components: PY1, PY2, and PY3
    - PY1 is the normal load contribution due to a ΔNY load gradient acting across the element.
    - PY2 is the shear load contribution due to NXY load in the adjacent panel.
    - PY3 is the shear load contribution due to ΔNY load gradient acting across the adjacent panel.
- Note that if the load gradient ΔNY = 0, then PY1 = PY3 = 0 and PNY = 0 and PSY = 1.
- Check to make sure that PY_{DBL} or PY is non-zero. If either value equals zero, use the DBL method to calculate the IBOLT element loads.

From Table **11.6-9** it can be seen that the load equations for the DBL method are also relatively straight forward. Again referring to the equations for Edge Position 1

- The normal boundary force resultants are set equal to the adjacent skin panel loads (NX and NY).
- The shear boundary force resultants are set equal and opposite the adjacent shear skin panel loads (due to NXY and/or ΔNY).
- PX and PY are then calculated using the equilibrium equations.

Example problem 4 provides a numerical example for a panel edge fastener with one edge free. The problem corresponds to the geometry of Edge Position 1 in Figure 11.6-29. Due to the free edge conditions, N1 = T1= 0. The adjacent panel loads are indicated in the panel area. The adjacent skin panel has in-plane loads NX 1500 lbs/in, NY = 1800 lbs/in, and NXY = 2400 lbs/in. Note that there is a load gradient ΔNY = 200 lbs/in across the element length. The IBOLT element is assumed to have dimensions A = B = 1.0 in. for clarity.

The PX, PY loads used in the Fixed Bearing Load method example has been idealized for clarity in that it matches the calculated PX, PY loads in the Derived Bearing Load method. In practice, these loads are likely to vary and large differences should be investigated to determine the cause. Engineering judgment may be required to resolve the differences and determine which approach is more accurate.

Copyright 2015 Lockheed Martin Corporation.
Note: The current version is always the version on the Lockheed Martin network.

11.6.3.4.1 Example 4 – Fastener Along a Panel Edge

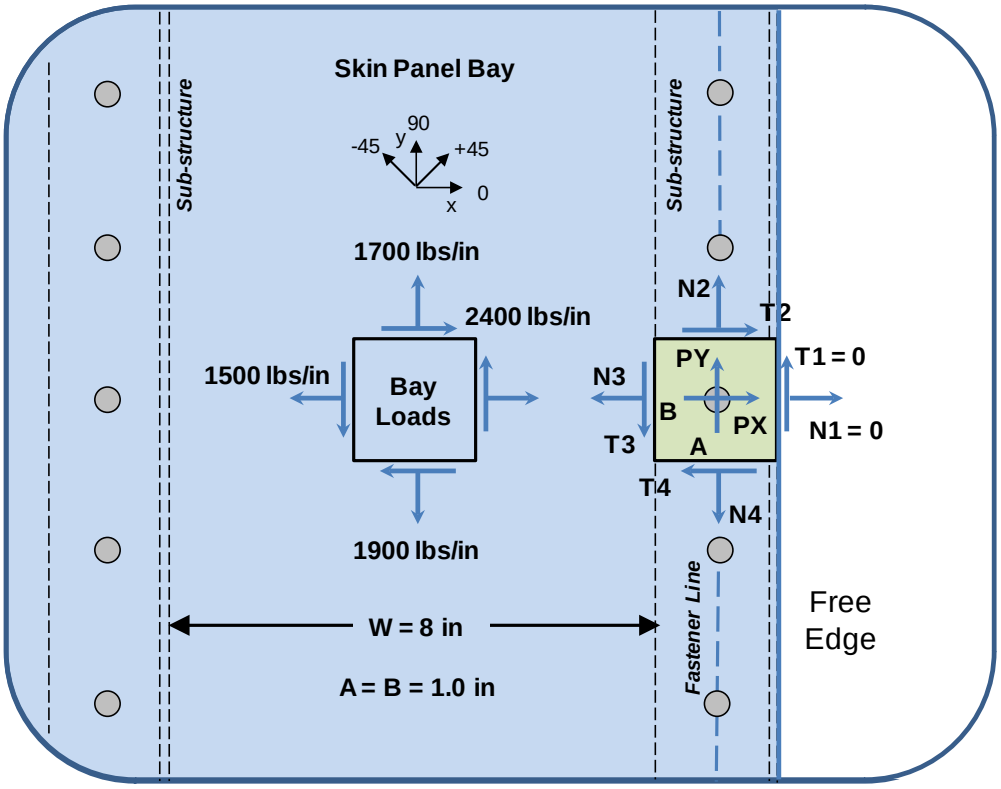

Problem Statement: Determine the IBOLT element loads for the center fastener using: a) the Fixed Bearing Load method; and b) the Derived Bearing Load method.

Known:

PX = 1500 lbs, PY = 3400 lbs

A = B = 1.0 in, Element dimensions

Adjacent Bay

NX = 1500 lbs/in

NY = 0.5 • (1700 + 1900) = 1800 lbs/in

NXY = 2400 lbs/in

ΔNY = 1900 – 1700 = 200 lbs/in

W1 = 8.0 in

a) ***Solution using the Fixed Bearing Load method***

Known: PX = 1500 lbs, PY = 3400 lbs

Determine: N1, N2, N3, N4, T1, T2, T3, T4 (Refer to Table **11.6-8**)

Preliminary observations:

a. The fastener is located along a panel edge with one edge free.

b. Is there a ΔNY load gradient in Y in either Bay? Yes, no load factor simplifications are applicable.

c. Is the bearing load PY = 0? No, then proceed with the FBL method.

1) Begin by calculating the bearing load components:

PX1 = PX = 1500 lbs

PX2 = PX3 = 0 lbs/in

Copyright 2015 Lockheed Martin Corporation.
Note: The current version is always the version on the Lockheed Martin network.

11.6.3.4.1 Example 4 Continued

PY1 = ΔNY • A = 200 • 1.0 = 200 lbs
PY2 = NXY • B = 2400 • 1.0 = 2400 lbs
PY3 = 0.5 • ΔNY • W = 0.5 • 200 • 8.0 = 800 lbs
PYT = PY1 + PY2 + PY3 = 200 + 2400 + 800 = 3400

2) Calculate bearing load factors:
RSY = (PY2 + PY3) / PYT = (2400 + 800) / 3400 = 0.941
RNY = 1.0 – RSY = 0.059

3) Calculate running loads along the IBOLT element boundary:
N1 = 0 lbs/in
N2 = NY − (1 − RSY) • 0.5 • PY / A = 1800 – 0.059 • 0.5 • 3400 = 1800 – 100 = 1700 lbs/in
N3 = PX / B = 1500 / 1.0 = 1500 lbs/in
N4 = NY + (1 − RSY) • 0.5 • PY / A = 1800 + 0.059 • 0.5 • 3400 = 1800 + 100 = 1900 lbs/in

T1 = 0 lbs/in
T2 = 0.5 • (T1 + T3) = 1600 lbs/in
T3 = RSY • PY / B = 0.941 • 3400 / 1.0 = 3200 lbs/in
T4 = 0.5 • (T1 + T3) = 1600 lbs/in

4) Verify using equilibrium equations 11.6-2:
PX = B • (N3 − N1) + A • (T4 − T2)
PX = 1.0 • (1500 − 0) + 1.0 • (1600 − 1600)
PX = 1500 lbs ✓

PY = A • (N4 − N2) + B • (T3 − T1)
PY = 1.0 • (1900 − 1700) + 1.0 • (3200 − 0)
PY = 3400 lbs ✓

T1 + T3 = T2 + T4
0 + 3200 = 1600 + 1600 = 1600 lb/in ✓

b) ***<u>Solution using the Derived Bearing Load method</u>***

Determine: N1, N2, N3, N4, T1, T2, T3, T4, PX, PY (Refer to Table **11.6-9**)

1) Calculate running loads along the IBOLT element boundary:
N1 = 0 lbs/in
N2 = NY − 0.5 • ΔNY = 1800 – 0.5 • 200 = 1700 lbs/in
N3 = NX = 1500 lbs/in
N4 = NY + 0.5 • ΔNY = 1800 + 0.5 • 200 = 1900 lbs/in

T1 = 0 lbs/in
T2 = 0.5 • (T1 + T3) = 1600 lbs/in
T3 = NXY + 0.5 • ΔNY • W = 2400 + 0.5 • 200 • 8.0 / 1.0 = 3200 lbs/in
T4 = 0.5 • (T1 + T3) = 1600 lbs/in

Copyright 2015 Lockheed Martin Corporation.
Note: The current version is always the version on the Lockheed Martin network.

11.6.3.4.1 Example 4 Continued

2) Calculate PX, PY from equilibrium equations 11.6-2:
PX = B • (N3 − N1) + A • (T4 − T2)
PX = 1.0 • (1500 − 0) + 1.0 • (1600 − 1600)
PX = 1500 lbs

PY = A • (N4 − N2) + B • (T3 − T1)
PY = 1.0 • (1900 − 1700) + 1.0 • (3200 − 0)
PY = 3400 lbs

Verify M_Z equilibrium:
T1 + T3 = T2 + T4
0 + 3200 = 1600 + 1600 = 1600 lb/in ✓

11.6.3.5 Fasteners at Skin Panel Corners: Two Edges Free

This section provides IBOLT element load equations for fasteners at skin panel corners with two edges free. The reference geometry for the four cases of skin panel corners is provided in Figure 11.6-29. Corner element positions and designations are given in Table 11.6-7. The orientation of the IBOLT element loads are shown in the center of the panel figure. The positive sign conventions for the local skin panel loads are indicated for each corner. The corner fastener for each corner is highlighted in green.

The key assumptions for two edges free are:
1) On each free edge, the normal and shear boundary force resultant must be equal to zero.
2) M_Z equilibrium (T1 + T3 = T2 + T4) must be satisfied.

Any normal load gradients (ΔNX or ΔNY) are assumed resolved at the corners, so there are no contributions to the load equations.

The IBOLT element load equations for the Fixed Bearing Load (FBL) method in which PX and PY are known are given in Table 11.6-10. There are several ways in which the loads could be resolved. Since PX and PY are known, engineering judgment must be used to obtain the boundary forces. The approach adopted here is to use the DBL method to determine the shear boundary force resultants with the assumption that the remaining bearing load is reacted by the normal force resultants.

The IBOLT element load equations for the Derived Bearing Load (DBL) method for which PX and PY are unknown are given in Table 11.6-11. Some key features of this approach are

- The non-zero normal boundary force resultants are set equal to the adjacent skin panel loads (NX and NY).
- The non-zero shear boundary force resultants are set to one-half the equal and opposite adjacent shear skin panel loads (0.5 • NXY).
- As shown in Figure 11.6-31, this is total amount of NXY shear that can be reacted while maintaining equilibrium with adjacent edge fastener elements.
- PX and PY are then calculated using the equilibrium equations.

Copyright 2015 Lockheed Martin Corporation.
Note: The current version is always the version on the Lockheed Martin network.

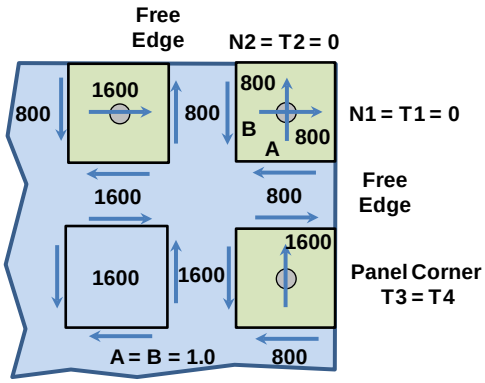

Figure 11.6-31 Example NXY shear reacted at Corner Position 2

Example problem 5 provides a numerical example for a fastener at a panel corner with two edges free. The problem corresponds to the geometry of Corner Position 2 in Figure 11.6-29. Due to the free edge conditions, N1 = T1= N2 = T2 = 0. The adjacent panel loads are indicated in the panel area. The IBOLT element has dimensions A = B = 1.0 in. PX, PY loads used in the FBL method example have been idealized for clarity in that it matches the calculated PX, PY loads in the DBL method. In practice, these loads are likely to vary and large differences should be investigated to determine the cause. Engineering judgment may be required to resolve the differences and determine which approach is more accurate.

Copyright 2015 Lockheed Martin Corporation.
Note: The current version is always the version on the Lockheed Martin network.

Table 11.6-10 IBOLT Element Loads for a Panel Corner Fastener using FBL Method with Bolt Load Unknown

Quantity	Units	2 − 45 Corner	4 − 135 Corner	6 − 225 Corner	8 − 315 Corner
Known	lbs	PX, PY	PX, PY	PX, PY	PX, PY
	in	A, B	A, B	A, B	A, B
	lbs/in	NX, NY, NXY	NX, NY, NXY	NX, NY, NXY	NX, NY, NXY
IBOLT Element Loads					
N1	lbs/in	0	− (1 − RSX) • PX / B	− (1 − RSX) • PX / B	0
N2	lbs/in	0	0	− (1 − RSY) • PY / A	− (1 − RSY) • PY / A
N3	lbs/in	(1 − RSX) • PX / B	0	0	(1 − RSX) • PX / B
N4	lbs/in	(1 − RSY) • PY / A	(1 − RSY) • PY / A	0	0
T1	lbs/in	0	0.5 • NXY	0.5 • NXY	0
T2	lbs/in	0	0	0.5 • NXY	0.5 • NXY
T3	lbs/in	0.5 • NXY	0	0	0.5 • NXY
T4	lbs/in	0.5 • NXY	0.5 • NXY	0	0
Bearing Load Components and Factors					
Define	lbs	PX1 = NX • B	PX1 = − NX • B	PX1 = − NX • B	PX1 = NX • B
	lbs	PX2 = 0.5 • NXY • A	PX2 = 0.5 • NXY • A	PX2 = − 0.5 • NXY • A	PX2 = − 0.5 • NXY • A
	lbs	PY1 = NY • A	PY1 = NY • A	PY1 = − NY • A	PY1 = − NY • A
	lbs	PY2 = 0.5 • NXY • B	PY2 = − 0.5 • NXY • B	PY2 = − 0.5 • NXY • B	PY2 = 0.5 • NXY • B
	---	RSX = PX2 / (PX1 + PX2)			
	---	RSY = PY2 / (PY1 + PY2)			
Check	---	If (PX1 + PX2 = 0) or (PY1 + PY2 = 0), Use DBL Method			

Copyright 2015 Lockheed Martin Corporation.
Note: The current version is always the version on the Lockheed Martin network.

Table 11.6-11 IBOLT Element Loads for a Panel Corner Fastener using DBL Method with Bolt Load Unknown

Quantity	Units	2 − 45 Corner	4 − 135 Corner	6 − 225 Corner	8 − 315 Corner
Known	in	A, B	A, B	A, B	A, B
	lbs/in	NX, NY, NXY	NX, NY, NXY	NX, NY, NXY	NX, NY, NXY
IBOLT Element Loads					
N1	lbs/in	0	NX	NX	0
N2	lbs/in	0	0	NY	NY
N3	lbs/in	NX	0	0	NX
N4	lbs/in	NY	NY	0	0
T1	lbs/in	0	0.5 • NXY	0.5 • NXY	0
T2	lbs/in	0	0	0.5 • NXY	0.5 • NXY
T3	lbs/in	0.5 • NXY	0	0	0.5 • NXY
T4	lbs/in	0.5 • NXY	0.5 • NXY	0	0
PX	lbs	PX = B • (N3 − N1) + A • (T4 − T2)			
PY	lbs	PY = A • (N4 − N2) + B • (T3 − T1)			

Copyright 2015 Lockheed Martin Corporation.
Note: The current version is always the version on the Lockheed Martin network.

11.6.3.5.1 Example 5 – Fastener at a Panel Corner

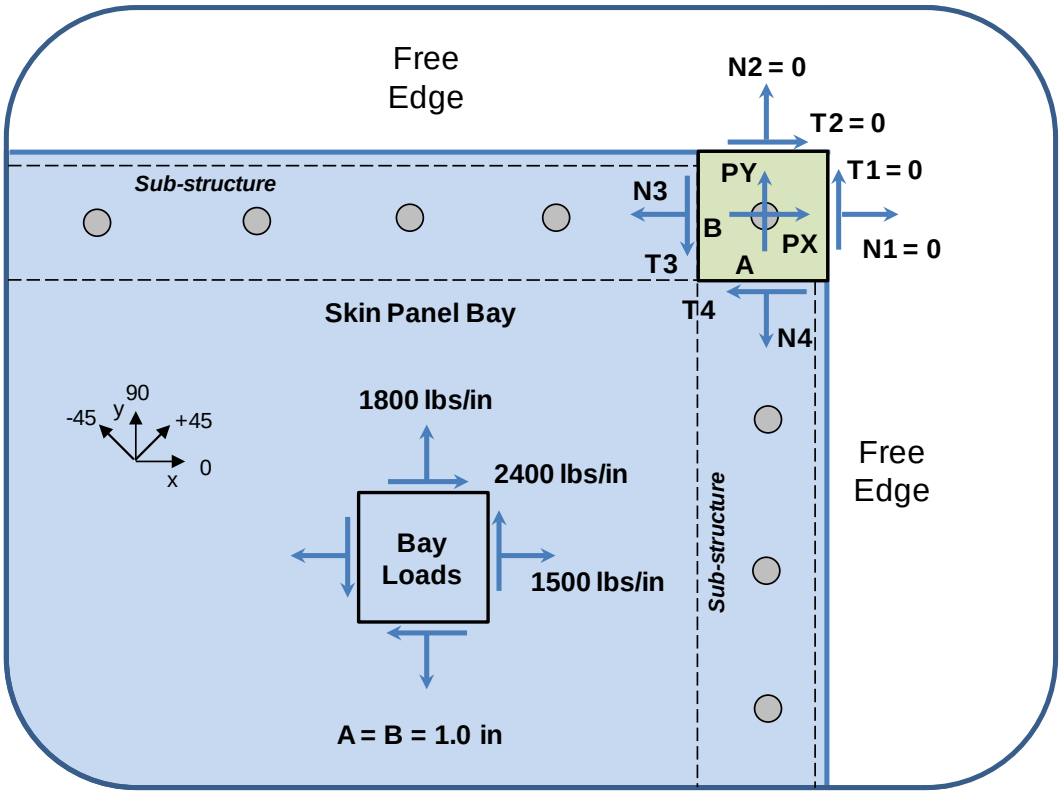

Problem Statement: Determine the IBOLT element loads for the center fastener using: a) the Fixed Bearing Load method; and b) the Derived Bearing Load method.

Known:
PX = 2700 lbs, PY = 3000 lbs
Adjacent Bay
NX = 1500 lbs/in
NY = 1800 lbs/in
NXY = 2400 lbs/in

A = B = 1.0 in, Element dimensions

a) ***Solution using the Fixed Bearing Load method***

Known: PX = 2700 lbs, PY = 3000 lbs
Determine: N1, N2, N3, N4, T1, T2, T3, T4 (Refer to Table 11.6-10)

Preliminary observations:
a. The fastener is located at a panel corner with two edges free.

1) Begin by calculating the bearing load components:
PX1 = NX • B = 1500 • 1.0 = 1500 lbs
PX2 = 0.5 • NXY • A = 0.5 • 2400 • 1.0 = 1200 lbs
PY1 = NY • A = 1800 • 1.0 = 1800 lbs
PY2 = 0.5 • NXY • B = 0.5 • 2400 • 1.0 = 1200 lbs

Copyright 2015 Lockheed Martin Corporation.
Note: The current version is always the version on the Lockheed Martin network.

11.6.3.5.1 Example 5 Continued

2) Calculate bearing load factors:
RSX = PX2 / (PX1 + PX2) = 1200 / 2700 = 0.444
RSY = PY2 / (PY1 + PY2) = 1200 / 3000 = 0.400
RNX = 1.0 – RSX = 0.556
RNY = 1.0 – RSY = 0.600

3) Calculate running loads along the IBOLT element boundary:
N1 = 0 lbs/in
N2 = 0 lbs/in
N3 = (1 − RSX) • PX / B = 0.556 • 2700 / 1.0 = 1500 lbs/in
N4 = (1 − RSY) • PY / A = 0.600 • 3000 / 1.0 = 1800 lbs/in

T1 = 0 lbs/in
T2 = 0 lbs/in
T3 = 0.5 • NXY = 1200 lbs/in
T4 = 0.5 • NXY = 1200 lbs/in

4) Verify using equilibrium equations 11.6-2:
PX = B • (N3 − N1) + A • (T4 − T2)
PX = 1.0 • (1500 − 0) + 1.0 • (1200 − 0)
PX = 2700 lbs ✓

PY = A • (N4 − N2) + B • (T3 − T1)
PY = 1.0 • (1800 − 0) + 1.0 • (1200 − 0)
PY = 3000 lbs ✓

T1 + T3 = T2 + T4
0 + 1200 = 0 + 1200 = 1200 lb/in ✓

b) ***<u>Solution using the Derived Bearing Load method</u>***

Determine: N1, N2, N3, N4, T1, T2, T3, T4, PX, PY (Refer to Table 11.6-11)

1) Calculate running loads along the IBOLT element boundary:
N1 = 0 lbs/in
N2 = 0 lbs/in
N3 = NX = 1500 lbs/in
N4 = NY = 1800 lbs/in

T1 = 0 lbs/in
T2 = 0 lbs/in
T3 = 0.5 • NXY = 1200 lbs/in
T4 = 0.5 • NXY = 1200 lbs/in

2) Calculate PX, PY from equilibrium equations 11.6-2:
PX = B • (N3 − N1) + A • (T4 − T2)
PX = 1.0 • (1500 − 0) + 1.0 • (1200 − 0)
PX = 2700 lbs

Copyright 2015 Lockheed Martin Corporation.
Note: The current version is always the version on the Lockheed Martin network.

11.6.3.5.1 Example 5 Continued

PY = A • (N4 − N2) + B • (T3 − T1)
PY = 1.0 • (1800 − 0) + 1.0 • (1200 − 0)
PY = 3000 lbs

Verify M_Z equilibrium:
T1 + T3 = T2 + T4
0 + 1200 = 0 + 1200 = 1200 lb/in ✓

11.6.4 Multiple Fastener Rows

This section provides guidance for defining IBOLT element loads for multiple fastener rows. The fastener row configurations are presented in the same order as the previous section:

1) Interior Skin Panel Fasteners: No Edges Free;
2) Fasteners along Panel Edges: One Edge Free; and
3) Fasteners at Skin Panel Corners: Two Edges Free.

The discussion will focus on a double row of fasteners to illustrate the procedures. The following assumptions are made with respect to the fastener rows discussed in this section:

- The stiffnesses of the joint elements do not vary from fastener to fastener. This includes:
  - The composite skin panel material, lay-up and thickness
  - The substructure material and thickness
  - The fastener type, diameter, fixity and bolt-to-hole tolerance
- The fastener rows are assumed to be an attachment between a single, continuous composite skin panel and a single, continuous substructure member, such as a spar or rib, with no splices.
- For panel corners, the substructure configuration may consist of multiple members provided that they are of same material and flange thickness such that any fastener-to-fastener stiffness variation can be neglected.

Under these assumptions, the fastener load distribution can be evenly distributed between adjacent fastener rows. Any variations in the joint stiffness from fastener to fastener will affect the fastener load distribution and must be accounted for in the joint loads modeling. Methods for determining fastener load distributions where stiffness variations exist from fastener to fastener are discussed in Section 11.6.5. Splices, spar-rib intersections, specialized fittings or nested groups of multiple fasteners for local load introduction are all beyond the scope of this section and will require fastener load distribution analysis using the methods discussed in Section 11.6.5.

<u>Interior Skin Panel Fasteners: No Edges Free</u>

This section considers the case of a double row of fasteners located within an interior skin panel where the IBOLT fastener elements have no edges free. The approach is to treat each adjacent pair of row fasteners along the length as an idealized single fastener, as shown in Figure 11.6-32, that is in equilibrium with the adjacent skin panel bays. Either the Derived Bearing Load (DBL) or Fixed Bearing Load (FBL) method of Section 11.6.3 may be used to determine the IBOLT element loads for the idealized single fastener. If the FBL method is used, the bearing loads PX and PY for each fastener pair are added together to obtain overall PX and PY bearing loads for the idealized single fastener. Once the IBOLT element loads have been determined for the idealized single fastener, these loads can then be used to determine the IBOLT loads for the corresponding pair of fasteners as shown in the figure. A numerical example of a double row of interior panel fasteners aligned with the Y-axis is shown in Figure 11.6-33.

Copyright 2015 Lockheed Martin Corporation.
Note: The current version is always the version on the Lockheed Martin network.

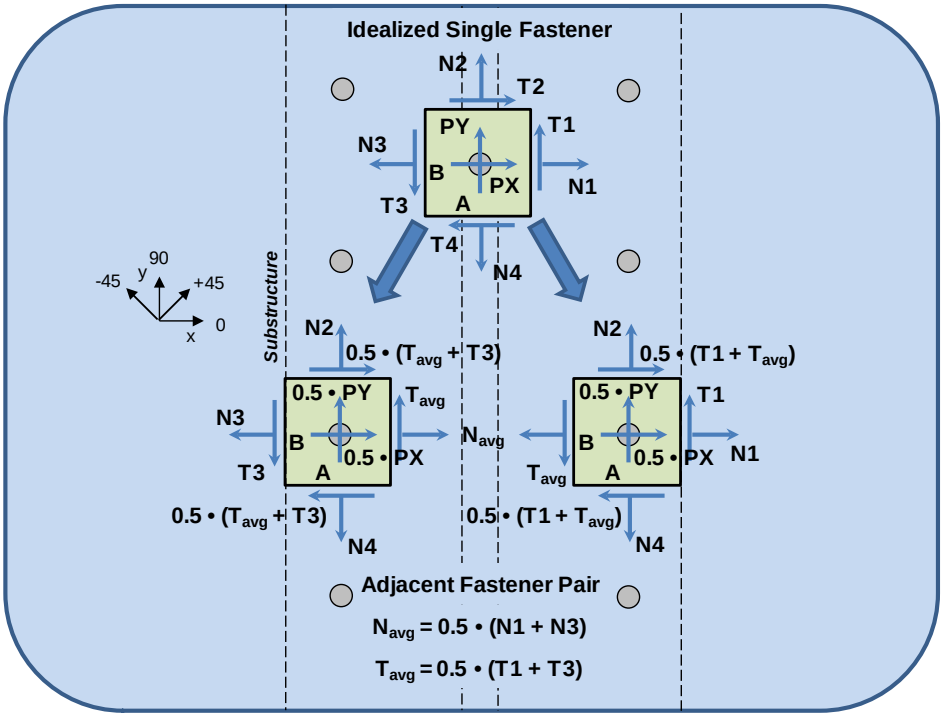

Figure 11.6-32 Idealized Single Fastener for a Double Row of Interior Panel Fasteners

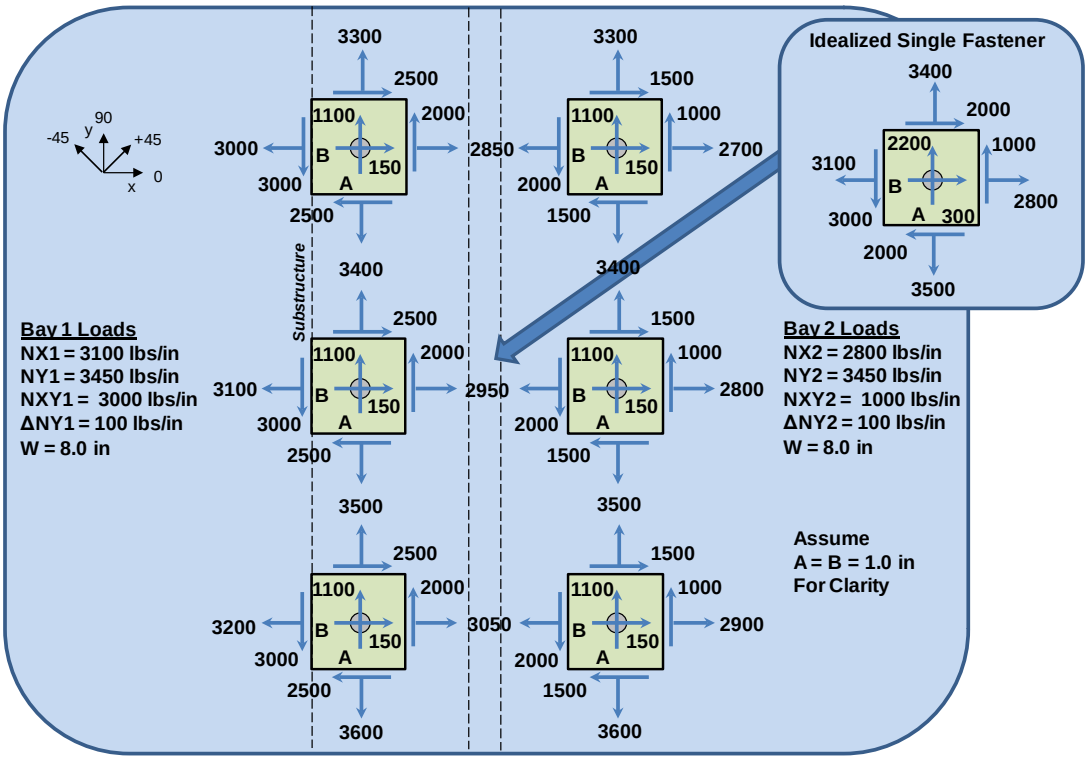

Figure 11.6-33 IBOLT Element Loads Example for a Double Row of Interior Panel Fasteners

Copyright 2015 Lockheed Martin Corporation.
Note: The current version is always the version on the Lockheed Martin network.

Fasteners along Panel Edges: One Edge Free

This section considers the case of a double row of fasteners located along the edge of a skin panel where the outermost IBOLT fastener elements have one edge free. As for interior panel fasteners, the approach is to treat each pair of row fasteners along the panel edge as an idealized single fastener that is in equilibrium with the adjacent skin panel bay. Either the Derived Bearing Load (DBL) or Fixed Bearing Load (FBL) method of Section 11.6.4 may be used to determine the IBOLT element loads for the idealized single fastener. If the FBL method is used, the bearing loads PX and PY for each fastener pair are added together to obtain overall PX and PY bearing loads for the idealized single fastener. Once the IBOLT element loads have been determined for the idealized single fastener, these loads can then be used to determine the IBOLT loads for the corresponding pair of fasteners as shown in Figure 11.6-34. A numerical example of a double row of panel edge fasteners is shown in Figure 11.6-35.

.

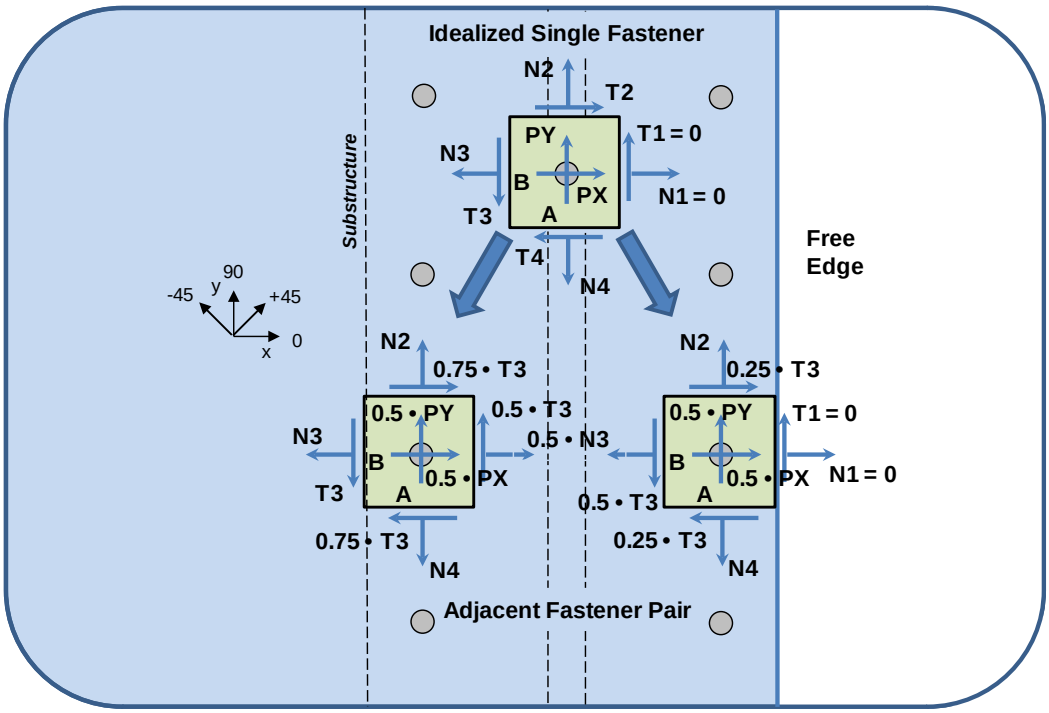

Figure 11.6-34 Idealized Single Fastener for a Double Row of Panel Edge Fasteners

Copyright 2015 Lockheed Martin Corporation.
Note: The current version is always the version on the Lockheed Martin network.

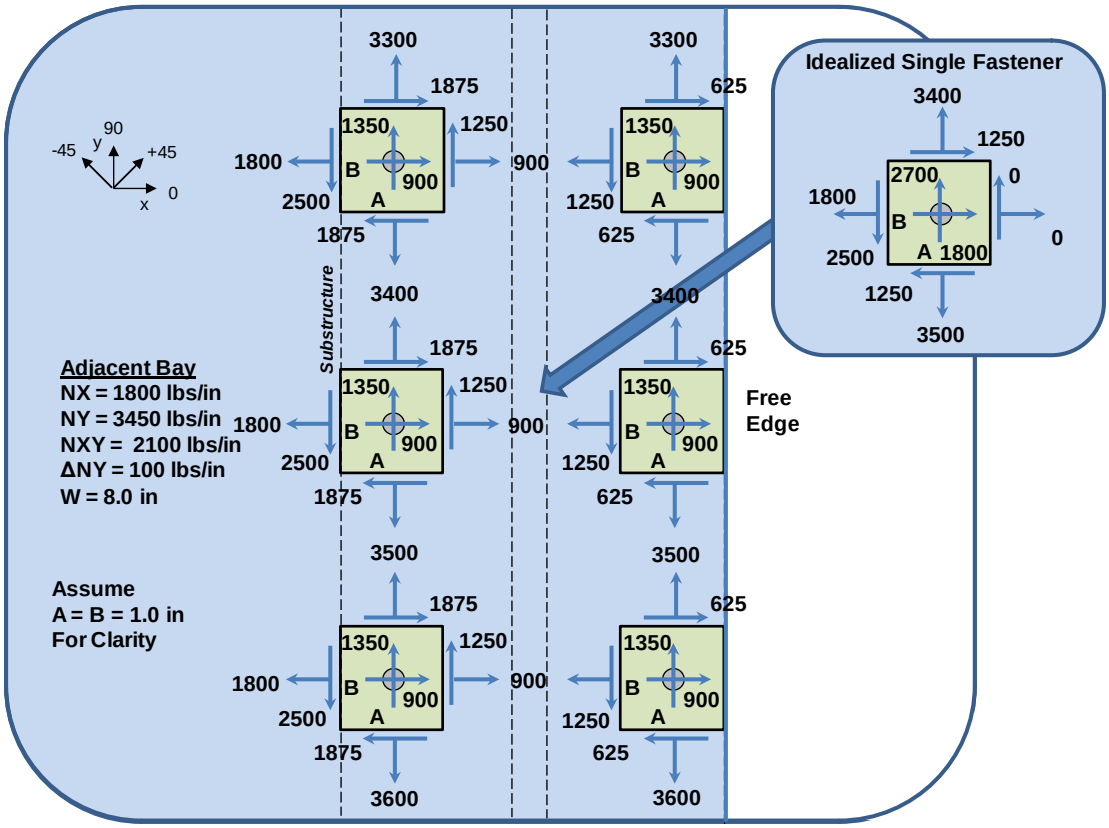

Figure 11.6-35 IBOLT Element Loads Example for a Double Row of Panel Edge Fasteners

Fasteners at a Panel Corner: Two Edges Free

This section considers the case of two double fastener rows intersecting at a panel corner where the corner IBOLT fastener element has two edges free. In this case, an idealized single corner fastener is used to determine element loads that are in equilibrium with the adjacent skin panel bay. The idealized single corner fastener loads will be used to define IBOLT element boundary running loads for the corresponding four elements that are shared members of the two double fastener rows. Either the Derived Bearing Load (DBL) or Fixed Bearing Load (FBL) method of Section 11.6.5 may be used to determine the IBOLT element loads for the idealized single fastener. If the FBL method is used, the bearing loads PX and PY for the four fasteners are added together to obtain overall PX and PY bearing loads for the idealized single fastener. Once the IBOLT element loads have been determined for the idealized single corner fastener, these running loads can then be used to determine the IBOLT boundary loads for the corresponding four fasteners as shown in Figure 11.6-36. The PX and PY bearing loads for each fastener are then calculated using element equilibrium Equations 11.6-1. A numerical example of two double fastener-rows that intersect at a panel corner is shown in Figure 11.6-37.

Copyright 2015 Lockheed Martin Corporation.
Note: The current version is always the version on the Lockheed Martin network.

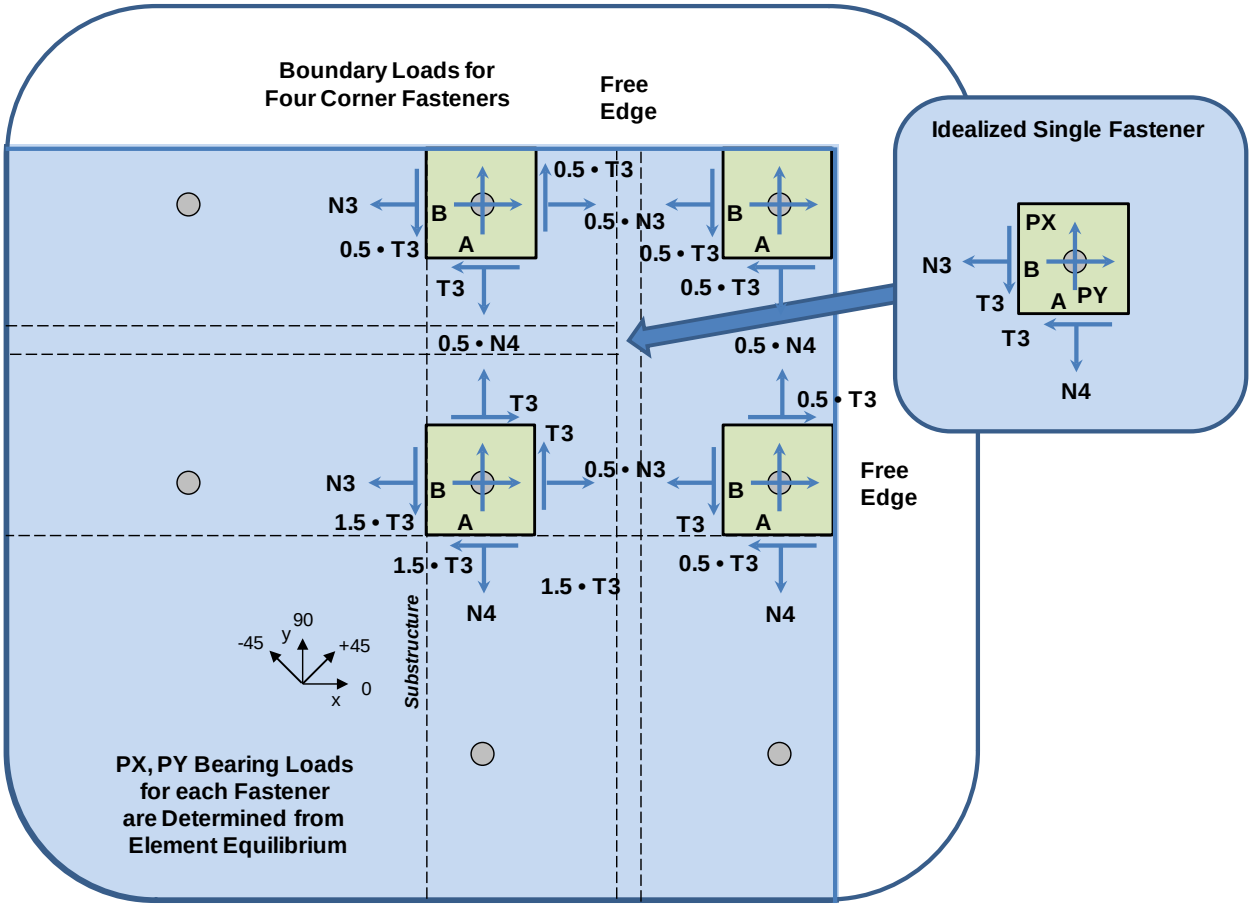

Figure 11.6-36 Idealized Single Fastener for a Double Row of Panel Corner Fasteners

Copyright 2015 Lockheed Martin Corporation.
Note: The current version is always the version on the Lockheed Martin network.

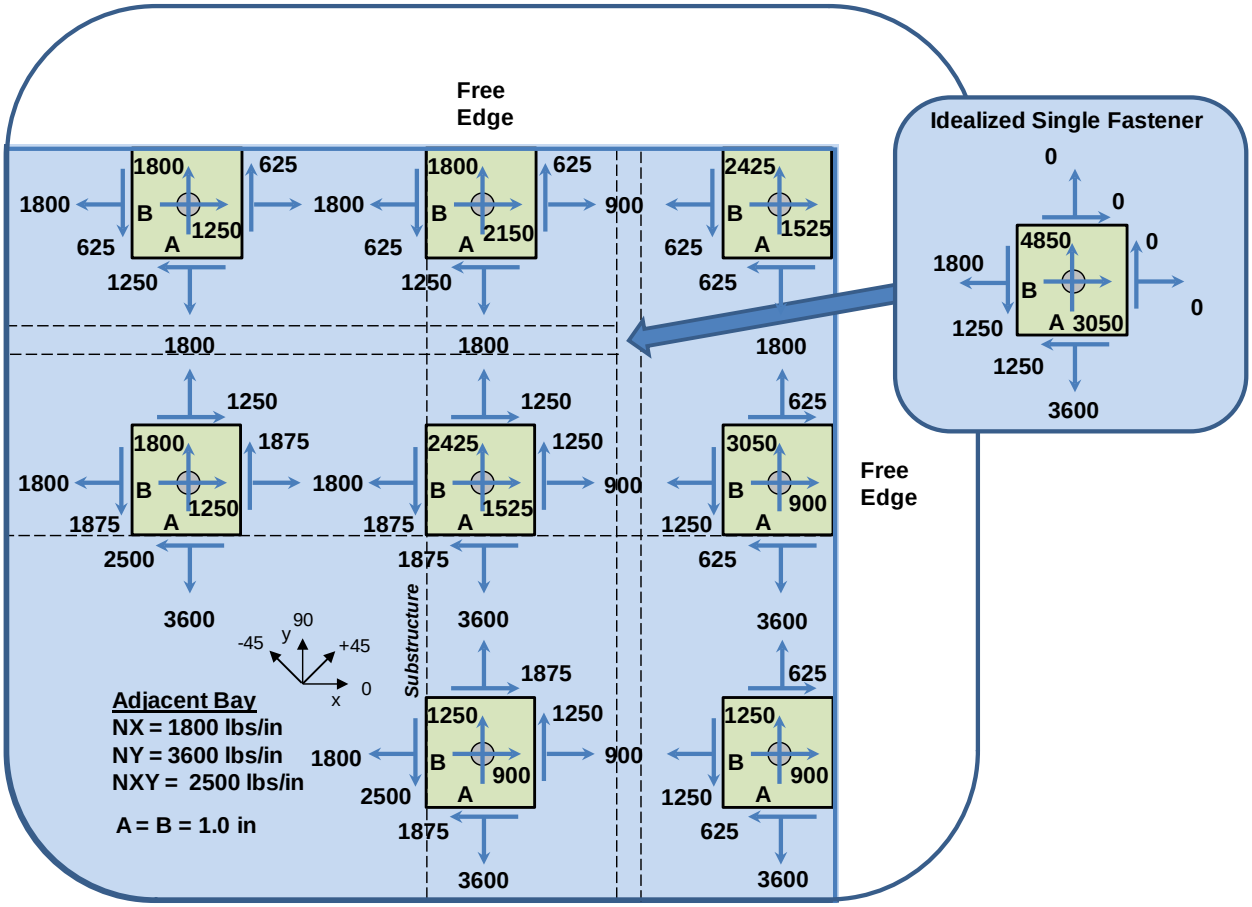

Figure 11.6-37 IBOLT Element Loads Example for Two Double Fastener Rows Intersecting at a Panel Corner

11.6.5 Coordinate Transformations

This section begins with a discussion of procedures for handling coordinate system transformations between finite element analysis loads, fastener line orientation, and the final rotation for alignment with the closest skin panel 0° fiber direction. Figure 11.6-38 illustrates a realistic situation where the coordinate systems for the finite element analysis loads, the fastener line orientation, and the closest panel fiber directions are not in alignment.

Copyright 2015 Lockheed Martin Corporation.
Note: The current version is always the version on the Lockheed Martin network.

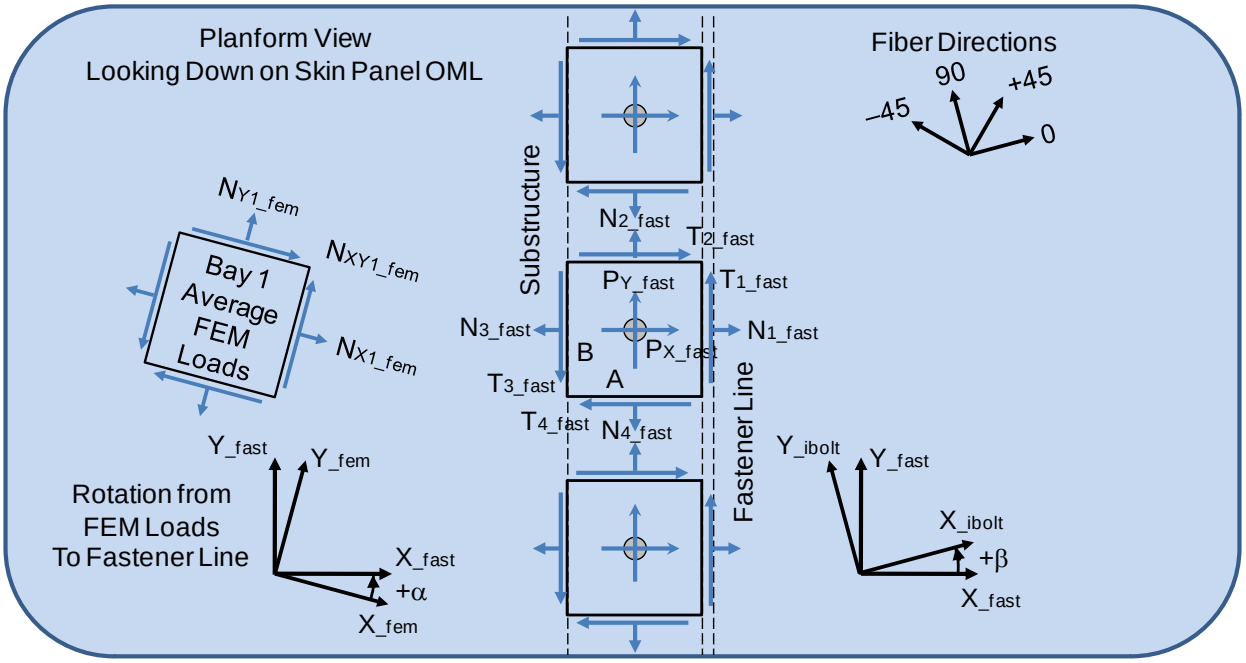

Figure 11.6-38 Coordinate systems between FEA loads, a fastener line, and skin fiber direction

The following procedures can be used to handle such a situation.

<u>Coordinate Transformation Procedures</u>

1) Rotate FEA Loads to Align with the Fastener Line

Rotate the finite element loads results (X_fem, Y_fem) for in-plane loads (NX, NY, NXY) in each bay so that they are in alignment with the fastener line (X_fast, Y_fast). As shown, this would be a planar coordinate transformation through angle +α using the equations for a planar stress transformation.

2) Define IBOLT element loads

Define the IBOLT element loads (PX, PY, N1–N4, T1–T4) with respect to the fastener line coordinate system (X_fast, Y_fast) using the FBL or DBL method defined in Section 11.6.3.

3) Identify the Nearest Skin Fiber Direction

Identify the nearest skin fiber direction to rotate the fastener element loads so that it is properly aligned for IBOLT strength analysis. As shown, this would be a planar coordinate transformation through angle + β using the equations from (X_fast, Y_fast) to (X_ibolt, Y_ibolt) coordinates.

4) Decompose the IBOLT Loads to Basic Load Cases for Transformation (Refer to Figure 11.6-27)

This step would involve the following:

a) Rotate Average In-Plane Loads from (X_fast, Y_fast) to (X_ibolt, Y_ibolt) coordinates.

b) Rotate the Bearing Load Components from (X_fast, Y_fast) to (X_ibolt, Y_ibolt) coordinates.

c) Adjust the Bearing Load Cases to match the transformed bearing load components.

d) Adjust the Transform portion of the Bypass Loads to match the transformed bearing load components.

Copyright 2015 Lockheed Martin Corporation.
Note: The current version is always the version on the Lockheed Martin network.

11.6.6 Fastener Load Distributions

This section discusses the determination of loads for multiple fastener configurations in which the load distribution is dependent upon the fastener pattern geometry and any variations in joint stiffness from fastener to fastener. The types of analysis discussed are:

1) Rigid-Body Fastener Pattern Analysis (Section 11.6.5.1)
2) Elastic Fastener Load Distributions Based on Joint Stiffness (Section 11.6.5.2)

A discussion of the use of discrete modeling of fasteners in finite element analysis to predict fastener loads may be found in Section 11.9.5.

11.6.6.1 Rigid-Body Fastener Pattern Analysis

In rigid-body fastener pattern analysis, the joint members are assumed to be relatively stiff enough such that the structure can be idealized as a rigid-body. The fastener loads are dependent on the geometry of the fastener pattern and the individual fastener properties such as location, diameter, orientation and axial, shear and bending stiffness. The method can be applied to 2-D and 3-D fastener configurations.

The methodology for rigid-body fastener pattern analysis is presented in Reference 11-1, Section 5.2.1. Method assumptions, equations, limitations and example problems are provided. There are several software tools available for rigid-body fastener pattern analysis. These tools include the IDAT programs PEERY for in-plane 2-D analysis and RIGIDBODY for full 3-D analysis.

11.6.6.2 Elastic Fastener Load Distributions Based on Joint Stiffness

In many aerospace structural applications, the flexibility of the joint members and joining fasteners must be taken in to account to obtain accurate fastener load distributions. This methodology accounts for the relative geometry and thermo-elastic properties of each individual structural joint member. This methodology is derived from the fastener loads distribution analysis presented in NACA TN 1051. The method develops a 2-D model of the joint that can handle multiple joint layers and predicts joint load distributions for mechanical and thermal loading. The method develops a system of n equations where n is the number of fasteners in the joint. The equations are $n-1$ recurrence relations and a force equilibrium equation. The $n-1$ recurrence equations sum up load contributions from constituent joint members assuming strain compatibility between adjacent layers of the joint stack-up. The system is solved for the load at each fastener. This method is described in Section 5.2.2 of Reference 11-1.

A similar type of elastic joint analysis is available using the IDAT/SPRING tool. This tool models a pin fastened joint using spring elements and accounts for mechanical and thermal loading. The spring model is constructed by defining a list of spring types and their associated stiffnesses. SPRING uses three basic spring types: extensional, shear, and bolt shear. Extensional springs are used to model the uniaxial stiffness of a joint layer. Shear springs are used to model the shear stiffness between two node points of a web-type structure. Bolt springs are used to model fastener shear stiffness. Bolt shear stiffness can be calculated using the IDAT/SS_JOINT tool, which is fully integrated in SPRING. The model is constructed by connecting node points with particular spring elements of these three types.

To solve the problem, SPRING assembles an overall joint stiffness matrix which is inverted to obtain a flexibility or compliance matrix. The flexibility matrix can be multiplied by applied forces to obtain displacements at each node. Individual spring forces are then determined by multiplying the difference in displacement of the spring's connecting nodes by the corresponding spring rate. Further details about SPRING can be found in Reference 11-43.

The IDAT/SPLICE tool is another joint analysis program that predicts joint loads for a single or double fastener row butt-strap splice joint connecting composite laminate panels. IDAT/SPLICE uses a two-dimensional nonlinear beam finite element analysis for predicting the joint response. The problem input consists of the following:

Copyright 2015 Lockheed Martin Corporation.
Note: The current version is always the version on the Lockheed Martin network.

- Panel dimensions
- Panel laminate filenames
- Fastener spacing
- Shim/gasket gap
- Fastener identification
- Fastener diameter
- Running load or applied strain
- Pressure load

SPLICE analysis generates an illustration showing the reaction loads and moments on the splice joint and a listing of the reaction loads and moments on the splice joint. Further details about SPLICE can be found in Reference 11-44.

11.6.7 Panel Pressure Induced Membrane and Bending Loads

For pressure loaded structure, pressure-induced membrane force and bending moment must be determined for use in IBOLT calculation. Coarse grid finite element models do not typically have sufficient fidelity to capture such loads, which can be nonlinear. Due to geometric effects, such as contour changes, these models may contain moment results in shell elements even when no pressure bending effects exist. In a highly localized margin calculation such as IBOLT it is often not representative of the actual margin of safety to use any moment results extracted from a coarse grid finite element model.

Consequently, pressure-induced membrane forces and moments are typically obtained using an external panel analysis method or software tool. These loads can be calculated by hand or by using the IDAT/PRESS tool, which is documented in Reference 11-45. PRESS calculates bending moments, in-plane loads, strains, strain margins of safety, and the maximum deflection of a flat, laminated, clamped, rectangular panel loaded with a uniform pressure distribution. Input data consists of panel dimensions, material, stacking sequence, and lateral pressure. PRESS panel boundary conditions may vary from fully clamped to simply-supported. PRESS laminate properties should be computed to agree with the orientation defined by the finite element mesh rosette. Figure 11.6-39 summarizes the conventions used in this analysis.

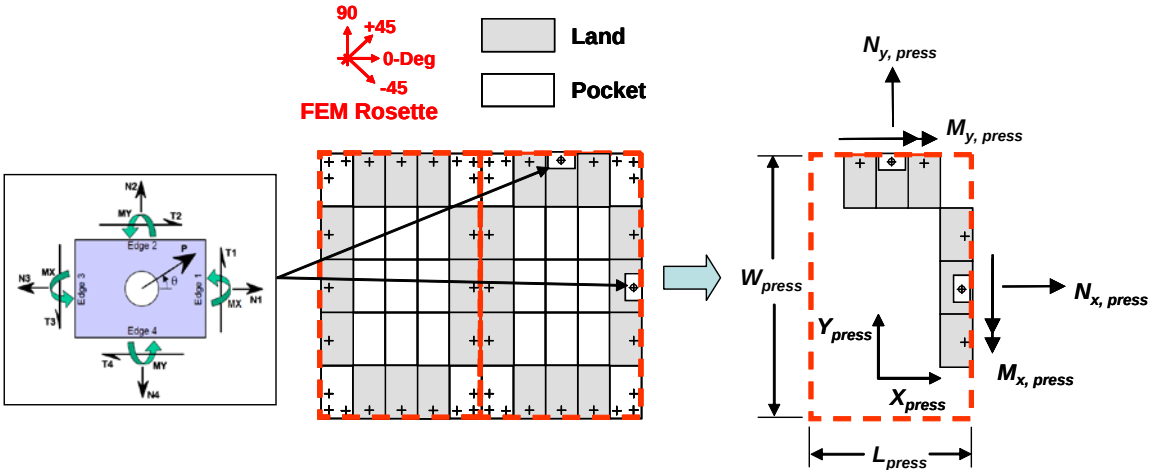

Figure 11.6-39 Method for Determining Pressure-Induced Loads to Include in IBOLT Free-body Loads

The analyst should be careful to ensure loads computed by hand or in the PRESS coordinate system are transformed to the local IBOLT analysis coordinate system. In particular, the analyst should note that the convention for positive moment direction in PRESS is reversed from IBOLT convention as shown in Figure 11.6-39. PRESS moment resultants, $M_{x,press}$, $M_{y,press}$, and $M_{xy,press}$, are applied directly to the IBOLT fastener element as discussed in Section 11.5.2.6 and in-plane membrane loads add to the finite element loads of Sections 11.6.2.

Copyright 2015 Lockheed Martin Corporation.
Note: The current version is always the version on the Lockheed Martin network.

In double fastener rows the inner fastener is assumed to carry the full bending moment. The IBOLT bolt load is modified for edge-of-part joints to react membrane load $N_{y,press}$.

Along a fastener line, the backup stiffness provided by attaching substructure constrains the laminate in a cylindrical bending condition such that no curvature is allowed in the direction of the fastener line. Consequently, along the fastener line the moment is a calculated reaction based on the ratio of bending (D_{11} and D_{22}) and twist (D_{13} and D_{23}) stiffnesses from the laminate stiffness matrix. Selection of the appropriate curvature restraints in IBOLT, as discussed in Section 11.5.2.6, will result in the correct moment calculations.

11.6.8 Pull Off Loads from Panel Pressure

Composite skins subjected to fastener tension loads induced from skin panel pressure or curvature should be analyzed at the substructure attachment for fastener pull-through and interlaminar shear (ILS) failure modes. Fastener pull-through load, also known as pull-off load, is the fastener tension load that results in a failure mode whereby the fastener pulls through the composite skin. Fastener pull-through loads induced by internal panel bay pressures are illustrated in Figure 11.6-40.

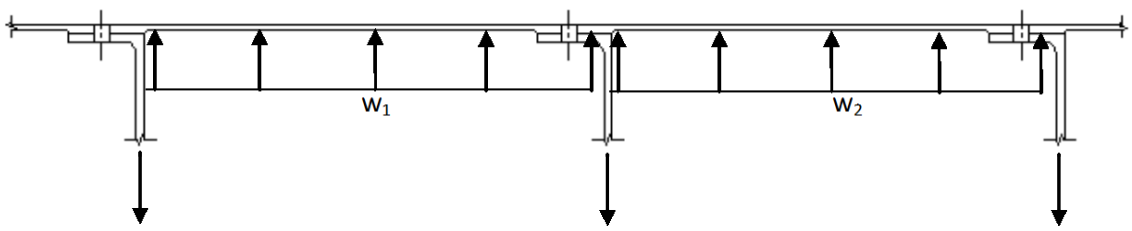

Figure 11.6-40 Normal Panel Pressure Induces Fastener Pull-Off Loads

This fastener tension also includes tension loading caused by the heel-toe prying effect of substructure flange reacting against skin as it deforms as shown in Figure 11.6-41. The fastener pull-through load (P_{tu}) and the associated heel-toe reaction load (R) are shown for a single flange substructure element. Note that the heel-toe reaction R may occur on the opposite side of the fastener for some design and loading configurations. Load reaction directions can also vary depending on the geometry and loading for the particular problem.

Copyright 2015 Lockheed Martin Corporation.
Note: The current version is always the version on the Lockheed Martin network.

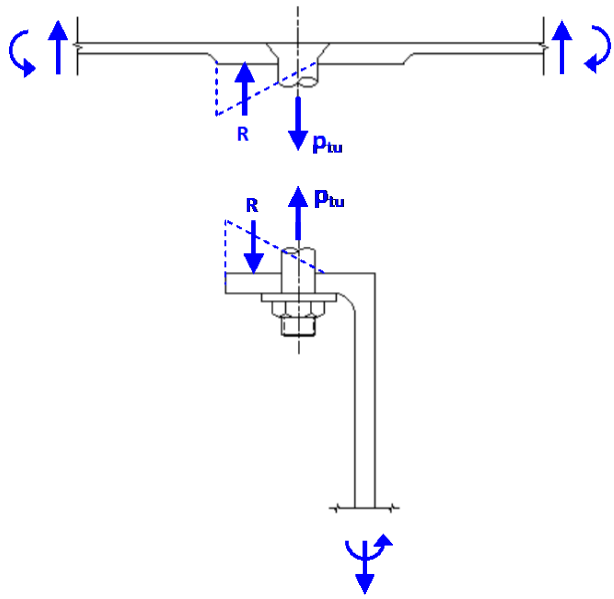

Figure 11.6-41 Free-Body of a Single Flanged Substructure Attachment

This section describes two approaches to determine the fastener pull-through load (P_{tu}) and the associated bending loads in the flange:

- Classical analysis (Section 11.6.7.1)
- Finite element analysis (Section 11.6.7.2)

The classical analysis method presented is a conservative hand analysis based on simplifying assumptions. A more accurate and less conservative loads determination method is through the use of two-dimensional finite element analysis that considers the stiffness of the skin and substructure.

Once the fastener pull-through load is known, fastener pull-through strength is determined by the method described in Section 11.5.3 using the IDAT tool PULL-THRU. Using the loads within the flange, the interlaminar shear strength is determined at the location of maximum transverse shear load using the method described in Section 11.5.4.1.

11.6.8.1 Pull-Off Loads from Classical Analysis

The analysis method provided is a conservative hand analysis method that uses overlapping moment support assumptions to make the problem statically determinate. The methods described include single and double flange substructure configurations, assumptions used for handling multiple fastener rows, and pull-through load calculations for curved skin panels.

The analysis considers only loads in the substructure flange due to normal pull-off loads. The pull-through load includes the heel-toe induced tension load due to the prying action of the flange against the skin. Additional loads will exist in the skin due to pressure induced membrane and bending as well as aircraft maneuver and thermally induced loads. These additional loads must be added to the internal loads calculated using this method to determine the total internal load state. While this section covers only the substructure and the heel-toe effect fastener tension load, the skin, substructure and fasteners also require additional strength analyses to the evaluate the overall loads not covered by this method.

Copyright 2015 Lockheed Martin Corporation.
Note: The current version is always the version on the Lockheed Martin network.

There are several general assumptions for the analysis as shown in Figure 11.6-42. The heel-toe reaction load due to the pull-through load P_{tu} where the flange makes contact with the skin is assumed to be a triangular distribution. For a single row of fasteners, the distribution extends from a maximum at the flange free edge inwards toward the assumed fastener pull-through load P_{tu} center located at point B. The fastener pull-through load P_{tu} center is located a distance of $d_1 = 2/3 \bullet D$ from the hole center toward the substructure web. The fastener nut/washer support and clamp up at the fastener hole is assumed to reduce the moment arm for the moment calculation by $2/3 \bullet D$ where D is the fastener hole diameter. The heel-toe reaction load R located at point A is the resultant of the assumed triangular load distribution. This is located at the centroid or *1/3* point along the span of the triangular load distribution. A fastener edge distance limit of two times the fastener hole diameter should be assumed for the heel-toe reaction triangular distribution for configurations with $e/D > 2D$.

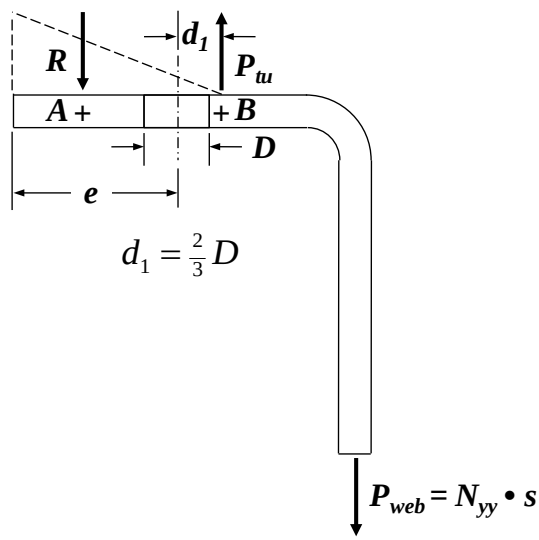

Figure 11.6-42 Assumptions Used in Flange Analysis

The assumed loads and heel-toe distribution are simplifying assumptions made to make the problem statically determinate. In addition, the problem is assumed two dimensional and local effects due to the ends and/or lengths of the skin panel and substructure are neglected. The effects of flange stiffener support and skin end fastening are also neglected. Due to the conservative assumptions used in this analysis, fastener hole net section effects are neglected.

Single Flange Substructure

The geometry and assumed loads for a typical single flange substructure is shown in Figure 11.6-43.

Copyright 2015 Lockheed Martin Corporation.
Note: The current version is always the version on the Lockheed Martin network.

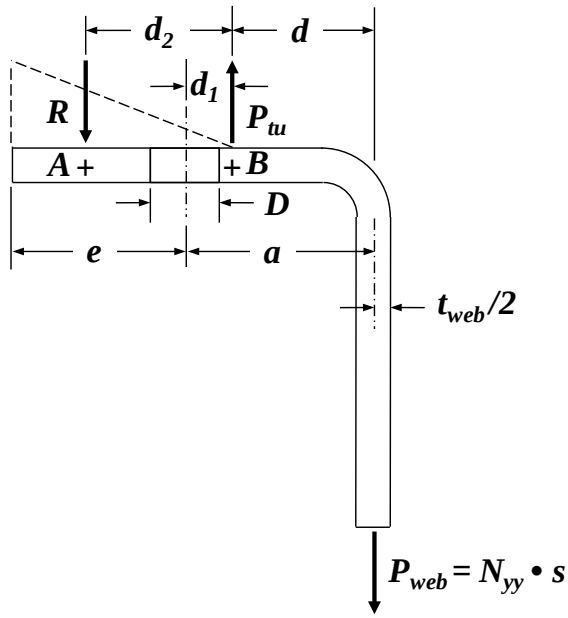

Figure 11.6-43 Free-Body Diagram of Single Flange Substructure

The pull-off load, p_{tu}, for single flange substructure is calculated by consideration of moment equilibrium at point A:

$$p_{tu} = N_{yy} \cdot s \cdot \left(1 + \frac{d}{d_2}\right)$$ **Equation 11.6-3**

where:

$$d_1 = \frac{2}{3} D$$

$$d = a - d_1 = a - \frac{2}{3} D$$

$$d_2 = \frac{2}{3}\left(e + \frac{2}{3} D\right)$$

s = fastener pitch (in)
e = fastener edge distance (in)
a = distance from web centerline to fastener centerline (in)
D = fastener diameter (in)
P_{web} = web load resultant (lbs)
N_{yy} = web normal running load (lbs/in)

The running moment within the flange may also be calculated which requires the definition of an effective width as shown in Figure 11.6-44. The effective width assumes a 45° degree load distribution angle from the fastener. The assumption is that the effective width is equal to 2 times the distance from the fastener center to the web centerline plus one fastener diameter up to a maximum of s where s = the fastener pitch.

Copyright 2015 Lockheed Martin Corporation.
Note: The current version is always the version on the Lockheed Martin network.

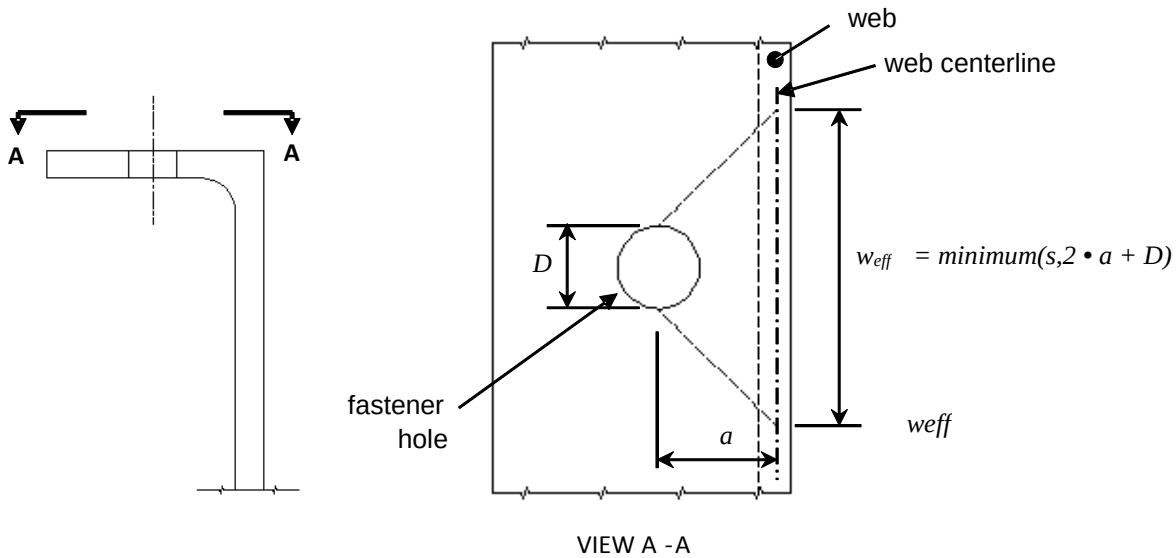

Figure 11.6-44 Flange Effective Width

The maximum flange bending moment occurs at point B in Figure 11.6-43. The running flange bending moment, m_B, is calculated:

$$m_B = N_{yy} \cdot d \cdot \frac{s}{w_{eff}}$$ **Equation 11.6-4**

where:
m_B = flange bending running moment at point B (in-lbs/in)
w_{eff} = min($2 \cdot a + D$, s) effective flange width (in)

<u>Double Flange Substructure</u>

Figure 11.6-45 shows the free-body diagram for double flange substructure that is symmetric about the web centerline.

Copyright 2015 Lockheed Martin Corporation.
Note: The current version is always the version on the Lockheed Martin network.

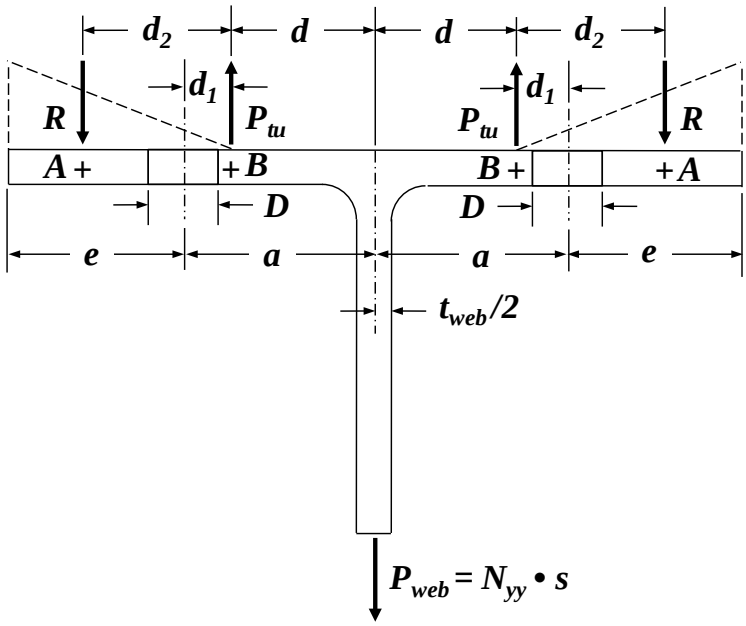

Figure 11.6-45 Free-Body Diagram of Double Flange Substructure

The pull-off load, p_{tu}, for double flange substructure is calculated:

$$p_{tu} = N_{yy} \cdot \frac{s}{2} \cdot \left(1 + \frac{d}{2 \cdot d_2}\right)$$ **Equation 11.6-5**

The running moment at the point B, m_B, for double flange substructure is calculated as follows:

$$m_B = \frac{N_{yy} \cdot d}{4} \cdot \frac{s}{w_{eff}}$$ **Equation 11.6-6**

If the flanges are unsymmetrical about the web centerline, then analyze each flange as if it were symmetric about the centerline.

Multiple Fastener Rows

The assumptions used previously are valid for pull-off loads calculation in substructure with multiple rows of fasteners as long as the triangular heel-toe assumption is applied to the fastener hole furthest from the web. The triangular distribution is assumed to extend from the flange free edge inward to the center of the fastener hole furthest away from the web. This only affects the calculation of the magnitude of the tension load in the fastener nearest the web which is dependent on the heel-toe reaction assumption. Figure 11.6-46 shows the free-body diagram for double flange substructure.

Copyright 2015 Lockheed Martin Corporation.
Note: The current version is always the version on the Lockheed Martin network.

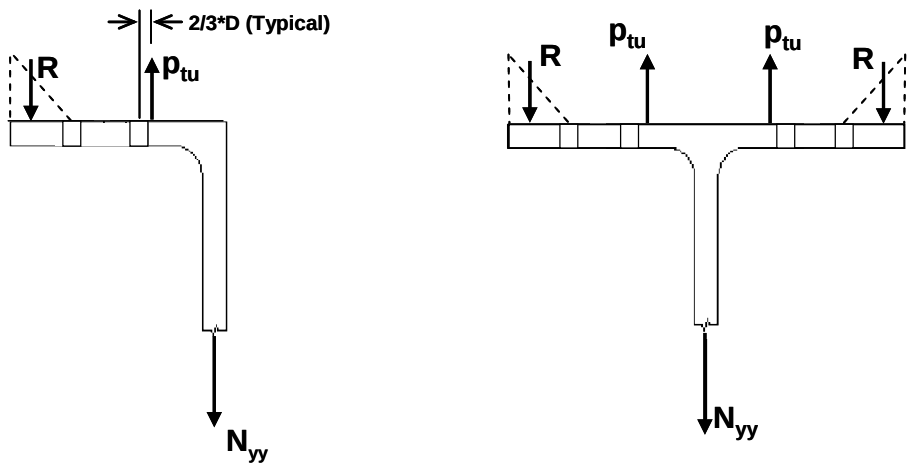

Figure 11.6-46 Free-Body Diagram of Double Flange Substructure with Multiple Fastener Rows

<u>Pull-Through Loads for Curved Panels</u>

Pull-through loads resulting from substructure attached to a curved panel are shown in Figure 11.6-47. Two configurations are possible when considering the curvature effects depending on the direction of the loading (tension or compression).

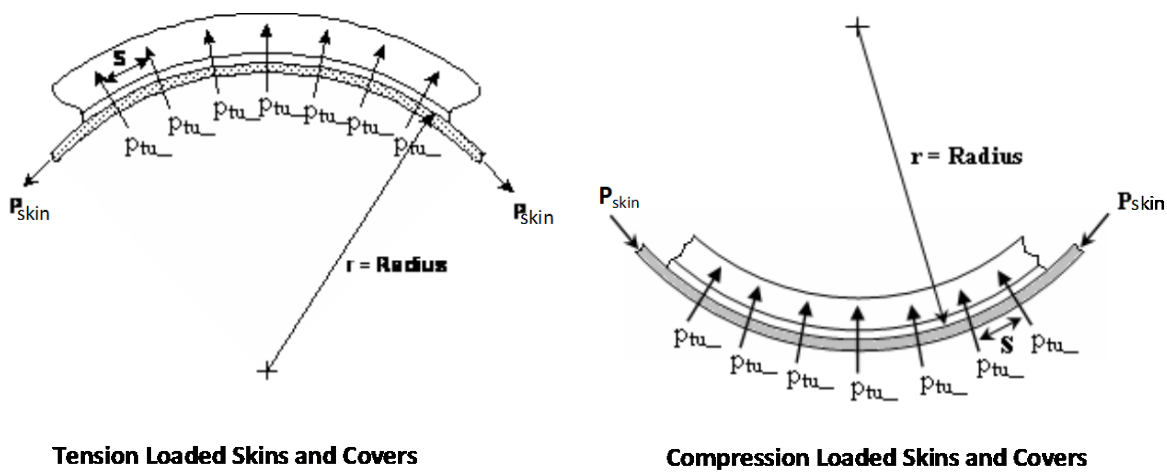

Figure 11.6-47 Pull-Off Loads in Curved Flanges

Bolt tension loads required to balance the axial load in a curved skin attached to a frame are calculated:

$$p_{tu} = \frac{P_{skin} \cdot s}{r \cdot n}$$ **Equation 11.6-7**

Copyright 2015 Lockheed Martin Corporation.
Note: The current version is always the version on the Lockheed Martin network.

Where:
P_{skin} = Axial load in skin (lbs)
r = local skin radius of curvature (in)
s = fastener spacing (in)
n = number of rows of bolts (Usually 1 for Angle and 2 for a Tee joint)
p_{tu} = pull-through tension load per fastener (lbs)

11.6.8.2 Pull-Off Loads from Finite Element Analysis

Finite element analysis may be used to obtain a more accurate prediction of pull-off and flange bending loads that account for the skin and substructure stiffness. Loads may be determined using a fine grid model in which the fasteners are modeled explicitly with spring elements. Guidelines for discrete modeling of fasteners may be found in Section 11.9.5.

Simplified two-dimensional finite element models of the skin and substructure may also be used to determine pull-off and flange bending loads. Care must be taken to ensure that flange-skin heel-toe effects are adequately modeled. Guidelines for the development of simplified 2-D models for flange pull-off analysis are described in Section 11.9.6.

The IDAT/FLANGE analysis tool provides a 2-D FEA-based nonlinear flange bending solution for the case of a pressure loaded substructure flange attached to a pressurized skin. This tool automatically sets up all of the problem elements, nodes, and boundary conditions properly per this approach and solves for flange internal loads that may be used for analysis. FLANGE does not calculate margins of safety since the flange pull-off internal loads must be combined with other internal loads due to aircraft loading besides flange pull-off prior to conducting the stress analysis of the flange. More information on the IDAT/FLANGE tool is available in the user's guide Reference 11-46. Figure 11.6-48 shows an example of the FLANGE GUI Input Screen.

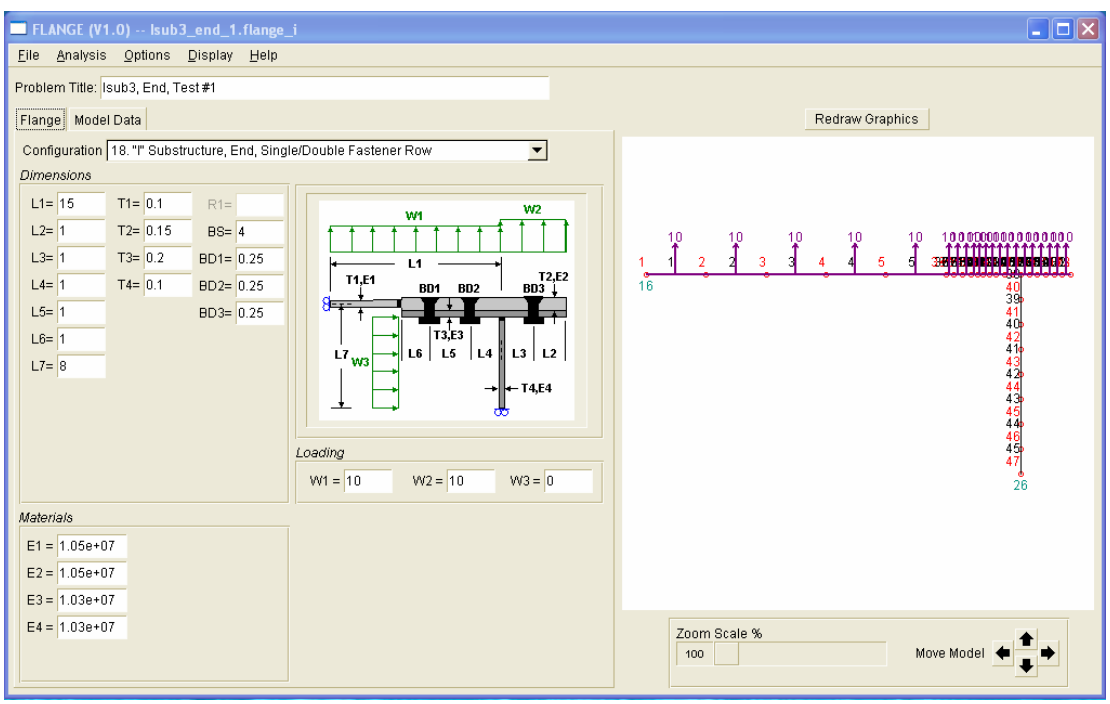

Figure 11.6-48 FLANGE GUI Input Screen Example

Copyright 2015 Lockheed Martin Corporation.
Note: The current version is always the version on the Lockheed Martin network.

Ten standard flange pull-off configurations have been incorporated into the IDAT/FLANGE tool. These flange pull-off configurations are shown in Figure 11.6-49. The flange moment, axial, and shear loads are extracted from the finite element model for use in conducting the stress analysis. The fastener pull-off load provided by FLANGE is used in the composite strength analysis for Fastener Pull through (Section 11.5.3) and Interlaminar Shear (Section 11.5.4). Other FLANGE results are used in flange bending analysis discussed in Reference 11-1 Section 5.

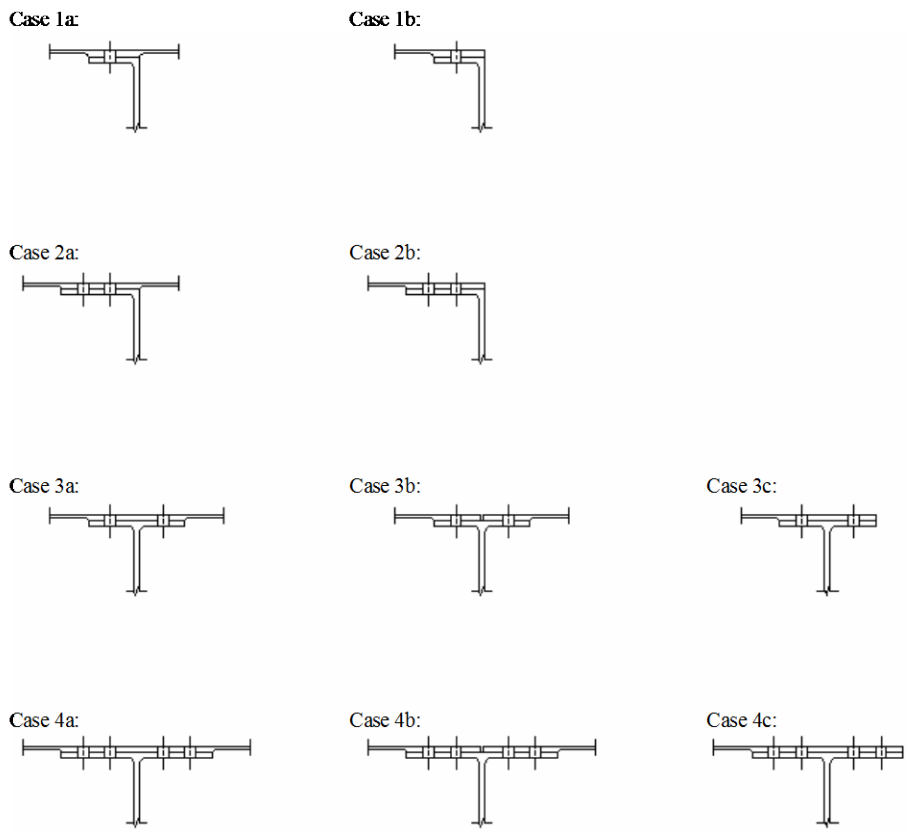

Figure 11.6-49 Standard FLANGE Pull-off Analysis Configurations

Copyright 2015 Lockheed Martin Corporation.
Note: The current version is always the version on the Lockheed Martin network.

11.7 Special Design Considerations

This section presents analysis guidelines for various configurations and features of bolted composite joints. Topics discussed are as follows:

- Multi-layer Joints
- Shims and Gaps
- Hole Reinforcements
- Countersinks
- Counterbores
- Seals and Seal Grooves
- Tapered Joints
- Interlaminar Shear Strength

11.7.1 Multi-Layer Joints

In some configurations, a single-shear joint with more than two members must be analyzed. This situation is commonly encountered in complex, built-up structures. The recommended approach for performing the IBOLT analysis in this situation is to divide the joint into a series of two-member, single-shear joints and to analyze each separately.

Engineering judgment must be exercised in applying this method. Unless a significant percentage of the total load is carried by the middle member, it is of similar stiffness as the remainder of the joint members and the middle member has low bolt-to-hole clearances, the middle member may need to be treated as a shim rather than assuming two single-shear joints. Failure to follow these guidelines can provide an unconservative prediction of static strength.

This method is best illustrated with an example problem, shown in Table 11.7-1. Note that:

1. Each layer of each problem must have a balanced free-body diagram.
2. The total free-body of the multilayer joint must be balanced.
3. Any layers that are common to more than one two-member single lap shear joint, must have the same loads in each two-member single lap shear joint.

Table 11.7-1 Multilayer Joint Example Problem

Given: Multilayer joint shown at right, middle figure	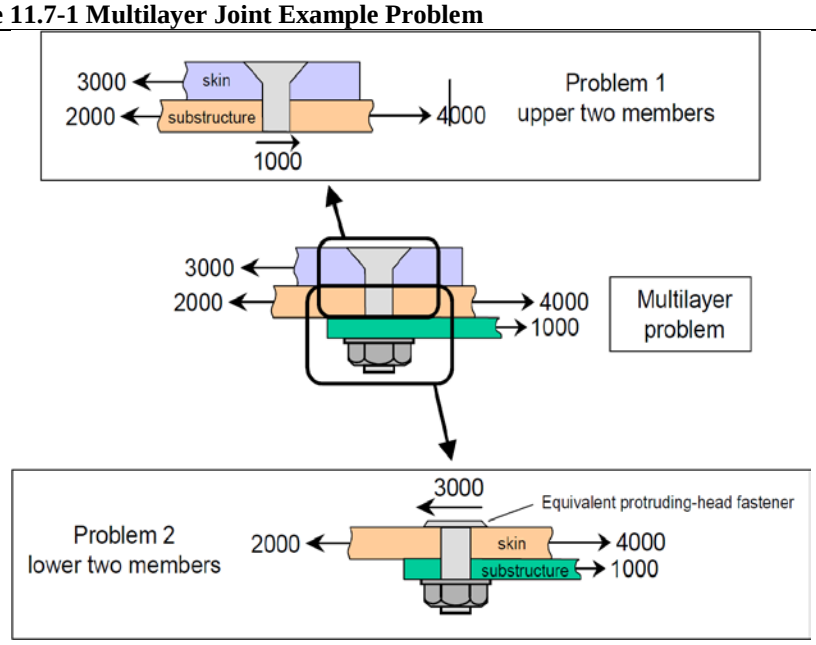
Approach: Split joint into two single layer joints, shown as • Problem 1 (Upper figure) • Problem 2 (Lower figure).	
The fastener load transfer from the uppermost layer is 3000 lbs because it is the end fastener in this skin and the skin has a 3000 lb load. The fastener load transfer from the lowermost layer is 1000 lb because it is the end fastener in this layer as	

Copyright 2015 Lockheed Martin Corporation.
Note: The current version is always the version on the Lockheed Martin network.

well and this layer has a 1000 lb load. The middle layer has to balance these fastener loads through a combination of applied load and bypass loads.		
Problem 1: IBOLT freebodies of each layer are shown to the right. Note that the total net fastener transfer is 1000 lbs to the left. This must be balanced by the fastener load of the bottom layer of Problem 2.	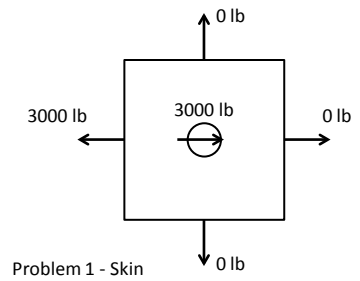	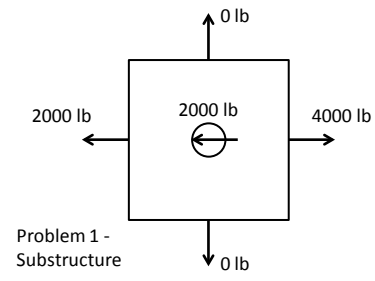
Problem 2: IBOLT freebodies of each layer are shown to the right. Note that the total net fastener transfer is 3000 lbs to the right. This must be balanced by the fastener load of the top layer of Problem 1. Note that in running IBOLT for Problem 2 both layers would use a protruding head fastener of similar shear strength.	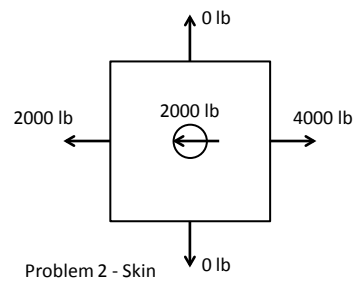	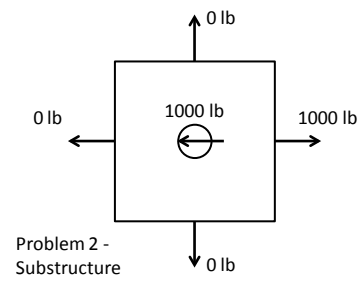
Note that 1. Each layer of each problem must have a balanced free-body diagram 2. The total free-body of the multilayer joint must be balanced 3. Any layers that are common to each problem statement must have the same loads in each instance, *e.g.*, Problem 1 Substructure and Problem 2 skin.		

Other approaches to the analysis of multilayer joints include the use of local finite element models with sufficient detail to model each fastener and layer or the use of a spring model such as IDAT/SPRING which can also model multiple layers.

11.7.2 Hybrid Laminates

The analyst should be aware of how IDAT/IBOLT treats hybrid laminates, made up of two or more materials as shown in Figure 11.7-2. There are logic rules built into the program on how to calculate the laminate properties which vary according to the type of property. Some properties are taken from the dominant material in the layup in terms of thickness. Other properties are obtained from a rule-of-mixtures algorithm based on the relative thickness fractions of the materials making up the hybrid laminate. This approach has correlated well with testing.

Copyright 2015 Lockheed Martin Corporation.
Note: The current version is always the version on the Lockheed Martin network.

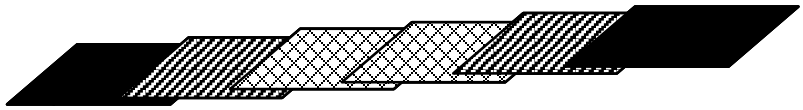

Figure 11.7-1 Illustration of a Hybrid Laminate

The hybrid laminate modulus is calculated using classical laminated plate theory where the stiffness properties are summed on a ply-by-ply basis. Unnotched laminate strengths at each of the 8 failure locations are calculated using the hybrid moduli multiplied by the failing strain value for the material system with the lowest failing strain after discounting materials which occupy less than 5 percent of the total thickness. The percent thickness calculation and strain allowable determination is performed in the tangential direction at each of the 8 failure locations. The 5 percent thickness check prevents the surface plies from dominating the strength characteristics of the laminate. The B-allowable statistical reduction factor is taken from the material system which determined the unnotched strength.

Strain energy release rates are based on rule of mixtures by summing contributions based on thickness fractions for each material. Bearing cutoff values are also based on rule of mixtures. The portions of the hybrid laminate used for the application of the various IBOLT empirical factors are also defined by the program algorithm. Table 11.7-2 summarizes the approach used by IDAT/IBOLT to calculate the various properties.

Table 11.7-2 Assumptions for Property Calculations in Hybrid Laminates

Property	Basis for Calculating Hybrid Laminate Property
Modulus	Lamination theory for hybrids
Strength	Lowest strain allowable for materials where $t_{matl} > 0.05t_{total}$
B-allowable Factors	Lowest strain allowable for materials where $t_{matl} > 0.05t_{total}$
Strain Energy Release Rate	Rule of mixtures based on thickness
Bearing Cutoffs	Rule of mixtures based on thickness
Empirical Factor : F_{DPLY}	Applied only to material with highest E_{11}
Empirical Factor : F_{PCTBC}	Rule of mixtures based on thickness
Empirical Factor : F_{PKBC}	Rule of mixtures based on thickness
Empirical Factor : F_{CSKBC}	Rule of mixtures based on thickness
Empirical Factor : F_{FILL}	Material with lowest strength for materials where $t_{matl} > 0.05t_{total}$
All other properties	Use value for material with highest percent thickness

11.7.3 Countersinks

The presence of a countersink influences strength at any hole. This is particularly true in laminated composites where the presence of a countersink reduces bearing-bypass strength, bearing cutoff strength, and bending capability over a straight hole. Additionally, a countersunk fastener installed sub-flush to the outer mold line (OML) reduces bearing strength. This section discusses analysis procedures for countersunk holes in composite plates.

IDAT/IBOLT includes empirical factors, calibrated to test data, to quantify the effect of a countersunk hole on bearing-bypass strength and bearing cutoff strength. IBOLT uses these factors which ratio strength without a countersink to strength with a countersink in margin of safety calculations for holes with a countersink. IBOLT treats the loss of bearing-bypass strength and bearing cutoff strength in the presence of a countersunk hole as a function of the fastener head geometry and the countersink depth, which is characterized by height-to-laminate thickness, h/t. The IBOLT Theory manual, Reference 11-11, discusses these empirical factors in detail.

Copyright 2015 Lockheed Martin Corporation.
Note: The current version is always the version on the Lockheed Martin network.

IBOLT accounts for the presence of a countersink in bending analysis by modifying applied moments to account for section geometry. The original moments are increased to account for the net section of the joint element using a bending factor and section factors. The bending factor, derived from notched flexure tests, is a function of fastener head type and whether or not the hole is filled by the fastener. The section factors adjust for fastener area, including diameter, head height, and countersink angle. The moments on the plate with the hole omitted are increased. Bending stress is calculated ply-by-ply using lamination theory on the remaining unnotched laminate. Section 11.4.4.4 discusses the factors and stress calculation in detail.

Some aircraft require countersunk fastener heads to lie at or below the outer mold line surface, which is defined to include non-structural plies. To satisfy this requirement, fasteners are typically installed targeting a nominal sub-flush countersink head depth. Additionally, as shown in Figure 11.7-3, each fastener installation varies from true perpendicular by some tilt angle. This causes the countersink depth to vary from a high value, "hi", on one side of the fastener head to a low value, "lo", on the opposite side.

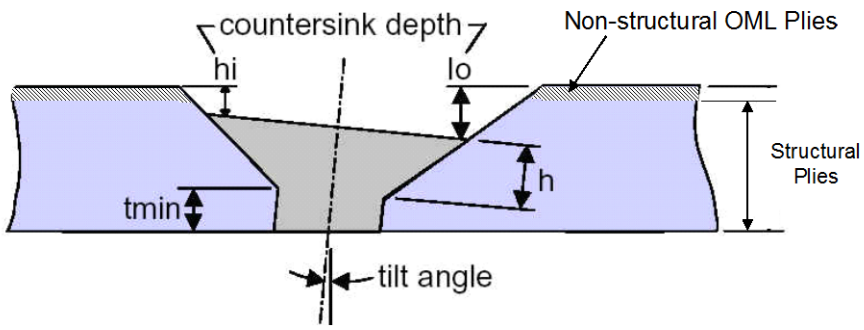

Figure 11.7-2 Deep Countersink Geometry

IDAT/IBOLT bearing-bypass and bearing cutoff margin of safety calculations, when a deep countersink is present, are based on strength reduction factors determined from test data. Details of this calculation can be found in Section 3.6 of Reference 11-11. The discussion below describes how to account for a deep countersink requirement in the IBOLT analysis problem setup.

Non-structural outer mold line (OML) plies, shown in Figure 11.7-2, should be accounted for in the countersink depth calculations; otherwise, all checks will be overly conservative. In an IBOLT analysis, this accounting is done by subtracting non-structural OML ply thickness from the total sub-flush countersink depth entered into IBOLT. If the Non-Structural OML ply thickness exceeds the nominal or maximum countersink depth, then a countersink depth of zero should be entered into IBOLT for the nominal or maximum countersink depth. Non-structural OML plies must not be considered as part of the structural laminate in an IBOLT analysis.

The countersink depth as input into IBOLT is based upon the "hi" side sub-flush depth, t_{min} in Figure 11.7-2. All subsequent computations within IBOLT are based upon a computed "lo" side value that is derived from the input. IBOLT assumes a nominal 1.45º tilt angle in calculating the low side and margins-of-safety. Table 11.7-3 provides reference values for the "hi" side countersink depth at nominal and maximum conditions based on manufacturing data from recent programs.

Table 11.7-3. "Hi" Side Countersink Depth (Reference Only)

	Nominal Condition	Maximum Condition
Fixed Panel	0.011 in.	0.019 in.
Removable Panel	0.002 in.	0.008 in.

Copyright 2015 Lockheed Martin Corporation.
Note: The current version is always the version on the Lockheed Martin network.

Table 11.7-4 shows an example calculation for the IBOLT "hi" side countersink input assuming a reference value of 0.007" non-structural OML ply thickness and the nominal conditions listed in Table 11.7-3. The reference values in these tables may be used for preliminary design but values used for detail analysis must be substantiated by each program.

Table 11.7-4 IBOLT "Hi" Side Input Example for Fixed Panel at 150% Design Limit Load (Reference Only)

	Fixed Panel	Removable Panel
"Hi" Side Nominal Countersink Depth	0.011 in.	0.002 in.
Non-structural OML Ply Thickness	0.007 in.	0.007 in
IBOLT "Hi" Side Countersink Depth Input	0.004 in.	0.000 in.

PM4057, Reference 11-1 Section 2.6.3 discusses highly variable structure according to the airframe certification requirements of Reference 11-47. Because of the tolerance on deep countersink holes, recent programs at Lockheed Martin Aeronautics have categorized deep countersinks in composite bolted joints as highly variable structure. Consequently, the nominal and maximum assembly conditions must have positive margins of safety at 150% and 100% of Design Limit Load (DLL), respectively. Program guidance may require the maximum assembly condition margin to be calculated as some increment of DLL such as 115% to 125%. This is generally performed at the same load level as the detrimental deformation analyses.

To verify that deep countersinks satisfy nominal and maximum assembly condition requirements, two analyses are performed:

- Ultimate Strength: Composite bolted joint strength sizing at 150% DLL assuming nominal countersink depth
- Limit Strength: Composite bolted joint strength sizing at 100% DLL assuming maximum countersink. Program guidance may require this margin calculation be performed at 115% to 125% DLL.

IBOLT computes a maximum permissible countersink depth for a given problem as shown in the example IBOLT output of Figure 11.7-3. Assuming a linear loading, the second Limit Strength/Maximum Countersink analysis is not required if the allowable "hi" side countersink, per the Ultimate Strength Check, is greater than the maximum countersink to be evaluated. Recall, the allowable hi side countersink on the IBOLT output is with non-structural plies removed.

Also note that the margins of safety shown at the bottom of the IBOLT output in Figure 11.7-3 are for a protruding head or a nominal flush countersunk fastener and cannot be used for a sub-flush analysis. All sub-flush analysis must be based on the "DEEP COUNTERSINK ANALYSIS" bearing-bypass and bearing cutoff margins of safety. All eight IBOLT analysis locations are evaluated in the deep countersink analysis but only the most critical is shown.

Copyright 2015 Lockheed Martin Corporation.
Note: The current version is always the version on the Lockheed Martin network.

```
                                ibolt_temp.ibolt_o

IBOLT V4.5h  03/22/12  LM Aero        28-Nov-2012        10:41:13        PAGE   1

        TITLE:       Example Problem
        SUBTITLE:    -65F
        INPUT FILE: ibolt_temp.ibolt_i
MATERIAL:
        B_IM7/977 TAPE -65A      B_IM7/977 FAB -65A
        B-BASIS FILE             B-BASIS FILE
        -65. F,  0.00 %MOIST     -65. F,  0.00 %MOIST
        Rev Date: 04-JAN-05      Rev Date: 14-APR-97

LAMINATE DEFINITION:
        (  4.%/ 27.%/ 13.%)      ( 17.%/ 21.%/ 17.%)
        Zone_8_Kick_neg65F.ls

              INITIAL                     SECANT
         LAMINATE PROPERTIES         LAMINATE PROPERTIES
        Ex   = 7.313E+06 psi        Ex   = 7.055E+06 psi
        Ey   = 9.008E+06 psi        Ey   = 8.7
        Gxy  = 3.007E+06 psi        Gxy  = 2.8
        NUxy = 0.265                NUxy = 0.2
        NUyx = 0.326                NUyx = 0.3

GEOMETRY: A =   1.875 in      B =   1.875 in
          D =   0.250 in      T =   0.239 in

LOADS: N1 =  -1306.2 lb/in     T1 =      0.0 lb/in     Mx =      0.0 in-lb/in
       N2 =  -2888.1 lb/in     T2 =      0.0 lb/in     My =      0.0 in-lb/in
       N3 =      0.0 lb/in     T3 =      0.0 lb/in     Mxy=      0.0 in-lb/in
       N4 =   -962.5 lb/in     T4 =      0.0 lb/in
       P BOLT =   4361.5 lb    THETA  =   55.84 deg    TORQUE =      0. in-lb

                                DEEP COUNTERSINK ANALYSIS:
                                 meas depth (hi)      0.004 in
                                 meas tilt angle      1.430 degrees
                                 brg/bypass MS        1.24
                                 brg cutoff MS        0.07

    5PTV4205E
    Interface n/a
    Es =1.04E+07 psi            FLUSH COUNTERSINK ANALYSIS:
                                                  Allow. Depth (in)
                                 strength (hi/lo)     0.018/0.029
                                 h/t     (no tilt)    0.085
                                 tmin    (no tilt)    0.108
                                 Csk Zone = 2

                                 BEND      COMB
                                STRESS    STRESS        B-MS
                                 (psi)     (psi)
                                    0.      -631.      145.46
                                    0.     16890.        4.46
                                    0.     37005.        1.31
                                    0.     -9284.        8.17
                                    0.    -16059.        4.75
                                    0.     -9284.        8.17
                                    0.     37005.        1.31
                                    0.     16891.        4.46

                                    0.     73057.        0.14
                                 be less than 15% of Bolt Diameter.
```

Input "hi" side nominal countersink, excluding non-structural plies

Margin based on input depth and tilt angle

High side countersink depth (0.018) and low side countersink depth (0.029) producing a zero M.S. for the applied loads. This does not include nonstructural plies.

Not valid margins if deep countersink condition exists. Use Deep countersink analysis

Figure 11.7-3 Sample IBOLT Deep Countersink Output

Copyright 2015 Lockheed Martin Corporation.
Note: The current version is always the version on the Lockheed Martin network.

11.7.4 Hole Reinforcements

Holes in composite laminates sometimes require some sort of liner to reinforce the hole, to correct for manufacturing variation, to repair damage, or to enable removability or interchangeability. These liners can be grommets, sleeves, or bushings. Grommets, which fit in countersunk holes, and sleeves, which fit in straight holes, are reinforcements that have thin walls and are deformable. Consequently, fastener-to-hole clearance with a grommet or sleeve present influences bypass strength. Bushings are relatively thick-walled reinforcements that deform little. The bushing-to-hole gap is assumed to be zero in bearing-bypass analysis since fastener-to-bushing fit does not influence bypass strength. There is no naming distinction between a bushing in a countersunk hole and a straight hole.

As described in the IBOLT Theory Manual, Reference 11-11, IBOLT accounts for the presence of fastener hole reinforcement in bearing-bypass analysis. For the analysis of joint elements where the hole contains a reinforcement such as a grommet, sleeve, or bushing, special attention is given to the IBOLT input values of hole diameter and fastener/hole clearance. Reinforcement dimensions are defined in an input dialog within the IBOLT graphical user interface. IBOLT then modifies hole configurations as discussed below.

The hole configuration for a straight shank fastener with a sleeve is shown in Figure 11.7-4. The input data are the sleeve inner diameter (ID), sleeve outer diameter (OD), and the bolt diameter (BD). In the analysis, the IBOLT bolt hole diameter (D_{hole}) is set to the sleeve outer diameter, and the IBOLT clearance is set to the difference between the sleeve inner diameter and the bolt diameter.

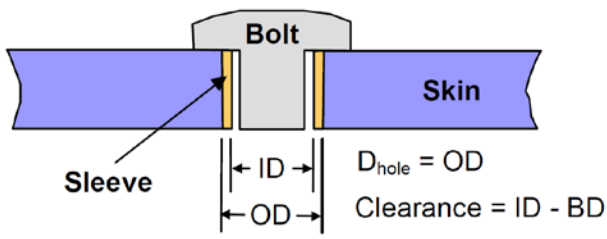

Figure 11.7-4 Hole Configuration with Sleeve

The hole configuration for a countersunk fastener with a grommet is shown in Figure 11.7-5. The input data are the grommet inner diameter (ID), grommet outer diameter (OD), bolt diameter (BD), grommet head diameter (HD), and grommet head height (HH). In the analysis, the IBOLT bolt hole diameter (D_{hole}) is set to the grommet outer diameter, and the IBOLT clearance is set to the difference between the grommet inner diameter and the bolt diameter.

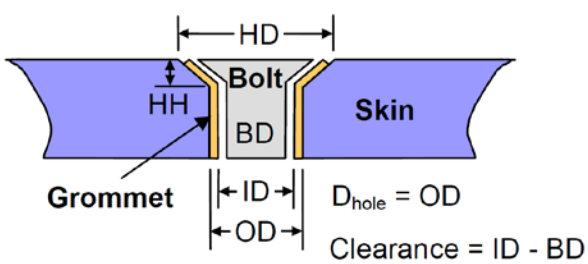

Figure 11.7-5 Hole Configuration with Grommet

Copyright 2015 Lockheed Martin Corporation.
Note: The current version is always the version on the Lockheed Martin network.

The hole configuration for a countersunk fastener with a bushing is shown in Figure 11.7-6. Because a bushing is generally a thicker walled, stiffer material, it is reasonable to assume it doesn't deflect under load. In the analysis, the IBOLT bolt hole diameter (D_{hole}) is set to the bushing outer diameter (OD), and the IBOLT clearance is set to zero.

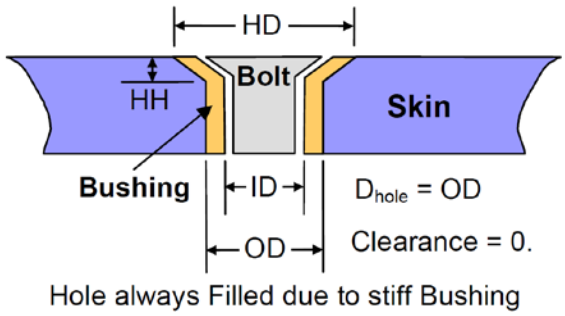

Figure 11.7-6 Hole Configuration with Bushing

A complicating factor for countersunk grommets and bushings is determining the head height (HH) and head diameter (HD) to be used for countersunk fasteners. Repair bushings in particular may have non-standard countersunk head geometry specific to the particular problem of interest. Therefore, IBOLT accepts the head height and diameter as user inputs. As a reference, IBOLT provides the head height and head diameter for each of the standard diameters of the specified fastener. Analysts should follow program guidance for specific fastener details. Table 11.7-5 summarizes how IBOLT analysis data items are affected by fastener reinforcement geometry, as defined in the figures above.

Table 11.7-5 IBOLT Analysis Data Items Modified by Fastener Reinforcements

IBOLT Analysis Data Item	Bushing Geometry	Grommet Sleeve Geometry
Laminate Hole Diameter	OD	OD
Clearance	0	ID – BD
Countersunk Fastener Head Height (as used in analysis)	HH	HH
Countersunk Fastener Head Diameter (as used in analysis)	HD	HD

IBOLT currently has some limitations in the implementation of reinforced hole analysis. IBOLT currently uses fastener material properties for the bushing/fastener combination in the beam-on-elastic-foundation bending analysis of the fastener. Additionally, the original head fixity of the fastener is used. Conservatively, the fixity is unadjusted for the presence of the bushing. Finally, the OD of the bushing is used as the fastener diameter through not only the skin, but also the substructure.

There are a number of special cases where the IBOLT bearing-bypass margin requires modification. The influence of fastener head/nut fixity on bearing strength is strictly associated with fastener type in IBOLT. Therefore, it is difficult to properly account for the influence of a bushing on peak bearing stress as well as the strength of blind bolts in bushings. Thus, the bushing is conservatively assumed to have the same head/nut fixity as the installed fastener. This is a reasonable assumption for all but the low-fixity blind bolts in the IDAT fastener database. It may also be appropriate for blind bolts in cases where the ratio of thickness to diameter, t/D, is large and their clamp-up is reacted through the bushing rather than the skin. However, in cases where bushings are used by design to achieve required bearing strength through decreased bearing stress peaking, some manual analysis modifications are warranted.

Copyright 2015 Lockheed Martin Corporation.
Note: The current version is always the version on the Lockheed Martin network.

Where a bushing is used, by design, in conjunction with a blind bolt in a composite skin and it meets the typical requirements of $t_{stack}/D_{bolt} < 3$, $t_{shim}/D_{bolt} < 0.25$, and $t_{skin}/D_{bushing} < 1.2$, then the IBOLT bearing cut-off margin of safety should be revised as

$$M.S._{bco\text{-}new} = F_{PKBC} \cdot (M.S._{bco\text{-}old} + 1) - 1.0 \qquad \textbf{Equation 11.7-1}$$

where
F_{PKBC} is the peaking factor obtained from the long format IBOLT output
$M.S._{bco\text{-}old}$ is the bearing cut-off margin of safety reported by IBOLT

The modified margin of safety given by Equation 11.7-1 may also be used in the analysis of discrepant parts. This applies if the outer diameter of the repair bushing is larger than that of the as-designed bushing and the bushing material is the same or stiffer than the original bushing.

Certain hole/sleeve configurations require modification to the standard IBOLT bearing margin calculation. For instance, program design guidelines[1] for removable door panels may suggest the use of bonded substructural sleeves for joint stack-ups that contain composite components. Bonded sleeve installations in composite substructure, as shown in Figure 11.7-7, are required when the door or panel is frequently opened.

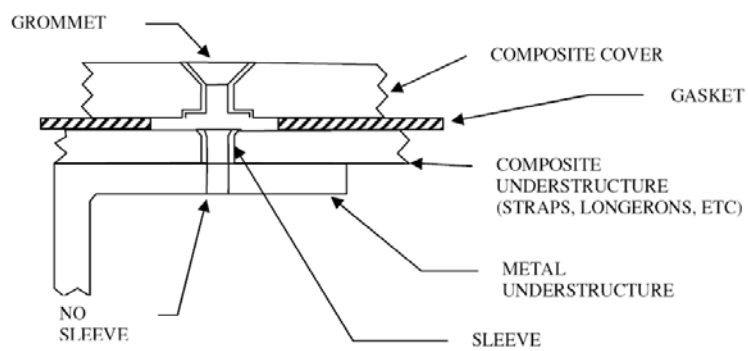

Figure 11.7-7 Removable Composite Cover and Associated Composite Substructure with Sleeve

In some composite joint applications, sleeve installation per instructions may result in sleeve depth less than laminate thickness. This undercut condition, shown in Figure 11.7-8 reduces bearing area and thus bearing strength for the hole. IBOLT does not automatically account for this undercut condition. Note that hole chamfering to accommodate installation of this flared sleeve causes negligible reduction in the bearing area of the hole and consequently does not require analysis modification.

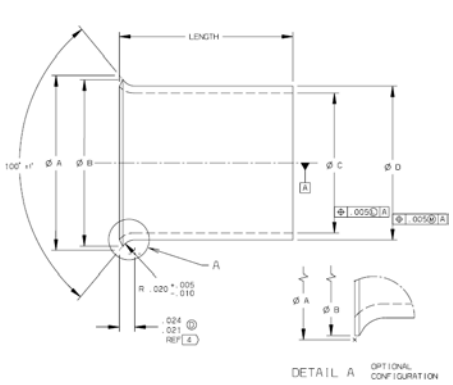

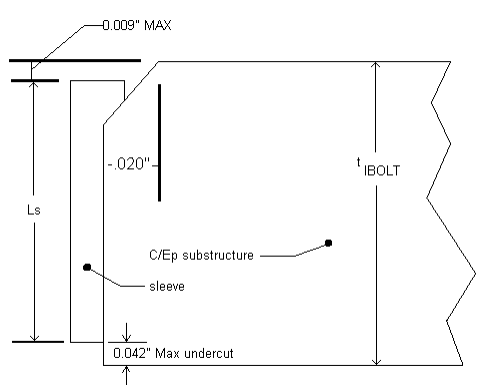

[1] *e.g.*, Reference 11-23

Copyright 2015 Lockheed Martin Corporation.
Note: The current version is always the version on the Lockheed Martin network.

Figure 11.7-8 Example of Sleeve and Sleeve Installation

This section provides an analytical means for quantifying the resulting reduction in bearing strength due to undercutting the sleeve. For situations in which composite substructure has bonded hole-liner sleeves that cannot be installed long and machined to full panel thickness:

- The undercut length should be limited to no more than 0.042 in. (worst-case for one size undercut)
- IBOLT bearing M.S. for the composite substructure should be reduced as follows

$$M.S._R = \left[M.S._{IBOLTbrg} + 1\right]\frac{L_s}{t_{IBOLT}} - 1 \qquad \text{Equation 11.7-2}$$

where
$M.S._R$ = Reduced margin of safety
$M.S._{IBOLTbrg}$ = IBOLT Full composite thickness bearing margin of safety
L_S = Sleeve length (in)
t_{IBOLT} = Full composite substructure thickness used in IBOLT (in)

IBOLT bypass margins-of-safety should use the full analysis thickness and not be reduced due to the short sleeve.

11.7.5 Shims and Gaps

A shim is a part or application of material designed to fill a gap or space and/or eliminate geometric mismatch between detail parts. This mismatch is typically due to tolerance build-up during manufacturing or structural fit up and assembly. Shims are commonly incorporated into structural design configurations to ensure that performance and affordability requirements are met in a producible manner. Shimming may also be required to fill gaps for sealing purposes or to prevent undesirable clamp-up preload.

There are three primary types of shims currently used on Lockheed Martin Aeronautics programs:

- **Moldable Plastic Shim (MPS) –** sometimes referred to as liquid shim, is a cast-in-place material that can be applied to a contoured or flat surface to a required thickness determined upon assembly.
- **Laminated Shim** – A laminated shim stock, sometimes referred to as peel shim, is made up of thin layers of solid metallic shim that are bonded together and can be peeled to allow custom adjustment of the shim thickness upon assembly.
- **Solid Shim** – is a shim fabricated from a solid material (metallic or composite) designed to fill a gap between structural members during assembly. A solid shim may have a predetermined shape or dimensions, or it may be custom machined during assembly per a specified process or drawing note.

Shimming design guidelines can be found in Reference 11-48 or in program-specific guidance such as Reference 11-49.

As shown in Figure 11.7-9 a shim can be either structural or non-structural in function. To be considered a structural shim, the shim material must be bonded, bolted or riveted to either joint member, must be capable of effective joint load transfer, and the shim must have a similar stiffness that is within 25 percent that of the joint member. Typically, the shim must span a minimum of 3 fastener diameters in order to be capable of reacting bearing loads. It also must have the same hole diameter and tolerance as the parent joint material. Moldable Plastic Shim and laminated shim are not considered structural shims due to their relative lack of stiffness and strength that prohibits effective load transfer.

Copyright 2015 Lockheed Martin Corporation.
Note: The current version is always the version on the Lockheed Martin network.

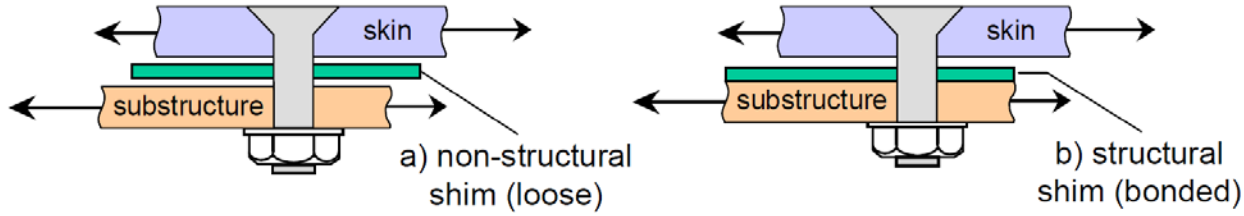

Figure 11.7-9 Structural versus Non-Structural Shims

As stated above, solid structural shims can be bonded using structural adhesives and bonding processes that provide efficient joint load transfer and strength. The bonding of shim to its adjacent structure is considered a secondary bond between two or more pieces of metal and/or precured composites. At a minimum, an explicitly defined hot bonding process specification must be used that requires the bond surfaces be cleaned down to the parent substrate material. A hot bonding process refers to a structural adhesive cured at elevated temperature. Fay-surface sealant or structural adhesive cured at room temperature is not sufficient to be considered structural.

Either metallic or carbon fiber composite solid shim, of sufficient modulus, may be considered structural if it is bonded to the structure as discussed above. Fiberglass shim bonded to the structure will be considered non-structural shim due to the low stiffness of the fiberglass relative to the structure, unless the parent joint member is fiberglass.

Composite skins may have co-cured graphite fabric sacrificial plies added to structural plies to compensate for cured thickness variation and machining and assembly tolerances of the laminate. While these plies have been shown to behave as structural shims, they should be treated conservatively as non-structural due to this geometric variation. For example, at assembly, they may be machined away. These sacrificial plies will be discussed later in this section.

The presence of a shimmed gap in mechanically fastened joint has an adverse effect on joint bearing strength. For all types of bolted joints, the presence of a shimmed gap increases the load transfer eccentricity. This increases the peaking of the bearing stress distribution in the joint members as shown in Figure 11.7-10. Also, a secondary bolt bending is induced. Figure 11.7-10 illustrates the composite skin bearing strength reduction with increasing non-structural shim-to-skin thickness ratios. For the example shown, as the shim thickness approaches the skin thickness, the bearing reduction is between 60 and 75 percent. The example shown is for a countersunk flush fastener, but the same trend is observed for protruding head fasteners as well.

Copyright 2015 Lockheed Martin Corporation.
Note: The current version is always the version on the Lockheed Martin network.

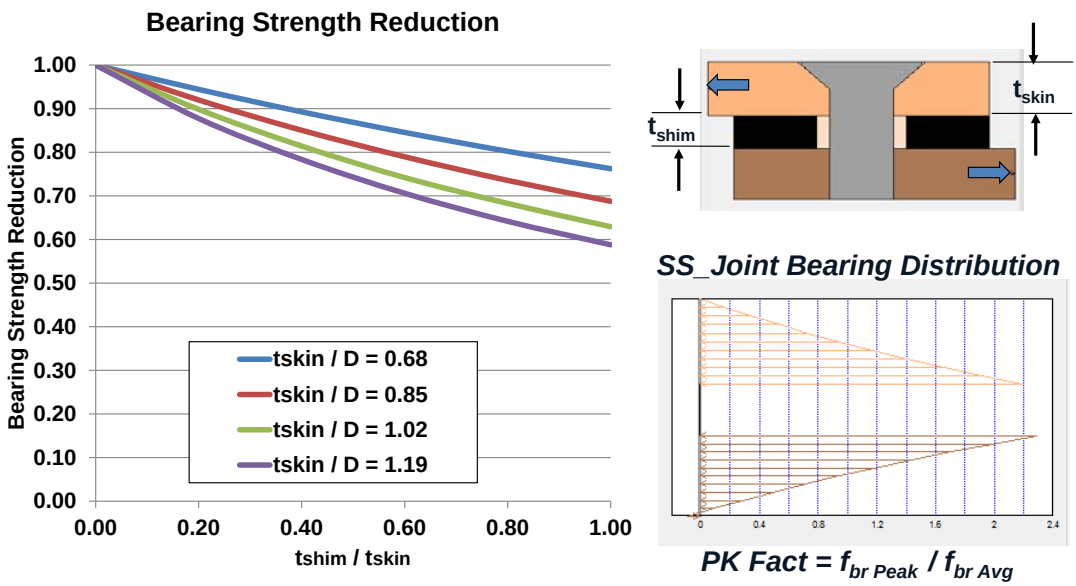

Increasing Load Eccentricity Increases the Peak Bearing Stress

Figure 11.7-10 Bearing Strength Loss in Composite Skins as Shim Thickness Increases

The adverse effect of load path eccentricity on the bearing distribution is the primary driver for Joint Design Guidelines 3 and 4 provided in Table 11.3-1. Guideline 3 defines the limitation of fastener diameter to laminate structural thickness for any given composite joint member as: Single Shear Joints, $1.0 < D/t$; Double Shear Joints, $2.0 < D/t$. Guideline 4 provides that the total joint thickness including all joint members, shim and gaps shall not exceed 3D, where D is the fastener diameter: $D/t_{total} \leq 3.0$. Note: IBOLT is limited by calibration data to $D/t_{total} \leq 2.0$ and will issue a user warning when this limit is exceeded.

Load path eccentricity created by shims can, if the shim is sufficiently thick, induce secondary loads to both the structure and to the fasteners within the shimmed joint. The effect is dependent on specific joint geometry and loads for that structure and must be examined on a case-by-case basis. The recommended maximum shim thickness for bolted joints loaded primarily in shear is 15 percent of the fastener diameter. Shims must be structural or the joint must be analyzed for fastener bending using the method of Section 5.2.3.4 of PM4057, Reference 11-1. The IDAT/SFBOLT tool may be used when at least one of the following conditions is true:

$$t_{shim} > 0.15 \cdot D$$
$$t/D > 1.0 \qquad \textbf{Equation 11.7-3}$$
$$t_{total}/D > 2.0$$

where
D is the nominal fastener diameter (in)
t_{shim} is the nominal shim thickness (in)
t is the nominal thickness of the thickest mating part (in)
t_{total} is the sum of the nominal thicknesses of all mating parts (in)

In many design configurations, the absence of a shim, either by design or by normal dimensional variability, would require part deformation to close gaps on assembly or allow undesirable deformation of part features during service life. Such deformations can lead to delaminations within the composite laminate. Pull up of gaps larger than 0.005 inch are not allowed when any of the parts being joined are composite.

Copyright 2015 Lockheed Martin Corporation.
Note: The current version is always the version on the Lockheed Martin network.

The IDAT/IBOLT composite joint strength analysis tool supports the analysis of both structural and non-structural shims. As part of bearing-bypass analysis, IBOLT calls IDAT/SS_JOINT to execute a beam-on-elastic-foundation analysis to determine the bearing load distributions within the composite laminate and substructure as discussed in Section 11.4.4. The available options for IBOLT problem input for structural and non-structural shims are discussed below with further details provided in the IBOLT User's Guide, Reference 11-24.

If a composite or metallic structural shim is attached to the substructure, then it can be considered as contributing to the substructure thickness and stiffness for IBOLT problem input. If a composite structural shim is attached to the skin, it can be included in the skin laminate definition for problem input. The exception is when the composite shim is considered sacrificial plies that will be machined for dimensional control. This case will be discussed separately below. If a metallic shim is attached to the composite skin, an approximate analysis must be conducted as IBOLT cannot consider metallic materials in the strength analysis of the skin laminate lay-up.

If a composite or metallic shim is classified as non-structural, then the shim type should be selected as Hard Shim during IBOLT problem input. The shim is treated as a spacer in the joint interface. This ensures the geometric effect of the gap between joint members is captured and does not contribute to either the skin or substructure stiffness. The fastener acts as an unsupported beam within the gap, representing the non-structural shim between the joint members. The non-structural shim may be composed of multiple materials such as metal, composite, moldable plastic shim and gasket materials. For rubber gaskets, the compressed thickness should be used for input.

In the case of discrepant part disposition stress analysis, the actual, measured bonded shim thickness and stiffness on an individual part may be included in the adjacent structural thickness for bolted joint and fastener analysis purposes.

Figure 11.7-11 shows an example configuration that illustrates potential layers within a joint attaching composite skin to metallic substructure. The numbers of layers, types of materials, and joining methods must all be considered to properly determine if the shim materials can be considered structural or non-structural for the appropriate IBOLT bearing-bypass analysis.

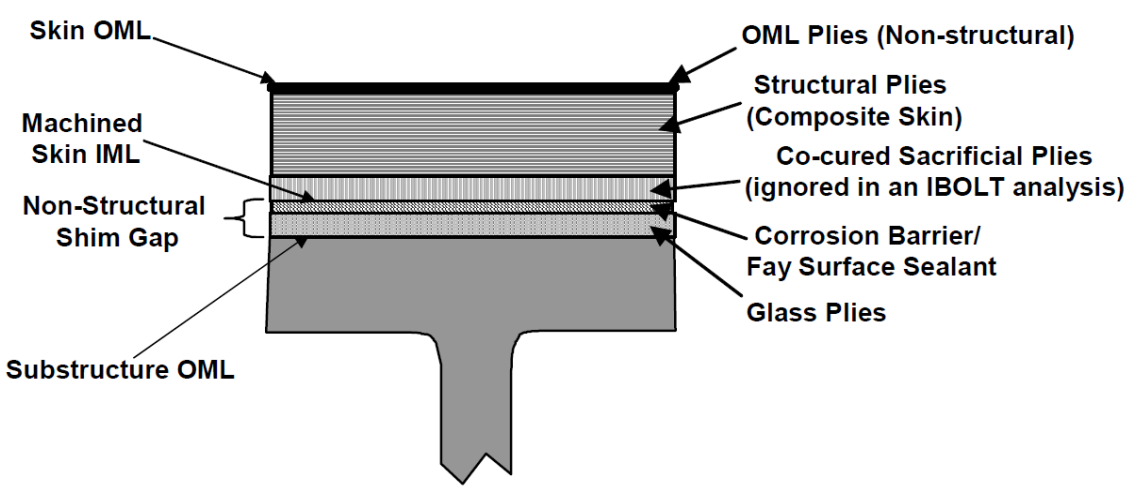

Figure 11.7-11 Sample Composite Bolted Joint Stack-up

In the manufacture of outer mold line (OML) composite skins, the skins may have co-cured fabric inner mold line (IML) sacrificial plies as shown in the figure that act as a substructure joint interface. The purpose of the sacrificial plies is a means of dimensional control. This is accomplished by pulling the skin OML down on a precisely defined

Copyright 2015 Lockheed Martin Corporation.
Note: The current version is always the version on the Lockheed Martin network.

tool to allow precision machining of the sacrificial plies to achieve a precise laminate skin thickness along the substructure interface. This process corrects any thickness variation of the composite skin that arises from the fabrication of the composite material system, lay-up of the detailed part, and cure of the composite laminate.

Static strength testing of composite joints with sacrificial plies has verified that the co-cured sacrificial fabric plies do act as a structural shim. Although the co-cured sacrificial plies could be treated as structural shims in an IBOLT analysis, their beneficial effect should be ignored due to uncertainty in the number of plies, or portions of plies, that remain after the IML machining process. *Therefore, for analysis purposes, the co-cured sacrificial plies must not be included in the make-up of the structural laminate or included in the non-structural shim gap.* They are simply ignored for the purpose of analysis.

Other shim materials, such as fiberglass shim packer plies, moldable plastic shim, or fiberglass buttons, may be secondarily bonded to the substructure to provide a machined medium for IML control. The gap thickness consists of the remaining machined shim material (conservatively assumed to be the maximum thickness), fay surface sealant thickness, and the thickness of any corrosion protection media applied to either of the machined surfaces. *These non-structural shim materials should be entered as a hard shim in the IBOLT joint configuration input.*

IBOLT composite joint strength checks should demonstrate positive margin at 150% Design Limit Load (DLL) using the maximum shim gap thickness while ignoring co-cured sacrificial plies.

11.7.6 Fuel Seals and Seal Grooves

While not structurally desirable, fuel seal grooves as shown in Figure 11.7-12 have been required in legacy aircraft designs. The stress concentration of the notched feature and interlaminar load transfer within the composite laminate leads to a different groove design from the metallic substructure groove. In addition to all usual analysis performed on solid laminates without seal grooves, two special strength checks are required:

- IBOLT analysis of the outer fastener row, assuming the discontinuous sublaminate is a non-structural shim
- Interlaminar strength analysis of tangency point at bottom of seal groove

Since the strap is tied to the substructure with a row of fasteners on either side of the seal groove, the joint clamp up is assumed to be sufficient to negate any interlaminar tension (ILT) stress effects.

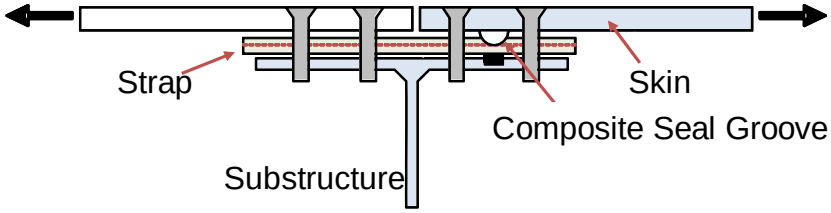

Figure 11.7-12 Typical Seal Groove in Laminated Strap

Nominal fastener centerlines, by design, should not be permitted to be closer than 2D to the seal groove centerline. A material review board discrepant part disposition specifying less than 2D requires an additional reduction factor.

When a seal groove is present in a composite bolted joint, bearing and bypass analysis should follow the IBOLT analysis methods outlined in Section 11.5.2. Also, the shim guidelines in Section 11.7.5, as applied to the sublaminate shown in Figure 11.7-13 should be followed. The sublaminate is the portion of the skin plies that contain the seal groove. For the analysis of fasteners 1 and 4, the sublaminate should be treated as a non-structural shim, which has the sublaminate primary stiffness, E_x, and thickness defined by the height of the seal groove. Only the outer row fasteners are analyzed in this fashion. This is because any delamination emanating from the seal

Copyright 2015 Lockheed Martin Corporation.
Note: The current version is always the version on the Lockheed Martin network.

groove is assumed to propagate only outward to the nearest free edge. Fasteners 2 and 3 are analyzed using the full structural thickness of the skin in the usual manner.

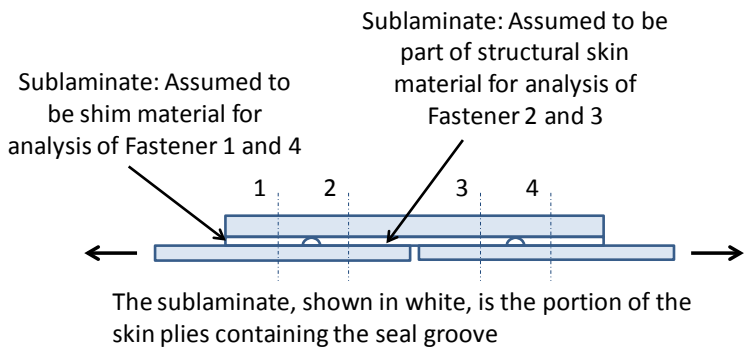

Figure 11.7-13 IBOLT Assumptions for Analysis of Seal Groove

The composite strap detail should also be checked for interlaminar strength. Ideally, the preferred approach would be to conduct an element level test program to determine in-plane design strain allowables that apply specifically to the intended design application. The element tests should be designed to replicate the bolted joint design with all joint members, composite strap with seal groove, and shimming materials included. Static and fatigue tests under in-plane loading can be performed at the design environmental conditions.

An alternate approach that has been successfully used in the past is to conduct an interlaminar strength analysis that is calibrated to element test results (Reference 11-50). At present, there are no closed-form analysis methods for predicting the three-dimensional stress state, so a finite element analysis using a 3-D solid model would be required. Depending upon the loading conditions, the problem may be reduced to generalized plane deformation with a finite element idealization such as that show in Figure 11.7-14.

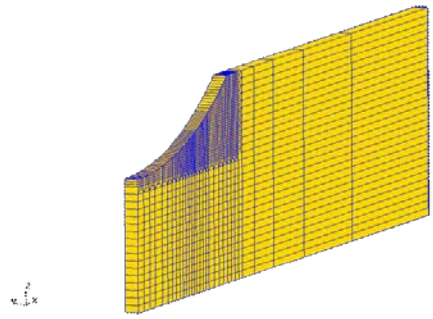

Figure 11.7-14 Example 3D Plane-Strain Solid Model

The strength analysis should be correlated to the results of a static strength testing program using a representative structural element and loading conditions. Depending upon the criticality of the structural application, testing may need to be expanded to cover the effects of environment, fatigue and defects.

The following approach may be used for this type of analysis.

1. Develop a 3-D solid finite element model using CHEXA and CPENTA elements, constructing the model parallel to the ply orientation that is most-nearly perpendicular to the seal groove. Groove geometry should be conservatively modeled to be perpendicular to the chosen fiber-direction.
2. Obtain loads from an airframe or detailed finite element model which represents the gross laminate as shell elements with no explicit modeling of the seal groove. Use Mohr's circle to rotate loads and moments by -45, 0, 45, or 90 degrees, as required to align with the seal groove geometry.

Copyright 2015 Lockheed Martin Corporation.
Note: The current version is always the version on the Lockheed Martin network.

3. Apply unit load cases to the 3-D model. Account for the shift in load line-of-action due to plies cut by the seal groove in axial unit load cases by multipoint (MPC) and slope contraints.
4. Extract stresses from the 3-D solid model at a characteristic distance[1] of R_c = 0.003 in. and factor up to actual design loads.
5. Calculate a combined interlaminar shear/tension margin of safety at each ply mid-plane, a distance R_c from the seal groove surface, using the following equations:

$$R = \left[\left(\frac{F_{13}^{su}}{f_{13}}\right)^2 + \left(\frac{F_{23}^{su}}{f_{23}}\right)^2 + \left(\frac{F_{33}^{tu}}{f_{33}}\right)^2\right]^{\frac{1}{2}}$$

$$M.S._{ILS-ILT} = \frac{1}{R} - 1 \qquad \text{Equation 11.7-4}$$

where
f_{13}, f_{23} is the interlaminar shear stress components extracted from 3-D solid finite element model (psi)
f_{33} is the interlaminar tensile stress component extracted from 3-D solid finite element model (psi). If f_{33} is compression, set $f_{33} = 0$
F_{13}^{su} is the B-basis interlaminar shear strength allowables, (TAU13) from IDAT/MATUTL (psi)
F_{23}^{su} is the B-basis interlaminar shear strength allowables, (TAU23) from IDAT/MATUTL (psi). If TAU23 is unavailable use TAU13.
F_{33}^{tu} is the B-basis interlaminar tensile strength allowable (SIG3) from IDAT/MATUTL (psi)

11.7.7 Counterbores

Counterbores are machined cylindrical flat bottomed holes, generally contentric with a through-hole, to accommodate some type of feature such as a fastener head, o-rings, or retention rings. In aircraft construction, counterbores may be required in certain holes in composite panels for the purposes of fuel sealing and/or fastener retention. This section discusses the structural analysis considerations of counterbores in these scenarios.

Program fuel sealing standards, such as Reference 11-51, may require fasteners installed in fixed outer mold line or closeout skins to be installed wet with polysulfide sealant and a counterbore seal at the base of the countersink, as shown in Figure 11.7-15. The counterbore is filled with sealant to produce an O-ring type of seal for the fastener. The counterbore seal addition does not affect the strength analysis. The depth requirement that the countersink cannot exceed 80 percent of the structural laminate (Section 11.3.1, Guideline 5) is measured from the intersection of the countersink and the straight hole. This is shown in Figure 11.7-16, such that the minimum structural thickness required in the shank portion of the fastener ignores the presence of the counterbore. Note that fastener installations that have grommets or sleeves do not have this counterbore seal requirement.

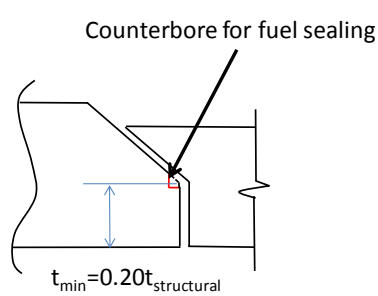

Figure 11.7-15 Counterbore Seal in Countersunk Hole in Composite Skin

[1] The characteristic is a distance from the edge of a feature where stresses should be taken for analysis. It is determined from correlation of analysis to test data.

Copyright 2015 Lockheed Martin Corporation.
Note: The current version is always the version on the Lockheed Martin network.

Counterbores may also be used in captive fastener retention for removable composite door and covers. One approach has required an inner mold line (IML) counterbore on the hole in the composite panel in order to accommodate the washer and retaining ring. Figure 11.7-16 shows an example of such a configuration. Note that in many fuel and environmental sealing applications it is required that t_g and t_w not overlap, *i.e.*, the washer may not protrude past the panel IML.

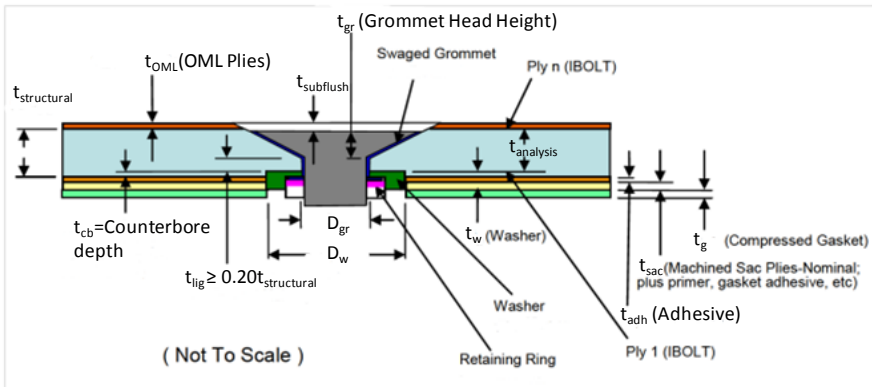

Figure 11.7-16 Captive Fastener with Counterbored Hole in Composite Panel

The test data used to calibrate captive fasteners in the current IBOLT fastener database is based on a test configuration where the captivated washer was always external to the panel IML, rather than counterbored into it. Consequently, for captive fastener configurations with a counterbored hole, some modifications must be made to the IBOLT analysis input. These modifications are intended to adjust the counterbored hole configuration in bearing where delamination is a likely failure mode without unduly affecting the bypass margins of safety. The K_t due to the larger counterbored hole in the IML is assumed to have a negligible effect on bypass failure, since it is assumed to be a small fraction of the structural thickness.

Composite panels having fastener systems with IML counterbored washers should be analyzed in IBOLT using a reduced analysis thickness, $t_{analysis}$, shown in Figure 11.7-16. $t_{analysis}$ is the thickness of the laminate minus the depth the counterbore extends into the laminate. Note that non-structural surface plies are excluded and a large effective IBOLT element size is used.

The counterbore depth and analysis thickness are defined as

$$t_{cb} = t_w - t_{sac} - t_{adh} \; (t_{cb,min} = 0.0) \qquad \textbf{Equation 11.7-5}$$

$$t_{analysis} = t_{structural} - t_{cb} \; \textit{(Rounded down to nearest whole ply)} \qquad \textbf{Equation 11.7-6}$$

where

t_{cb} is the counterbore depth into the structural plies (in)
t_{sac} is the nominal machined thickness of sacrificial plies, primer, and adhesive, if applicable (in)
$t_{structural}$ is the composite laminate thickness excluding protective surface plies and sacrificial plies (in)
$t_{analysis}$ is the reduced analysis thickness (in)
t_w is the washer thickness (in)
t_{adh} is the nominal adhesive thickness for bonding sacrificial plies (in)

Copyright 2015 Lockheed Martin Corporation.
Note: The current version is always the version on the Lockheed Martin network.

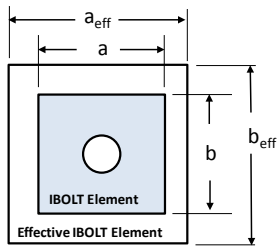

Figure 11.7-17 Effective IBOLT Element Size for Counterbore Hole Analysis.

The effective IBOLT element dimensions shown in Figure 11.7-17 are defined as

$$a_{eff} = (a \cdot t_{structural} - D_w \cdot t_{cb}) / t_{analysis}$$
$$b_{eff} = (b \cdot t_{structural} - D_w \cdot t_{cb}) / t_{analysis}$$

Equation 11.7-7

where:
a = IBOLT element width (in)
b = IBOLT element height (in)
D_w = Washer diameter (in.)

For analysis of counterbored holes, the basic requirement continues to be that no structural failure shall occur at 150% DLL. The IBOLT analysis check should be executed at 150% DLL using the nominal thickness definitions of Figure 11.7-16 along with the effective element dimensions. Any sub-flush requirements will still need to be included in the analysis.

Additionally, the analyst must ensure that the remaining ligament, shown in Figure 11.7-16 is greater than the minimum requirement. This is expressed as

$$t_{lig} = t_{structural} + t_{oml} - t_{subflush} - t_{cb} \geq 0.20 \cdot t_{analysis}$$

Equation 11.7-8

where
t_{lig} is the ligament height (in)
t_{oml} is the OML protective surface ply thickness (in)
$t_{subflush}$ is the fastener head depth below OML (in)

Note that the countersink depth requirements are based on nominal dimensions. Also, note that the shim thickness entered in IBOLT includes the following:

- Maximum thickness shim or seal-frame, if any
- Compressed gasket, if present
- Washer thickness minus the grommet and washer thickness (0.019-inch for all diameters) below $t_{analysis}$.

The IBOLT shim thickness should be determined by

$$t_{shim,IBOLT} = t_{shim,max} + t_g + t_w - 0.019 \text{ in.}$$

Equation 11.7-9

where
$t_{shim,max}$ is the maximum shim thickness (in.)
t_g is the compressed gasket thickness (in.)
t_w is the washer thickness (in.)
0.019 in. is the grommet and washer bearing thickness below $t_{analysis}$

Use caution when minimizing counterbore depth for weight efficiency and take care to avoid pull-through delamination failures on bolt installation due to high torque.

11.7.8 Tapered Joints

When composite laminates are tapered at a bolted connection, some modifications must be made to the standard IBOLT bearing and bypass analysis methods outlined in Section 11.5. The laminate could be tapered through a

Copyright 2015 Lockheed Martin Corporation.
Note: The current version is always the version on the Lockheed Martin network.

machining process as shown in Figure 11.7-18 or through internal ply drops as shown in Figure 11.7-19. In either of these configurations, the cross-sectional area's ability to resist the bearing and bypass stresses is reduced and analysis must account for the differences from the formulation of the IBOLT theory.

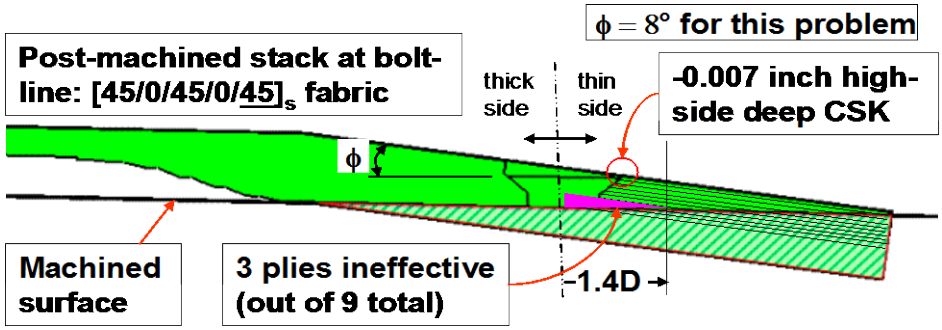

Figure 11.7-18 Example of Internal Ply-Drop Taper

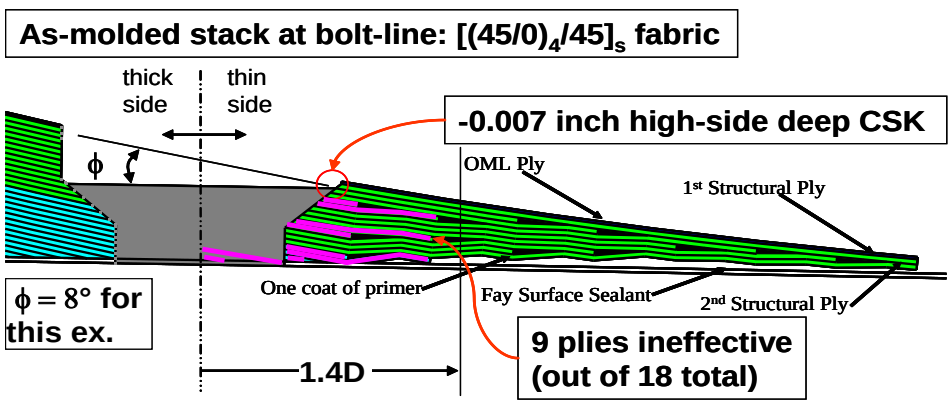

Figure 11.7-19 Example of Internal Ply-Drop Taper

For tapered composite laminates joined with structural fasteners and requiring IBOLT bearing and bypass analysis, perform three IBOLT runs as follows:

- Bearing into the laminate
- Bearing toward the free edge
- Bypass

To analyze a tapered laminate for bearing into the laminate or bearing in the thick-side direction:

1. Set laminate thickness to the laminate stack at the centerline of the fastener hole;
2. Use high-side, *i.e.*, thin-side nominal countersink depth (see Figure 11.7-18 and Figure 11.7-19) for the IBOLT "Deep Csk Hi-side" entry
3. Use all other parameters per Section 11.5
4. Develop IBOLT element loads, as appropriate per Section 11.6.3

To analyze a tapered laminate for bearing toward the free edge or bearing in the thin side direction:

1. Plies terminating within 1.4D (Reference 11-52 test data) of the fastener centerline as shown in Figures Figure 11.7-18 and Figure 11.7-19 should be assumed to be ineffective and omitted from the laminate stack. Thus,

$$t_{analysis} = t_{structural} - 1.4 \cdot D \cdot \tan\varphi$$

Copyright 2015 Lockheed Martin Corporation.
Note: The current version is always the version on the Lockheed Martin network.

where
$t_{structural}$ is
D is the nominal fastener diameter (in)
φ is the angle the fastener head makes with the OML surface (degrees)

2. Use high-side, *i.e.*, thin-side nominal countersink depth (see Figure 11.7-18 and Figure 11.7-19) for the IBOLT "Deep Csk Hi-side" entry
3. Use all other parameters per Section 11.5
4. Develop IBOLT element loads, as appropriate per Section 11.6.3

To analyze a tapered laminate for bypass loading

1. Set the fastener hole diameter, D, to the head diameter of the countersunk fastener
2. Select a protruding head fastener of the same material as the real countersunk bolt
3. Set the laminate thickness to the laminate stack at the centerline of the fastener hole
4. Set Tilt Angle = 0°;
5. Use all other parameters per Section 11.5
6. Develop IBOLT element loads, as appropriate per Section 11.6.3

Report the deep countersink bearing-bypass margin of safety and bearing cutoff margin of safety from whichever of the three approaches is applicable.

For bearing loads in a direction between parallel to edge-of-part and 90° outward from edge-of-part, conservatively use method 2 with the load oriented toward the edge of the part for initial screening. This uses the thinnest laminate and the most conservative load direction. If necessary, then separate parallel and normal to edge-of-part load components, run separately using appropriate geometry and approach for each. The combined margin of safety can then be calculated by combining the deep countersink bearing cutoff margin of safety and bearing-bypass margin of safety as

$$R_{brg-byp} = \frac{1}{M.S._{IBOLT\ Deep\ CS\ Brg-Byp} + 1}$$

$$R_{brg} = \frac{1}{M.S._{IBOLT\ Deep\ CS\ Brg} + 1}$$

$$M.S. = \frac{1}{\sqrt{R_{Brg-Byp}^2 + R_{Brg}^2}} - 1$$

Equation 11.7-10

where
$M.S._{IBOLT\ Deep\ CS\ Brg\text{-}Byp}$ is the margin reported as Deep Countersink Bearing-Bypass Cutoff
$M.S._{IBOLT\ Deep\ CS\ Brg}$ is the margin reported as Deep Countersink Bearing Cutoff

Copyright 2015 Lockheed Martin Corporation.
Note: The current version is always the version on the Lockheed Martin network.

11.8 Unix / PC Calculations

There are a number of Lockheed Martin computer programs referenced in Section 11 that are used in bolted joint analysis. All of these tools reside in the Integrated Detail Analysis Tool (IDAT) suite. Table **11.8-1** provides a summary list of the tools with a description of their application to various aspects of bolted joint analysis. IDAT is available in both Windows and Linux versions.

Table 11.8-1 **Summary of IDAT Tools[1] used in Bolted Joint Analysis**

IDAT Tool Name	Description	Application in Bolted Joint Analysis	Section Reference
A4EI	Bonded Joint Strength Analysis	Bonded Shims or Doublers	11.7.5
BDAT	Batch Detail Analysis Tools	Multiple options for loads extraction using batch tools: BIBOLT (loads extraction and IBOLT Execution), SHELL_FRCS, SLIMGPFB, SLIMJNT	11.9.3
Fastener Database	Bolt/Nut Selector Dialog	Provides a convenient reference list of available bolt/nuts with material, modulus, strengths, and joint factors	11.5.5
FLANGE	Flange Bending Analysis	Analysis of substructure flanges and determination of pull-off loads	11.6.7.2
IBOLT	Bolted Joint Analysis	Analysis of composite materials for bearing and bearing-bypass failures	11.4, 11.5
LAMINATE	Laminate Stack Editing Tool	Used to create a laminate file definition; Also can generate IBOLT bearing-bypass interaction diagrams	11.4
LAM_PERCT	Laminate Percent File Editing Tool	Used to create a laminate percent file in terms of % 0°,+45°,-45°, and 90° plies	11.4
MATUTL	Engineering Material Properties Tool	For use in obtaining various material properties for laminate; Also can generate joint strength related carpet plots	11.5.2.1, 11.5.3, 11.7.6
PEERY	Eccentric (Rigid) Fastener Pattern Analysis	Determines fastener loads in a two dimensional eccentric fastener pattern.	11.6.5.2
PRESS	Flat Panel Pressure Loading	Analysis of flat panels under transverse pressure loading for determining panel membrane and bending loads	11.6
PULLTHRU	Fastener Pull-Through Analysis	Strength analysis for fastener pull-through failure in composite materials	11.5.3
RIGIDBODY	Three Dimensional Rigid Body Analysis	For use in determining reactions/fastener loads in a three dimension rigid body	11.6.5.2
SFBOLT	Fastener Static and Fatigue Analysis	Analysis of the fastener in a bolted joint	11.5.5.2
SPLICE	Bolted Butt Strap Joint Analysis	Fastener distribution in single and double row composite butt splice joints	11.6.5.2
SPRING	One Dimensional Spring Analysis	Obtain load distributions in simple joints	11.6.5.2
SS_JOINT	Bolted Joint Beam-on-an-Elastic Foundation Analysis	Prediction of bearing stress distribution through the laminate/joint thickness	11.3.3, 11.4, 11.5.5.2, 11.6.5, 11.7.5

[1] IDAT material reference file generation is supported using the utility program MATGEN which is not available for general usage. Contact the IDAT support team for more information on generating material reference files.

Copyright 2015 Lockheed Martin Corporation.
Note: The current version is always the version on the Lockheed Martin network.

11.9 FEA Modeling Conventions and Considerations

This section discusses finite element modeling practices for composite bolted joint analysis. Fastener loads are frequently determined through the use of finite element models. A complete discussion of finite element modeling practices is beyond the scope of this manual. However, some discussion of finite element modeling is necessary here because fastener loading can be quite sensitive to finite element joint idealization and stiffness values defined in the finite element model.

The finite element model idealization and the mechanics of extracting fastener loads from a given idealization are critical to proper composite bolted joint bearing-bypass analysis. The related topics covered to this point may be summarized as follows. Finite element model idealization of aircraft structure and loads developed from substructure and composite skin panels was described in general within Section 11.6.2. Specific methods for defining IBOLT element loads from finite element results were described in Section 11.6.3. Procedures for handling multiple fastener rows and coordinate transformations were described in Sections 11.6.4 and 11.6.5, respectively.

The topics discussed in this section are:

- Joint Loads from a Coarse Grid Finite Element Model (11.9.1)
- Joint Loads from a Fine Grid Finite Element Model (11.9.2)
- Automated Loads Extraction for Coarse Grid Models using the IDAT/BDAT tool (11.9.3)
- Transforming Nastran Results to the IBOLT Element Coordinate System (11.9.4)
- FEA Modeling of Discrete Fasteners (11.9.5)
- FEA Modeling for Flange Pull-Off Analysis (11.9.6)

11.9.1 Joint Loads from a Coarse Grid Finite Element Model

In a coarsely meshed finite element model, such as a preliminary design model or global air vehicle internal loads model, fastened joint idealizations will likely not represent individual fasteners explicitly. These models are used for bearing-bypass analysis of critical bolted joints prior to freezing fastener locations so explicit fastener definition is not desired. In such models, bolted joints may be represented as a T-intersection, as shown in Figure 11.9-1, formed from a combination of shell elements and 1-dimensional elements, such as rods or bars, which model the area build-up at the intersection that potentially includes both skin and substructure cap areas. In some coarse finite element models, the joint idealization might include explicitly modeled flanges or spring elements to account for panel effectivity.

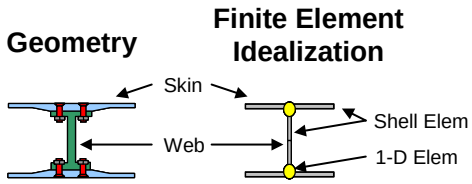

Figure 11.9-1 Bolted Joint Idealization in a Coarse Grid Finite Element Model

As shown in Figure 11.9-2, the consequence of a coarse grid T-intersection finite element idealization of bolted joints is that the nodes and elements in the finite element model do not coincide with the location and number of fastener elements used in IDAT/IBOLT bearing-bypass analysis. Therefore, a methodology is needed to extract shear flow and element forces in order to develop bolt loads and the IBOLT fastener element free-body loads for input to bearing-bypass analysis.

Copyright 2015 Lockheed Martin Corporation.
Note: The current version is always the version on the Lockheed Martin network.

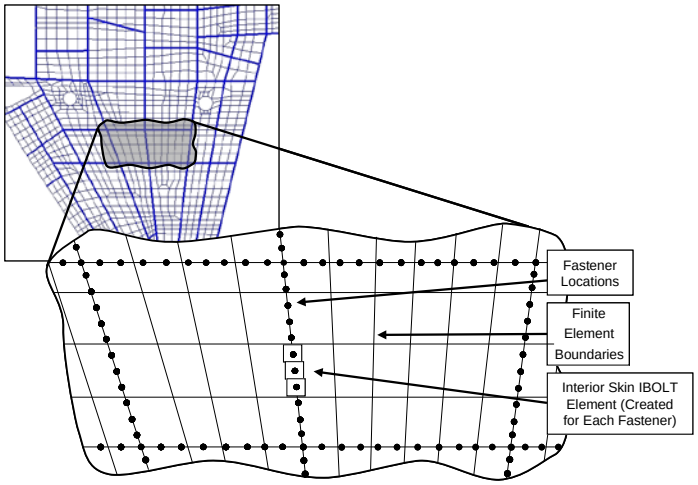

Figure 11.9-2 Coarse Finite Element Mesh Does not Align with IBOLT Fastener Elements

The basic procedure for determining IBOLT loads from a coarse grid finite element model involves the following steps:

- Isolate analysis regions by defining lands and pockets in the structure
- Map the IBOLT fastener element onto the finite element mesh for both size and orientation
- Assign free-body type based on fastener location and joint configuration
- Calculate free-body loads - bolt loads, pressure-induced loads, bypass tractions

Section 11.6.3 discusses in detail the process of defining IBOLT element loads once finite element loads have been extracted from model results. This section is concerned with the extraction of the element and grid forces from the FEM results.

11.9.1.1 Isolating the Analysis Regions

The first step in determining IBOLT loads from a coarse grid finite element model is to identify and isolate analysis regions by defining lands and pockets in the structure as shown in Figure 11.9-3. In general, land elements intersect with substructure (*e.g.*, bars/beams/rods, webs, and flanges) and pocket elements are unsupported structure (*e.g.*, skin, webs, and panels away from joints). It is assumed that a fastener can lie anywhere within a given land element.

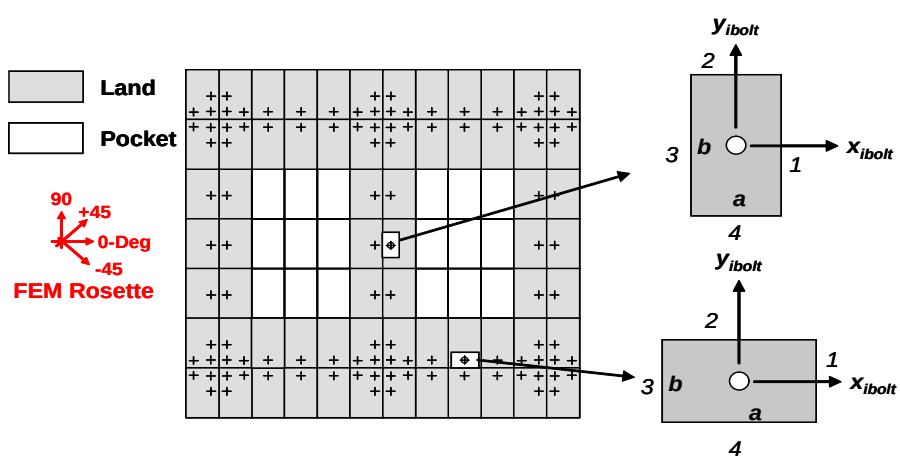

Looking Down on Fastener Heads

Figure 11.9-3 Plan View of Finite Element Model Showing Regions of Land and Pocket Elements

Copyright 2015 Lockheed Martin Corporation.
Note: The current version is always the version on the Lockheed Martin network.

11.9.1.2 Mapping an IBOLT Element onto a Finite Element Mesh

After the regions are defined, the next step in determining IBOLT loads from a coarse grid finite element model is to map the IBOLT fastener element onto the finite element mesh. First, determine if the IBOLT fastener head is aligned or opposed to the finite element normal vector. Refer to Section 11.9.4 for specific guidance and equations regarding mapping the Nastran element coordinate system to the IBOLT element coordinate system. The finite element mesh should be oriented in a view looking down on the fastener head to determine the 0º fiber direction using the mesh rosette.

As discussed in Section 11.5.2.4, the IBOLT fastener element must be aligned with one of the four fiber directions. The IBOLT x-direction is assumed to align with the laminate x-direction for bookkeeping purposes and is in agreement with the convention used for the IDAT/BDAT tool (Reference 11-53) discussed in Section 11.9.3. Free-body diagrams can be similarly generated with the IBOLT coordinate system rotated to a different orientation, such as alignment with a panel edge or bypass fastener row. Section 11.6.3 discusses the development of the IBOLT element loads.

11.9.1.3 Assigning Free-Body Type

After correctly aligning the IBOLT fastener element, the free-body type must be determined to define the set of equations used to calculate free-body loads within an element. The three possible free-body types are defined as follows:

- No Edges Free (Interior Panel Fasteners) – Continuous skin joined to substructure away from edges, corners, and intersections. Skin elements are attached to FEM with a bar/beam/rod and a web element. This free-body is discussed in Section 11.6.3.3.
- One Edge Free (Fasteners along Panel Edges) – Edge of skin joined to substructure away from corners and intersections. Skin elements are attached to FEM with a bar/beam/rod and a web element. Found near boundaries of cutouts, panels, and mate joints. This free-body is discussed in Section 11.6.3.4.
- Two Edges Free (Fasteners at Panel Corners) – Corner of skin joined to substructure. Skin elements are attached to FEM with a bar/beam/rod and a web element. Found near corners of panels and mate joints. This free-body is discussed in Section 11.6.3.5.

11.9.1.4 Calculating Free-Body Loads

Development of the IBOLT fastener element free-body loads is critical to accurate bolted joint bearing-bypass analysis and is sensitive to the method used. Grid point forces are extracted to define the IBOLT fastener load, which is then combined with shell element forces to derive the in-plane running loads at the IBOLT fastener element boundary, as shown for a no-edge-free free-body type in Figure 11.9-4. Because the coarse mesh does not align with actual fastener locations, finite element load gradient information is not detailed enough to determine individual fastener load changes along a single finite element edge. Therefore, a single IBOLT fastener element represents a group of fasteners along a single finite element edge.

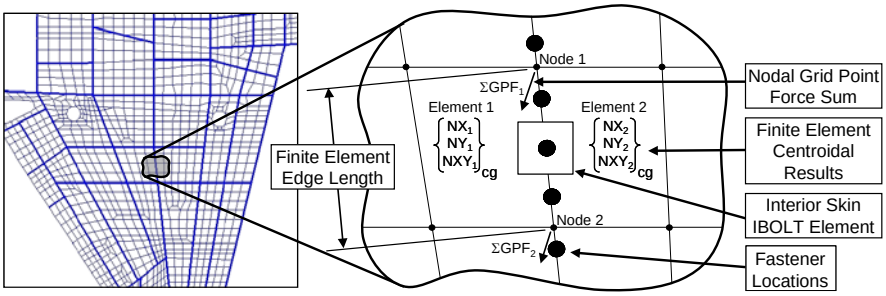

Figure 11.9-4 Finite Element Results Used to Determine IBOLT Fastener Element Loads for No Edges Free

Copyright 2015 Lockheed Martin Corporation.
Note: The current version is always the version on the Lockheed Martin network.

The normal and shear running loads and moments, N_i, T_i, and M_i in Figure 11.9-1, that are applied to the IBOLT fastener element boundaries to develop a balanced free-body are determined from the following contributions:

- Bolt load components, P_{edge} and P_{trans}, determined from finite element grid point forces
- Pressure-induced membrane force and bending moment from hand calculations or IDAT/PRESS. Refer to Section 11.6.7.
- Shell element forces, NX, NY, and NXY, from land finite elements. Refer to Section 11.6.2.

11.9.1.5 Fastener Bearing Load Calculation

The first calculation that must be made is the fastener bearing load. Grid point forces capture the running load gradient at a substructure interface better than element forces so IBOLT fastener loads should be determined from finite element grid point force results at these interfaces.

A notional skin-to-substructure joint free-body, Figure 11.9-5, shows that the skin carries in-plane membrane and shear load internally and transfers load through fastener shear to the substructure. If the skin-to-substructure free-body is split into separate skin and substructure free-bodies, as shown in Figure 11.9-6, this fastener shear interface load exists on each free-body.

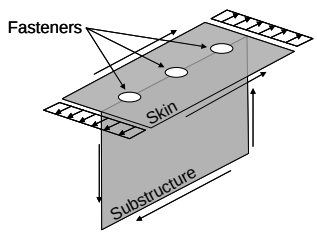

Figure 11.9-5 Notional Skin-to-Substructure Joint Free-Body

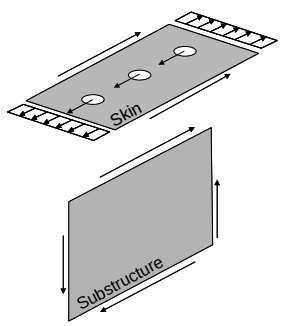

Figure 11.9-6 Separate Skin and Substructure Free-Bodies

In a finite element model, grid points connect the skin and substructure elements, as shown in Figure 11.9-7, and internal grid point forces at the joint must sum to zero to satisfy static equilibrium. If the substructure is removed as

Copyright 2015 Lockheed Martin Corporation.
Note: The current version is always the version on the Lockheed Martin network.

shown in Figure 11.9-8, nonzero grid point force resultants exist at the interface in order to maintain static equilibrium. Thus, grid point force resultants represent the fastener shear load transfer along the joint.

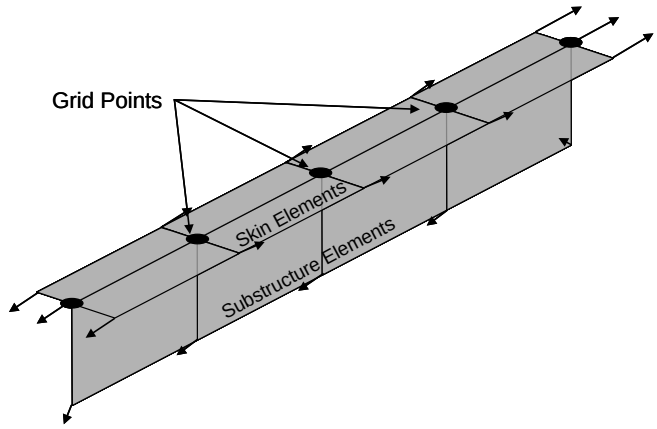

Figure 11.9-7 Grid Points Connecting the Skin and Substructure Elements in a Finite Element Model

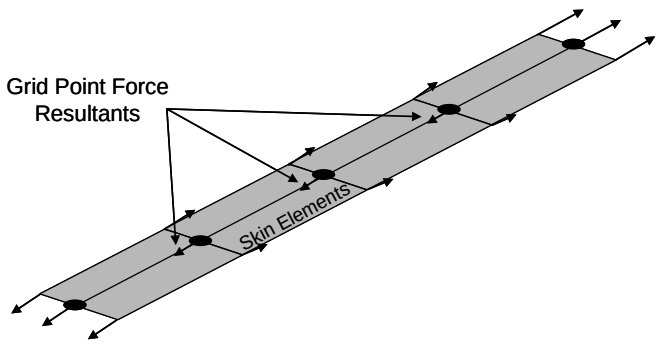

Figure 11.9-8 Nonzero Grid Point Force Resultants Exist on the Skin Free-body with Substructure Removed

In order to calculate shear flow along an edge, the grid point force resultants must be split into the appropriate contributions to each edge. In the regularly structured meshes, shown previously in Figure 11.9-2 and Figure 11.9-4, sequential element edges along a fastener row are approximately the same length. Therefore to calculate the shear flow along the edge of the element, grid point forces can be apportioned approximately equally to the adjacent element edges. However, as shown in Figure 11.9-9, the more general case is substantial variation in finite element geometry that leads to differences in element edge lengths, *i.e.*, $len_1 \neq len_e \neq len_2$. In this case, the appropriate portion of each grid point force, ΣGPF_i, must be allocated to each of the element edges adjacent to it. Because len_e in Figure 11.9-9 is greater than len_1, more of ΣGPF_1 should be allocated to the len_e edge in the shear flow calculation.

Copyright 2015 Lockheed Martin Corporation.
Note: The current version is always the version on the Lockheed Martin network.

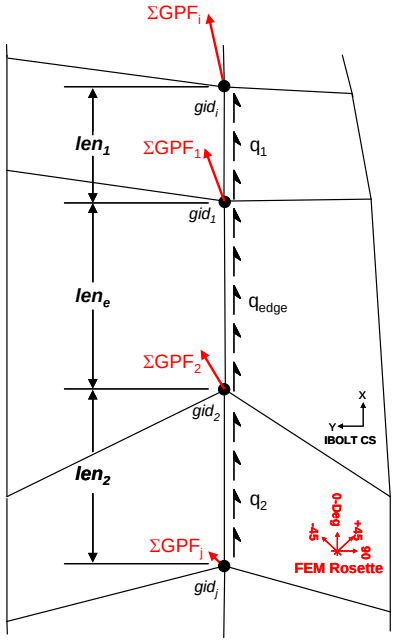

Figure 11.9-9 Shear Flow in a Coarse Grid Finite Element Model with Variation in Element Geometry

A more general procedure for allocating grid point forces to adjacent edges is to use a linear ratio of edge lengths. Thus, the appropriate portion of the grid point force, $\Sigma GPF_{i,j}$, is allocated to each edge *j* from the node *i* on either end, as shown in Figure 11.9-10. So ΣGPF_1 would be split into $\Sigma GPF_{1,1}$ and $\Sigma GPF_{1,e}$. Likewise, ΣGPF_2 would be split into $\Sigma GPF_{2,e}$ and $\Sigma GPF_{2,2}$. $\Sigma GPF_{1,e}$ and $\Sigma GPF_{2,e}$ would then be allocated to the current element edge where the current fastener is located, having length len_e, and used in the shear flow calculation for that edge. The calculations for $\Sigma GPF_{1,e}$ and $\Sigma GPF_{2,e}$ are given in Equation 11.9-1 and Equation 11.9-2.

Copyright 2015 Lockheed Martin Corporation.
Note: The current version is always the version on the Lockheed Martin network.

$$\sum \mathbf{GPF_{1,e}} = \frac{len_e}{(len_1 + len_e)} \sum \mathbf{GPF_1} \qquad \textbf{Equation 11.9-1}$$

$$\sum \mathbf{GPF_{2,e}} = \frac{len_e}{(len_2 + len_e)} \sum \mathbf{GPF_2} \qquad \textbf{Equation 11.9-2}$$

Where
$\Sigma GPF_{1,e}$ = portion of the grid point force resultant at node 1 allocated to current element edge (lbs)
$\Sigma GPF_{2,e}$ = portion of the grid point force resultant at node 2 allocated to current element edge (lbs)
ΣGPF_1 = total grid point force resultant at node 1 (lbs)
ΣGPF_2 = total grid point force resultant at node 2 (lbs)
len_e = length of current element edge (in)
len_1, len_2 = lengths of element edges adjacent to current element edge (in)

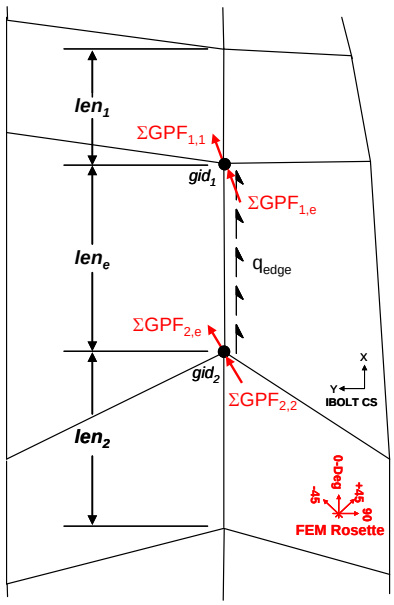

Figure 11.9-10 Weighted Average Grid Point Shear Flow Accounts for Element Geometric Variation

The shear flow, q_{edge}, acting on the current element edge can then be calculated by summing the portions of the grid point force resultants allocated to this edge and dividing by the edge length.

$$\mathbf{q_{edge}} = \frac{1}{len_e}\left(\sum \mathbf{GPF_{1,e}} + \sum \mathbf{GPF_{2,e}}\right) \bullet \mathbf{edgvec} \qquad \textbf{Equation 11.9-3}$$

Where
q_{edge} = current element edge shear flow (lbs/in)
$\Sigma GPF_{1,e}$ = Portion of node 1 grid point force resultant allocated to current element edge (lbs)
$\Sigma GPF_{2,e}$ = Portion of node 2 grid point force resultant allocated to current element edge (lbs)
len_e = length of current element edge (in)
len_1, len_2 = length of element edges adjacent to current element edge (in)
edgvec = unit direction vector of current element edge

Finally, if the IBOLT element width, *a*, is equal to the fastener spacing, *s*, which is the typical case except as described in Section 11.5.2.5, then the IBOLT fastener load in the edgewise direction, as shown in Figure 11.9-11, is calculated as:

Copyright 2015 Lockheed Martin Corporation.
Note: The current version is always the version on the Lockheed Martin network.

$$\mathbf{P_{edge}} = a \cdot \mathbf{q_{edge}}$$ **Equation 11.9-4**

Where
P_{edge} = fastener load in the edgewise direction (lbs)
a = IBOLT element x-direction boundary width (in)

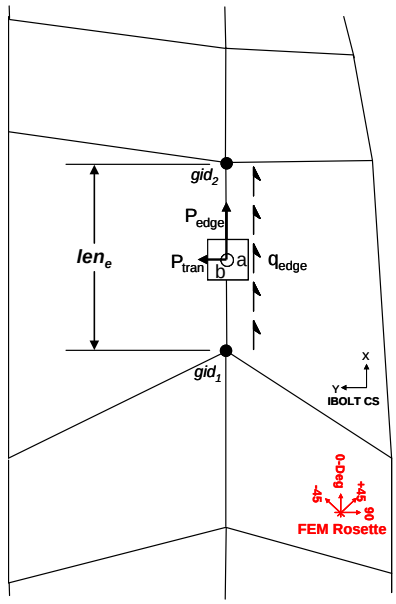

Figure 11.9-11 IBOLT Fastener Load Calculated From Element Edge Shear Flow

Using the same procedure as above, a transverse running load can be calculated by taking the transverse components of the grid point force resultants.

$$\mathbf{q_{tran}} = \frac{1}{len_e}\left(\sum \mathbf{GPF_{1,e}} + \sum \mathbf{GPF_{2,e}}\right) \bullet \mathbf{tranvec}$$ **Equation 11.9-5**

Where
q_{tran} = current element edge transverse running load (lbs/in)
$\Sigma GPF_{1,e}$ = fraction of node 1 grid point force resultant allocated to current element edge (lbs)
$\Sigma GPF_{2,e}$ = fraction of node 2 grid point force resultant allocated to current element edge (lbs)
len_e = length of current element edge (in)
tranvec = unit direction vector of in-plane normal to current element edge

As previously, if the IBOLT element width, *a*, is equal to the fastener spacing, *s*, the IBOLT fastener load in the transverse direction is

$$\mathbf{P_{tran}} = a \cdot \mathbf{q_{tran}}$$ **Equation 11.9-6**

Where
P_{tran} = fastener load in the edgewise direction (lbs)
a = IBOLT element x-direction boundary width (in)

If the IBOLT element width, *a*, is not equal to fastener spacing, *s*, then fastener spacing should be used in Equations 11.9-5 and 11.9-6.

Copyright 2015 Lockheed Martin Corporation.
Note: The current version is always the version on the Lockheed Martin network.

11.9.2 Joint Loads from a Fine Grid Finite Element Model

In a more detailed finite element model, fasteners may be modeled explicitly at grid point locations, as shown in Figure 11.9-12. Individual fastener loads can be determined directly from the grid point forces and IBOLT element running loads from the surrounding finite element force results. Such an idealization requires knowledge of the location of each individual fastener and usually requires substantial effort to construct and respond to detailed engineering changes. The benefit of such a model is an increased ability to automate analysis and process load updates. Consequently, this type of model is typically used in a mature design after the design configuration has stabilized and changes are less frequent.

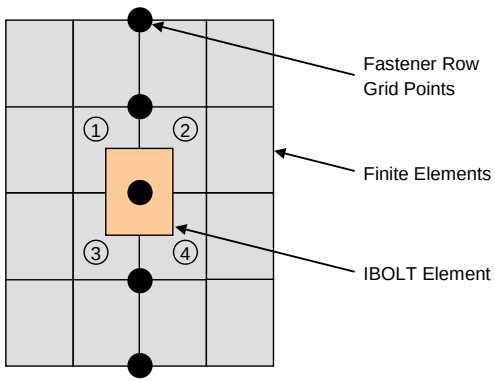

Figure 11.9-12 Fasteners Modeled Explicitly in a Fine Grid Finite Element Model

The method presented here assumes one element between fastener nodes. As element size decreases in a finite element mesh, element force results rise significantly in the immediate vicinity of singularities, such as nodal attachments. For this reason, further refinement is not recommended at fastener attachments in shell element idealizations. If a finer mesh is used then consideration should be given to methods for alleviating result peaks. Methods for accomplishing this include averaging across elements or excluding elements adjacent to singularities. The approach taken depends on the element size used.

IBOLT bearing-bypass analysis requires user input of the fastener bearing load and edge running loads from a balanced free-body in static equilibrium. In the fine grid approach, the fastener bearing load comes from the force value at a grid point corresponding to a fastener location. Skin panel running loads are calculated from the sum of finite element results and the reaction to the fastener load. The finite element results used in the running calculation are centroidal forces and moments from adjacent elements averaged at the analysis node as shown in Figure 11.9-13. Calculations needed to bring the applied fastener bearing load and element edge running loads into static equilibrium are given in Section 11.6.3.

Copyright 2015 Lockheed Martin Corporation.
Note: The current version is always the version on the Lockheed Martin network.

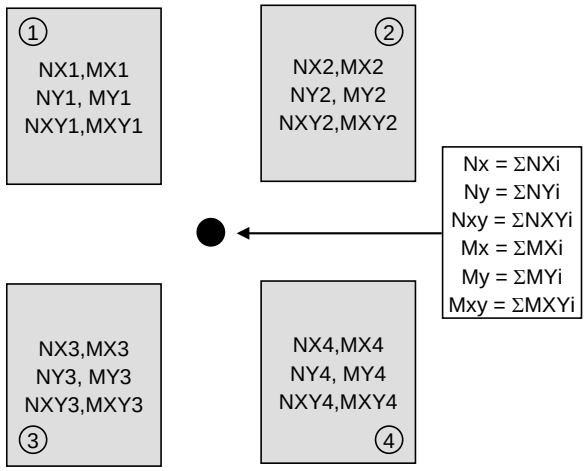

Figure 11.9-13 Adjacent Element Centroidal Forces and Moments Averaged at Analysis Node

As discussed in Section 11.5.2.4 the IBOLT analysis coordinate system must align with one of the laminate fiber directions. Additionally, for simplicity, it is preferred to align the IBOLT fastener edge 1 (normal to the IBOLT x-direction) to a panel edge where one exists. The closest fiber angle to the panel edge should be used. A swap angle can be defined for the IBOLT analysis element as the rotation from the laminate coordinate system to the ply angle that will be used as the IBOLT x-direction, which is also the new zero degree ply. The IBOLT element is rotated using a right-hand rule in increments of 45 degrees (-135, -90, -45, 0, 45, 90, 135, or 180). The laminate can be rotated using the Rotate Laminate feature within IBOLT.

Figure 11.9-14 gives examples of these rotations at various locations on a sample composite panel. Note that in this figure the IBOLT element normal points into the structure to align with the finite element normal vector so a positive rotation is in the clockwise direction. Additionally, the laminate stacking sequence starts with the first ply at the outer mold line so in this case the laminate stacking sequence must be reversed for IBOLT analysis as discussed in Section 11.9.4. The laminate stacking sequence can be reversed using the Reverse Laminate File feature in IBOLT.

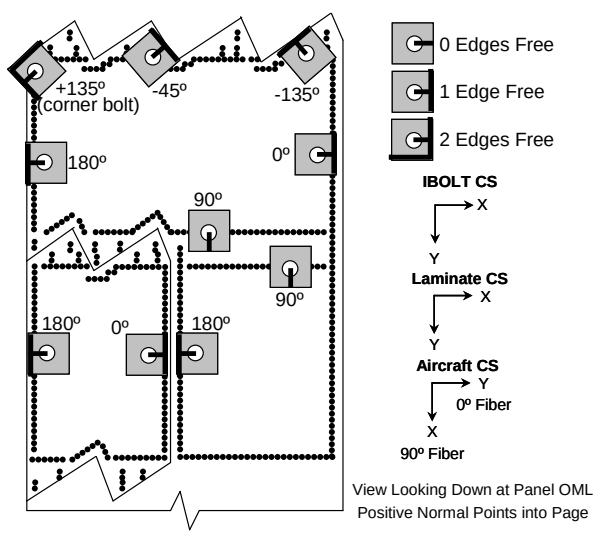

Figure 11.9-14 Example IBOLT Element Rotations

Copyright 2015 Lockheed Martin Corporation.
Note: The current version is always the version on the Lockheed Martin network.

After the swap angle has been determined, the running loads, moments and fastener loads must be transformed, using this swap angle, to the IBOLT analysis coordinate system. Care should be taken to apply the appropriate transformations from Section 11.9.4. The finite element node-averaged loads (Nx, Ny, Nxy) should be rotated using a Mohr's circle transformation to the IBOLT analysis coordinate system loads (Nx_t, Ny_t, Nxy_t). The finite element node-averaged moments (Mx, My, Mxy) should be similarly rotated and also sign-changed, where appropriate, to the IBOLT analysis coordinate system moments (Mx_t, My_t, Mxy_t). The fastener bearing load components (Px, Py), which come from grid point force summation, should be rotated, by the swap angle, to the IBOLT analysis coordinate system.

11.9.3 Automated Loads Extraction for Coarse Grid Models

Lockheed Martin has a batch processing tool for developing fastener bearing and free-body element loads from a coarse grid finite element model. The IBOLT load batch processing tool is called BIBOLT, or Batch IBOLT, and is contained in the Batch Detail Analysis Tool (BDAT) utilities within IDAT. Details on this tool are found in Reference 11-53. The BIBOLT program, illustrated in Figure 11.9-15, performs batch processing of composite bearing-bypass analyses using the IBOLT sub-program with loads extracted automatically from a finite element model. Figure 11.9-14 shows BIBOLT data for finite elements along a fastener row with IBOLT fastener elements represented by black squares. The tool has utilities for efficient pre-processing of fastener row definition, automated execution of high volume analysis, and tabulated results reporting highlighting critical locations. The output results are associated to finite element IDs for visualization within post-processing tools and are tabulated for reporting.

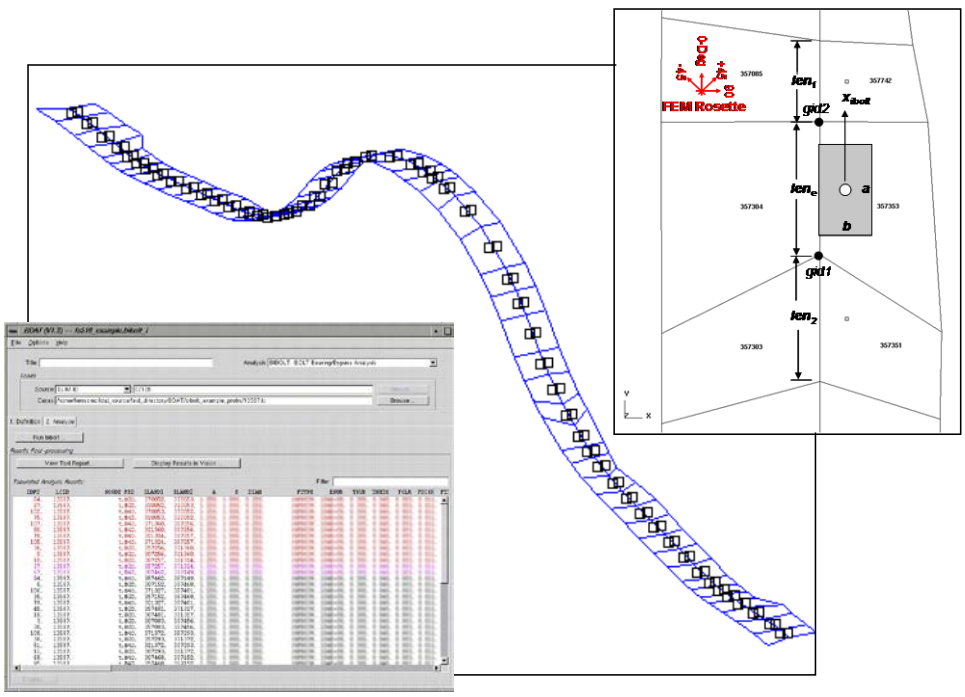

Figure 11.9-15 Batch IBOLT Automation Tool

BIBOLT was released prior to the development of the free-body equations discussed in Section 11.6.3, so be aware that there are differences in the assumptions and load equations between BIBOLT and the approach recommended in Section 11.6.3. The intent is to bring these methods into alignment in the future.

A BIBOLT option is provided to calculate pressure-induced loads using IDAT/PRESS and combine those loads with the FEM free-body loads as discussed in Section 11.6.7. The results of a BIBOLT analysis are written to a text output file (*.bibolt_o) and consists of the following information:

Copyright 2015 Lockheed Martin Corporation.
Note: The current version is always the version on the Lockheed Martin network.

- Summary of the most critical margins and failure modes for each SET of finite elements
- Sorted critical margins for each failure mode
- Summary of critical load cases and associated margins
- Critical margins and failure modes for each joint
- Summary of critical free-body loads for each joint
- Summary of deep countersink margins for each joint

The IDAT Batch Detail Analysis Tool (BDAT) contains a few additional tools that can be useful in extracting loads from finite element models. These additional tools are summarized below and can be executed as batch command line processes. Further details about them can be found in Reference 11-53. These tools interface with SLIM and Vision, which are commercial software tools, developed by Third Millennium Productions (TMP). SLIM is used for finite element load results data archiving. Vision is used for finite element data and results post-processing. Additional loads extraction tools in BDAT are as follows:

- SHELL_FRCS - extracts SLIM force data for CQUAD4 and CTRIA3 elements for a set of element id's and desired load conditions from the SLIM databases. It sorts the forces and writes the peak values to the output file and to a VISION readable file. It also computes the area weighted averaged section forces for all of the elements in the element file. The summary of maximum /minimum averages is printed to a file. All area-weighted-averaged loads can be printed to a separate file for use by other programs.
- SLIMGPFB - This program gets SLIM free-body grid point forces from SLIM databases for a list of elements and load cases and then outputs the data to a VISION results file. The FEM for the list of elements will also be written to a VISION output file.
- SLIMJNT - This program is used to sum grid point forces for a set of nodes from SLIM databases in order to determine a total joint load in a locally defined coordinate system. The program does this by reading the grid point forces for a list of elements that make up a free-body cut from the FEM. The program will either read all load cases in the SLIM ID or read a list of user provided load cases. It uses a joint definition file to resolve the free-body forces into a joint load given a list of node ID's and effectivities. The forces are then resolved into a local coordinate system which is defined in the joint definition file. The joint load is sorted to determine the maximum joint load values for output based on the output vector X, Y, and/or Z as specified by the user for each joint definition. The joint free-body forces for X, Y, Z, and the resultant are output for the user defined local coordinate system. All free-body moments are ignored by this program.
- SLIMP – This is a pre-processor for SLIMJNT and simplifies creation of joint definition files (*.jinp).

The methodology outlined above for developing a bolt and free-body loads model is well-suited for automated IBOLT analysis batch scripts to process large numbers of fasteners and load conditions for a relatively coarse grid model. It, does not work for fine grid models and each program and team develops and supports its own tools and scripts for post-processing of fine grid model results.

11.9.4 Transforming Nastran Results to IBOLT Coordinates

In extracting loads from finite element model results for use in IBOLT analysis, the analyst should exercise caution to ensure loads are being transformed and calculated correctly in IBOLT free-body formulations. Figure 11.9-16 and Figure 11.9-17 present equations for transforming NASTRAN-coordinate-system results to the IBOLT-coordinate-system. Figure 11.9-16 gives the transformation equations for the case where NASTRAN and IBOLT normal directions are aligned and Figure 11.9-17 gives the equations for the case where NASTRAN and IBOLT normal directions are reversed. These finite element free-bodies view the bolt from the countersink head side, *i.e.*, normal direction into the page. If a finite element tool other than NASTRAN is used, the analyst should consult the tool's documentation to determine the correct transformation.

Note that the diagrams in these figures assume that the laminate stack is defined with ply 1 at the inner mold line (IML) surface of the laminate. If outer mold line (OML) tooling is used on a program, the finite element normal direction may point into the structure and laminate stacks may be defined in the NASTRAN model with the first ply on the OML surface. In these cases, the IBOLT element normal may also be reversed (aligned with the finite

Copyright 2015 Lockheed Martin Corporation.
Note: The current version is always the version on the Lockheed Martin network.

element normal) and the laminate stacking sequence would be reversed in IBOLT, using the Reverse Laminate File feature in IBOLT, to properly orient the countersunk fastener head in the analysis. The ply stacking sequence transformations given in Figure 11.9-16 and Figure 11.9-17 would be reversed in these cases.

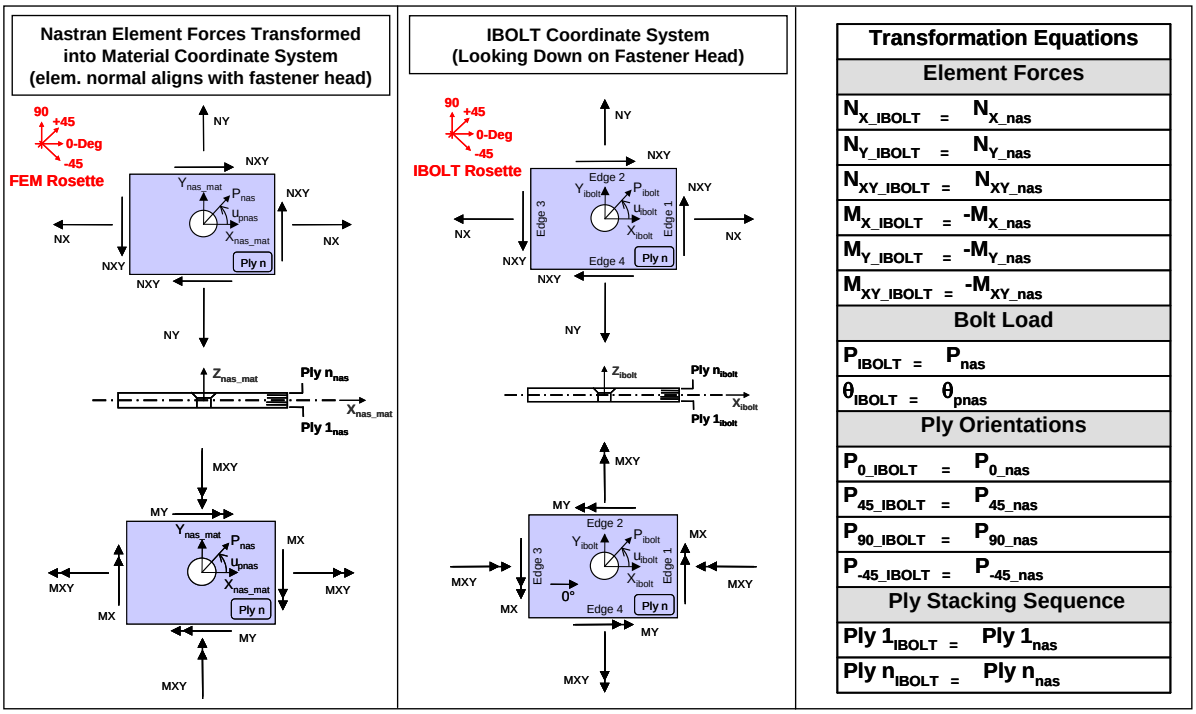

Figure 11.9-16 Transforming Nastran Results to IBOLT When NASTRAN and IBOLT Normals Agree

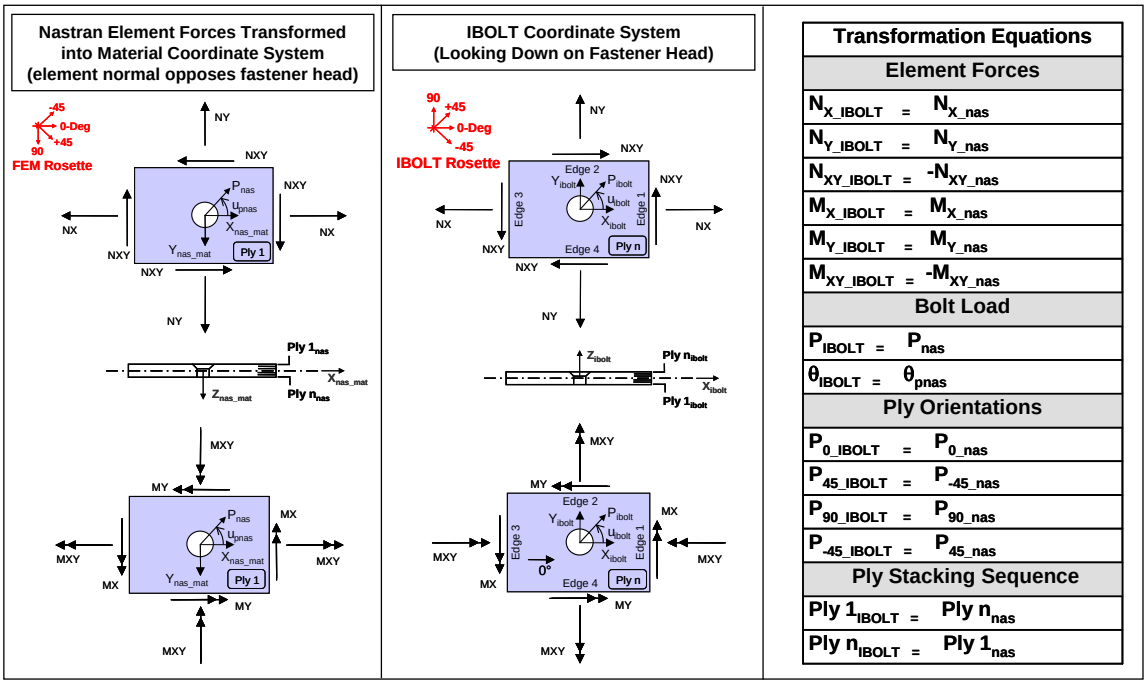

Figure 11.9-17 Transforming Nastran Results to IBOLT When NASTRAN and IBOLT Normals Reversed

Copyright 2015 Lockheed Martin Corporation.
Note: The current version is always the version on the Lockheed Martin network.

11.9.5 FEA Modeling of Discrete Fasteners

There are a variety of ways to represent mechanically fastened joints in finite element analysis, depending on the joint geometry and level of model detail. Fastener connections are typically modeled using: shared grid points of nodes; nodes connected by elements which may be rigid (MPC, RBE), elastic (CBAR, CBEAM), spring (CBUSH, CELASi) or gap (CGAP) elements; or newer mesh independent fastener elements (CFAST). Figure 11.9-18 shows some possible examples of these connections.

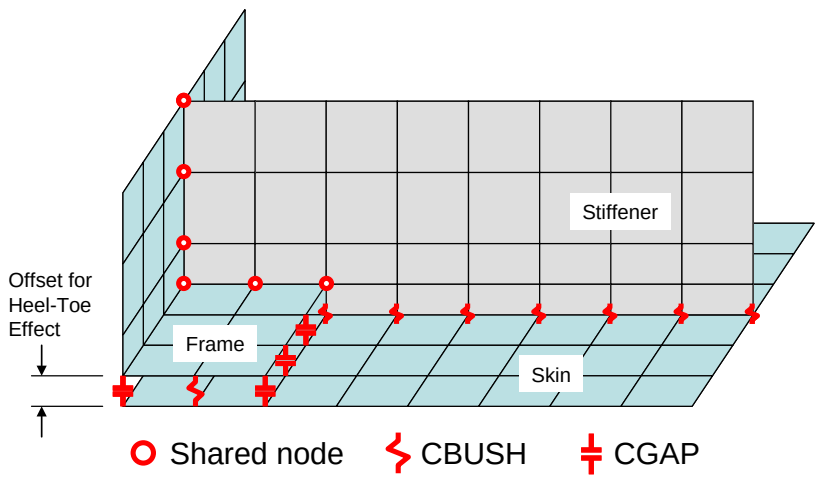

Figure 11.9-18 Possible Finite Element Fastener Connections using NASTRAN Element Types

A coarse grid finite element model used for preliminary design and full vehicle internal loads development typically does not explicitly model fasteners. Fastener loads must be calculated from the skin to substructure load transfer with the overall bearing-bypass load state determined from the analysis of adjacent skin panel loads as described in Section 11.6.3. A fine grid finite element model for detailed analysis may have fasteners explicitly modeled using spring or fastener elements in order to calculate fastener loads directly. The various types of connection are discussed in more detail below.

Shared Node Connection — Used for Close Fit Tolerance Holes

A shared grid point node connection has infinite stiffness and therefore transfers 100% of the load between modeled components. This fastener modeling option is used only for tight, close fit tolerance holes (*Diametric bolt-to-hole clearance* $\leq$ *0.004 in.)*. If a grid point corresponds to a fastener location, then the grid point forces may be used directly for the fastener load. Otherwise, the grid point forces along the fastener line will need to be resolved into individual fastener loads, such as the method illustrated in Figure 11.6-17. Refer to Section 11.6.2 for more information.

Spring Connection — Used for Close Fit Tolerance Holes

Spring elements, as shown in Figure 11.9-19 may also be used to represent fasteners for close fit tolerance holes. This may be desired for situations in which a detailed fastener load distribution for a specific fastener pattern is desired. This may also be necessary when trying to model multi-layer joints and/or account for effects of differences in fastener stiffness, geometry, properties of joint members, etc.

Copyright 2015 Lockheed Martin Corporation.
Note: The current version is always the version on the Lockheed Martin network.

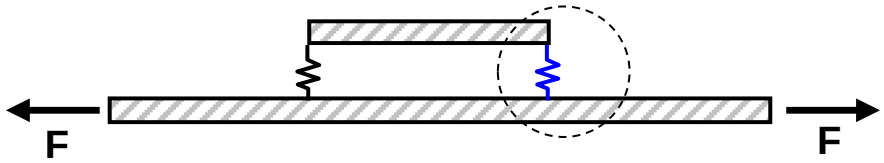

Figure 11.9-19 Finite Element Spring Connection for a Bolted Joint

Spring elements, such as through the use of a NASTRAN CBUSH element, model the joint load transfer in terms of a nodal force, P_{node}, and deflection, u_{node}, as shown in Figure 11.9-20.

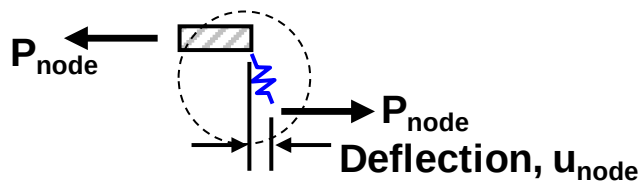

Figure 11.9-20 Nodal Force and Deflection in a Finite Element Spring Connection

For a linear structural response, spring stiffness, or spring rate, is the slope of the line that relates nodal force to nodal deflection due to spring extension as shown in Figure 11.9-21. The spring rate is a function of joint configuration details, including composite skin stiffness, fastener type, and bolt-to-hole clearance, particularly for the case of interchangeable and replaceable (IR) panels. Directional spring stiffnesses must be related to an element coordinate system and are supplied as a property input to the finite element model. Additionally, an offset value may be defined to account for geometric offsets.

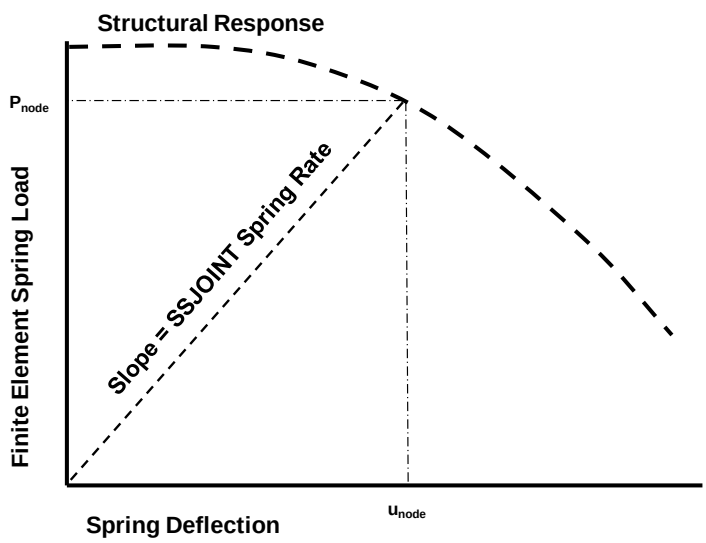

Figure 11.9-21 Spring Rate Relation between Force and Deflection

Directional spring stiffnesses must be defined for in-plane shear stiffness, out-of-plane normal stiffness, and the three rotational stiffness components. Relative to in-plane shear, the stiffness values for the fastener axial direction (normal to the skin) and the three rotational components are typically an order of magnitude greater. Consequently,

Copyright 2015 Lockheed Martin Corporation.
Note: The current version is always the version on the Lockheed Martin network.

the spring rates for tension and moment components (degrees of freedom 3, 4, 5, and 6) may be set at an assumed value of an order of magnitude higher, typically 10 msi, as compared to the fastener shear stiffness.

The fastener shear stiffness for a spring element can be determined using the IDAT/SSJOINT tool which models bolted joint deformation using a beam-on-elastic-foundation approach. If the fastener spacing aligns with nodal spacing then the SSJOINT stiffness value can be used directly for the spring element. Otherwise, the spring stiffness value must be adjusted to account for the actual fastener spacing as follows:

$$K_{FE,shear} = \frac{S_{FE}}{S_{actual}} \cdot K_{SS_JOINT}$$ **Equation 11.9-7**

Where
$K_{FE,shear}$ = Finite element spring shear stiffness (lbs/in)
S_{FE} = Nodal spacing along component interface in finite element model (in)
S_{actual} = Actual fastener spacing as designed (in)
K_{SS_JOINT} = Single fastener stiffness value determined from SS_JOINT (lbs/in)

Spring Connection — Used for Loose Fit Tolerance Holes

Composite panels are frequently used in interchangeability/replaceability (IR) applications where they must be removed at various maintenance intervals over the life of the aircraft. In these situations, loose fit tolerance holes are typically used with diametric bolt-to-hole clearance greater than 0.004 in. where the composite joint does not transfer load until the gap is closed. In such joints, movement in the bolted connection to close the gap must be accounted for in the analysis. There are multiple ways of doing this including the use of CGAP elements, reduced panel stiffness and reduced spring stiffness. The method discussed here is the reduction of the spring stiffness through the use of a secant spring rate as shown in Figure 11.9-22.

When a loose fit gap is present, the close fit tolerance spring rate obtained from SSJOINT must be shifted as shown to account for the radial gap. Initial application of load closes the gap until edge contact occurs. Once contact is made with the edge of the hole, load is transferred between components at the calculated SSJOINT spring rate. The secant spring rate relates nodal force to the resultant deflection that includes this gap closing behavior. The secant spring rate can be estimated based on test data, engineering experience, classical analysis or from finite element analysis.

Copyright 2015 Lockheed Martin Corporation.
Note: The current version is always the version on the Lockheed Martin network.

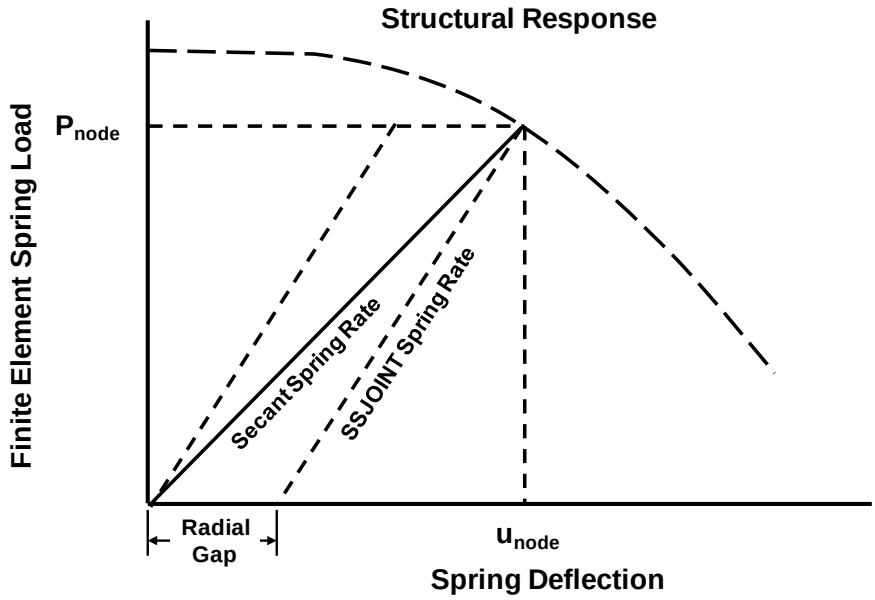

Figure 11.9-22 Spring Behavior with Gap Present

<u>Spring Sizing Assumptions and Considerations</u>

Joint load path eccentricity must be accurately represented through the selection of reference surfaces (OML, mid-surface, or IML) and appropriate element offsets. As an example, the joint may be modeled with coincident nodes on the OML surface and load path eccentricity represented through element offsets. This simplifies surface and joint definition and provides a single-value to manage model updates.

Diametric bolt-to-hole gaps for loose fit fasteners such as for IR panels are usually defined by standard hole tolerance categories. Fasteners are assumed to be initially centered in holes and no load is transferred until deflection closes the gap. A linear spring rate applies after the gap closes.

In order to ensure a balance between appropriate conservatism and minimum weight design, certain load conditions may be specified for which the removable panels should be considered highly effective for load transfer, while others load conditions are specified for low effectivity. Spring rate calculations account for load transfer effectivity through the definition of the gap size as shown in Figure 11.9-23. Standardized definitions for a high effectivity gap and a low effectivity gap may also be specified based on some multiple of the nominal bolt-to-hole radial gap. Recommended values for these multiples are as follows:

- High effective runs use 0.5 times nominal gap
- Low effective runs use 1.5 times nominal gap

Copyright 2015 Lockheed Martin Corporation.
Note: The current version is always the version on the Lockheed Martin network.

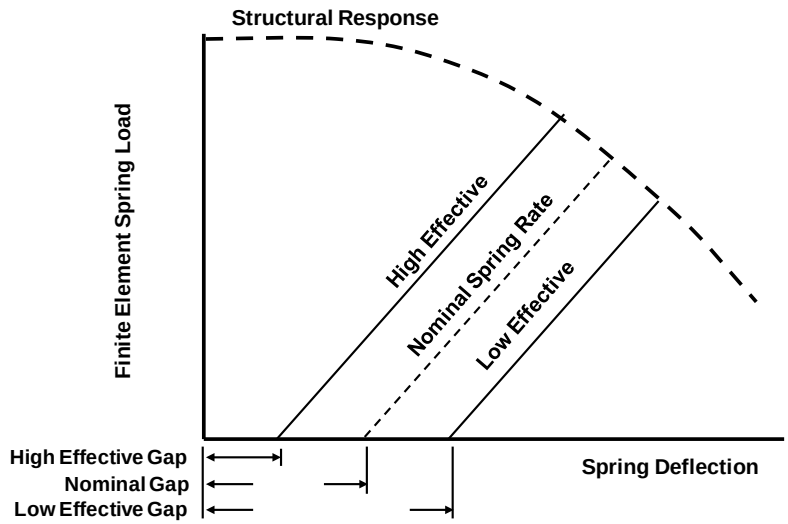

Figure 11.9-23 Gap Size Adjustment from Panel Effectivity Definition

To minimize the effort in calculating fastener spring rates, fasteners should be grouped into stiffness zones whenever possible. The fasteners may be grouped by similar hole fit category, fastener type, diameter, and skin, substructure and shim modulus and thickness.

Modeling Heel-Toe Effects for Substructure Flanges

Fine grid finite element models of aircraft structure may model substructure details such as flanges explicitly. In this idealization, it may be necessary to model heel-toe effects, where compressive load is transferred between the flange and skin, but tensile load is not. Since contact modeling is not typically feasible in a practical loads model, the heel-toe effect may be modeled using gap elements (NASTRAN CGAP), as shown in Figure 11.9-18, through using dummy spring elements, or through combinations of pinned elements that reflect an assumed heel-toe reaction distribution. Refer to Section 11.9.6 for more discussion on modeling flange heel-toe effects.

11.9.6 FEA Modeling for Flange Pull-Off Analysis

This section outlines a simple finite element modeling approach for flange pull-off analysis including:

- Assumed structure for 2-D finite element model
- Assumed model boundary conditions
- Finite element modeling guidelines

In addition to the simple approach defined below, fine grid finite element models may also be used to explicitly model individual fasteners and thereby accurately determine fastener loads. To generate valid fastener pull-off loads, the models must have mesh refinement sufficient to explicitly model individual fasteners and must include a mechanism for capturing the prying load heel-toe effects of flanges shown in Figure 11.6-41.

The flange pull-off problem is a two dimensional representation that is limited to a representative portion of the substructure web and flange and attached skin. The skin portion modeled is to the half-way point between the substructure fastener attachments on either side of the flange being analyzed. The substructure web is modeled either to the half-way point between the upper and lower flange for full depth webs, *eg*, spars, ribs, some longerons,

Copyright 2015 Lockheed Martin Corporation.
Note: The current version is always the version on the Lockheed Martin network.

etc., or to the nearest internal flange location for structure without full-depth webs. The assumed structure for a single flange / single fastener / continuous skin configuration is shown in Figure 11.9-24.

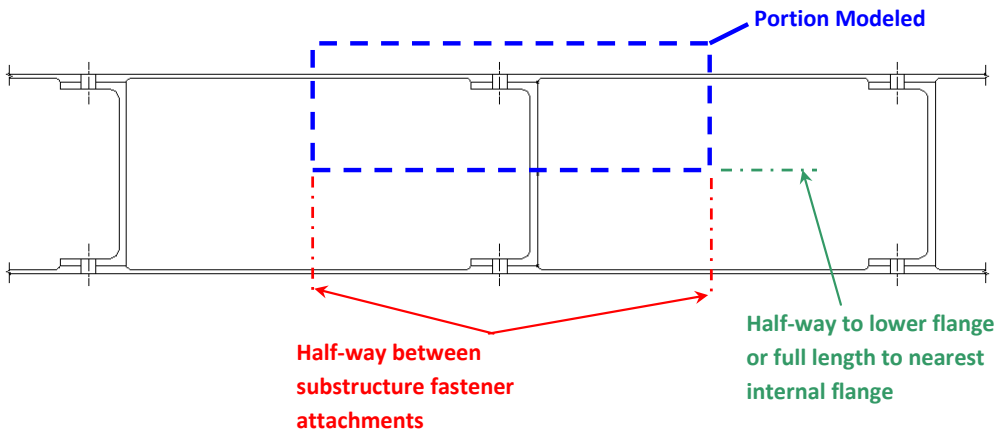

Figure 11.9-24 Assumed Structure for 2-D finite element model

The structure is divided into skin, flange, and web beam elements with representative bending and axial stiffness. An example for a single flange, single fastener row, continuous skin configuration as shown in Figure 11.9-25 where the elements are labeled as elements "a" through "g". Similarly, the element nodes are labeled as "1" through "8". Each element “a” through “g” may actually be represented by multiple elements based on the degree of discretization required to obtain a converged solution. More elements will result in better deflected shape plots when post-processing the FEM. A geometric nonlinear analysis may be required particularly for thin structural members.

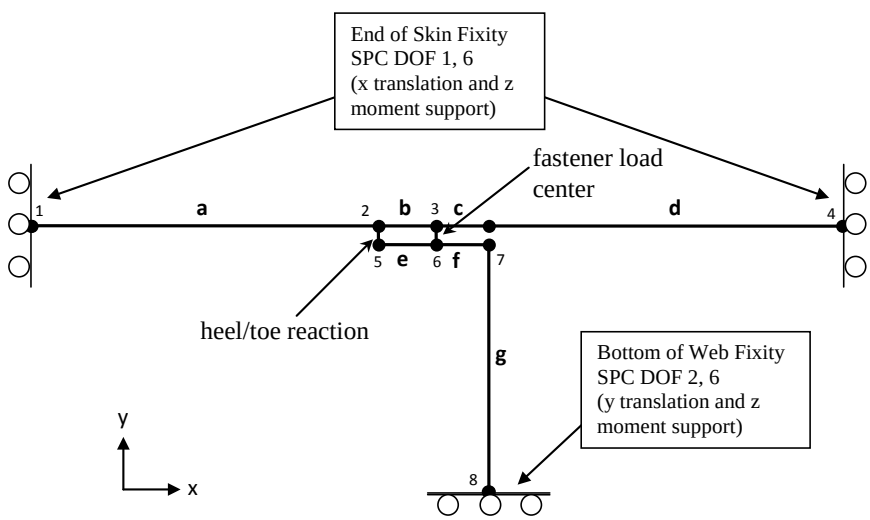

Figure 11.9-25 Assumed Boundary Conditions for Flange Pull-off Model

The following finite element modeling guidelines should be followed with respect to model fixity, fastener connectivity, heel-toe reaction, and skin splice idealizations.

Copyright 2015 Lockheed Martin Corporation.
Note: The current version is always the version on the Lockheed Martin network.

- Fixity—the model boundary conditions or fixity assumptions to be used for the FEM approach to flange pull-off analysis are shown in Figure 11.9-25.

- Fastener Connectivity—the fastener attachment is a pinned connection between the substructure flange and skin with connected degrees of freedom 1 and 2 (DOF = 1, 2). The fastener load center is assumed to be at a location that is at a distance *2/3·D* from the fastener center in the direction opposite from the heel-toe reaction where D is the fastener hole diameter. Refer to nodes 3 and 6 in Figure 11.9-25. This assumes that the fastener nut/washer support at the fastener hole causes a reduction in the moment arm by *2/3·D* while under loading as shown in Figure 11.9-26. This is consistent with the classical analysis assumptions described in Section 11.6.8.1

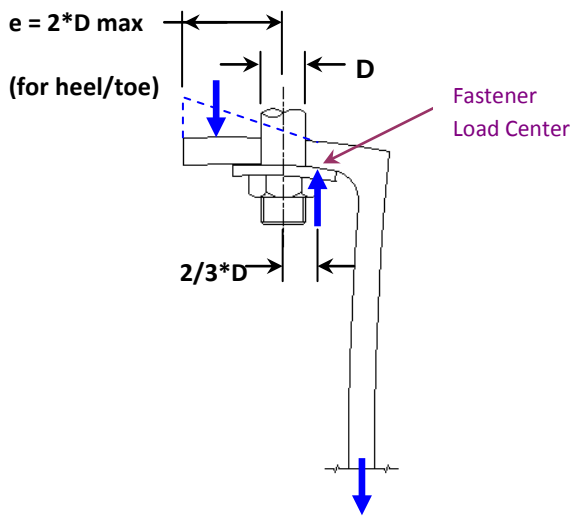

Figure 11.9-26 Fastener Loading and Heel-Toe Assumption

- Heel-Toe Reaction—the heel-toe reaction is assumed to be a triangular distribution between the fastener load center and the flange edge, as shown in Figure 11.9-26, and is modeled as a vertical-only connection between the skin and flange FE grid points (DOF = 2). Refer to nodes 2 and 5 in Figure 11.9-25.

  In general, the heel-toe reaction may occur on either side of the fastener (web or free edge side) depending on the problem geometry and loading. Therefore, both heel-toe configurations must be considered for analysis. The correct heel-toe configuration can be determined based on the relative deflection between the flange and skin grid points as determined from an analysis run in which no heel-toe reaction is used. The heel-toe reaction will be evident from this analysis as occurring on the side where the flange and skin elements pass through each other.

  In keeping with the heel-toe triangular distribution assumption, the center of the heel-toe reaction is assumed to occur at a point 2/3 the distance from the fastener load center and the flange edge (Figure 11.6-41 and Figure 11.9-26). A fastener edge distance limit of two times the fastener hole diameter should be assumed for the heel-toe reaction triangular distribution for configurations with $e/D > 2D$.

- Skin Splice Modeling—skin splice breaks are represented by two coincident grid points at the end of each skin segment as shown in Figure 11.9-27. These grids are also coincident with the flange grid at the splice location. The heel-toe reaction may occur at the skin splice location, and when it does, it is modeled as a vertical load (DOF = 2) connection between the flange grid and each skin segment grid at that location.

Copyright 2015 Lockheed Martin Corporation.
Note: The current version is always the version on the Lockheed Martin network.

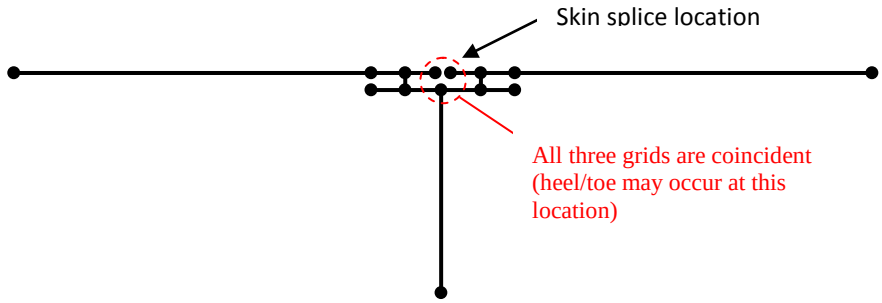

Figure 11.9-27 Skin Splice Modeling

- Applied Pressure Loads—pressure loading is applied to the skin and substructure web elements as a distributed loading. At the location where the substructure flange and skin elements are coincident, the pressure load is applied to the skin when gapping can occur between the flange and skin and to the flange where gapping does not occur. In general, the pressure may be different on each skin and web, w_1, w_2, and w_3 as shown in Figure 11.9-28. Typically, $w_3 = w_2 - w_1$ for the condition shown below without external pressure. There must be an appropriate level of detail in the skin and substructure web to correctly model any non-linear behavior due to the pressure loads. This may also require a nonlinear solution.

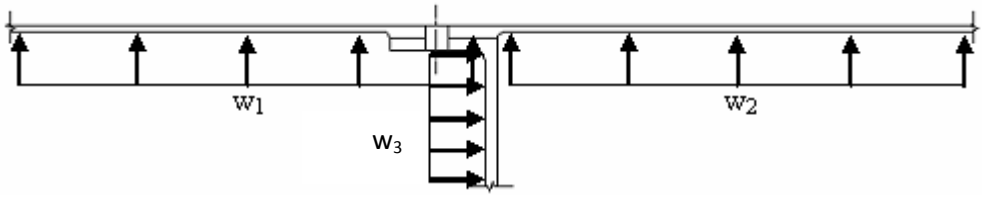

Figure 11.9-28 Pressure Loading Configuration

Copyright 2015 Lockheed Martin Corporation.
Note: The current version is always the version on the Lockheed Martin network.